Journal of the Serbian Chemical Society

VOLUME 80

No 10

BELGRADE 2015

Available on line at

www.shd.org.rs/JSCS/

CONTENTS

REVIEW

Formic acid oxidation at platinum–bismuth catalysts[•]

KSENIJA Đ. POPOVIĆ[*#] and JELENA D. LOVIĆ[#]

ICTM – Institute of Electrochemistry, University of Belgrade, Njegoševa 12, P. O. Box 473, 11000 Belgrade, Serbia

Abstract: The field of heterogeneous catalysis, specifically catalysis on bimetallic surfaces, has seen many advances over the past few decades. Bimetallic catalysts, which often show electronic and chemical properties that are distinct from those of their parent metals, offer the opportunity to obtain new catalysts with enhanced selectivity, activity, and stability. The oxidation of formic acid is of permanent interest as a model reaction for the mechanistic understanding of the electro-oxidation of small organic molecules and because of its technical relevance for fuel cell applications. Platinum is one of the most commonly used catalysts for this reaction, despite the fact that it shows a few significant disadvantages, such as high cost and extreme susceptibility to poisoning by CO. To solve these problems, several approaches have been used, but generally, they all consist in the modification of platinum with a second element. Especially, bismuth has received significant attention as a Pt modifier. According to the results presented in this review dealing with the effects influencing formic acid oxidation, it was found that two types of Pt–Bi bimetallic catalysts (bulk and low loading deposits on GC) showed superior catalytic activity in terms of lower onset potentials and oxidation current densities, as well as exceptional stability compared to Pt. The findings in this report are important for an understanding of the mechanism of formic acid electro-oxidation on the bulk alloy and decorated surface, for the development of advanced anode catalysts for direct formic acid fuel cells, as well as for the synthesis of novel low-loading bimetallic catalysts. The use of bimetallic compounds as anode catalysts is an effective solution to overcoming the problems of current stability in the oxidation of formic acid during long-term applications. In the future, the tolerance of both CO poisoning and electrochemical leaching should be considered as the key factors in the development of electrocatalysts for anodic reactions.

Keywords: formic acid oxidation; Pt–Bi catalysts; alloy; metal clusters; fuel cell anode catalysts.

CONTENTS

1. INTRODUCTION

For many years, much attention has been focused on low-temperature fuel cells with energy conversion based on the electrocatalytic oxidation of small organic molecules, such as methanol, ethanol and formic acid. The fuel cell industry has focused the majority of its research on the development of cost-effective, reactive, and durable catalysts.

Electrochemical oxidation of formic acid is under comprehensive investigation for two main reasons: formic acid can be used as a fuel in direct formic acid fuel cell (DFAFC) and can serve as a model reaction that provides a simplified example of the oxidation of more complex organic molecules that can also be used for this purpose.[1] A direct formic acid–oxygen fuel cell with a polymer electrolyte membrane (PEM) has some advantages over a direct methanol fuel cell. Oxidation of formic acid commences at a lower positive potential than methanol oxidation and the crossover of formic acid through the polymer membrane is lower than that of methanol.[2,3] Moreover, formic acid is a relatively benign and non-explosive fuel, which makes it facile in handling and distribution, as compared to hydrogen. On the other hand, it has a lower energy content with respect to hydrogen or methanol. Recent data showed, however, that formic acid fuel cells are attractive alternatives for small portable fuel cell applications.[4,5]

Electrochemical oxidation of formic acid has been widely studied on different metal electrodes. Among them, platinum was shown to exhibit the highest catalytic activity of all the pure metals. This reaction has been investigated at platinum since the early work of Breiter[6] and the results were reviewed by Par-

sons and Van der Noot[1], and Jarvi and Stuve.[7] Many results have been reported concerning the electrocatalytic oxidation of formic acid from the fundamental viewpoint[8–12] in contrast to the limited information on the properties of formic acid as a fuel. However, in the last few years, this reaction has attracted more attention.[13,14]
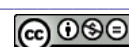
As already mentioned above, formic acid oxidation on platinum is considered as a model reaction in electrocatalysis, because the oxidation of formic acid is a simple structure-sensitive process. In spite of the apparent simplicity of the process, that is, the oxidation only requires the elimination of two hydrogen atoms in the form of protons and the transfer of the two corresponding electrons, the oxidation mechanism has a double pathway. Thus, the oxidation of formic acid on Pt electrodes follows the dual path mechanism introduced by Capon and Parsons,[15,16] involving a direct path (dehydrogenation) and an indirect path (dehydratation), both generating CO_2 as the final reaction product. This finding was later confirmed by differential electrochemical mass spectrometry (DEMS) measurements.[3] Both routes are structure sensitive and there is a clear dependence of the reactivity on the surface structure, as experiments with single crystal electrodes revealed:[17–21]
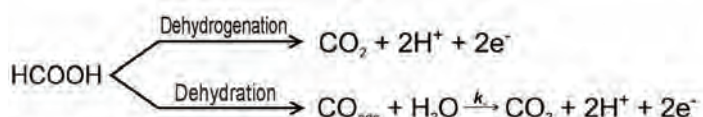
In the direct path, formic acid is oxidized through a reactive intermediate to CO_2, while in the indirect path, formic acid is first dehydrated to the adsorbed CO intermediate, as a poisoning species that hinders the direct reaction path, followed by oxidation of the adsorbed CO by OH formed at higher potentials.

The direct path that proceeds through an active intermediate is the simplest one. Formic acid adsorbs on the surface, probably transferring one electron, to form an active intermediate, and then this intermediate is oxidized to CO_2. Regarding the nature of the active intermediate, the question is not yet fully resolved.[22–24] Adsorbed formate (HCOO), rather than the formic acid fragment (COOH), was proposed as the reactive intermediate[23,25–27] and this assumption was confirmed by direct surface-enhanced infrared absorption spectroscopy (SEIRAS).[28]

In the indirect pathway, the first step is a dehydration step with the loss of an oxygen atom to form adsorbed CO, which was detected by IR spectroscopy.[10,29] CO adsorbs strongly on the surface, and for this reason, the route is also known as the poisoning route. Thus, adsorbed CO blocks the active sites on the surface and prevents the reaction from proceeding. Accordingly, the catalytic performance of Pt is significantly reduced at low potentials due to CO poisoning.

However, besides being a poisoning species, CO may act as a reactive intermediate, whereby some fraction of CO_{ads} can be oxidized with OH_{ads} to produce CO_2.[12]

Nevertheless, platinum is an unavoidable material and considered as one of the most efficient catalysts for the oxidation of small organic molecules but, on the other hand, has several significant disadvantages: high cost and extreme susceptibility to poisoning due to strongly adsorbed intermediates, which are formed during the oxidation processes.[30] Taking this into account, the ideal electrocatalysts would be one that accelerates the direct route and prevents the formation of CO.

It is now well known that these requirements are fulfilled by bimetallic catalysts, which often show electronic and chemical properties that are distinct from those of their constituent metals and offer the chance to obtain new catalysts with enhanced selectivity, activity and stability.

Several approaches have been taken to achieve these goals, but in general, they consist of the modification of platinum with a second element. This modification is usually realized by alloying or by modification of the Pt surface with adsorbed foreign metals in an amount less than a full monolayer.[31,32] The presence of a foreign metal alters the properties of Pt in the bimetallic surfaces.[12,33] The effects of these atoms can be classified in three main categories: electronic, bifunctional and third body effects. The first one, which involves ligand and strain effects, relates to a change in the electronic properties of the catalytically active material. The bifunctional effect is present when the second metal becomes the source of the oxygen required for the oxidation of the fuel. The third body effect implies a change in the distribution of the active adsorption sites due to dilution of the catalytically active material. Generally, more than one of these factors controls the enhanced properties of bimetallic surfaces making separation of the individual contributions difficult.

In order to improve Pt electrocatalytic activity towards HCOOH oxidation and tolerance to CO, addition of metals such as Ru, Pb, Os, Li, Pd, Fe, Bi *etc*.[12,34–39] were applied. Especially, bismuth has received significant attention as a Pt-modifier,[18,31,32,40,41] and different systems, such as PtBi intermetallics,[42–46] PtBi alloys,[39,47,48] electrochemically co-deposited carbon supported PtBi (PtBi/C),[49] or Pt modified by Bi either by underpotential deposition (UPD) or irreversible adsorption[50,51] were proposed as good catalysts for formic acid oxidation.

Besides the many methods for the synthesis of bimetallic catalysts, a new method for the preparation of noble metal coatings was recently proposed. This procedure includes the replacement of the surface layer of a less precious metal (Ru, Cu, Pb and Ti) with a more noble metal (Pt and Pd) by spontaneous electroless exchange upon immersion into a complex solution of Pt or Pd ions.[52,53]

An additional approach for the formation of low dimensional systems is electro-deposition of mono or multilayer metals on different substrates.[54–56] This concept of bimetallic mono and multilayer catalysts has received much attention regarding its possibility to reduce the noble metal quantity and maintain the activity by replacing the under-layer (bulk of the catalyst) with a less noble metal. Moreover, unlike other bimetallic catalysts where the second metal is either in the form of an adatom or as a component of a surface alloy, this type of catalyst allows the study of the electronic effect of the second metal under-layer on the noble catalyst over-layer, as the only operating factor.

In addition, from a practical point of view, long-term stability of the investigated catalysts for formic acid oxidation is very important. Therefore, it is necessary to determine which of the factors mostly affected the improvement of the formic acid oxidation rate and the stability of the catalyst.

In this paper, recent advances in HCOOH oxidation research are presented with focus on the progresses that have been made on Pt–Bi catalysts for the possible use in DFAFCs. Different preparation methods were employed to adapt the properties of Pt. Each method will be emphasized for its advantage and discussed in terms of its limitations, based on the physicochemical and electrochemical characterizations of the catalysts in order to explain the mechanism of action of bismuth added to platinum, the importance of surface composition and surface morphology for the reaction of formic acid oxidation.

2. BULK CATALYSTS FOR ELECTRO-OXIDATION OF FORMIC ACID

2.1. Activity of bulk catalysts

2.1.1. Platinum electrodes

Platinum, the most studied catalyst for formic acid oxidation, is very susceptible to poisoning species, which significantly reduces its catalytic performance at low potentials, as is well known from the literature.[12] Traditional single crystals represent an ideal model surfaces for the oxidation reaction of small organic molecule and are suitable for surface characterization methods both *in situ* and *ex situ*. Studies on single crystal Pt samples showed that formic acid oxidation is a strongly structure sensitive reaction. The most complete study on formic acid structure sensitivity was realized by the Motoo group,[57] using a complete series of stepped surfaces around the stereographic triangle. The studies of this reaction on stepped Pt surfaces were performed in order to clarify how exactly the step density influences this reaction, *i.e.* higher index or stepped surfaces were used to verify the active site assumption, whether low coordination sites are particularly active. The less poisoned surface was Pt(111), as indicated by the low observed hysteresis, but the activity toward formic acid oxidation was low. It should be noted that the presence of defects, especially on (100) steps, considerably increased the activity of a Pt(111) electrode. For example, in order

to achieve higher rates at moderate poisoning, electrodes having 5–6 atoms wide (111) terraces were the best under the experimental conditions used.

The oxidation of formic acid is a structure sensitive reaction, which implies the existence of adsorption steps in the process. In an electrochemical environment, the adsorption processes have to be considered as complex steps since they always involve the competitive adsorption of anions, water and/or hydrogen, which can have different dependences on concentration, and affects the relative rates of dissociative adsorption in a complex way.[21]

These kind of studies are relevant not only from a fundamental point of view but also from a practical one, because in practical applications, the stepped surfaces may be considered as models for surface defects always present on polycrystalline electrodes.

Remembering that the cyclic voltammogram for an as-prepared polycrystalline Pt electrode (Fig. 1a) is described by a region of hydrogen adsorption//desorption ($E < 0.05$ V vs. SCE), separated by a double layer from the region of surface oxide formation ($E > 0.45$ V vs. SCE). The absence of well-developed peaks at an as-prepared Pt polycrystalline electrode in the hydrogen adsorption//desorption region is caused by the employed preparation procedure.

The activity of Pt electrode towards formic acid oxidation is given in Fig. 2a. The cyclic voltammogram shows a well-established feature for formic acid oxidation.[7] In the forward scan, the current slowly increases reaching a plateau at ≈0.25 V vs. SCE followed by an ascending current starting at 0.5 V vs. SCE, which attains a maximum at ≈0.62 V vs. SCE. Such behavior could be explained considering the dual path mechanism, $i.e.$, dehydrogenation assigned as the direct path, based on the oxidation of formate,[28] and dehydration, indirect path, assumes the formation of CO_{ads}, both generate CO_2 as the final reaction product. At low potentials, HCOOH oxidizes through the direct path with the simultaneous formation of CO_{ads}. Increasing coverage with CO_{ads} reduces the Pt sites available for the direct path and current slowly increases reaching a plateau. Subsequent formation of oxygen-containing species on Pt enables the oxidative removal of CO_{ads}, more Pt sites become available for HCOOH oxidation and current increases until Pt oxide, inactive for HCOOH oxidation, is formed, which results in a current peak at ≈0.62 V vs. SCE. In the backward scan, the sharp increase in the HCOOH oxidation current coincides with the reduction of Pt oxide. The currents are much higher than in the forward sweep, because the Pt surface is freed of CO_{ads}.

2.1.2. Effect of Bi adatoms

The addition of foreign metals to Pt surfaces in amounts less than a full monolayer results in modified surface catalytic properties. Therefore, surfaces of bimetallic electrodes often show improved electrocatalytic behavior. It was reported in earlier studies that Bi modification of platinum electrodes could exceptionally increase their reactivity toward HCOOH oxidation, depending on the
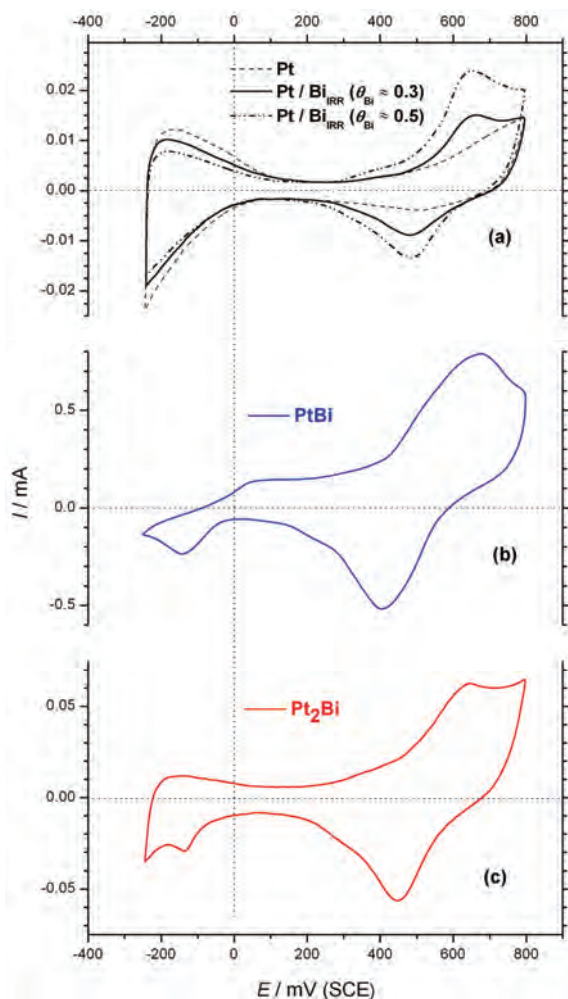
Fig. 1. Basic voltammograms for Pt and Pt/Bi$_{IRR}$ (a), PtBi alloy (b) and Pt$_2$Bi (c) bulk electrodes in 0.1 M H$_2$SO$_4$. Scan rate: 50 mV s^{-1}. ω = 1500 rpm. T = 295 K.

Bi surface coverage.[40,47] Most current studies exploring structure/property/activity relationships based on experimental approaches either use well-defined single crystals as a model or are based on modified noble single crystal surfaces. Feliu and co-workers[58,59] as well as Abruna and co-workers[60,61] reported that bismuth-modified platinum low and high-index single crystal surfaces, which were prepared *via* the under-potential deposition (UPD) process, exhibited extraordinary enhancement in reactivity towards formic acid oxidation.

Irreversibly adsorbed Bi[40,47,51,62] inhibits poison formation simultaneously enhancing dehydrogenation,[51] *i.e.*, this modification is an efficient way to hinder the dehydration path (CO-intermediate pathway) in favor of the direct path.[63] This increased selectivity for dehydrogenation was proposed to be an "ensemble effect"[64,65] in which the adsorbed Bi divides the Pt surface into small domains

where only dehydrogenation can occur. A correlation between ensemble size and formic acid oxidation activity was also established.[66] According to literature data, the activity of Pt catalysts modified with Bi depends on the shape of the Pt nanocrystals,[67] and varies with the size of the particles[68] and the loading of the Pt catalyst.[63]
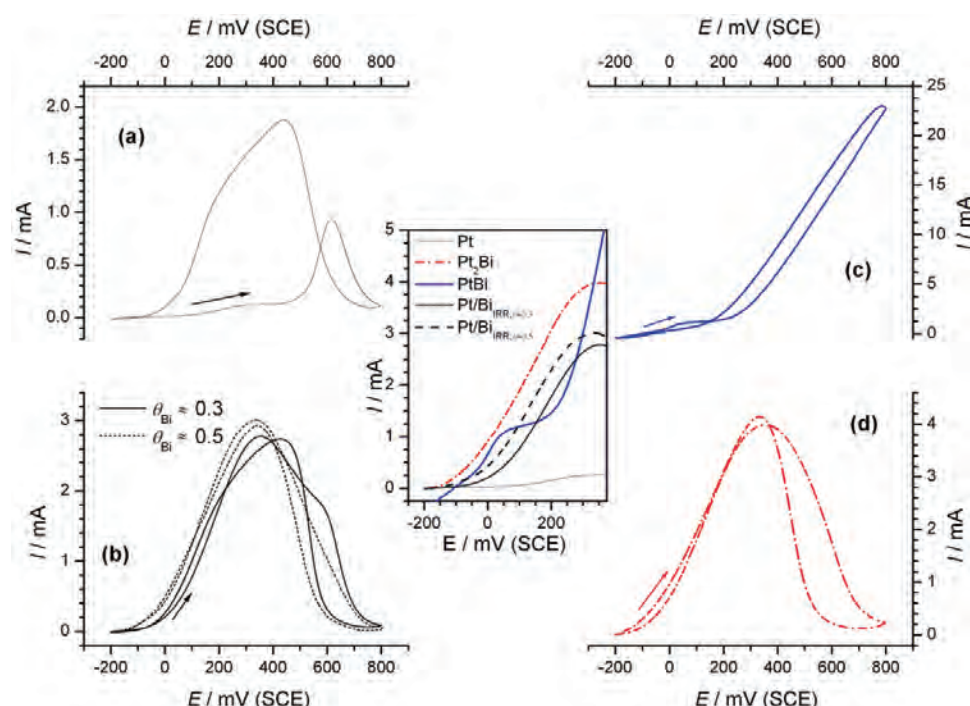
Fig. 2. Cyclic voltammograms for the oxidation of 0.125 M HCOOH in 0.1 M H_2SO_4 solution on: a) Pt, b) Pt/Bi$_{IRR}$, c) PtBi and d) Pt$_2$Bi catalysts. Inset: magnification of the onset potential region. Scan rate: 50 mV s^{-1}. ω = 1500 rpm. T = 295 K.

The beneficial effect of Bi on Pt for this reaction could be due to changes in the Pt–Pt distance that favor the direct route in formic acid oxidation,[69] or to the formation of surface Bi oxides that participate in the oxidation of intermediates,[39,70] or to electronic effects by lowering the electron density of the 5d orbitals, resulting in a considerable decrease of the CO binding strength to Pt,[33,71] or to the ensemble effect creating an appropriate size of Pt domains and thereby providing direct oxidation of HCOOH to CO_2.[48,64] Depending on the preparation of the catalysts and their resulting surface composition, the contribution of the above effects may vary.

In the research performed by our group,[72] the oxidation of formic acid was studied on polycrystalline Pt modified by irreversibly adsorbed Bi (Pt/Bi$_{IRR}$) (Fig. 2b). The experiments were realized without Bi cations in solution, as

opposed to modification by an UPD metal, thereby avoiding competition between adsorption/reaction steps of the reactant and modifier. The results were contrasted to pure Pt (Fig. 2a). Modification of the Pt electrode was performed at the open circuit potential, as described elsewhere.[65] After modification, the electrode was rinsed with water and transferred into a cell containing supporting electrolyte. The fraction of the sites covered by Bi (denoted $Pt/Bi_{IRR;\theta}$) was estimated from the decrease in the charge for desorption of hydrogen, due to the fact that hydrogen does not adsorb on Bi,[73] *i.e.*, only the Pt sites not blocked by Bi were available for hydrogen adsorption. In order to avoid Bi dissolution, the anodic potential limit was set at 0.5 V *vs*. SCE, since it was established that the initial amount of Bi was almost completely retained when the upper potential limit was fixed below 0.75 V *vs*. RHE.[74] This finding is in agreement with that reported using electrochemical quartz crystal microbalance (EQCM) analysis of the Bi oxidation mechanism on smooth Pt electrodes.[75]

The activities of Pt/Bi_{IRR} and Pt electrodes towards formic acid oxidation are compared in Fig. 2a and b and the results showed that the onset potential for the reaction on the Pt/Bi_{IRR} ($\theta_{Bi} \approx 0.3$) was about 0.1 V less positive than on the Pt electrode. The current reached a peak that corresponded to the oxidation of HCOOH to CO_2 *via* the direct path, occurring on Pt sites that were not blocked by the poisoning CO_{ads} species. On the descending part of the curve, a shoulder appeared at almost the same potential as the peak on the curve for the pure Pt electrode, which arises from the HCOOH oxidation on the sites being freed by CO_{ads} oxidation. Thus, HCOOH oxidation on $Pt/Bi_{IRR;\theta\approx0.3}$ proceeded predominantly by the dehydrogenation path with some minor degree of dehydratation also occurring.

HCOOH oxidation was also tested on a Pt/Bi_{IRR} electrode with larger coverage by Bi ($\theta_{Bi} \approx 0.5$). Bell-shaped voltammogram clearly suggests that oxidation of HCOOH on this electrode proceeds through dehydrogenation path. It is noticeable that the dehydration path is completely suppressed. The increased selectivity toward the dehydrogenation path on Pt/Bi_{IRR} compared to Pt was mainly the result of an ensemble effect caused by Bi reducing the continuous Pt sites necessary for dehydration. Nevertheless, the ensemble effect on the Pt/Bi_{IRR} catalyst was enabled by adsorbed Bi, which practically had no influence on the neighboring free Pt atoms.

2.1.3. PtBi ordered intermetallic compounds

Recently, Abruna and co-workers[42,43,45,69] studied the electro-oxidation of formic acid on the surface of ordered intermetallic compounds PtBi and $PtBi_2$. The choice of PtBi was based on extensive earlier studies in which the enhanced activity of Pt surfaces modified with irreversibly adsorbed Bi adlayers toward the oxidation of formic acid was established.[40,60–62]

Intermetallics are binary or multi-elemental metallic compounds that, since they have well-defined crystalline structures, offer predictable control over structural, geometric, and electronic effects in a manner that is not available when disordered alloys are used. In principle, the electronic and atomic structures, both of which are well known to be important parameters for electrocatalytic activity, can be significantly controlled. As the order in intermetallic phases arises from the high enthalpy of mixing, a high chemical and structural stability could be expected. Therefore, in contrast to disordered alloys, all Pt (and Bi) atoms on the surface of an ordered intermetallic phase have the same local geometry and thus, the same activity.

The results obtained in these studies relating to formic acid oxidation indicated that the PtBi ordered intermetallic phase has properties and reactivity that are dramatically different from those of bare platinum surfaces. Especially, the onset potential for the electrocatalytic oxidation of formic acid is significantly shifted (by over 300 mV) to more negative values and the current density (at a given potential) is significantly enhanced when compared to pure Pt. Moreover, PtBi displayed virtual immunity to CO poisoning.[69] Oana *et al.*[76] found for the intermetallic structures that the susceptibility for CO adsorption on Pt was drastically reduced on $PtBi_2$ and PtBi surfaces, with respect to Pt, due to an increase in the Fermi level of the system induced by Bi.

According to Abruna and co-workers,[45,69] the origin of the catalytic activity was related to electronic effects enhancing the affinity of PtBi for formic acid adsorption and producing surface oxides at low potentials, as well as to geometric effects that reduces the affinity for CO poisoning. The shift in the onset potential and the increase in the current density are due to electronic effects. In essence, the formation of the PtBi ordered intermetallic results in a charge redistribution (as a first approximation arising from work function differences), which enhances the affinity of PtBi towards formic acid and further gives rise to the formation of surface oxides at much lower potentials. Regarding the geometric effect, contrary to any Pt-based alloy where the Pt–Pt distance for nearest-neighbor Pt atoms is essentially the same as in Pt metal (2.78 Å), in ordered intermetallic compounds, the Pt–Pt distances can be modulated over a range of a factor of 2. For example, in PtBi the Pt–Pt distance in the (001) plane is 4.32 Å. Such distances were expected to diminish significantly CO poisoning, by reducing bridge sites and eliminating 3-fold hollow adsorption sites. However, some electronic effects could also be involved.

Therefore, ordered intermetallic compounds, which were proposed as powerful catalysts for formic acid oxidation,[42–46] not only exhibited greatly enhanced electrocatalytic activity (especially relative to Pt), but they could also serve as model systems to explore structure/composition/property/activity relationships.

2.1.4. PtBi alloys

The fact that formic acid is a good candidate for DFAFCs initiated the study of its oxidation on so-called real catalysts, such as bulk PtBi alloy and two-phase Pt_2Bi catalysts.[39,48,72]

In one of our previous works, formic acid oxidation was investigated on PtBi alloy samples obtained according to the Bi–Pt phase diagram[39] by melting the pure elements under an inert atmosphere in the proportion of Bi to Pt of 1:1, and the alloy was characterized by X-ray photoelectron spectroscopy (XPS) and by X-ray diffraction (XRD) analysis.[39,48]

XPS analysis revealed three chemical states of Bi, *i.e.*, PtBi or Bi(0), Bi_2O_3 and BiO(OH) on the catalyst surface (Table I).[39] These results suggested a model in which the PtBi alloy was covered by a layer of Bi_2O_3 and the very top of this layer contained BiO(OH) species.

TABLE I. XPS analysis of the surface composition of differently treated PtBi 1:1 alloy; BE – the binding energies of the Bi $4f_{7/2}$ excitation; FWHM – the full width at half maximum; take-off angle (90 or 15°) is next to the sample name in brackets[39]

Sample	BE Bi $4f_{7/2}$, eV	FWHM, eV	Approximate composition, %	Species
Polished electrode	157.3	0.9	34.3	Bi–Pt
	158.8	1.42	65.7	Bi^{3+}
Equilibrated at OCP (90°)	157.4	0.9	63.2	Bi–Pt
	158.3	1.6	31.8	Bi^{3+}
	159.6	1.9	4.9	BiO(OH)
Equilibrated at OCP (15°)	157.5	1.0	64.7	Bi–Pt
	158.5	1.6	22.0	Bi^{3+}
	159.5	1.7	13.3	BiO(OH)
Oxidized at 0.8 V *vs*. SCE (90°)	157.5	0.9	43.2	Bi–Pt
	158.5	1.3	44.1	Bi^{3+}
	159.3	1.8	12.6	BiO(OH)
Oxidized at 0.8 V *vs*. SCE (15°)	157.8	1.1	34.4	Bi–Pt
	158.8	1.2	51.8	Bi^{3+}
	159.6	1.3	13.8	BiO(OH)

XRD characterization of the PtBi alloy was performed to determine its phase composition. The diffraction pattern reveals peaks characteristic for hexagonal structure of the PtBi alloy and very small additional maxima that were assigned to traces of platinum cubic phase (≈0.7 wt. %).[48]

Electrochemical characterization showed that PtBi followed the behavior of its constituents.[39] In the potential range up to 0.05 V *vs*. SCE, the electrode activity and the processes involved were determined by the behavior of pure Bi. It was established that the activity of PtBi was highly dependent on the reduction/oxidation of Bi species. Dissolution of Bi, *i.e.*, leaching from the alloy matrix, proceeded all along the anodic potential scan.[39,42] Comparison of the

basic voltammograms for PtBi and Pt (Fig. 1a and b) showed that the deposition/dissolution of Bi completely suppressed hydrogen adsorption/desorption on Pt, as well as that the surface oxidation on PtBi was initiated at significantly lower positive potentials. The fact that adsorption/desorption of hydrogen was completely suppressed on the PtBi surface, as well as absolute inactivity of both the Bi and PtBi surfaces for the adsorption of CO, made determination of the real surface area impossible. Therefore, comparison of activity was given by the geometric surface area.

The voltammograms for the oxidation of formic acid on Pt and PtBi alloy electrodes, given in Fig. 2a and c, respectively, clearly indicated a dependence of the activity on the reduction/oxidation processes of Bi. Oxidation of formic acid does not occur on pure Bi[39,77] and, consequently, does not occur on PtBi covered by Bi. Hence, the beginning of the reaction must be linked to free Pt sites on the PtBi. Relative to Pt, the onset potential on the PtBi electrode was shifted towards negative potentials by more than 0.25 V and the current densities at 0.05 V *vs.* SCE were higher by about two and half orders of magnitude.

The exceptional activity of PtBi is caused by UPD phenomena of Bi on Pt, which was electrochemically detected. Namely, after recording the voltammogram for PtBi, this electrode was replaced with Pt and voltammograms were taken in the supporting solution with and without HCOOH. The voltammetric profiles obtained in the supporting solution indicated an underpotential deposition of Bi on Pt, evidencing that dissolved Bi could be adsorbed on Pt sites as an UPD layer. In the presence of formic acid, voltammogram displayed typical features for formic acid oxidation on a Bi-modified Pt surface,[12] clearly suggesting that this reaction on the PtBi alloy occurs on the Bi modified Pt sites on the PtBi surface and the huge increase in catalytic activity relative to polycrystalline Pt was attributed to UPD phenomena of Bi leached from the alloy matrix and re-adsorbed on Pt.

In addition, based on XPS analysis, it is proposed that some contribution of a bifunctional action, enabled by the presence of hydroxylated Bi species, should be taken into consideration.

Our studies of Pt_2Bi electrode,[48,72] a two-phase material consisting of PtBi alloy and pure Pt, revealed that this is a powerful catalyst for formic acid oxidation. Characterization of the catalyst was realized by XRD spectroscopy (phase composition), STM (surface morphology) and CO_{ads} stripping voltammetry (surface composition).

Comparison of the basic voltammograms of Pt_2Bi electrode and Pt in the potential range up to 0.05 V *vs.* SCE revealed that the presence of Bi suppressed hydrogen adsorption/desorption to a large extent (Fig. 1c). The cathodic peak at approximately –0.1 V *vs.* SCE could be correlated to the reduction of Bi oxide species and adsorbed Bi^{3+}, species formed in the positive going scan.[39,43] Com-

prehensive oxide formation/reduction was presented by the anodic and cathodic peaks that are superimposed over those of Pt oxide formation and reduction, although the peak position that corresponds to oxide reduction on Pt_2Bi was slightly shifted towards negative potentials with respect to Pt, indicating some electronic interaction between Pt and Bi. A similar behavior was reported for smooth polycrystalline Pt electrodes in the presence of Bi(III) ions[78] and for PtBi (1:1) alloy.[39]

The cyclic voltammogram for formic acid oxidation on Pt_2Bi is presented in Fig. 2d. On Pt_2Bi catalyst, formic acid oxidation commenced more than 0.2 V earlier than on Pt. The currents increased reaching a peak with a current ≈30 times higher than the plateau on Pt and than diminished up to the positive potential limit. As Bi does not adsorb formic acid,[39,77] the oxidation of formic acid occurred on pure Pt domains and on Pt atoms on PtBi domains. The bell-shaped voltammogram for formic acid oxidation suggests that the reaction on Pt_2Bi proceeded through the dehydrogenation path with the dehydration path being completely suppressed. Compared to Pt, the high activity of the Pt_2Bi catalyst could be explained by increased selectivity toward the dehydrogenation path caused by an ensemble effect originating from the interruption of continuous Pt sites by Bi atoms.

CO_{ads} stripping voltammetry recorded at Pt_2Bi and Pt[48] demonstrated that onset potential and the peak position at Pt_2Bi were slightly shifted to more negative potentials relative to Pt, indicating the presence of some electronic modification of the Pt surface atoms, capable for CO adsorption, by Bi. Since Bi[74] and PtBi[69] are inactive for CO adsorption, the oxidation of CO occurs only on the Pt domains. Therefore, the charge under the CO_{ads} peak at Pt_2Bi reflecting a process at the surface of the Pt phase was used for determining the contribution of pure Pt in the surface composition of the Pt_2Bi catalyst. The estimated contribution of pure Pt on the Pt_2Bi surface corresponded closely to bulk composition, thus indicating that adsorbed CO also prevents leaching of Bi.

In order to test whether the surface morphology of Pt_2Bi changes during formic acid oxidation, STM measurements were performed before and after the reaction and insignificant changes in the surface morphology and roughness were found. Consequently, it appears that the Pt_2Bi surface became kinetically stabilized due to the competition between the oxidation of formic acid at the electrode/ /solution interface and Bi leaching, *i.e.*, corrosion/oxidation processes of the electrode surface itself.[79] Accordingly, the main reasons for high stability of Pt_2Bi catalyst is the suppression of Bi leaching, as well as inhibition of dehydration path in the reaction of formic acid oxidation.

On the other hand, the lower onset potential for HCOOH oxidation and higher reaction currents on Pt_2Bi alloy compared to both Pt/Bi_{IRR} electrodes were the result of ensembles that were created by alloyed Bi atoms incorporated

into the Pt lattice, causing a shift in the d-band center of the adjacent Pt atoms. Therefore, Bi in the alloy also exhibited an electronic effect, which could enhance the affinity towards HCOOH adsorption and thus increasing the interaction of HCOOH molecules with the catalyst surface.

It was found that all the investigated bimetallic catalysts were more active than Pt with the onset potentials shifted to more negative values and the currents at 0.0 V *vs*. SCE (under steady state conditions) improved by up to two order of magnitude (Table II).

TABLE II. Activity of the respective catalysts at E = 0.0 V (SCE) determined under steady--state conditions

Activity parameter	Catalyst			
	Pt poly	Pt/Bi$_{IRR, \theta \approx 0.3}$	Pt/Bi$_{IRR, \theta \approx 0.5}$	Pt$_2$Bi
j / mA cm^{-2}	0.0038	0.058	0.36	0.48
$j_{Pt_2Bi}/j_{respective\ catalyst}$	127	8.3	1.33	1

Comparison of the results obtained for these different bulk Pt–Bi catalysts indicated that Bi in the alloy and irreversibly adsorbed Bi exhibited different effects on the catalytic activity. This enables distinguishing between the role of the ensemble and electronic effects in the oxidation of formic acid on Pt–Bi electrodes. The electronic effect, existing only on the alloy, contributes to an earlier start of the reaction, while the maximum current originates from an ensemble effect. During potential cycling of the Pt/Bi$_{IRR}$ electrode, Bi was leached from the electrode surface and the ensemble effect was reduced over time, or lost.

2.2. Stability of bulk catalysts

From a practical point of view, long-term stability of the investigated catalysts for the oxidation of formic acid is very important. The stabilities of the Pt–Bi catalysts were tested by chronoamperometric measurements and by prolonged potential cycling in the supporting solution as well as in the supporting solution containing formic acid. The aim of the study was to establish which factors mostly affected the improvement of the oxidation rate of formic acid and the stability of the catalyst. Additionally, a parallel study on a Pt electrode was performed to verify the promotional role of Bi.

Cyclic voltammograms recorded on Pt$_2$Bi catalyst in the formic acid containing electrolyte are shown in Fig. 3. Over the potential cycling up to 0.8 V *vs*. SCE, the activity of Pt$_2$Bi electrode slowly decreased during the first 5–7 cycles reaching values of ≈85 % of the initial currents. After these first few sweeps, the currents remain unchanged with further cycling. On the contrary, the cycling of Pt$_2$Bi in supporting electrolyte led to enhancement of the currents related to the oxidation of Bi species, indicating some surface decomposition caused by Bi leaching/dissolution process (Fig. 3, inset A). It appears, consequently, that sta-

bility of Pt_2Bi during oxidation of formic acid could be induced by the presence of formic acid in the electrolyte.
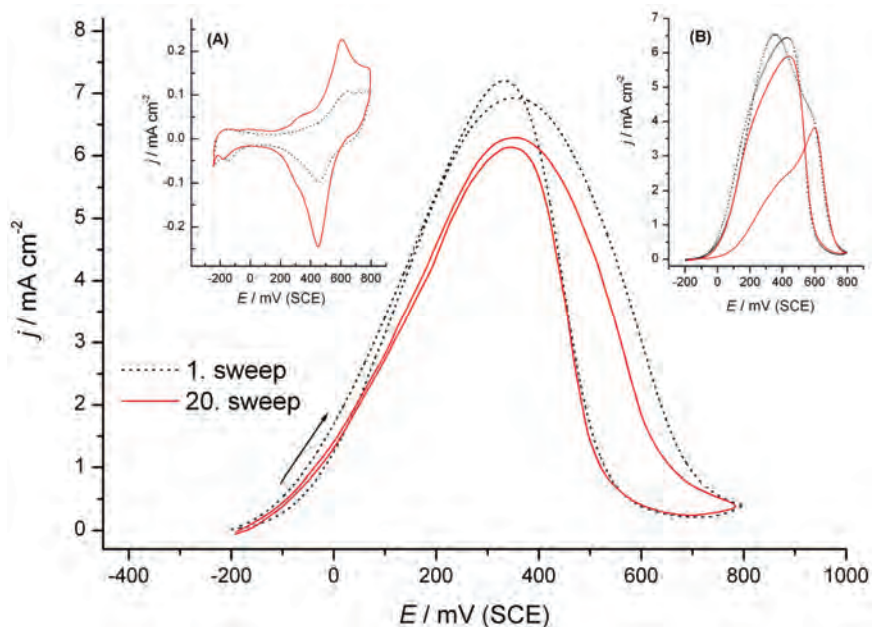
Fig. 3. Cyclic voltammograms (1st and 20th sweep) for the oxidation of 0.125 M HCOOH in 0.1 M H_2SO_4 solution at a Pt_2Bi catalyst. Insets: A) basic voltammograms (1st and 20th sweep) for Pt_2Bi electrode in 0.1 M H_2SO_4 solution and B) cyclic voltammograms (1st and 20th sweep) for the oxidation of 0.125 M HCOOH in 0.1 M H_2SO_4 solution at $Pt/Bi_{IRR; \theta \approx 0.3}$ electrode. Scan rate: 50 mV s^{-1}. $\omega = 1500$ rpm. $T = 295$ K.

Contrary to the Pt_2Bi catalyst, the Pt/Bi_{IRR} electrode shows significant changes with continuous cycling in the solution containing formic acid (Fig. 3, inset B).[72] Repetitive cycling up to 0.8 V *vs*. SCE shifted the onset potential for formic acid oxidation to more positive values, decreased the reaction currents, while anodic peak diminished and a new peak starts to emerge and grow at ≈0.6 V *vs*. SCE. This transformation of the cyclic voltammograms indicated modification of the surface composition due to continuous Bi dissolution. Apparently, re--adsorption of Bi species from the solution was rather low, so the initial voltammogram was never restored, which is in accordance with results obtained for formic acid oxidation on bismuth-coated mesoporous Pt microelectrodes.[80]

To test the assumption that the presence of formic acid stabilizes the catalyst, a Pt_2Bi electrode was subjected to potential cycling in the supporting electrolyte and after 20 cycles the electrode was replaced by a Pt electrode (Fig. 4a). The results of this experiment showed a slightly reduced charge of hydrogen adsorption/desorption indicating underpotential deposition of the previously leached/

/dissolved Bi. The same procedure was repeated in the electrolyte containing formic acid. The voltammogram of formic acid oxidation recorded on Pt in this experiment almost retraced the characteristic profile of pure Pt, suggesting that leaching of Bi was suppressed in the presence of formic acid. This was confirmed by STM measurements performed before and after the oxidation of formic acid, indicating a small difference in roughness and an insignificant change in the surface morphology.[48]
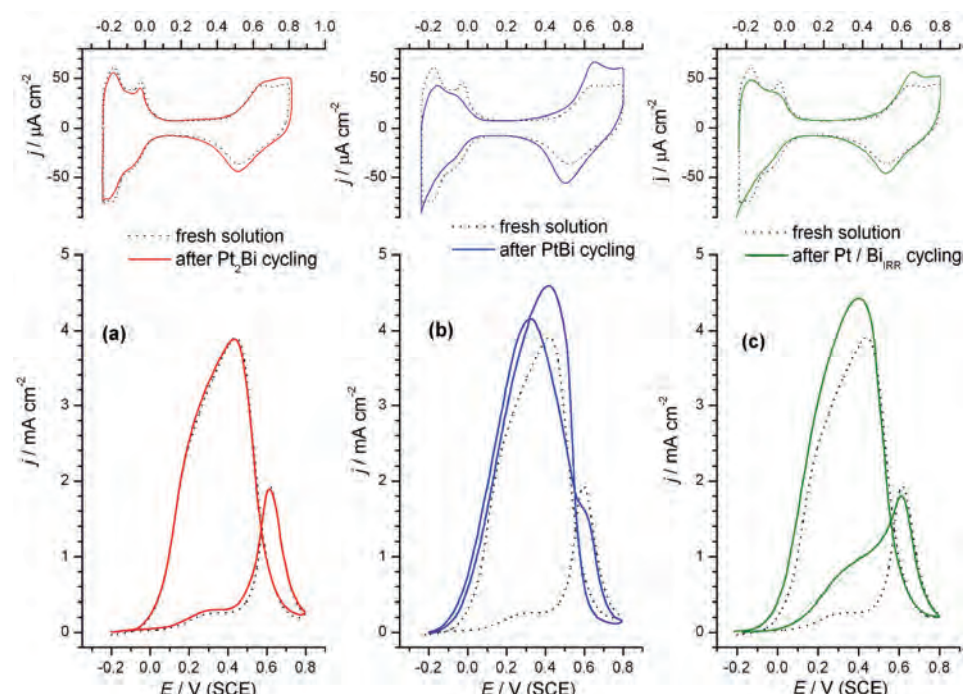
Fig. 4. Comparison of cyclic voltammograms recorded after replacement of: a) Pt_2Bi, b) PtBi and c) Pt/Bi_{IRR} with polycrystalline Pt in 0.1 M H_2SO_4 solution and in 0.125 M HCOOH solution. Scan rate: 50 mV s^{-1}. ω = 1500 rpm. T = 295 K.

It should be noted that the experiment performed after replacing the PtBi alloy with Pt revealed significant Bi leaching under the same experimental conditions, meaning that Pt_2Bi was more resistant to Bi leaching than PtBi (Fig. 4b). The same experiment conducted with the Pt/Bi_{IRR} electrode showed considerable changes in surface composition due to Bi dissolution. Upon prolonged cycling, the electrode surface became enriched in platinum and exhibited a Pt-like electrochemical behavior in acid electrolyte containing formic acid (Fig 4c).

Although Pt/Bi_{IRR} shows remarkable initial activity compared to pure Pt, this electrode was not stabilized by formic acid oxidation, since the desorption of Bi was not suppressed in the presence of formic acid. In addition, the poisoning

effect induced by the dehydration path was not avoided and Bi_{IRR} did not provoke any significant modification of the electronic environment. Therefore, Pt/Bi_{IRR} catalysts are less active than the corresponding alloy.

Chronoamperometric experiments were performed to prove the activity and stability of the investigated catalysts (Fig. 5). Insight into the chronoamperometric curves confirmed the advantage of alloys, *i.e.*, the necessity of alloying Pt with Bi to obtain a catalyst with stable activity.
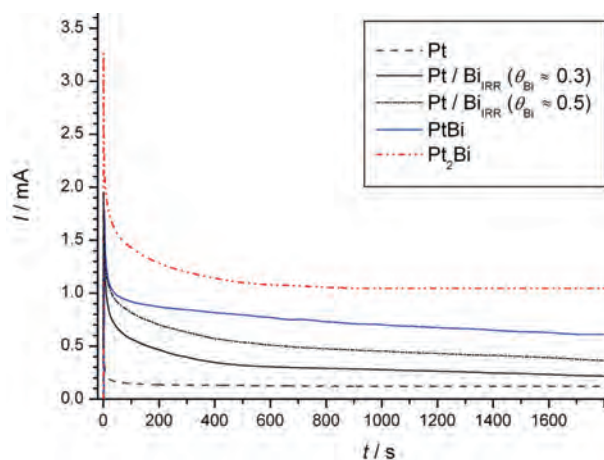
Fig. 5. Chronoamperometric curves for the oxidation of 0.125 M HCOOH at 0.2 V in 0.1 M H_2SO_4 solution on PtBi, Pt_2Bi, Pt/Bi_{IRR} and Pt catalysts. $\omega = 1500$ rpm. $T = 295$ K.

In summary, the main reason for the high stability of the Pt_2Bi catalyst is the inhibition of the dehydration path in the reaction, as well as suppression of Bi leaching in the presence of formic acid, which is specified by a minor change in the surface morphology and roughness.[48,72] Comparing the results obtained for the two types of Pt–Bi catalysts, polycrystalline Pt modified by irreversible adsorbed Bi and for Pt_2Bi catalyst, the role of the ensemble effect and electronic effect in the oxidation of formic acid was distinguished.[48] The electronic effect contributes to a lower onset potential of the reaction, while the maximum current comes from the ensemble effect. During the potential cycling treatment of the Pt/Bi_{IRR} electrode, Bi is dissolved from the electrode surface and the ensemble effect is reduced or lost over time. On the other hand, the high stability of the Pt_2Bi catalyst, confirmed by chronoamperometric experiments, proves an advantage of alloys, i.*e*., the necessity of alloying Pt with Bi to obtain a corrosion resistant catalyst. According to Liu *et al*.,[79] the high stability of the PtBi intermetallic is due to suppressed leaching of Bi in the presence of formic acid because of the effective competition between oxidation of the organic molecule at the electrode surface and the corrosion/oxidation of the electrode surface itself.

3. LOW-LOADING Pt–Bi CATALYSTS

3.1. Activity of low-loading catalysts

The concept of bimetallic mono and multilayer catalysts has received much attention regarding its possibility to reduce the noble metal loading and maintain the activity by replacing the under-layer (or bulk of the catalyst) with a less noble metal. In addition, unlike other bimetallic catalysts where the second metal is either in the form of an adatom or as a surface alloy component, this type of catalyst allows the study of the electronic effect of the second metal under-layer to the noble catalyst over-layer, as the only operating factor.

3.1.1. Pt/GC catalyst

Pt was deposited onto a glassy carbon substrate (Pt/GC) using chronocoulometry at the potential corresponding to Pt limiting current plateau.[70] For the sake of comparison, a Pt/GC electrode was prepared using the same electrochemical procedure and the quantity analogous to one for a bimetallic electrode.

AFM imaging of the Pt deposit on the GC substrate showed randomly distributed clusters (agglomerates), which consisted of spherical nanoparticles with a regular size distribution of 5.7±1.5 nm, as revealed by STM measurements.[70]

Catalytic activity of Pt/GC electrode for formic acid oxidation was examined by potentiodynamic and quasi steady-state measurements. The reaction proceeds through both paths featured by higher first and lower second anodic, indicating lower poisoning of this Pt surface compared to the Pt bulk electrode and a shift in the reaction towards the direct path. STM analysis of this electrode revealed rather small, loosely packed particles with a diameter of ≈5 nm, which should have a lower number of defects and smaller Pt ensembles exposed to the reaction. Such morphology of the particles should lead to a more pronounced direct path in formic acid oxidation. These results are in accordance with a previously reported conclusion[81] that the particle structure, *i.e.*, morphology, rather than the particle size plays a predominant role in the activity of Pt catalysts for formic acid oxidation. The particle structure is directed by particle growth, which is influenced by the support morphology and saturation of the active centers of the support by a metal precursor.

3.1.2. Pt@Bi/GC clusters

Formic acid oxidation was studied on a Pt–Bi catalyst obtained using an unusual approach for the preparation, *i.e.*, modification of the Bi deposit with a Pt overlayer.[70] Briefly, platinum–bismuth deposits on a glassy carbon (GC) rotating disk electrode were prepared by a two-step process. Electrochemical deposition of a controlled amount of Bi was performed at –0.1 V *vs*. SCE onto a mirror-like polished GC substrate. Subsequently, the electrodes were rinsed and transferred to the solution for deposition of Pt. It should be stressed that Pt deposition was realized at a potential of –0.1 V *vs*. SCE, which corresponded to the Pt limiting current plateau, in order to avoid any displacement reaction between Pt

and the less noble Bi and/or GC substrate. For the same reason, the GC and GC/Bi electrodes were immersed and pulled out from the solution for Pt deposition at –0.1 V *vs*. SCE. The electrodes prepared in such manner, denoted as Pt@Bi/GC, were characterized by AFM spectroscopy, which indicated that Pt crystallized preferentially onto the previously formed Bi particles.

Analysis of the current *vs*. time transient responses demonstrated compliance with theoretical curves for progressive 3D nucleation[82] in all three cases, *i.e*., for Bi deposition on a GC substrate, for Pt deposition on Bi/GC surface and Pt deposited alone on a GC support. The density of nuclei at saturation imply not only higher coverage of GC surface by Bi in comparison to Pt, but also that Pt could be better spread over Bi than over GC.

The issue of Bi leaching (dissolution) from PtBi catalysts, and their catalytic effect alongside the HCOOH oxidation is rather unresolved. In order to control Bi dissolution, as prepared electrode were subjected to electrochemical oxidation by slow sweep in the supporting electrolyte within the relevant potential range. Such oxidized electrodes are denoted as "treated Pt@Bi/GC". This procedure led to quantitative oxidation of Bi partially occluded by Pt, but simultaneously to the formation of Bi oxide, accordingly creating a surface composed of Pt and Bi oxide.

The SEM micrographs of the as-prepared and treated Pt@Bi/GC electrodes are shown in Fig. 6a and b, respectively. The SEM image of the as-prepared sample shows well separated, randomly distributed clusters (agglomerates), with size of about 700 nm, which were formed from smaller particles. After electrochemical treatment of Pt@Bi agglomerates, the SEM image showed a decrease in the number and size of the isolated clusters, indicating some dissolution of uncovered/unprotected Bi deposit.

Anodic striping charges indicated that along oxidation procedure about 70% of the quantity of deposited Bi was oxidized (Fig. 6c). The shape of the stripping peak implies the possibility of its deconvolution into two peaks, a sharp one that corresponds to Bi dissolution and a broader one at more positive potential that suits Bi oxide formation.[83] ICP mass spectroscopic analysis of the electrolyte after this electrochemical treatment revealed that Bi was only partially dissolved, which confirmed the possibility of the formation of some Bi oxide species.

These assumptions were confirmed by EDX spectra, which evidenced the presence of Pt, Bi and O, showing a decrease in Bi quantity in the Pt@Bi/GC electrode after the slow sweep and significant increase in the oxygen content, which may be attributed to Bi oxide formation (Fig. 6d). Thus, the composition of the treated Pt@Bi/GC obtained by EDX analysis corresponded qualitatively well to the results obtained by the deconvolution of the stripping peak.

In this way, the prepared electrode exhibited significantly high activity and exceptional stability in comparison to the Pt/GC electrode. Formic acid oxidation

proceeded predominantly through the dehydrogenation path on the treated Pt@Bi/GC electrode, resulting in its high activity. The onset potential was shifted by 150 mV to more negative values and the currents were about 10 times higher than those at the same potential on Pt/GC, as revealed both by potentiodynamic as well as by quasi-steady state measurements (Fig. 7).
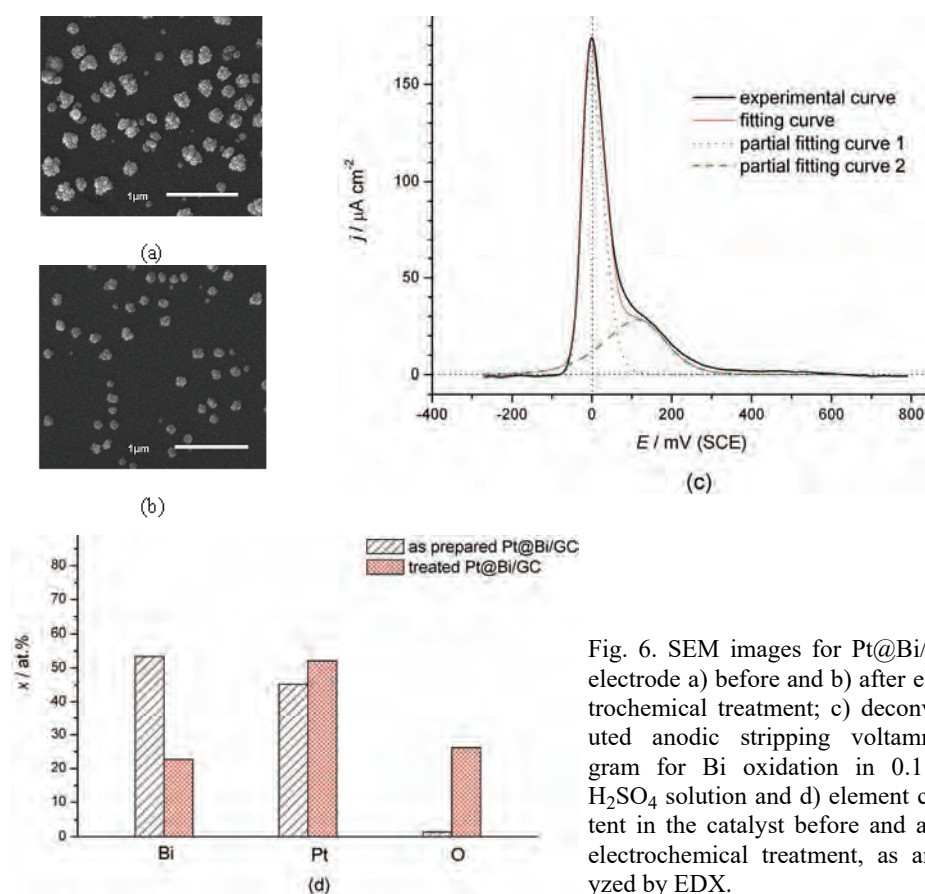
Fig. 6. SEM images for Pt@Bi/GC electrode a) before and b) after electrochemical treatment; c) deconvoluted anodic stripping voltammogram for Bi oxidation in 0.1 M H$_2$SO$_4$ solution and d) element content in the catalyst before and after electrochemical treatment, as analyzed by EDX.

This high activity and increased selectivity toward dehydrogenation is the result of well-balanced ensemble effect originating from the interruption of continuous Pt sites by Bi-oxide domains. The possibility of some electronic effect of non-oxidized Bi under the Pt on the activity of the Pt@Bi/GC electrode could not be excluded. Prolonged cycling and chronoamperometry tests revealed exceptional stability of the catalyst during formic acid oxidation.[70] This low loading Pt-based electrode exhibited activity for the oxidation of formic acid similar to that of bulk Pt$_2$Bi alloy, which has been shown to be one of the best Pt–Bi bimetallic catalysts for the oxidation of formic acid.[48]
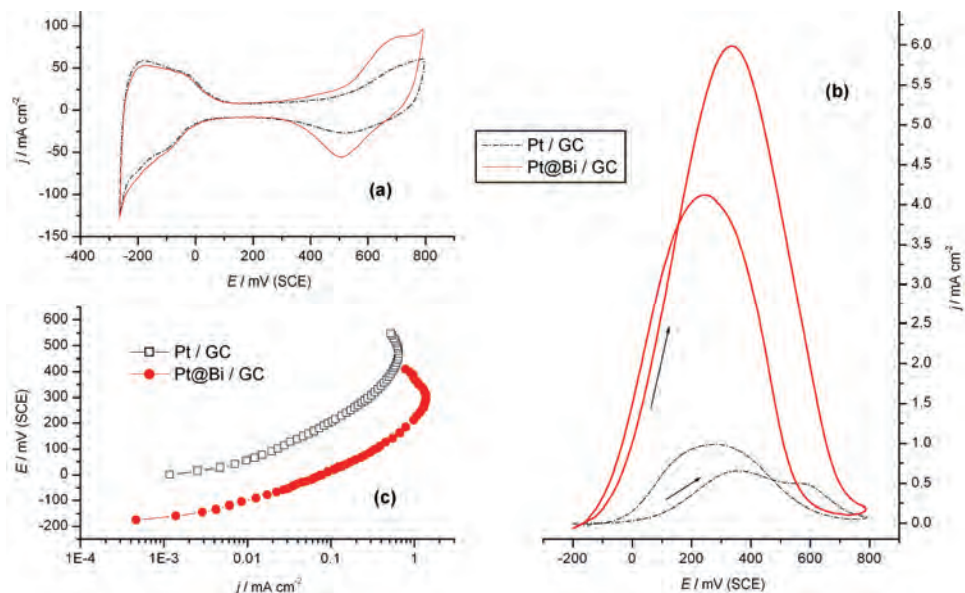
Fig. 7. Initial cyclic voltammograms: a) for treated Pt/GC and treated Pt@Bi/GC electrodes in 0.1 M H_2SO_4 solution and b) for the oxidation of 0.125 M HCOOH in 0.1 M H_2SO_4 solution (scan rate 50 mV s^{-1}); c) corresponding Tafel plots (scan rate 1 mV s^{-1}). ω = 1500 rpm. T = 295 K.

3.2. Stability of low-loading catalysts

As already stated, upon treatment of as prepared Pt@Bi/GC clusters by a slow anodic sweep, a unique bimetallic structure consisting of a Bi core occluded by Pt and a Bi-oxide was obtained. Consideration of the stability of the Pt@Bi//GC catalyst was realized by applying prolonged potential cycling up to 0.8 V *vs*. SCE (hereinafter referred to as a cycling protocol) in supporting electrolyte or in supporting electrolyte containing formic acid and the results were compared with data obtained at a Pt/GC electrode treated in the same manner. An attempt was made to correlate the electrochemical response with the structural features of these two catalysts and to signify the effects that determine the electrode stability in formic acid oxidation.[84]

The difference in activity between Pt@Bi/GC and Pt/GC catalyst after the application of cycling protocol in appropriate electrolyte revealed a complex phenomenology, suggesting that the interplay of several factors, such as nanoparticle size, surface morphology, influence of formic acid and its intermediate CO_{ads}, determines the performance of the catalysts in formic acid oxidation.

Oxidation of HCOOH at the Pt@Bi/GC electrode occurred directly through dehydrogenation to CO_2 enabled by the well-balanced Bi-oxide domains and small Pt ensembles, which resulted in remarkable stability of this catalyst. Seri-

ous formic acid oxidation effectively competes with oxidation of the electrode surface, *i.e*., dissolution of Bi.[79] Leaching of Bi from Pt@Bi/GC in the presence of formic acid was not prevented but highly suppressed due to the source of Bi, *i.e*., Bi core. Since this electrode is composed of a Bi core occluded by Pt and Bi oxide, the morphology of the surface slightly changes and facilitates high activity and stability of this catalyst.

Pt@Bi/GC catalyst exhibited excellent stability during prolonged oxidation of formic acid even above the potentials of Bi dissolution, as revealed by the negligible decrease in activity (Fig. 8a). Such stability of the catalyst was confirmed by quasi-steady state measurements performed on the surface previously treated by potential cycling in supporting electrolyte containing formic acid. The data obtained under slow sweep conditions corroborated the difference in the activities of investigated catalysts, as was found by the potentiodynamic measurements. These measurements also showed high selectivity of this surface toward the dehydrogenation path. Tafel slops of 120 mV obtained at Pt@Bi/GC electrode after 1, 20 and 100 cycles in the supporting electrolyte containing formic acid indicate that the dehydrogenation path in formic acid oxidation proceeded on a surface free of adsorbed CO species. Contrary to the Pt@Bi/GC electrode, which possessed high stability and unusual cycling performance in formic acid oxidation, the activity of the Pt/GC electrode during the cycling protocol in the presence of formic acid in the supporting electrolyte continuously decreased (Fig. 8b). Even more, while at Pt@Bi/GC electrode, the reaction proceeded continuously through the direct path, in the case of Pt/GC, the reaction mechanism changes during cycling. As can be seen from Fig. 8b, in the first cycle, the current raises and reaches a peak that indicates predominant direct oxidation of HCOOH, while the appearance of a well-defined shoulder on the descending part of the curve signifies the indirect path in the reaction as well. As the number of cycles increases, the currents related to dehydrogenation diminish and simultaneously, the well-defined shoulder transforms into a peak, indicating the increased role of the indirect path in the reaction.

This decrease in the activity of Pt/GC electrode could not only be due to a gradual accumulation of reaction residues, *i.e*., poisoning, on the electrode surface, but also to structural adjustments of the platinum nanoparticles as a result of the changes in the potentials during the scanning in acidic solutions, especially in the presence of the organic compound. The Tafel slope obtained for Pt/GC electrode of 140 mV (Fig. 8b) indicates that the reaction occurred on the surface partially covered by CO_{ads}, not only through the dehydrogenation path, but also *via* the dehydration path occurring in parallel. Significant decreases in the currents and increases in the Tafel slope after 20 and 100 cycles indicate retardation of the reaction due to adsorption and accumulation of CO on the surface.
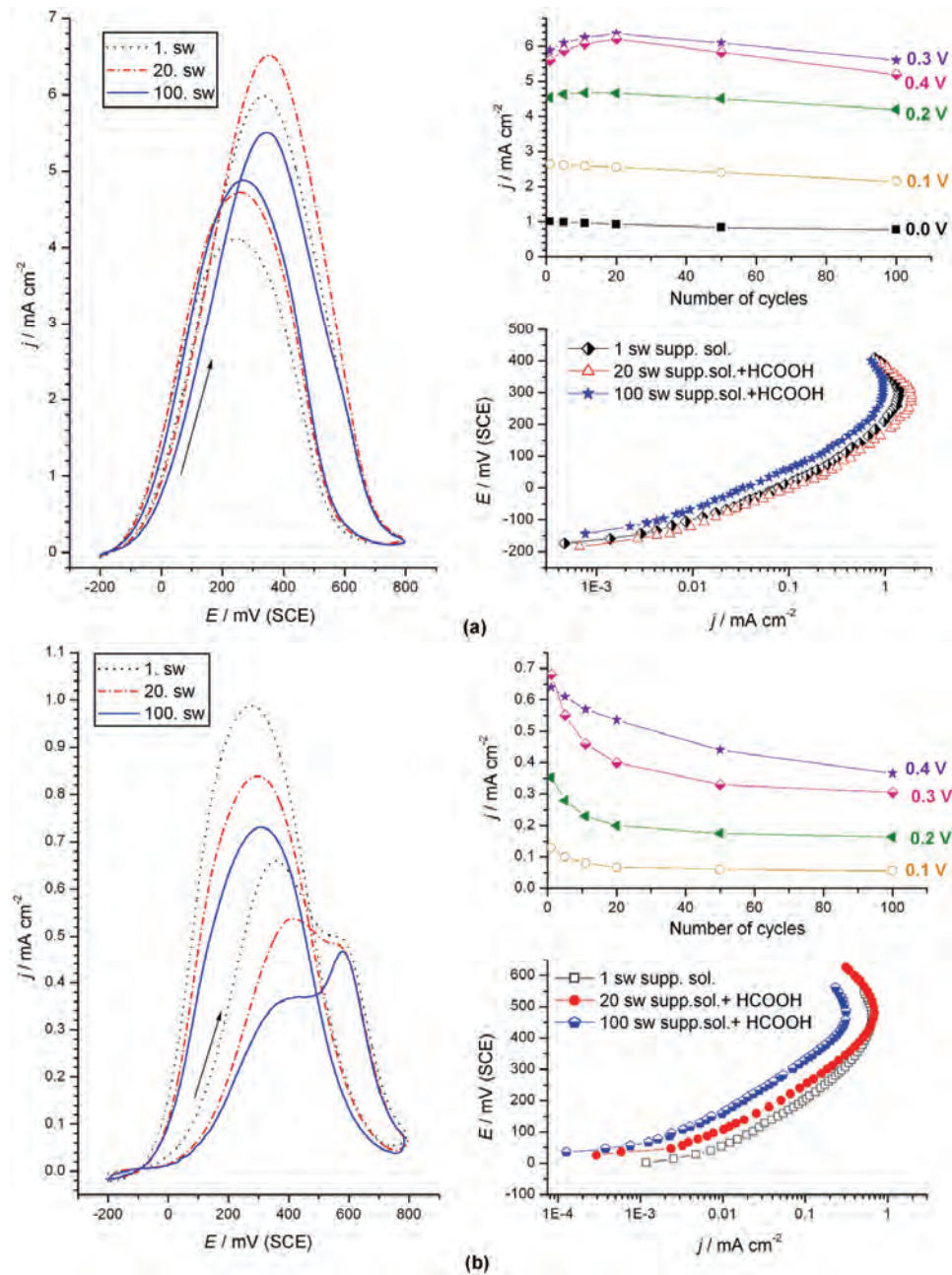
Fig. 8. Cyclic voltammograms for the oxidation of 0.125 M HCOOH in 0.1 M H$_2$SO$_4$ (1st, 20th and 100th sweep at a rate of 50 mV s^{-1}); effect of cycling – plots of current density *vs.* number of cycles and corresponding Tafel plots (scan rate 1 mV s^{-1}) obtained a) on a Pt@Bi/GC electrode and b) on a Pt/GC electrode. ω = 1500 rpm. T = 295 K.

The oxidation of adsorbed CO, usually used for surface characterization, was also employed to determine the electrochemically active surface area (*ECSA*) of a catalyst. The values calculated for Pt@Bi/GC and Pt/GC electrodes revealed that, regardless of the presence or absence of HCOOH in the supporting electrolyte, the *ECSA* of the Pt@Bi/GC electrode increased during the cycling protocol, while the *ECSA* decreased for the Pt/GC electrode (Fig. 9). However, the degree of *ECSA* change upon cycling for both electrodes significantly depended on whether the supporting electrolyte contained HCOOH. The *ECSA* of the Pt@Bi/ /GC electrode slightly increased during this treatment in presence of formic acid due to some Bi dissolution and was confirmed in the experiments with polycrystalline Pt (Fig. 10b).
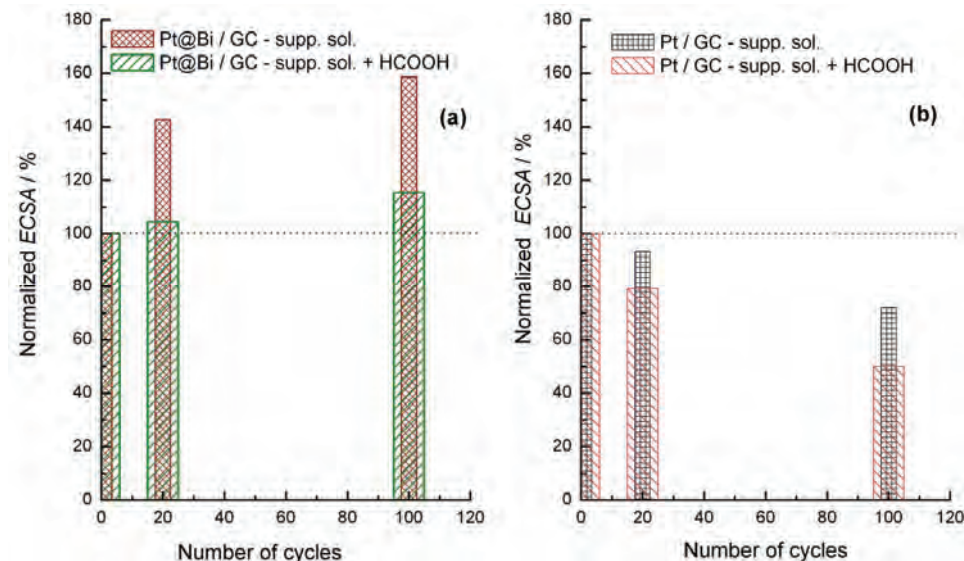
Fig. 9. Normalzed *ECSA* values calculated with CVs upon potential cycling in supporting solution and in supporting solution containing 0.125 M HCOOH on: a) Pt@Bi/GC and b) Pt/GC electrodes. The normalized *ECSA* values were calculated by dividing the *ECSA* value after a certain number of potential cycles by that of the first cycle.

However, when this electrode was cycled in pure supporting electrolyte, the *ECSA* value increased significantly during the treatment (Fig. 9) because of intense leaching of Bi from the electrode, which was confirmed by the experiment with polycrystalline Pt (Figs. 10a and b).

On the other hand, the Pt/GC electrode exhibited completely opposite properties upon similar treatment in the supporting electrolyte with or without formic acid. When this electrode was subjected to potential cycling in the absence of HCOOH, the *ECSA* value decreased slightly (Fig. 9), which was primarily due to the coalescence and agglomeration of the particles. Some negli-

gible dissolution of Pt could also be possible.[85] The result of these phenomena was the formation of defects on the surface that led to some negative shift of the onset and the peak potential of the oxidation of CO_{ads}, which indicates a slight change in the surface morphology had occurred. The consequence of these minor surface alternations was a small decrease in the activity for the oxidation of formic acid.
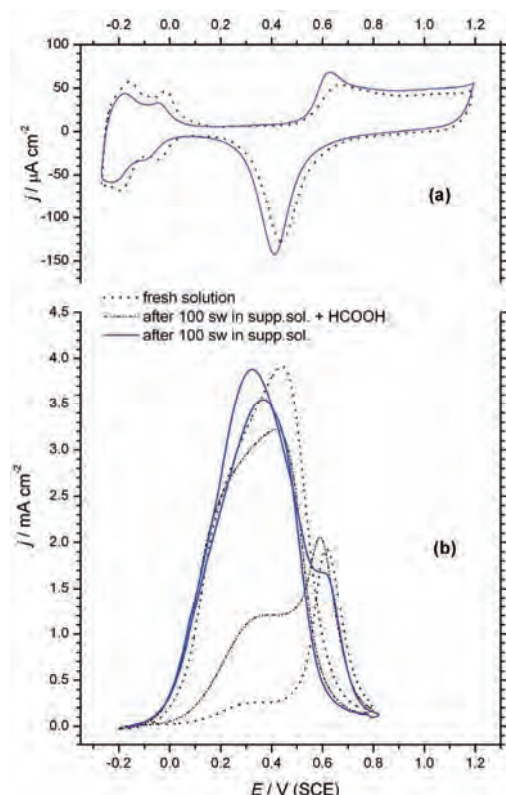
Fig. 10. Cyclic voltammograms recorded a) after replacement of Pt@Bi/GC that has been exposed to cycling protocol with a polycrystalline Pt electrode in 0.1 M H_2SO_4 solution and b) for the oxidation of 0.125 M HCOOH in 0.1 M H_2SO_4. Scan rate: 50 mV s^{-1}. ω = 1500 rpm. T = 295 K.

Furthermore, when the Pt/GC electrode was similarly treated in the presence of HCOOH, the *ECSA* decreased much more (Fig. 9) and a larger shift of the CO_{ads} stripping peaks in the negative direction was observed, indicating to a considerable perturbation in the surface morphology. The consequence of these changes was a significantly lower activity of these surfaces. Considering that formic acid oxidation proceeds on a Pt/GC electrode through both the direct dehydrogenation and the indirect dehydration path, and that during cycling the reaction turns more to the latter one in which CO adsorbs on the surface, it seems that adsorption of CO and its oxidation contribute not only to particle agglomeration but even more to Pt dissolution.

High stability of Pt@Bi/GC electrode is confirmed in chronoamperometric experiment (Fig. 11). Current density recorded on treated Pt@Bi/GC during 1800 s at a constant potential of 0.2 V was again significantly higher than on the Pt/GC electrode. At Pt/GC electrode, the current decayed rapidly reaching a low steady state value within a few minutes. Contrarily, the current decreased slowly at the Pt@Bi/GC electrode and stabilized at a value that was more than 10 times higher than for the other electrode. This experiment also demonstrated the higher stability of the Pt@Bi/GC electrode in comparison to the Pt_2Bi catalyst[48] since under the same conditions, the decrease in the currents for HCOOH oxidation at the Pt@Bi/GC electrode was much lower compared to the decrease registered for the Pt_2Bi catalyst.
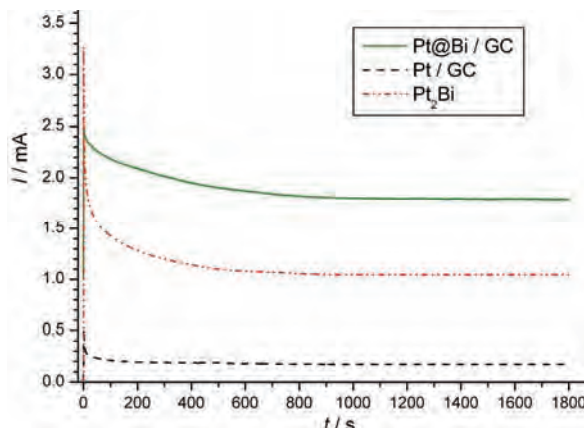
Fig. 11. Chronoamperometric curves for the oxidation of 0.125 M HCOOH in 0.1 M H_2SO_4 solution at 0.2 V on Pt@Bi/GC and Pt/GC electrodes. $\omega = 1500$ rpm. $T = 295$ K.

3.3. Pt(Bi)/GC shell–core catalyst

The bimetallic PtBi electrodes, as catalysts for formic acid oxidation, were examined in terms of obtaining a steady state electrode surface. The catalyst, denoted as Pt(Bi)/GC was produced using a similar methodology of preparation as previously described for the Pt@Bi/GC catalyst, *i.e.*, by sequential deposition of Bi followed by deposition of Pt. In contrast to the experiments to test the stability of the Pt@Bi/GC catalyst, when its activation was performed by two slow sweeps up to 0.8 V *vs*. SCE, the Pt(Bi)/GC electrodes after metal deposition were activated by cycling the potential at a scan rate of 50 mV s^{-1} between hydrogen and oxygen evolution (–0.27 up to 1.2 V *vs*. SCE) in 0.1 M H_2SO_4 solution, prior to use as catalysts for the oxidation of formic acid. Generally, potential cycling is an electrochemical treatment that determines the degree of surface reconstruction and the size of the electrochemically active area. In the case of the Pt(Bi)/GC electrodes, this treatment was applied to quantify the amount of remaining Bi and Bi oxide in order to explain the importance of the composition and morphology of the surface for the reaction of formic acid oxidation.[86]

EDX and ICP-MS analysis, and AFM and electrochemical characterization, revealed that initially unfinished core–shell structures were formed. AFM characterization of the electrode surface indicated that Pt was preferentially deposited on the previously formed Bi particles, but cyclic voltammetry revealed leaching of Bi, meaning that Bi was not completely occluded by Pt.

The Pt(Bi)/GC catalysts were not stable at potentials beyond 0.4 V *vs*. SCE due to Bi leaching/dissolution from the surface, which occurred through the oxidation of the less-noble metal. Electrochemical treatment by potential cycling of the as-prepared electrode (Fig. 12a) led to quantitative oxidation of Bi from the
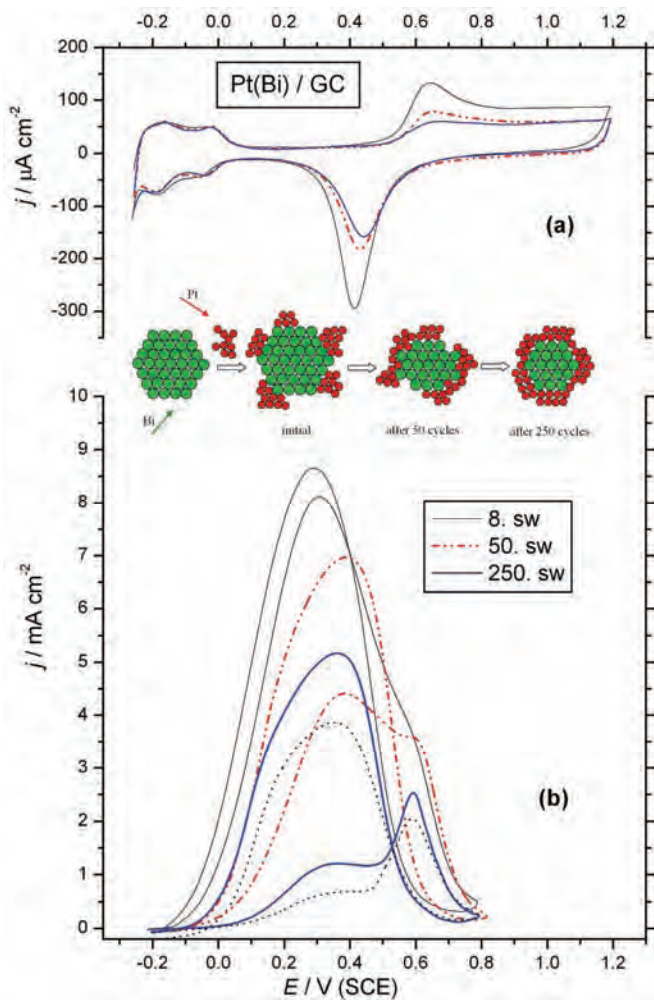
Fig. 12. Cyclic voltammograms recorded on the Pt(Bi)/GC electrode: a) in 0.1 M H_2SO_4 and b) for the oxidation of 0.125 M HCOOH in 0.1 M H_2SO_4 after 8, 50 and 250 cycles. Scan rate: 50 mV s^{-1}. ω = 1500 rpm. T = 295 K.

unprotected core and the simultaneous formation of Bi oxide, consequently creating a shell composed of Pt and Bi-oxide. By prolonged cycling, the amount of surface oxides diminished creating finally a Pt@Bi shell–core structure.

These electrodes exhibit enhanced electrocatalytic activity in formic acid oxidation in comparison to Pt/GC electrode treated in the same manner (Fig. 12b). This behavior could be explained primarily by an ensemble effect induced by surface Bi oxides interrupting the Pt domains, but to some extent, could also be attributed to the influence of the under-lying Bi onto the Pt surface layer, affecting the extent of poison adsorption on the Pt.

Electronic modification of Pt both by surface and sub-surface Bi can play some role as well. Significantly prolonged potential cycling in supporting electrolyte of Pt(Bi)/GC electrodes previously stabilized by Bi oxide led to considerably lower Bi leaching and was accompanied by dissolution and redeposition of Pt, resulting in a Pt shell over a Bi core. The Pt@Bi/GC (shell–core) catalysts, with only Pt in the surface layer exhibit somewhat enhanced activity due to the electronic effect of the remaining under-lying Bi, which depended on the thickness of the Pt layer determined by the quantity of Bi in the core. This observation was confirmed by results obtained at three catalysts with different ratio of Pt and Bi (different underlying thickness of Bi).[86]

In this way, by controlling the thickness of the Bi and Pt layers using electrochemical techniques, it was possible to improve the electrocatalytical properties of Pt(Bi)/GC in HCOOH oxidation and to create a low-loaded Pt-based catalyst with comparable activity to that of the bulk metal alloy.

4. CONCLUSIONS

According to the results presented in this work dealing with the effects influencing the overall formic acid oxidation, it was found that both types of Pt–Bi bimetallic catalysts (bulk and low-loaded deposits on GC) showed superior catalytic activity compared to Pt, in terms of the lower onset potential and higher oxidation current density. Both types of Pt–Bi catalysts were investigated in order to establish how Bi atoms affect the adsorption characteristics of Pt towards formic acid.

It was found that among all the tested Pt–Bi bimetallic bulk catalysts, Pt_2Bi is the most powerful for formic acid oxidation, exhibiting high activity and stability. High activities of the bulk bimetallic catalysts result from the fact that formic acid oxidation proceeds completely through the dehydrogenation path. Increased selectivity toward dehydrogenation is caused by an ensemble effect. The high stability of Pt_2Bi surfaces are induced by the suppression of Bi leaching, as was evidenced by the insignificant changes in the morphology and roughness of the surfaces before and after electrochemical treatment in formic acid containing solution. The results presented indicate that Bi in alloy and irreversibly adsorbed

Bi exhibit different effects on the catalytic activity. Bi in the alloy not only induces an ensemble effect, but also has an electronic effect, which could be the reason for better performance of this catalyst resulting in higher currents and a lower onset potential. The activity of PtBi alloy is caused by UPD phenomena of Bi on Pt, which was electrochemically detected. In addition, based on XPS analysis, it is proposed that the activity of PtBi could also be caused by the bifunctional action of hydroxylated Bi species.

Comparing the results obtained for these bulk Pt–Bi catalysts, the role of the ensemble effect and electronic effect in the oxidation of formic acid could be distinguished. The electronic effect, existing only on the alloy, contributed to the earlier start of the reaction, while the enhanced maximum current originates from the ensemble effect. Thus, the stability of the catalytic activity of Pt–Bi bimetallic electrodes is strongly related to the leaching tolerance of the electrode surface during formic acid oxidation. The leaching tolerance of anodic catalysts was greatly enhanced by the formation of alloy between Pt and Bi, *i.e.*, it is necessary to alloying Pt with Bi to obtain a corrosion stable bulk catalyst.

Electrochemical deposition of low loading Pt layer over Bi deposits on a GC electrode resulted in the formation of approximately spherical clusters of Bi covered by Pt. Treatment of the as-prepared electrode in the relevant potential range and supporting electrolyte leads to quantitative oxidation of Bi partially occluded by Pt, and simultaneously to the formation of Bi oxide, thus creating a surface composed of Pt and Bi-oxide. The so-prepared electrode exhibits higher activity and exceptional stability in comparison to a pure Pt/GC electrode. Formic acid oxidation proceeds predominantly through dehydrogenation path on treated Pt@Bi/GC electrode resulting in its high activity. The increased selectivity toward dehydrogenation is caused by an ensemble effect originating from the interruption of continuous Pt sites by Bi-oxide domains. The possibility of some electronic effect of non-oxidized Bi under the Pt on the activity of Pt@Bi//GC cannot be excluded. Such stability is induced by the stability of the Bi-oxide formed during electrode pre-treatment. This low loading Pt-based electrode exhibits activity for the oxidation of formic acid similar to the activity of bulk Pt_2Bi alloy, which has been shown to be one of the best Pt–Bi bimetallic catalysts for the oxidation of formic acid.

The use of bimetallic compounds as anode catalysts is an effective solution to overcome the problems with stability of the formic acid oxidation current for long-term applications. In the future, the tolerance of both CO poisoning and electrochemical leaching should be considered as the key factors in the development of electrocatalysts for anodic reactions.

И З В О Д

ОКСИДАЦИЈА МРАВЉЕ КИСЕЛИНЕ НА КАТАЛИЗАТОРИМА ПЛАТИНА–БИЗМУТ

КСЕНИЈА Ђ. ПОПОВИЋ и ЈЕЛЕНА Д. ЛОВИЋ

ИХТМ – Центар за електрохемију, Универзитет у Београду, Његошева 12, п. пр. 473, 11000 Београд

Електрохемијска оксидација мравље киселине је предмет истраживања последњих деценија као модел реакција за разумевање механизма оксидације малих органских молекула, као и због њене могуће примене у горивним спреговима. Платина је један од најчешће коришћених катализатора за ову реакцију упркос томе што показује неколико значајних недостатака који спречавају њену широку практичну примену: има високу цену и показује врло изражен пад ефикасности услед тровања површине адсорбованим интермедијерима (CO$_{ads}$). Да би се превазишли ови проблеми и побољшале каталитичка својства катализатора, платина се модификује другим металима, па се стога све више користе биметални платински катализатори. Посебна пажња је усмерена на Bi као модификатор платине. Оксидација мравље киселине испитивана је на два типа Pt–Bi електрода: на масивним електродама и на електродама добијеним таложењем танких филмова на носаче од стакластог угљеника. Оба типа биметалних катализатора показују знатно већу активност и изузетну стабилност у поређењу са чистом Pt. Резултати приказани у овом прегледу значајни су за разумевање механизма електрооксидације мравље киселине на легурама Pt–Bi и Pt модификованој бизмутом, за развој нових анода побољшаних карактеристика за примену у горивим спреговима са мрављом киселином као горивом (DFAFC), као и за синтезу биметалних катализатора са малим садржајем Pt на бази танких филмова. Коришћењем ових биметалних катализатора превазишао би се и проблем стабилности анодног материјала за дугорочну примену у горивним спреговима.

(Примљено 18. марта, ревидирано 24. априла, прихваћено 5. маја 2015)

REFERENCES

1. R. Parsons, T. Van der Noot, *J. Electroanal. Chem.* **257** (1988) 9
2. X. Wang, J.-M. Hu, I.-M. Hsing, *J. Electroanal. Chem.* **562** (2004) 73
3. J. Willsau, J. Heitbaum, *Electrochim. Acta* **31** (1986) 943
4. X. Yu, P. G. Pickup, *J. Power Sources* **182** (2008) 124
5. C. Rice, S. Ha, R. I. Masel, A. Wieckowski, *J. Power Sources* **111** (2002) 83
6. M. W. Breiter, *Electrochim. Acta* **8** (1963) 447
7. T. D. Jarvi, E. M. Stuve, in *Electrocatalysis*, J. Lipkovski, P. N. Ross, Eds., Wiley–VCH, New York, 1998, pp. 75–154
8. T. J. Schmidt, R. J. Behm, B. N. Grgur, N. M. Marković, P. N. Ross, *Langmuir* **16** (2000) 8159
9. J. M. Feliu, E. Herrero, in: *Handbook of Fuel Cells-Fundamentals Technology and Applications*, *Vol. 2: Electrocatalysis*, W. Vielstich, A. Lamm, H.A. Gasteiger (Eds.), John Wiley & Sons Ltd., Chichister, 2003, pp. 625–634
10. S. Park, Y. Xie, M. J. Weaver, *Langmuir* **18** (2002) 5792
11. E. Levia, T. Iwasita, E. Herrero, J. M. Feliu, *Langmuir* **13** (1997) 6287
12. N. M. Marković, P. N. Ross Jr., *Surf. Sci. Rep.* **45** (2002) 117
13. A. Boronat-González, E. Herrero, J. M. Feliu, *J. Solid State Electrochem.* **18** (2014) 1181
14. N. V. Rees, R. G. Compton, *J. Solid State Electrochem.* **15** (2011) 2095
15. A. Capon, R. Parsons, *J. Electroanal. Chem.* **44** (1973) 1
16. A. Capon, R. Parsons, *J. Electroanal. Chem.* **45** (1973) 205

17. J. Clavilier, R. Parsons, R. Durand, C. Lamy, J. M. Leger, *J. Electroanal. Chem.* **124** (1981) 321
18. R. R. Adžić, A. Tripković, V. B. Vešović, *J. Electroanal. Chem.* **204** (1986) 329
19. A. Tripković, K. Popović, *J. Serb. Chem. Soc*. **60** (1995) 297
20. A. Tripković, K. Popović, R. Adžić, *J. Chim. Phys*. **88** (1991) 1635
21. T. Iwasita, X. Xia, E. Herrero, H. D. Liess, *Langmuir* **12** (1996) 4260
22. G. Samjeske, A. Miki, S. Ye, M. Osawa, *J. Phys. Chem., B* **110** (2006) 16559
23. M. F. Mrozek, H. Luo, M. J. Weaver, *Langmuir* **16** (2000) 8463
24. A. Cuesta, G. Cabello, C. Gutierrez, M. Osawa, *Phys. Chem. Chem. Phys.* **13** (2011) 20091
25. C. Lamy, J. M. Leger, *J. Chim. Phys*. **88** (1991) 1649
26. V. Grozovski, F. J. Vidal-Iglesias, E. Herrero, J. M. Feliu, *ChemPhysChem* **12** (2011) 1641
27. H. Okamoto, Y. Numata, T. Gojuki, Y. Mukouyama, *Electrochim. Acta* **116** (2014) 263
28. A. Miki, S. Ye, M. Osawa, *Chem. Commun.* (2002) 1500
29. S.-C. Chang, L.-W. H. Leung, M. J. Weaver, *J. Phys. Chem. B* **94** (1990) 6013
30. P. K. Babu, H. S. Kim, J. H. Chung, E. Oldfield, A. Wieckowski, *J. Phys. Chem. B* **108** (2004) 20228
31. R. Adžić, A. V. Tripković, N. Marković, *J. Electroanal. Chem.* **150** (1983) 79
32. R. R. Adžić, in *Advances in Electrochemistry and Electrochemical Engineering*, H. Gerischer, C. W. Tobias, Eds., Wiley, New York, 1984, p. 159
33. N. de-los-Santos-Alvarez, L. R. Alden, E. Rus, H. Wang, F. J. Di Salvo, H. D. Abruna, *J. Electroanal. Chem.* **626** (2009) 14
34. L. J. Zhang, Z. Y. Wang, D. G. Xia, *J. Alloy. Compd.* **426** (2006) 268
35. W. Liu, J. Huang, *J. Power Sources* **189** (2009) 1012
36. Z. Awaludin, T. Okajima, T. Ohsak, *Electrochem. Comm.* **31** (2013) 100
37. O. Winjobi, Z. Zhang, C. Liang, W. Li, *Electrochim. Acta* **55** (2010) 4217
38. W. Chen, J. Kim, S. Sun, S. Chen, *Langmuir* **23** (2007) 11303
39. A. V. Tripković, K. Dj. Popović, R. M. Stevanović, R. Socha, A. Kowal, *Electrochem. Comm.* **8** (2006) 1492
40. J. Clavilier, A. Fernandez-Vega, J. M. Feliu, A. Aldaz, *J. Electroanal. Chem*. **258** (1989) 89
41. M. Ball, C. A. Lucas, N. M. Marković, B. M. Murphy, P. Steadman, T. J. Schmidt, V. Stamenković, P. N. Ross, *Langmuir* **17** (2001) 5943
42. D. Volpe, E. Casado-Rivera, L. Alden, C. Lind, K. Hagerdon, C. Downie, C. Korzniewski, F. J. Di Salvo, H. D. Abruna, *J. Electrochem. Soc*. **151 (**2004) A971
43. H. Wang, L. Alden, F. J. Di Salvo, H. D. Abruna, *Phys. Chem. Chem. Phys*. **10** (2008) 3739
44. C. Roychowdhury, F. Matsumoto, V. B. Zeldovich, S. C. Warren, P. F. Mutolo, M. J. Ballesteros, U. Wiesner, H. D. Abruna, F. J. Di Salvo, *Chem. Mater.* **18** (2006) 3365
45. E. Casado-Rivera, D. J. Volpe, L. Alden, C. Lind, C. Downie, T. Vazquez-Alvarez, A. C. D. Angelo, F. J. Di Salvo, H. D. Abruna, *J. Am. Chem. Soc*. **126** (2004) 4043
46. J. Sanabria-Chinchilla, H. Abe, F. J. Di Salvo, H. D. Abruna, *Surf. Sci*. **602** (2008) 1830
47. E. Herrero, A. Fernandez-Vega, J. M. Feliu, A. Aldaz, *J. Electroanal. Chem.* **350** (1993) 73
48. J. D. Lović, M. D. Obradović, D. V. Tripković, K. Dj. Popović, V. M. Jovanović, S. Lj. Gojković, A. V. Tripković, *Electrocatalysis* **3** (2012) 346
49. X. Yu, P. G. Pickup, *Electrochim. Acta* **56** (2011) 4037

50. S. Daniele, S. Bergamin, *Electrochem. Comm.* **9** (2007) 1388
51. B.-J. Kim, K. Kwon, C. K. Rhee, J. Han, T.-H. Lim, *Electrochim. Acta* **53** (2008) 7744
52. S. R. Branković, J. X. Wang, R. R. Adžić, *Surf. Sci. Lett.* **747** (2001) L173
53. S. Papadimitriou, S. Armyanov, E. Valova, A. Hubin, O. Steenhaut, E. Pavlidou, G. Kokkinidis, S. Sotiropoulos, *J. Phys. Chem., C* **114** (2010) 5217
54. R. G. Freitas, E. C. Pereira, *Electrochim. Acta* **55** (2010) 7622
55. R. G. Freitas, E. P. Antunes, E. C. Pereira, *Electrochim. Acta* **54** (2009) 1999
56. A. Tegou, S. Papadimitriou, G. Kokkinidis, S. Sotiropoulos, *J. Solid State Electrochem.* **14** (2010) 175
57. S. Motoo, N. Furuya, *Ber. Bunsenges. Phys. Chem.* **91** (1987) 457
58. R. Carbo, R. Albalat, J. Claret, J. M. Feliu, *J. Electroanal. Chem.* **446** (1998) 79
59. J. M. Feliu, A. Fernandez-Vega, J. M. Orts, A. Aldaz, *J. Chim. Phys.* **88** (1991) 1493
60. S. P. E. Smith, H. D. Abruna, *J. Electroanal. Chem.* **467** (1999) 43
61. S. P. E. Smith, K. F. Ben-Dor, H. D. Abruna, *Langmuir* **15** (1999) 7325
62. J. Clavilier, A. Fernandez-Vega, J. M. Feliu, A. Aldaz, *J. Electroanal. Chem.* **261** (1989) 113
63. A. Sáez, E. Expósito, J. Solla-Gullón, V. Montiel, A. Aldaz, *Electrochim. Acta* **63** (2012) 105
64. A. Lopez-Cudero, F. J. Vidal-Iglesias, J. Solla-Gullon, E. Herrero, A. Aldaz, J. M. Feliu, *Phys. Chem. Chem. Phys.* **11** (2009) 416
65. J. Clavilier, J. M. Feliu, A. Aldaz, *J. Electroanal. Chem.* **243** (1988) 419
66. J. Kim, C. K. Rhee, *Electrochem. Comm.* **12** (2010) 1731
67. Q.-S. Chen, Z.-Y. Zhou, F. J. Vidal-Iglesias, J. Solla-Gullon, J. M. Feliu, S.-G. Sun, *J. Am. Chem. Soc.* **133** (2011) 12930
68. C. Jung, T. Zhang, B.-J. Kim, J. Kim, C. K. Rhee, T.-H. Lim, *Bull. Korean Chem. Soc.* **31** (2010) 1543
69. E. Casado-Rivera, Z, Gal, A. C. D. Angelo, C. Lind, F. J. Di Salvo, H. D. Abruna, *ChemPhysChem.* **4** (2003) 193
70. J. D. Lović, S. I. Stevanović, D. V. Tripković, V. V. Tripković, R. M. Stevanović, K. Dj. Popović, V. M. Jovanović, *J. Electrochem. Soc.* **161** (2014) H547
71. L. R. Alden, D. K. Han, F. Matsumoto, H. D. Abruna, F. J. Di Salvo, *Chem. Mater.* **18** (2006) 5591
72. J. D. Lović, D. V. Tripković, K. Dj. Popović, V. M. Jovanović, A. V. Tripković, *J. Serb. Chem. Soc.* **78** (2013) 1189
73. R. Gomez, J. M. Feliu, A. Aldaz, *Electrochim. Acta* **42** (1997) 1675
74. T. J. Schmidt, B. N. Grgur, R. J. Behm, N. M. Marković, P. N. Ross Jr., *Phys. Chem. Chem. Phys.* **2** (2000) 4379
75. S. Uhm, Y. Yun, Y. Tak, J. Lee, *Electrochem. Comm.* **7** (2005) 1375
76. M. Oana, R. Hoffmann, H. D. Abruna, F. J. Di Salvo, *Surf. Sci.* 574 (2005) 1
77. N. Kapur, B. Shan, J. Hyun, L. Wang, S. Yang, J. B. Nicholas, K. Cho, *Mol. Simulat.* **37** (2011) 648
78. V. Pautienienė, L. Tamašauskaitė-Tamašiūnaitė, A. Sudavičius, G. Stalnionis, Z. Jusys, *J. Solid State Electrochem.* **14** (2010) 1675.
79. Y. Liu, M. A. Lowe, F. J. Di Salvo, H. D. Abruna, *J. Phys. Chem., C* **114** (2010) 14929
80. S. Daniele, C. Bragato, D. Battistel, *Electroanalysis* **24** (2012) 759
81. D. Tripković, S. Stevanović, A. Tripković, A. Kowal, V. M. Jovanović, *J. Electrochem. Soc.* **155** (2008) B281

82. F. Gloaguen, J. M. Leger, C. Lamy, A. Marmanna, U. Stimming, R. Vogel, *Electrochim. Acta* **44** (1999) 1805
83. W. S. Li, X. M. Long, J. H. Yan, J. M. Nan, H. Y. Chen, Y. M. Wu, *J. Power Sources* **158** (2006) 1096.
84. J. D. Lović, S. I. Stevanović, D. V. Tripković, A. V. Tripković, R. M. Stevanović, V. M. Jovanović, K. Dj. Popović, *J. Solid State Electrochem* **19** (2015) 2223
85. L. Tang, B. Han, K. Persson, C. Friesen, T. He, K. Sieradzki, G. Ceder, *J. Am. Chem. Soc*. **132** (2010) 596
86. J. D. Lović, S. I. Stevanović, D. V. Tripković, V. M. Jovanović, R. M. Stevanović, A. V. Tripković, K. Dj. Popović, *J. Electroanal. Chem*. **735** (2014) 1.

Journal of the Serbian Chemical Society

Antimicrobial and anticancer evaluation of a novel synthetic tetracyclic system obtained by Dimroth rearrangement

SOBHI M. GOMHA[1]*, IKHLASS M. ABBAS[1], MOHAMED A. A. ELNEAIRY[1],
MAHMOUD M. ELAASSER[2] and BAZADA K. A. MABROUK[1]

[1]*Department of Chemistry, Faculty of Science, Cairo University, Giza, Egypt and* [2]*Regional Center for Mycology and Biotechnology, Al-Azhar University, Cairo, Egypt*

Abstract: A series of pyrido[3′,2′:4,5]thieno[2,3-*e*][1,2,4]triazolo[4,3-*c*]pyrimidines were prepared *via* oxidative cyclization of 4-(2-arylidenehydrazinyl)pyrido[3′,2′:4,5]thieno[3,2-*d*]pyrimidines. Dimroth rearrangement of such a series yielded pyrido[3′,2′:4,5]thieno[2,3-*e*][1,2,4]triazolo[1,5-*c*]pyrimidines. A reaction mechanism was proposed and the products were screened for their antimicrobial and anticancer activities. From the antimicrobial screening results, it could be seen that compounds **8c**, **9f** and **10c** showed excellent activity against Gram-positive bacteria while compounds **10d** and **8c** showed the highest activity against Gram-negative bacteria. The results of the anticancer activities showed that compound **9c** was the most active against HepG-2 and MCF-7 with *IC*$_{50}$ values of 1.19 and 3.46 µg/mL, respectively.

Keywords: hydrazones; oxidative cyclizations; thienopyridines; reaction mechanism.

INTRODUCTION

The synthesis of fused triazolopyrimidine moieties has been described by many investigators and it was shown that these have pronounced biological activities.[1–6] Previous observations revealed that [1,2,4]triazolo[4,3-*c*]pyrimidine derivatives can isomerize under different suitable reaction conditions to the thermodynamically more stable [1,2,4]triazolo[1,5-*c*]pyrimidines.[7–9] This isomerization was first reported by Miller and Rose[10,11] when they treated [1,2,4]triazolo[4,3-*c*]pyrimidine derivatives with an acid, base, or thermally.

In continuation of an ongoing search for new bioactive heterocycles[12–20] based on the above-mentioned research results, the goal of this study was to synthesize some novel pyrido[3′,2′:4,5]thieno[2,3-*e*][1,2,4]triazolo[4,3-*c*]pyramidines not only to study their isomerization to pyrido[3′,2′:4,5]thieno[2,3-*e*][1,2,4]-

1251

triazolo[1,5-*c*]pyrimidines, but also to obtain new compounds which were expected to find notable pharmacological applications.

RESULTS AND DISCUSSION

Chemistry

Detailed analytical and spectral data of the synthesized compounds are given in the Supplementary material to this paper.

Synthesis of compound **4** was achieved through two synthetic pathways. The first pathway involved the conversion of **1**[21] to 7,9-bis(4-methoxyphenyl)-pyrido[3′,2′:4,5]thieno[3,2-*d*]pyrimidin-4(3*H*)-one (**2**) through its cyclization with formic acid (Scheme 1). The IR spectra of **2** displayed no cyano group absorptions.
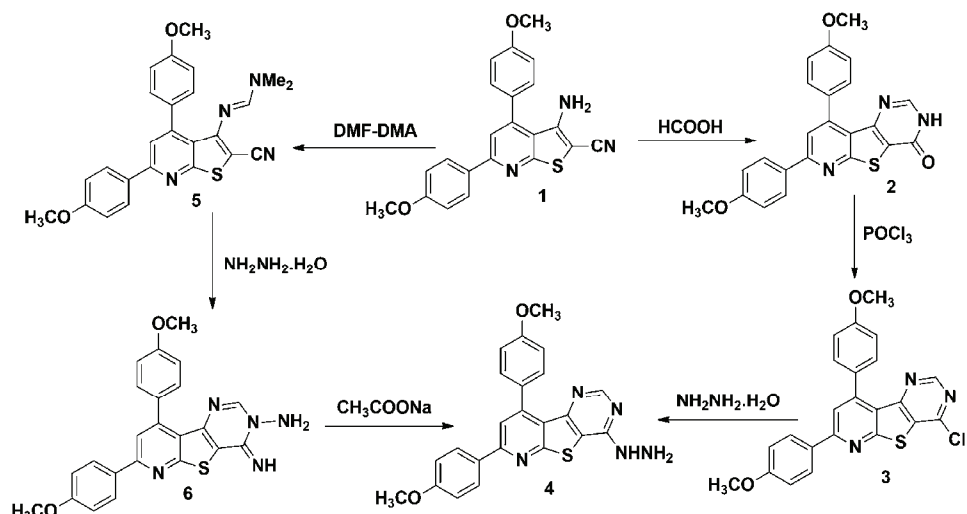
Scheme 1. Synthesis of the starting materials **4** and **6**.

Chlorination of **2** with phosphorus oxychloride under reflux afforded **3**. Nucleophilic displacement of the 4-chloro group in **3** was achieved by heating under reflux with hydrazine hydrate to give compound **4**.[22] The IR spectrum of the titled compound **4** showed the appearance of absorption bands at 3424–3291 cm^{-1} for NH and NH$_2$), its ^{1}H-NMR spectrum showed the presence of characteristic peaks at δ 5.01 and 9.02 ppm of NH$_2$ and NH groups, respectively, while the mass spectrum showed a molecular ion peak at *m/z* 429 corresponding to its molecular formula C$_{23}$H$_{19}$N$_5$O$_2$S. Detailed analytical and spectral data are given in the Supplementary material to this paper. These results confirmed the chemical structure of compound **4** (Scheme 1).

The second pathway was the reaction of **1** with DMF–DMA under reflux for 4 h to give *N'*-(2-cyano-4,6-bis(4-methoxyphenyl)thieno[2,3-*b*]pyridin-3-yl)- -*N*,*N*-dimethylformimidamide (**5**).

IR spectrum of **5** showed an absorption band at 2191 cm^{-1} assigned to the cyano group (CN). Furthermore, its ^{1}H-NMR spectrum showed two singlet signals at 2.64 and 2.87 ppm, which were indicative of the $N(CH_3)_2$ group in this structure. The mass spectrum of **5** showed the molecular ion peak at *m/z* 442 corresponding to its molecular formula $C_{25}H_{22}N_4O_2S$.

Reaction of the latter compound with hydrazine hydrate (99 %) in ethanol afforded **6**. The formation of compound **6** was assumed to proceed *via* the loss of a dimethylamine from **5** followed by intramolecular cyclization into **6.** The IR spectrum of **6** revealed the absence of the cyano group and the appearance of absorption bands at 3472, 3341 and 3220 cm^{-1} for NH and NH_2. Its ^{1}H-NMR spectrum showed three singlets at *δ* 4.92, 9.02 and 8.44 ppm which indicated the presence of NH_2, NH and the pyrimidine proton, respectively.

Isomerization of **6** to its corresponding more thermodynamically stable hydrazine compound **4** was realized by refluxing **6** in dioxane in the presence of sodium acetate through a Dimroth-type rearrangement, which involves a sequence of ring opening and ring closure reactions under basic conditions, as shown in Scheme 2.[23,24]
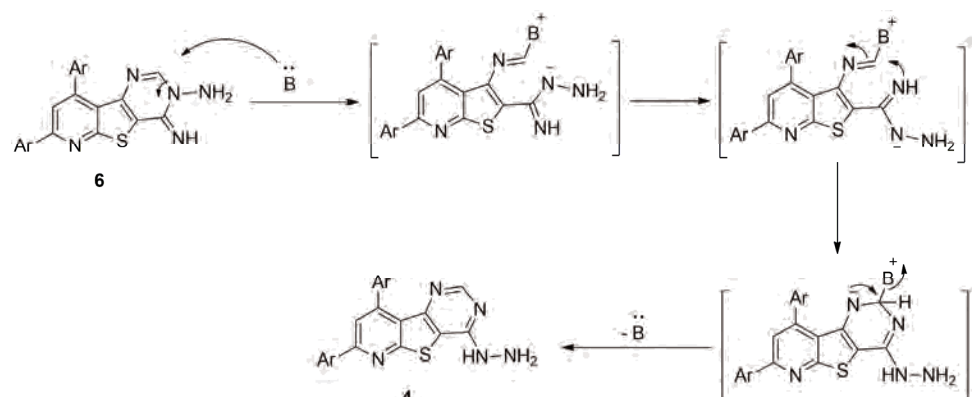
Scheme 2. Mechanism of the rearrangement of compound **6** to **4**.

The identity of compounds **4** and **6** was proven based on their melting points (m.p.), thin layer chromatography (TLC) and spectral data.

Condensation of equimolar quantities of 4-hydrazinylpyrido[3′,2′:4,5]thieno[3,2-*d*]pyrimidine (**4**) with the aldehydes **7a**–**h** gave the corresponding 4-(2- -benzylidenehydrazinyl)-pyrido[3′,2′:4,5]thieno[3,2-*d*]pyrimidines **8a**–**h** (Scheme 3). The structures of the products **8a**–**h** were confirmed based on their elemental analysis and spectral data (see the Supplementary material to this paper).

7,8-11: **a**, R = C₆H₅; **b**, R = 4-MeC₆H₄; **c**, R = 4-MeOC₆H₄; **d**, R = 4-ClC₆H₄; **e**, R = 4-NO₂C₆H₄;
f, R = 2-HOC₆H₄; **g**, R = 2,4-diClC₆H₃; **h**, R = CH₃
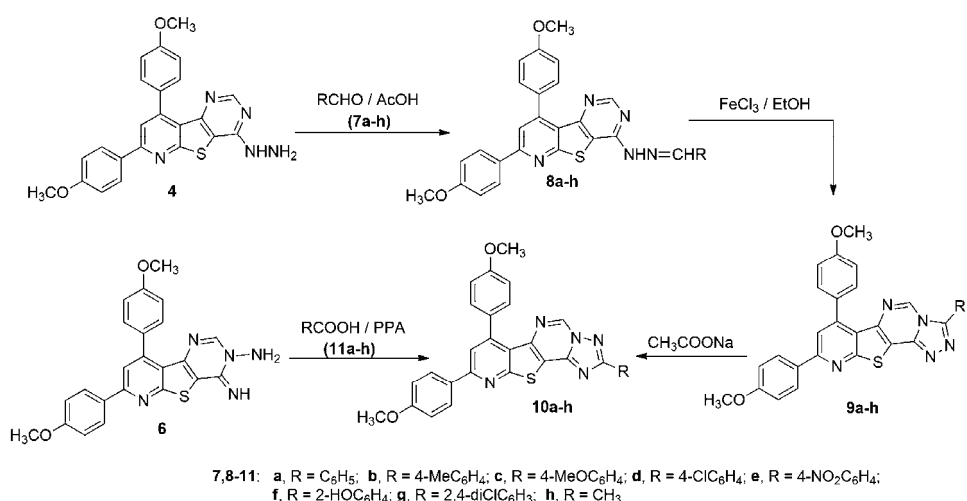
Scheme 3. Synthesis of fused [1,2,4]triazolo[1,5-*c*]pyrimidine derivatives **10a**–**h**.

The IR spectrum of **8a**, taken as a typical example of the prepared series, revealed an absorption band at 3440 cm⁻¹ due to the NH group. Their ¹H-NMR spectra showed the presence of hydrazone (–CH=N–NH–)protons as two singlets at δ 8.82 and 12.16 ppm, respectively (see Supplementary material).

Next, the oxidative cyclization of the hydrazone derivatives **8a**–**h** with iron (III) chloride in ethanol yielded the respective triazolo[4,3-*c*]pyrimidine derivatives **9a**–**h** (Scheme 3).

TLC analysis of the crude products isolated from the foregoing dehydrogenative cyclization method indicated that only one product was formed in each ease. The mass spectra of the isolated products showed high intensity molecular ion peaks at the expected *m/z* values that were less by two than those of the corresponding hydrazone **8**. Their IR spectra showed the disappearance of the NH group. Their ¹H-NMR spectra lacked the characteristic signals for the azomethine (–CH=N–) and the hydrazone (–C=N–NH–) protons present in the spectra of **8**.

The conversion of **8** into **9** is reminiscent of other related oxidative cyclization of aldehyde *N*-heteroarylhydrazones with bromine in acetic acid in the presence of sodium acetate or iron(III) chloride, which have been reported to proceed *via* the generation of the respective nitrilimines, which undergo *in situ* 1,5-electrocyclization to give the respective fused heterocycles.[25–27]

When each of the triazolo[4,3-*c*]pyrimidine derivatives **9a**–**h** was heated in ethanol in the presence of sodium acetate, they isomerized to the thermodynamically more stable triazolo[1,5-*c*]pyrimidine derivatives **10a**–**h** through tandem ring opening and ring closure reactions, as shown in Scheme 4. This rearrangement is consistent with those reported in some earlier reports.[8,28] The structure

elucidation of all compounds **10a**–**h**, which have not been reported, hitherto, was based on their spectral and analytical data (see the Supplementary material). In the mass spectra, all compounds gave the molecular ions at the expected m/z values, which in most cases are not the base peaks. The ^{1}H-NMR spectra were also consistent with their proposed structures.
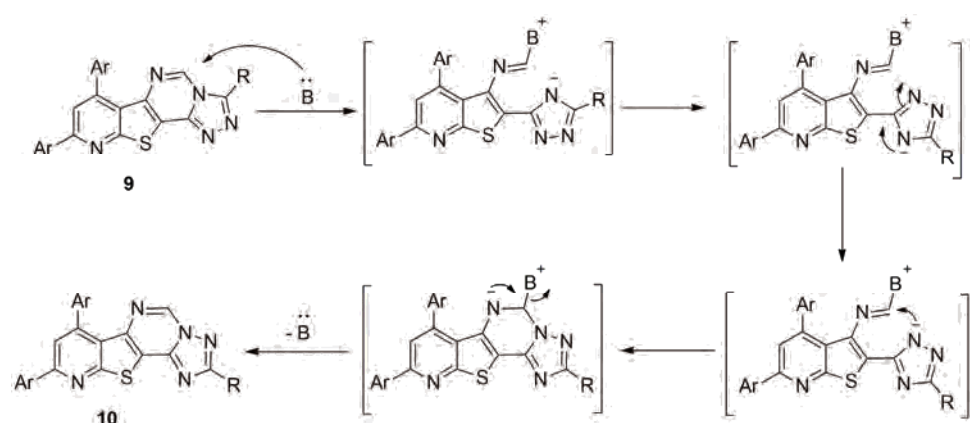
Scheme 4. Mechanism of the rearrangement of compounds **9a**–**h** to **10a**–**h**.

To provide decisive evidence for this rearrangement, the products **10a**–**h** were compared with authentic samples prepared by an alternative synthesis. Thus, treatment of **6** with the respective aromatic carboxylic acids **11a**–**h** in presence of polyphosphoric acid gave products **10a**–**h**, which proved identical in all respects (m.p., mixed m.p., IR and ^{1}H-NMR spectra) with those obtained above from base-catalyzed rearrangement of **9a**–**h** (Scheme 3). This finding confirmed the base-catalyzed rearrangement of **9** into **10** (Scheme 3). The driving force for the observed rearrangement is the fact that the [1,2,4]triazolo[1,5-*c*]pyrimidine ring system is thermodynamically more stable than its isomer, namely [1,2,4]-triazolo[4,3-*c*]pyrimidine.[29]

Antimicrobial evaluation

The synthesized compounds were evaluated for their *in vitro* antimicrobial activity at 5 mg mL^{-1} using the agar well diffusion method against a representative panel of pathogenic strains, *i.e.*, *Staphylococcus aureus* and *Bacillis subtilis* as examples of Gram-positive bacteria as well as *Pseudomonas aeruginosa* and *Escherichia coli* as examples of Gram-negative bacteria while *Aspergillus fumigatus* and *Candida albicans* were used as the fungal strains. DMSO was used for dissolving the tested compounds and showed no inhibition zones, confirming that it has no influence on growth of the tested microorganisms. The results of the testing for antibacterial and antifungal effects summarized in Table I showed that

the new derivatives tested displayed variable *in vitro* antibacterial and antifungal actions. In general, the chemical structure of the whole molecule, comprising the nature of the heterocyclic system as well as the type of the substituted function present in the heterocyclic ring structure, has a pronounced effect on the anti-microbial activity. Most of the substituted analogues produced high inhibitory effects against bacteria, which were comparable to the effects of reference drugs.

TABLE I. *In vitro* antibacterial and antifungal activity of the compounds tested by the well-diffusion agar assay expressed as the diameter (mm) of the inhibition zone in the form of mean ± *SD*

Tested compound	Gram-positive bacteria		Gram-negative bacteria		Fungi	
	B. subtilis	*S. aureus*	*E. coli*	*P. aeruginosa*	*A. fumigatus*	*C. albicans*
8a	6.7±0.4	7.8±0.5	11.8±0.9	9.4±0.7	0	0
8b	6.1±0.3	6.4±0.4	9.2±0.3	7.3±0.6	0	0
8c	22.4±0.7	20.1±0.9	21.9±0.8	18.2±0.7	0	6.9±0.3
8f	6.5±0.4	6.8±0.6	7.1±0.4	6.9±0.5	22.1±0.8	13.3±0.7
9e	6.3±0.3	6.6±0.4	6.2±0.4	6.7±0.6	0	0
9f	20.9±0.6	21.4±0.8	16.9±0.9	12.1±0.7	19.3±0.4	7.4±0.3
9h	17.3±0.7	15.9±0.5	13.7±0.6	8.4±0.5	16.8±0.6	6.7±0.4
10c	19.8±0.7	13.8±0.8	7.2±0.5	6.5±0.4	19.7±0.8	10.6±0.6
10d	14.3±0.6	17.0±0.6	24.8±0.7	19.5±0.8	11.2±0.6	0
10f	18.9±0.5	14.1±0.6	6.7±0.4	6.6±0.5	10.4±0.7	0
10g	0	0	15.4±0.7	13.6±0.7	0	0
Penicillin G	26.4±0.7	24.6±0.6	–	–	–	–
Streptomycin	–	–	26.7±0.9	20.4±0.5	–	–
Amphotericin B	–	–	–	–	25.9±0.8	20.1±0.7

From the screening results, it could be seen that compounds **8c**, **9f** and **10c** showed excellent activity against the Gram positive bacteria and compounds **10f**, **9h** and **10d** showed moderate effects. The highest activity against Gram negative bacteria were exerted by **10d** and **8c**. Selective antimicrobial activity was observed under these screening conditions for compound **10g** against the tested Gram-negative bacteria. Compounds **4**, **6**, **8d**, **8e**, **8g**, **8h**, **9a**–**d**, **9g**, **10a**, **10b**, **10e** and **10h** were completely inactive under these screening conditions. The rest of the compounds showed non-significant activity against the tested bacteria compared with the standard drugs.

Interestingly, compounds **8f, 10c** and **9h** showed promising inhibitory activity against *A. fumigatus* and *C. albicans* compared with amphotericin B as a reference drug.

The mean values of the inhibition zone diameter obtained for these compounds suggested that some of the synthesized compounds possess significant antimicrobial activity against the tested organisms used in these assays, and therefore, the minimum inhibitory concentration (*MIC*) of the active compounds were evaluated *in vitro* using the microdilution technique, while the lowest con-

centration showing no growth was taken as the *MIC*. The fungicides amphotericin B and griseofulvin as well as the bactericides penicillin G and streptomycin were used as reference drugs to evaluate the potency of the tested compounds under the same conditions. The results of the *MIC* determinations reported in Table II showed that compounds **8f**, **9f**, **9h**, **10c**, **10d** and **10f** exhibited broad spectrum action against both Gram-positive and Gram-negative bacteria as well as fungi. Compound **8c** had broad-spectrum antibacterial activity. Compound **9f** reached the highest potency with *MIC* values of 15.6 and 31.25 μg mL^{-1} against the Gram-positive bacteria *B. subtilis* and *S. aureus*, respectively. The highest activity (31.25 μg mL^{-1}) against *E. coli* was detected for compound **10d**. Moreover, significant *MIC* values were determined for compounds **8f** and **9f** against *A. fumigatus* compared with the reference drugs.

TABLE II. Antimicrobial activity expressed as minimum inhibitory concentration (*MIC* / μg mL^{-1}) of the synthesized bioactive compounds compared with standard drugs

Tested compound	Microorganism					
	Gram-positive bacteria		Gram-negative bacteria		Fungi	
	B. subtilis	*S. aureus*	*E. coli*	*P. aeruginosa*	*A. fumigatus*	*C. albicans*
8c	62.5	62.5	62.5	125	–	–
8f	500	500	500	500	31.25	250
9f	15.63	31.25	250	125	31.25	500
9h	125	125	125	250	125	500
10c	62.5	250	250	250	62.5	500
10d	125	125	31.25	125	250	–
10f	125	250	500	500	250	–
Penicillin G	0.03	0.06	–	–	–	–
Streptomycin	–	–	0.03	3.9	–	–
Amphotericin B	–	–	–	–	0.3	2.9
Griseofulvin	–	–	–	–	100	250

Cytotoxic activity

The *in vitro* growth inhibitory activity of the synthesized compounds was investigated in comparison with the well-known standard anticancer drug doxorubicin using the crystal violet colorimetric viability assay. For comparison purposes, the cytotoxicity of imatinib (2-substituted aminopyrimidine derivative; Gleevec®), a standard antitumor drug used for the treatment of gastrointestinal tract tumors, was also evaluated under the same conditions. Data generated were used to plot a dose response curve of which the concentration of test compounds required to kill 50 % of the cell population (*IC*$_{50}$) was determined. The cytotoxic activity was expressed as the mean *IC*$_{50}$ of three independent experiments (Table III) and the results revealed that all the tested compounds showed inhibitory activity to the tumor cell lines in a concentration dependent manner.

The results presented in Table III and Figs. S-1–S-3 of the Supplementary material showed that compounds **9c**, **8h, 9f**, **8g** and **10h** had significant anti-cancer activity against the two tumor cell lines MCF-7 and HepG-2, compared with reference drug imatinib. Interestingly, compound **9c** was the most active against HepG-2 and MCF-7 with IC_{50} values of 1.19 and 3.46 µg mL^{-1}, respectively, comparable to doxorubicin. However, compounds **8a**–**f**, **6**, **9a**, **9e**, **9g**, **9h** and **10b**–**g** were less active than imatinib. Moreover, compound **10a** was almost inactive under the employed screening conditions.

TABLE III. The *in vitro* inhibitory activity of tested compounds against tumor cell lines expressed as IC_{50} values (µg mL^{-1}) ± standard deviation from six replicates

Tested compound	Tumor cell line	
	MCF-7	HepG2
4	15	20
6	> 50	35.5
8a	32.6	40.5
8b	37.7	27.9
8c	34.3	31.1
8d	44.9	49.7
8e	22.9	21.7
8f	38.2	43.4
8g	19.7	10.7
8h	8.67±0.31	2.94±0.12
9a	39.7	40.6
9b	20.1	29.4
9c	3.46±0.24	1.19±0.07
9d	39.9	43.6
9e	24.6	35.1
9f	7.7	17.6
9g	22.5	27.9
9h	48.6	> 50
10a	> 50	> 50
10b	45.6	36.9
10c	29.1	25.4
10d	30.4	35.2
10e	44.3	47.4
10f	36.1	39.3
10g	33.9	41.1
10h	22.4	16.1
Doxorubicin	0.46	0.42
Imatinib	24.6	18.9

EXPERIMENTAL

Chemistry

The melting points were recorded on a Gallenkamp electrothermal apparatus. The structures of the synthesized compounds were confirmed by their spectral (MS, IR and ^{1}H-NMR)

data and elemental analyses. The infrared spectra (KBr) were determined on a Pye Unicam SP-3000 infrared spectrophotometer. The ^{1}H-NMR spectra were obtained on a Varian Gemini 300 spectrometer (300 MHz) in DMSO-d_6 with TMS as the internal standard. The mass spectra were recorded on a GCMS-QP 1000 EX Shimadzu spectrometer. Elemental analyses were realized at the Microanalytical Center, University of Cairo, Giza, Egypt. The biological evaluation of the products was performed at the Regional Center for Mycology and Biotechnology at Al-Azhar University, Cairo, Egypt.

*Synthesis of 7,9-bis(4-methoxyphenyl)pyrido[3',2':4,5]thieno[3,2-*d*]pyrimidin-4(3*H*)-one (2)*. A mixture of 3-amino-4,6-bis(4-methoxyphenyl)thieno[2,3-*b*]pyridine-2-carbonitrile (**1**) (3.87 g, 10 mmol) and formic acid (20 mL) was refluxed for 2 h. The solution was cooled and then poured onto water. The resulting solid was collected and recrystallized from ethanol to give **2** as yellow crystals.

*Synthesis of 4-chloro-7,9-bis(4-methoxyphenyl)pyrido[3',2':4,5]thieno[3,2-*d*]pyrimidine (3)*. A mixture of compound **2** (4.15 g, 10 mmol) and phosphorus oxychloride (20 mL) was heated at reflux for 12 h and the excess of phosphorus oxychloride was removed by distillation under reduced pressure. The residue was treated with dry benzene (10 mL), the solvent was distilled off under vacuum to remove the last traces of phosphorus oxychloride and the resultant gummy residue was triturated with ice and sodium bicarbonate solution. The thus obtained solid was collected, dried and taken for the next step without any purification.

*Synthesis of 4-hydrazinyl-7,9-bis(4-methoxyphenyl)pyrido[3',2':4,5]thieno[3,2-*d*]pyrimidine (4)*. A mixture of compound **3** (4.33 g, 10 mmol) and hydrazine hydrate (30 mL) was refluxed for 4 h. The reaction mixture was poured onto crushed ice. The thus obtained white solid was filtered, dried and recrystallized from dioxane as white crystals.

*Synthesis of N'-(2-cyano-4,6-bis(4-methoxyphenyl)thieno[2,3-*b]pyridin-3-yl)-N,N-*dimethylformimidamide (5)*. A mixture of compound **1** (3.87 g, 10 mmol) and dimethylformamide dimethylacetal (DMF-DMA) (1.33 mL,10 mmol) in dry dioxane (30 mL) was heated under reflux for 6 h, then allowed to cool and poured into cold water (40 mL). The solid product was collected and recrystallized from ethanol to give **5** as brown crystals.

*Synthesis of 4-imino-7,9-bis(4-methoxyphenyl)pyrido[3',2':4,5]thieno[3,2-*d*]pyrimidin--3(4*H*)-amine (6)*. A mixture of compound **5** (4.42 g, 10 mmol) and hydrazine hydrate (10 mL) in ethanol (30 mL) was refluxed for 3 h, and then allowed to cool. The solid product was collected and recrystallized to give **6** as white crystals.

Preparation of hydrazones 8a–h

General procedure. A mixture of hydrazine **4** (0.858 g, 2 mmol) and the appropriate aldehyde (2 mmol) in acetic acid (30 mL) was heated under reflux for 4 h and then cooled. The mixture was diluted with water and the solid that precipitated was filtered off, washed with water, dried and crystallized from dioxane to give the respective hydrazones **8a**–**h**. The physical constants of the hydrazones **8a**–**h** are listed in the Supplementary material.

*Synthesis of pyrido[3',2':4,5]thieno[2,3-*e]-1,2,4-triazolo[4,3-c]pyrimidines 9a–h*

General procedure. To the appropriate hydrazone **8** (14 mmol) in ethanol (40 mL), a solution of iron(III) chloride (2M, 5 mL) was added. The mixture was refluxed for 20 min, and then left overnight at room temperature. The excess solvent was distilled off under reduced pressure, and solid residue remaining was washed with water several times, dried and finally crystallized from the appropriate solvent to give the respective products **9**. The physical constants of the products **9a**–**h** are given in the Supplementary material.

*Rearrangement of **9a**–**h** to **10a**–**h***

General procedure. To a solution of the appropriate **9a**–**h** (1 mmol) in ethanol (50 mL) was added sodium acetate (0.164 g, 2 mmol) and the mixture was refluxed for 6 h and then cooled. The precipitated solid was filtered off, washed with water and then with ethanol and finally crystallized from dimethylformamide to give pyrido[3′,2′:4,5]thieno[2,3-*e*]-1,2,4-triazolo[1,5-*c*]pyrimidines **10a**–**h**.

*Alternate synthesis of **10a**–**g***

A mixture of **6** (0.429 g, 1 mmol) and polyphosphoric acid (10 mL) was heated to 50–60 °C under stirring. A substituted benzoic acid (1 mmol) was added portionwise. The mixture was then heated at 180–200 °C for 3 h under stirring. After completion of the reaction, the reaction mixture was poured into ice and neutralized with concentrated aqueous ammonia solution. The crude product was filtered, washed with water and recrystallized from DMF to afford a product that was found to be identical in all respects (m.p., mixed m.p. and IR) with product **10a**–**g** but in higher yields.

*Alternate synthesis of **10h***

To a solution of **6** (0.429 g, 1 mmol) in glacial acetic acid (10 mL), acetic anhydride (0.204 g, 2 mmol) was added and the mixture was refluxed for 2 h. After refluxing, the reaction mixture was cooled and poured into ice-cold water. The solid product that was formed was collected by filtration and crystallized from DMF to give a product that was identical in all respects with **10h** prepared from the rearrangement of **9h**.

Antimicrobial activity assay

The preliminary antimicrobial activity was investigated on a dozen of the newly synthesized compounds in order to increase the selectivity of these derivatives towards the test microorganisms. All microbial strains were provided from culture collection of the Regional Center for Mycology and Biotechnology (RCMB), Al-Azhar University, Cairo, Egypt.

The antimicrobial profile was tested against two Gram-positive bacterial species (*Bacillus subtilis* and *Staphylococcus aureus*), two Gram-negative bacterial species (*Escherichia coli* and *Pseudomonas aeruginosa*) and two fungi (*Aspergillus fumigatus* and *Candida albicans*) using a modified well diffusion method.[30,31] Briefly, 100 μL of the test bacteria/fungi were grown in 10 mL of fresh media Mueller–Hinton and Sabouraud agar (Oxoid, UK), respectively, until they reached a count of approximately 10^8 cells mL^{-1} for the bacteria or 10^5 cells mL^{-1} for the fungi. One hundred μL of microbial suspension was spread onto agar plates corresponding to the broth in which they were maintained and tested for susceptibility by the well diffusion method. One hundred μL of each sample (at 5 mg ml^{-1}) was added to each well (10 mm diameter holes cut in the agar gel). The plates were incubated for 24–48 h at 37 °C (for the bacteria and yeast) and for 48 h at 28 °C (for the filamentous fungi). After incubation, the growth of the microorganism was observed. The plates were performed in triplicate and the resulting inhibition zone diameters were measured in mm and used as criterion for the antimicrobial activity. The size of the clear zone is proportional to the inhibitory action of the compound under investigation. A solvent control (DMSO) was included in every experiment as a negative control. Penicillin G and streptomycin (Sigma–Aldrich, USA) were used as a positive control against the Gram-positive and Gram-negative bacteria, respectively. Amphotericin B (Sigma–Aldrich, USA) was used as a positive control for the fungi.

MIC *determination using the broth microdilution method*. All the newly synthesized compounds were screened *in vitro* for their antibacterial and antifungal activities by the broth dilution method as described by CLSI[32] to determine the lowest concentration inhibiting the

growth of an organism, which was recorded as the *MIC* value. DMSO was used as the diluent. Stock solutions at 1000 μg mL^{-1} were prepared, from which serial dilutions were prepared for screening the tested compounds. Mueller–Hinton broth was used as the nutrient medium to grow and dilute the drug suspensions for the tested bacteria, and Sabouraud dextrose broth was used for fungal nutrition. The inoculum size for test strain was adjusted to 10^8 CFU (colony forming units) per mL by comparing the turbidity. For the broth microdilution test, 50 μL of each microbial suspension in suitable growth medium was added to the wells of a sterile 96-well microtiter plate already containing 50 μL of two-fold serially diluted tested compound. Control wells were prepared with culture medium, microbial suspension only, tested compound only and DMSO in amounts corresponding to the highest quantity present. The contents of each well were mixed on a microplate shaker (Eppendorf, Hamburg, Germany) at 900 rpm for 1 min prior to incubation for 24–48 h under the above-described cultivation conditions. The *MIC* was the lowest concentration where no viability was observed after 24––48 h based on the metabolic activity. To indicate respiratory activity, the presence of color was determined after the addition of 10 μL well^{-1} of TTC (2,3,5-triphenyltetrazolium chloride, Sigma) dissolved in water (20 mg mL^{-1}) and incubation under appropriate cultivation conditions for 30 min in the dark.[33,34] After incubation, the optical density was measured using a Microplate Reader (Sunrise, Tecan, Inc., USA). Positive controls were wells with a microbial suspension in an appropriate growth medium in amounts corresponding to the highest quantity present in the broth microdilution assay. Negative controls were wells with growth medium and a tested compound. All measurements of the *MIC* values were performed in triplicate. Penicillin G and streptomycin (Sigma Aldrich, USA) were used as standard antibacterial while griseofulvin and amphotericin B (Sigma Aldrich, USA) were used as standard antifungal drugs.

Evaluation of the antitumor activity using a viability assay. Human breast carcinoma (MCF-7) and human hepatocellular carcinoma (HepG2) cell lines were obtained from the American Type Culture Collection (ATCC, Rockville, MD, USA). The cells were grown in RPMI-1640 medium supplemented with 10 % inactivated fetal calf serum and 50 μg ml^{-1} gentamicin. The cells were maintained at 37 °C in a humidified atmosphere with 5 % CO_2 and were subcultured two to three times a week.

The potential cytotoxicity of the compounds was evaluated on tumor cells using the method of Gangadevi and Muthumary.[35] The cells were grown as monolayers in growth RPMI-1640. The monolayers of 10^4 cells adhered at the bottom of the wells in a 96-well microtiter plate incubated for 24 h at 37 °C in a humidified incubator with 5 % CO_2. The monolayers were then washed with sterile phosphate-buffered saline (0.01 M, pH 7.2) and simultaneously the cells were treated with 100 μL from different dilutions of the tested sample in fresh maintenance medium and incubated at 37 °C. A control of untreated cells was made in the absence of the tested sample. Positive controls containing the drugs imatinib or doxorubicin were also tested as references for comparison. Six wells were used for each concentration of the test sample. Every 24 h, the cells were observed under an inverted microscope. The number of surviving cells was determined by staining the cells with crystal violet[35,36] followed by cell lysing using 33 % glacial acetic acid and the absorbance at 590 nm was read using a microplate reader (Sunrise, Tecan, Inc, USA) after well mixing. The absorbance values from untreated cells were considered as corresponding to 100 % proliferation.

The number of viable cells was determined using microplate reader as previously mentioned before and the percentage viability was calculated as:

$$\text{Cell viability, \%} = 100\frac{OD_t}{OD_c}$$

where OD_t is the mean optical density of the wells treated with the tested sample and OD_c is the mean optical density of untreated cells. The relation between surviving cells and drug concentration was plotted to obtain the survival curve of each tumor cell line after treatment with a specified compound. The 50 % inhibitory concentration (IC_{50}), the concentration required to cause toxic effects in 50 % of intact cells, was estimated from graphical plots.

CONCLUSIONS

In conclusion, a general and convenient method for the synthesis of novel pyrido[3′,2′:4,5]thieno[2,3-*e*]-1,2,4-triazolo[1,5-*c*]pyrimidine derivatives in moderate to excellent yields was reported herein. The protocol features initial oxidative cyclization of the respective pyrimidinylhydrazones followed by Dimroth rearrangement under basic conditions. The synthesized compounds were evaluated for their *in vitro* antimicrobial activity at 5 mg mL^{-1} against a representative panel of pathogenic strains using the agar well diffusion method and the results indicated that compounds **8c**, **9f**, **10c** and **10d** showed excellent activity against bacteria. In addition, the *in vitro* growth inhibitory activity of the synthesized compounds was investigated in comparison with the well-known anticancer standard drug doxorubicin using the crystal violet colorimetric viability assay and the results indicated that compounds **9c**, **8h**, **9f**, **8g** and **10h** had significant anticancer activity against the two tumor cell lines MCF-7 and HepG-2. Interestingly, compound **9c** was the most active against HepG-2 and MCF-7 with IC_{50} values of 1.19 and 3.46 µg mL^{-1}, respectively.

SUPPLEMENTARY MATERIAL

The analytical and spectral data of the synthesized compounds and *in vitro* inhibitory activities, Figs. S-1–S-3, are available electronically from http://www.shd.org.rs/JSCS/, or from the corresponding author on request.

ИЗВОД
ИСПИТИВАЊЕ АНТИМИКРОБНЕ И АНТИКАНЦЕРСКЕ АКТИВНОСТИ НОВИХ ТЕТРАЦИКЛИЧНИХ СИСТЕМА ДОБИЈЕНИХ ДИМРОТОВИМ ПРЕМЕШТАЊЕМ

SOBHI M. GOMHA[1], IKHLASS M. ABBAS[1], MOHAMED A. A. ELNEAIRY[1], MAHMOUD M. ELAASSER[2] и BAZADA K. A. MABROUK[1]

[1]*Department of Chemistry, Faculty of Science, Cairo University, Giza, Egypt и* [2]*Regional Center for Mycology and Biotechnology, Al-Azhar University, Cairo, Egypt*

Синтетисана је серија деривата пиридо[3',2':4,5]тиено[2,3-*e*]-1,2,4-триазоло[4,3-*c*]-пиримидина оксидативном циклизацијом 4-(2-арилиденхидразинил)пиридо [3',2':4,5]-тиен[3,2-*d*]пиримидина. Добијени интермедијери Димротовим премештањем дају пиридо[3',2':4,5]тиено[2,3-*e*]-1,2,4-триазоло[1,5-*c*]пиримидине. Испитана је антимикробна и антиканцерска активност добијених деривата. На основу добијених резултата једињења **8c**, **9f** и **10c** показују изузетну активност према Грам-позитивним бактеријама, а деривати **10d** и **8c** показују најбољу активност према Грам-негативним бактеријама. Испи-

тивања антиканцерске активности су показала да дериват **9c** показује најбољу активност према HepG-2 и MCF-7, са IC_{50} вредностима 1,19 и 3,46 µg mL^{-1}, редом.

(Примљено 22. децембра 2014, ревидирано 18. фебруара, прихваћено 4. марта 2015)

REFERENCES

1. S. M. Gomha, *Monatsh. Chem.* **140** (2009) 213
2. A. H. Shamroukh, A. E. Rashad, H. S. Ali, F. M. E. Abdel-Megeid, *J. Heterocycl. Chem.* **50** (2013) 758
3. N. Boechat, L. C. S. Pinheiro, T. S. Silva, A. C. C. Aguiar, A. S. Carvalho, M. M. Bastos, C. C. P. Costa, S. Pinheiro, A. C. Pinto, J. S. Mendonça, K. D. B. Dutra, A. L. Valverde, O. A. Santos-Filho, I. P. Ceravolo, A. U. Krettli, *Molecules* **17** (2012) 8285
4. P. G. Baraldi, M. A. Tabrizi, R. Romagnoli, F. Fruttarolo, S. Merighi, K. Varani, S. Gessi, P. A. Borea, *Curr. Med. Chem.* **12** (2005) 1319
5. M. M. Kandeel, A. M. Kamal, E. K. A. Abdelall, H. A. H. Elshemy, *Eur. J. Med. Chem.* **59** (2013) 183
6. P. G. Baraldi, B. Saponaro, M. A. Tabrizi, S. Baraldi, R. Romagnoli, A. R. Moorman, K. Varani, P. A. Borea, D. Petri, *Eur. J. Med. Chem.* **20** (2012) 1046
7. A. S. Shawali, S. M. Gomha, *Tetrahedron* **58** (2002) 8559
8. A. E. Rashad, O. A. Heikal, A. O. H. El-Nezhawy, F. M. E. Abdel-Megeid, *Heteroatom Chem.* **16** (2005) 226
9. A. E. Rashad, M. I. Hegab, R. E. Abdel-Megeid, M. M. Ali, F. M. E. Abdel-Megeid, *Phosphorus Sulfur Silicon Relat. Elem.* **185** (2010) 74
10. G. W. Miller, F. L. Rose, *J. Chem. Soc.* (1963) 5642
11. G. W. Miller, F. L. Rose, *J. Chem. Soc.* (1965) 3357
12. S. M. Gomha, K. D. Khalil, *Molecules* **17** (2012) 9335
13. S. M. Gomha, S. M. Riyadh, I. M. Abbas, M. A. Bauomi, *Heterocycles* **87** (2013) 341
14. S. M. Gomha, H. A. Abdel-Aziz, *Bull. Korean Chem. Soc.* **33** (2012) 2985
15. S. M. Gomha, S. M. Riyadh, *Molecules* **16** (2011) 8244
16. S. M. Gomha, T. M. A. Eldebss, M. M. Abdulla, A. S. Mayhoub, *Eur. J. Med. Chem.* **82** (2014) 472
17. S. M. Gomha, A. S. Shawali, A. O. Abdelhamid, *Turk. J. Chem.* **38** (2014) 865
18. S. M. Gomha, H. A. Abdel-Aziz, *J. Serb. Chem. Soc.* **78** (2013) 1119
19. S. M. Gomha, Kh. D. Khalil, A. M. El-Zanate, S. M. Riyadh, *Heterocycles* **87** (2013) 1109
20. S. M. Gomha, *Int. J. Pharm. Pharm. Sci.* **5** (2013) 42
21. B. Kh. A. Mabrouk, *M.Sc. Thesis*, Cairo University, Egypt, 2012
22. M. Z. A. Badr, A. A. Geies, M. S. Abbady, A. A. Dahy, *Phosphorus Sulfur Silicon Relat. Elem.* **179** (2004) 2581
23. M. I. Hegab, N. A. Hassan, A. E. Rashad, A. A. Fahmy, F. M. E. Abdel-Megeid, *Phosphorus Sulfur Silicon Relat. Elem.* **182** (2007) 1535
24. P. G. Baraldi, H. El-Kashef, A. Farghaly, P. Vanelle, F. Fruttarolo, *Tetrahedron* **60** (2004) 5093
25. A. S. Shawali, H. M. Hassaneen, N. Kh. Shurrab, *Tetrahedron* **64** (2008) 10339
26. M. A. Shaban, A. Z. Nasr, *Adv. Heterocycl. Chem.* **49** (1999) 277
27. A. S. Shawali, H. M. Hassaneen, N. K. Shurrab, *Heterocycles* **75** (2008) 1479
28. B. Abdelfattah, M. M. Kandeel, M. Abdel-Hakeem, Z. M. Fahmy, *J. Chin. Chem. Soc.* **53** (2006) 403

29. C. J. Shisho, M. B. Devani, G. V. Ullas, S. Ananthan, V. S. Bhadi, *J. Heterocycl. Chem.* **18** (1981) 43
30. G. Fischer, *Adv. Heterocycl. Chem.* **57** (1993) 81
31. M. A. Pfaller, L. Burmeister, M. S. Bartlett, M. A. Ghorab, M. G. Rinaldi, *J. Clin. Microbiol.* **26** (1988)1437
32. CLSI, Clinical and Laboratory Standards Institute, Twentieth informational supplement, M100-S22. Wayne, PA, 2012
33. NCCLS, National Committee for Clinical Laboratory Standards, M38-A, Wayne, PA, 2002
34. A. Klančnik, S. Piskernik, B. Jeršek, S. S. Možina, *J. Microbiol. Methods* **81** (2010) 121
35. V. Gangadevi, J. Muthumary, *Afr. J. Biotechnol.* **6** (2007) 1382
36. T. Mosmann, *J. Immunol. Methods* **65** (1983) 55.

Antimicrobial and anticancer evaluation of a novel synthetic tetracyclic system obtained by Dimroth rearrangement

SOBHI M. GOMHA[1]*, IKHLASS M. ABBAS[1], MOHAMED A. A. ELNEAIRY[1],
MAHMOUD M. ELAASSER[2] and BAZADA K. A. MABROUK[1]

[1]*Department of Chemistry, Faculty of Science, Cairo University, Giza, Egypt and* [2]*Regional Center for Mycology and Biotechnology, Al-Azhar University, Cairo, Egypt*

ANALYTICAL AND SPECTRAL DATA OF THE SYNTHESIZED COMPOUNDS

7,9-Bis(4-methoxyphenyl)pyrido[3',2':4,5]thieno[3,2-d]pyrimidin-4(3H)-one (2). Yield: 70 %; m.p.: 224 °C; Anal. Calcd. for $C_{23}H_{17}N_3O_3S$ (FW: 415.46): C, 66.49; H, 4.12; N, 10.11 %. Found: C, 66.27; H, 4.29; N, 10.03 %. IR (KBr, cm^{-1}): 3154 (NH), 1664 (C=O), 1600 (C=N); ^{1}H-NMR (300 MHz, DMSO-d_6, δ / ppm): = 3.83 (3H, *s*, OCH$_3$), 3.86 (3H, *s*, OCH$_3$), 7.03–8.27 (8H, *m*, Ar-H), 7.88 (1H, *s*, pyridine-H5), 8.12 (1H, *s*, pyrimidine-H2), 12.79 (1H, *s*, D$_2$O exchangeable, NH); MS (70 eV, *m/z* (relative abundance, %)): 415 (M$^+$, 100), 256 (16), 129 (29), 57 (85).

4-Hydrazinyl-7,9-bis(4-methoxyphenyl)pyrido[3',2':4,5]thieno[3,2-d]pyrimidine (4). Yield: 71 %; m.p.: 240–242 °C; Anal. Calcd. for $C_{23}H_{19}N_5O_2S$ (FW: 429.49): C, 64.32; H, 4.46; N, 16.31 %. Found: C, 64.18; H, 4.31; N, 16.10 %; IR (KBr, cm^{-1}): 3424–3291 (NH$_2$ and NH), 1605 (C=N); ^{1}H-NMR (300 MHz, DMSO-d_6 δ / ppm): 3.85 (6H, *s*, 2OCH$_3$), 5.01 (2H, *s*, NH$_2$, D$_2$O exchangeable), 7.06–8.35 (10H, *m*, Ar-H, pyridine-H5 and pyrimidine-H2), 9.02 (1H, *s*, NH, D$_2$O exchangeable); MS (70 eV, *m/z* (relative abundance, %)): 429 (M$^+$, 16), 358 (100), 285 (60), 57 (22).

N'-(2-Cyano-4,6-bis(4-methoxyphenyl)thieno[2,3-b]pyridin-3-yl)-N,N-dimethylformimidamide (5). Yield: 72 %; m.p.: 200–202 °C; Anal. Calcd. for $C_{25}H_{22}N_4O_2S$ (FW: 442.53): C, 67.85; H, 5.01; N, 12.66 %. Found: C, 67.69; H, 5.13; N, 12.48 %; IR (KBr, cm^{-1}): 3097 (=C–H), 2924 (C–H), 2191 (CN), 1627(C=N); ^{1}H-NMR (300 MHz, DMSO-d_6, δ / ppm): 2.64 (6H, *s*, N(CH$_3$)$_2$), 2.87 (6H, *s*, N(CH$_3$)$_2$), 3.88 (3H, *s*, OCH$_3$), 3.89 (3H, *s*, OCH$_3$), 6.94–8.10 (9H,

---

* Corresponding author. E-mail: s.m.gomha@hotmail.com

m, Ar-H and CH=N), 7.57 (1H, *s*, pyridine-H5); MS (70 eV, *m/z* (relative abundance, %)): 443 (M$^+$+1, 30), 442 (M$^+$, 100), 383 (54), 221 (7), 59 (49).

*4-Imino-7,9-bis(4-methoxyphenyl)pyrido[3',2':4,5]thieno[3,2-d]pyrimidin--3(4*H)*-amine (6)*. Yield: 74 %; m.p.: 264–266 °C; Anal. Calcd. for C$_{23}$H$_{19}$N$_5$O$_2$S (FW: 429.49): C, 64.32; H, 4.46; N, 16.31 %. Found: C, 64.20; H, 4.34; N, 16.17 %; IR (KBr, cm^{-1}): 3472, 3341, 3220 (NH$_2$ and NH), 1605 (C=N); ^{1}H-NMR (300 MHz, DMSO-*d*$_6$, *δ* / ppm): 3.82 (3H, *s*, OCH$_3$), 3.85 (3H, *s*, OCH$_3$), 4.92 (2H, *s*, NH$_2$, D$_2$O exchangeable), 7.02–8.23 (9H, *m*, Ar-H and pyridine-H5), 8.44 (1H, *s*, pyrimidine-H2), 9.02 (1H, *s*, NH, D$_2$O exchangeable); MS (70 eV, *m/z* (relative abundance, %)): 429 (M$^+$, 97), 399 (100), 355 (23), 192 (22), 58 (7).

Benzaldehyde, 2-(7,9-bis(4-methoxyphenyl)pyrido[3',2':4,5]thieno[3,2-d]-pyrimidin-4-yl)hydrazone (8a). Yield: 78 %; white solid; m.p.: 312–314 °C; Anal. calcd. for C$_{30}$H$_{23}$N$_5$O$_2$S (FW: 517.60): C, 69.61; H, 4.48; N, 13.53%. Found: C, 69.48; H, 4.32; N, 13.27 %; IR (KBr, cm^{-1}): 3440 (NH), 3049 (=CH), 2932 (CH), 1605 (C=N); ^{1}H-NMR (300 MHz, DMSO-*d*$_6$, *δ* / ppm): 3.84 (6H, *s*, 2OCH$_3$), 7.04–7.65 (13H, *m*, Ar-H), 7.88 (1H, *s*, pyridine-H2), 8.22 (1H, *s*, pyrimidine-H5), 8.82 (1H, *s*, N=CH), 12.16 (1H, *s*, NH, D$_2$O exchangeable); MS (70 eV, *m/z* (relative abundance, %)): 517 (M$^+$, 15), 516 (100), 421 (63), 311 (81), 240 (42), 130 (26), 77 (12).

4-Methylbenzaldehyde, 2-(7,9-bis(4-methoxyphenyl)pyrido-[3',2':4,5]thieno-[3,2-d]pyrimidin-4-yl)hydrazone (8b). Yield: 73 %; white solid; m.p.: 330–332 °C; Anal. Calcd. for C$_{31}$H$_{25}$N$_5$O$_2$S (FW: 531.63): C, 70.04; H, 4.74; N, 13.17 %. Found: C, 69.91; H, 4.70; N, 13.03 %; IR (KBr, cm^{-1}): 3432 (NH), 3044 (=CH), 2911 (CH), 1605 (C=N); ^{1}H-NMR (300 MHz, DMSO-*d*$_6$, *δ* / ppm): 2.37 (3H, *s*, CH$_3$), 3.84 (6H, *s*, 2OCH$_3$), 7.05–7.71 (12H, *m*, Ar-H), 7.79 (1H, *s*, pyridine--H5), 8.21 (1H, *s*, pyrimidine-H2), 8.42 (1H, *s*, N=CH), 12.12 (1H, *s*, NH, D$_2$O exchangeable); MS (70 eV, *m/z* (relative abundance, %)): 531 (M$^+$, 12), 424 (38), 232 (76), 137 (59), 91 (90), 53 (100).

4-Methoxybenzaldehyde, 2-(7,9-bis(4-methoxyphenyl)pyrido-[3',2':4,5]thi-eno[3,2-d]pyrimidin-4-yl)hydrazone (8c). Yield: 70 %; pale yellow solid; m.p.: 334–335 °C; Anal. Calcd. for C$_{31}$H$_{25}$N$_5$O$_3$S (FW: 547.63): C, 67.99; H, 4.60; N, 12.79 %. Found: C, 67.75; H, 4.48; N, 12.54 %. IR (KBr, cm^{-1}): 3435 (NH), 3045 (=CH), 2953 (CH), 1605 (C=N); ^{1}H-NMR (300 MHz, DMSO-*d*$_6$, *δ* / ppm): 3.86 (9H, *s*, 3OCH$_3$), 7.09–7.71 (12H, *m*, Ar-H), 7.84 (1H, *s*, pyridine-H5), 8.28 (1H, *s*, pyrimidine-H2), 8.43 (s, 1H, N=CH), 12.06 (s, D$_2$O exchangeable, 1H, NH); MS (70 eV, *m/z* (relative abundance, %)): 547 (M$^+$, 6), 258 (31), 179 (100), 143 (84), 57 (16).

4-Chlorobenzaldehyde, 2-(7,9-bis(4-methoxyphenyl)pyrido[3',2':4,5]thieno-[3,2-d]pyrimidin-4-yl)hydrazone (8d). Yield: 78 %; white solid; m.p.: 338––340 °C; Anal. Calcd. for C$_{30}$H$_{22}$ClN$_5$O$_2$S (FW: 552.05): C, 65.27; H, 4.02; N, 12.69 %. Found: C, 65.13; H, 4.14; N, 12.43 %; IR (KBr, cm^{-1}): 3421 (NH),

3044 (=CH), 2908 (CH), 1599 (C=N); ^{1}H-NMR (300 MHz, DMSO-d_6, δ / ppm): 3.84 (6H, *s*, 2OCH$_3$), 7.07–7.71 (12H, *m*, Ar-H), 7.83 (1H, *s*, pyridine-H5), 8.22 (1H, *s*, pyrimidine-H2), 8.42 (1H, *s*, N=CH), 12.10 (1H, *s*, NH, D$_2$O exchangeable); MS (70 eV, *m/z* (relative abundance, %)): 554 (M$^+$+2, 3), 552 (M$^+$, 10), 447 (100), 330 (28), 272 (65), 142 (73), 57 (79).

*4-Nitrobenzaldehyde, 2-(7,9-Bis(4-methoxyphenyl)pyrido[3',2':4,5]thieno-[3,2-*d]*pyrimidin-4-yl)hydrazone (8e)*. Yield: 76 %; pale yellow solid; m.p.: 342––344 °C; Anal. Calcd. for C$_{30}$H$_{22}$N$_6$O$_4$S (FW: 562.60): C, 64.05; H, 3.94; N, 14.94 %. Found: C, 64.17; H, 3.82; N, 14.72 %; IR (KBr, cm^{-1}): 3418 (NH), 3040 (=CH), 2909 (CH), 1599 (C=N); ^{1}H-NMR (300 MHz, DMSO-d_6, δ / pm): 3.85 (3H, *s*, OCH$_3$), 3.87 (3H, *s*, OCH$_3$), 7.03–8.31 (12H, *m*, Ar-H), 7.88 (1H, *s*, pyridine-H5), 8.39 (1H, *s*, pyrimidine-H2), 8.51 (1H, s, N=CH), 11.91 (s, 1H, NH, D$_2$O exchangeable); MS (70 eV, *m/z* (relative abundance, %)): 562 (M$^+$, 21), 444 (19), 415 (100), 388 (56), 120 (49), 56 (73).

*4-Hydroxybenzaldehyde, 2-(2-(7,9-Bis(4-methoxyphenyl)pyrido[3',2':4,5]-thieno[3,2-*d]*pyrimidin-4-yl)hydrazine (8f)*. Yield: 73 %; brown solid; m.p.: 286––288 °C; Anal. Calcd. for C$_{30}$H$_{23}$N$_5$O$_3$S (FW: 533.60): C, 67.53; H, 4.34; N, 13.12 %. Found: C, 67.43; H, 4.19; N, 13.03 %; IR (KBr, cm^{-1}): 4425 (OH and NH), 3044 (=CH), 2908 (CH),1604 (C=N); ^{1}H-NMR (300 MHz, DMSO-d_6, δ / / ppm): 3.85 (3H, *s*, OCH$_3$), 3.86 (s, 3H, OCH$_3$), 6.94–8.28 (12H, *m*, Ar-H), 7.87 (1H, *s*, pyridine-H5), 8.43 (1H, *s*, pyrimidine-H2), 8.58 (1H, *s*, N=CH), 10.12 (1H, *s*, OH, D$_2$O exchangeable), 12.11 (1H, *s*, NH, D$_2$O exchangeable); MS (70 eV, *m/z* (relative abundance, %)): 533 (M$^+$, 2), 429 (100), 415 (42), 272 (75), 121 (39), 58 (68).

*4-Dichlorobenzaldehyde, 2-(7,9-bis(4-methoxyphenyl)pyrido[3',2':4,5]thi-eno[3,2-*d]*pyrimidin-4-yl)hydrazine (8g)*. Yield: 76 %; white solid; m.p.: 350––352 °C; Anal. Calcd. for C$_{30}$H$_{21}$Cl$_2$N$_5$O$_2$S (FW: 586.49): C, 61.44; H, 3.61; N, 11.94 %. Found: C, 61.31; H, 3.32; N, 11.75 %; IR (KBr, cm^{-1}): 3425 (NH), 3055 (=CH), 2910 (CH), 1599 (C=N); ^{1}H-NMR (300 MHz, DMSO-d_6, δ / ppm): 3.84 (3H, *s*, OCH$_3$), 3.89 (3H, *s*, OCH$_3$), 7.04–7.77 (11H, *m*, Ar-H), 7.91 (1H, *s*, pyridine-H5), 8.23 (1H, *s*, pyrimidine-H2), 8.54 (1H, *s*, N=CH), 12.12 (1H, *s*, NH, D$_2$O exchangeable); MS (70 eV, *m/z* (relative abundance, %)): 586 (M$^+$, 2), 388 (100), 359 (45), 273 (39), 178 (47), 59 (77).

*Acetaldehyde, 2-(7,9-bis(4-methoxyphenyl)pyrido[3',2':4,5]thieno[3,2-*d]*py-rimidin-4-yl)hydrazine (8h)*. Yield: 84 %; green solid; m.p.: 240–241 °C; Anal. Calcd. for C$_{25}$H$_{21}$N$_5$O$_2$S (FW: 455.53): C, 65.92; H, 4.65; N, 15.37 %. Found: C, 65.75; H, 4.60; N, 15.14 %; IR (KBr, cm^{-1}): 3375 (NH), 3047 (=CH), 2939 (CH), 1608 (C=N); ^{1}H-NMR (300 MHz, DMSO-d_6, δ / ppm): 1.42 (3H, *d*, *J* = = 5.7 Hz, CH$_3$), 3.89 (3H, *s*, OCH$_3$), 3.92 (3H, *s*, OCH$_3$), 7.03 (1H, *q*, *J* = 5.7 Hz, N=CH), 7.26–8.17 (8H, *m*, Ar-H), 7.71 (1H, *s*, pyridine-H5), 7.99 (1H, *s*,

pyrimidine-H2), 12.17 (1H, *s*, NH, D$_2$O exchangeable); MS (70 eV, *m/z* (relative abundance, %)): 455 (M$^+$, 3), 415 (100), 388 (38), 207 (11), 136 (14), 56 (12).

*7,9-Bis(4-methoxyphenyl)-3-phenylpyrido[3',2':4,5]thieno[2,3-*e*][1,2,4]tri-azolo[4,3-*c*]pyrimidine (**9a**)*. Yield: 67 %; orange solid; m.p.: 354 °C (dioxane); Anal. Calcd. for C$_{30}$H$_{21}$N$_5$O$_2$S (FW: 515.59): C, 69.89; H, 4.11; N, 13.58 %; Found: C, 69.79; H, 4.02; N, 13.44 %; IR (KBr, cm^{-1}): 3060, 3000 (=C–H), 2935 (C–H), 1604 (C=N); ^{1}H-NMR (300 MHz, DMSO-d_6, *δ* / ppm): 3.81 (3H, *s*, OCH$_3$), 3.97 (3H, *s*, OCH$_3$), 7.04–8.23 (14H, *m*, Ar-H and pyridine-H5), 9.20 (1H, *s*, pyrimidine-H2); MS (70 eV, *m/z* (relative abundance, %)): 515 (M$^+$, 51), 485 (18), 380 (10), 121 (100), 50 (93).

*7,9-Bis(4-methoxyphenyl)-3-*p-*tolylpyrido[3',2':4,5]thieno[2,3-*e*][1,2,4]tri-azolo[4,3-*c*]pyrimidine (**9b**)*. Yield: 70 %; yellow solid; m.p.: 318 °C (dioxane); Anal. Calcd. for C$_{31}$H$_{23}$N$_5$O$_2$S (FW: 529.61): C, 70.30; H, 4.38; N, 13.22 %. Found: C, 70.27; H, 4.19; N, 13.03 %; IR (KBr, cm^{-1}): 3060, 3010 (=C–H), 2958, 2932 (C–H), 1606 (C=N); ^{1}H-NMR (300 MHz, DMSO-d_6, *δ* / ppm): 2.42 (3H, *s*, CH$_3$), 3.82 (3H, *s*, OCH$_3$), 3.88 (3H, *s*, OCH$_3$), 7.04–8.25 (13H, *m*, Ar-H and pyridine-H5), 9.18 (1H, *s*, pyrimidine-H2); MS (70 eV, *m/z* (relative abundance, %)): 529 (M$^+$, 18), 511 (23), 247 (100), 205 (40), 118 (36), 92 (49), 77 (69).

*3,7,9-Tris(4-methoxyphenyl)pyrido[3',2':4,5]thieno[2,3-*e*][1,2,4]triazolo-[4,3-*c*]pyrimidine (**9c**)*. Yield: 69 %; yellow solid; m.p.: 326–328 °C (dioxane); Anal. Calcd. for C$_{31}$H$_{23}$N$_5$O$_3$S (FW: 545.61): C, 68.24; H, 4.25; N, 12.84 %. Found: C, 68.11; H, 4.20; N, 12.72 %; IR (KBr, cm^{-1}): 3063, 2999 (=C–H), 2932(C–H), 1607 (C=N); ^{1}H-NMR (300 MHz, DMSO-d_6, *δ* / ppm): 3.83 (3H, *s*, OCH$_3$), 3.86 (3H, *s*, OCH$_3$), 3.89 (3H, *s*, OCH$_3$), 7.06–8.43 (13H, *m*, Ar-H and pyridine-H5), 9.16 (1H, *s*, pyrimidine-H2); MS (70 eV, *m/z* (relative abundance, %)):= 545 (M$^+$, 3), 444 (100), 388 (48), 108 (59).

*3-(4-Chlorophenyl)-7,9-bis(4-methoxyphenyl)pyrido[3',2':4,5]thieno[2,3-*e*]-[1,2,4]triazolo[4,3-*c*]pyrimidine (**9d**)*. Yield: 73 %; reddish-brown solid; m.p.: 346–348 °C (dioxane); Anal. Calcd. for C$_{30}$H$_{20}$ClN$_5$O$_2$S (FW: 550.03): C, 65.51; H, 3.67; N, 12.73 %. Found: C, 65.38; H, 3.61; N, 12.54 %; IR (KBr, cm^{-1}): 3067, 3001 (=C–H), 2958, 2933 (C–H), 1606 (C=N); ^{1}H-NMR (300 MHz, DMSO-d_6, *δ* / ppm): 3.82 (3H, *s*, OCH$_3$), 3.87 (3H, *s*, OCH$_3$), 7.01–8.31 (13H, *m*, Ar-H and pyridine-H5), 9.14 (1H, *s*, pyrimidine-H2); MS (70 eV, *m/z* (relative abundance, %)): 552 (M$^+$+2, 19), 550 (M$^+$, 59), 414 (44), 388 (53), 247 (14), 178 (100), 77 (56).

*7,9-Bis(4-methoxyphenyl)-3-(4-nitrophenyl)pyrido[3',2':4,5]thieno[2,3-*e*]-[1,2,4]triazolo[4,3-*c*]pyrimidine (**9e**)*. Yield: 73 %; brown solid; m.p.: 312–314 °C; (DMF); Anal. Calcd. for C$_{30}$H$_{20}$N$_6$O$_4$S (FW: 560.58): C, 64.28; H, 3.60; N, 14.99 %. Found: C, 64.20; H, 3.47; N, 14.76 %; IR (KBr, cm^{-1}): 3074, 3005 (=C–H), 2937 (C–H), 1605 (C=N); ^{1}H-NMR (300 MHz, DMSO-d_6, *δ* / ppm):

3.83 (3H, *s*, OCH$_3$), 3.86 (3H, *s*, OCH$_3$), 7.00–8.28 (13H, *m*, Ar-H and pyridine--H5), 9.15 (1H, *s*, pyrimidine-H2); MS (70 eV, *m/z* (relative abundance, %)): 560 (M$^+$, 20), 433 (31), 354 (47), 247 (14), 44 (100).

*2-(7,9-Bis(4-methoxyphenyl)pyrido[3',2':4,5]thieno[2,3-*e*][1,2,4]triazolo-[4,3-*c*]pyrimidin-3-yl)phenol (9f)*. Yield: 72 %; brown solid; m.p.: 284–286 °C (dioxane); Anal. Calcd. for C$_{30}$H$_{21}$N$_5$O$_3$S (FW: 531.58): C, 67.78; H, 3.98; N, 13.17 %. Found: C, 67.63; H, 3.69; N, 13.08 %; IR (KBr, cm^{-1}): 3064 (=C–H), 2955 (C–H), 1605 (C=N); ^{1}H-NMR (300 MHz, DMSO-*d*$_6$, *δ* / ppm): 3.84 (3H, *s*, OCH$_3$), 3.85 (3H, *s*, OCH$_3$), 7.03–8.29 (13H, *m*, Ar-H and pyridine-H5), 9.08 (1H, *s*, pyrimidine-H2), 11.24 (1H, *s*, OH, D$_2$O exchangeable); MS (70 eV, *m/z* (relative abundance, %)): 531 (M$^+$, 5), 432 (31), 309 (94), 247 (78), 92 (71), 40 (100).

*3-(2,4-Dichlorophenyl)-7,9-bis(4-methoxyphenyl)pyrido[3',2':4,5]thieno-[2,3-*e*][1,2,4]triazolo[4,3-*c*]pyrimidine (9g)*. Yield: 70 %; brown solid; m.p.: 318 °C (dioxane); Anal. Calcd. for C$_{30}$H$_{19}$Cl$_2$N$_5$O$_2$S (FW: 584.48): C, 61.65; H, 3.28; N, 11.98 %. Found: C, 61.66; H, 3.20; N, 11.75 %; IR (KBr, cm^{-1}): 3066, 3000 (=C–H), 2953, 2931 (C–H), 1606 (C=N); ^{1}H-NMR (300 MHz, DMSO-*d*$_6$, *δ* / ppm): 3.85 (3H, *s*, OCH$_3$), 3.94 (3H, *s*, OCH$_3$), 7.06–8.25 (12H, *m*, Ar-H and pyridine-H5), 9.03 (1H, *s*, pyrimidine-H2); MS (70 eV, *m/z* (relative abundance, %)): 584 (M$^+$, 12), 531 (40), 354 (78), 279 (51), 193 (39), 173 (91), 40 (100).

*7,9-Bis(4-methoxyphenyl)-3-methylpyrido[3',2':4,5]thieno[2,3-*e*][1,2,4]tri-azolo[4,3-*c*]pyrimidine (9h)*. Yield: 76 %; green solid; m.p.: 312–314 °C (ethanol); Anal. Calcd. for C$_{25}$H$_{19}$N$_5$O$_2$S (FW: 453.52): C, 66.21; H, 4.22; N, 15.44 %. Found: C, 66.39; H, 4.15; N, 15.31 %; IR (KBr, cm^{-1}): 3062, 2998 (=C–H), 2930 (C–H), 1605 (C=N); ^{1}H-NMR (300 MHz, DMSO-*d*$_6$. *δ* / ppm): 2.74 (3H, *s*, CH$_3$), 3.83 (3H, *s*, OCH$_3$), 3.92 (3H, *s*, OCH$_3$), 7.04–8.34 (9H, *m*, Ar-H and pyridine-H5), 9.15 (1H, *s*, pyrimidine-H2); MS (70 eV, *m/z* (relative abundance, %)): 453 (M$^+$, 34), 309 (62), 281 (100), 239 (68), 92 (62), 44 (52).

*7,9-Bis(4-methoxyphenyl)-2-phenylpyrido[3',2':4,5]thieno[2,3-*e*][1,2,4]tri-azolo[1,5-*c*]pyrimidine (10a)*. Yield: 66 %; orange solid; m.p.: 351–353 °C; Anal. Calcd. for C$_{30}$H$_{21}$N$_5$O$_2$S (FW: 515.59): C, 69.89; H, 4.11; N, 13.58 %. Found: C, 69.68; H, 4.00; N, 13.39 %; IR (KBr, cm^{-1}): 3044 (=C–H), 2911 (C–H), 1600 (C=N); ^{1}H-NMR (300 MHz, DMSO-*d*$_6$, *δ* / ppm): 3.81 (3H, *s*, OCH$_3$), 3.87 (3H, *s*, OCH$_3$), 7.04–8.27 (14H, *m*, Ar-H and pyridine-H5), 8.45 (1H, *s*, pyrimidine-H2); MS (70 eV, *m/z* (relative abundance, %)): 515 (M$^+$, 51), 413 (18), 350 (21), 149 (22), 93 (58), 65 (100).

*7,9-Bis(4-methoxyphenyl)-2-*p*-tolylpyrido[3',2':4,5]thieno[2,3-*e*][1,2,4]tri-azolo[1,5-*c*]pyrimidine (10b)*. Yield: 65 %; yellow solid; m.p.: 308–310 °C; Anal. Calcd. for C$_{31}$H$_{23}$N$_5$O$_2$S (FW: 529.61): C, 70.30; H, 4.38; N, 13.22 %. Found: C, 70.21; H, 4.23; N, 13.01 %; IR (KBr, cm^{-1}): 3048 (=C–H), 2934 (C–H), 1602 (C=N); ^{1}H-NMR (300 MHz, DMSO-*d*$_6$, *δ* / ppm): 2.36 (3H, *s*,

CH$_3$), 3.81 (3H, *s*, OCH$_3$), 3.85 (3H, *s*, OCH$_3$), 6.79–8.32 (13H, *m*, Ar-H and pyridine-H5), 8.40 (1H, *s*, pyrimidine-H2); MS (70 eV, *m/z* (relative abundance, %)): 529 (M$^+$, 37), 447 (65), 378 (100), 198 (91), 142 (55), 50 (62).

*2,7,9-Tris(4-methoxyphenyl)pyrido[3',2':4,5]thieno[2,3-*e*][1,2,4]triazolo-[1,5-*c*]pyrimidine (10c)*. Yield: 69 %; yellow solid; m.p.: 326–328 °C; Anal. Calcd. for C$_{31}$H$_{23}$N$_5$O$_3$S (FW: 545.61): C, 68.24; H, 4.25; N, 12.84 %. Found: C, 68.07; H, 4.22; N, 12.57 %; IR (KBr, cm^{-1}): 3046 (=C–H), 2909 (C–H), 1601 (C=N); ^{1}H-NMR (300 MHz, DMSO-d_6, δ / ppm): 3.83 (3H, *s*, OCH$_3$), 3.87 (3H, *s*, OCH$_3$), 3.89 (3H, *s*, OCH$_3$), 7.05–8.44 (13H, *m*, Ar-H and pyridine-H5), 9.09 (1H, *s*, pyrimidine-H2); MS (70 eV, *m/z* (relative abundance, %)): 545 (M$^+$, 32), 413 (45), 262 (27), 149 (81), 65 (100).

*2-(4-Chlorophenyl)-7,9-bis(4-methoxyphenyl)pyrido[3',2':4,5]thieno[2,3-*e*]-[1,2,4]triazolo[1,5-*c*]pyrimidine (10d)*. Yield: 69 %; brown solid; m.p.: 346–348 °C; Anal. Calcd. for C$_{30}$H$_{20}$ClN$_5$O$_2$S (FW: 550.03): C, 65.51; H, 3.67; N, 12.73 %. Found: C, 65.31; H, 3.59; N, 12.50 %; IR (KBr, cm^{-1}): 3050 (=C–H), 2911 (C–H), 1603 (C=N); ^{1}H-NMR (300 MHz, DMSO-d_6, δ / ppm): 3.80 (3H, *s*, OCH$_3$), 3.89 (3H, *s*, OCH$_3$), 7.07–8.29 (13H, *m*, Ar-H and pyridine-H5), 9.04 (1H, *s*, pyrimidine-H2); MS (70 eV, *m/z* (relative abundance, %)): 552 (M$^+$+2, 11), 550 (M$^+$, 39), 414 (100), 387 (49), 274 (41), 137 (35).

*7,9-Bis(4-methoxyphenyl)-2-(4-nitrophenyl)pyrido[3',2':4,5]thieno[2,3-*e*]-[1,2,4]triazolo[1,5-*c*]pyrimidine (10e)*. Yield: 67 %; brown solid; m.p.: 312–314 °C; Anal. Calcd. for C$_{30}$H$_{20}$N$_6$O$_4$S (FW: 560.58): C, 64.28; H, 3.60; N, 14.99 %. Found: C, 64.25; H, 3.42; N, 14.79 %; IR (KBr, cm^{-1}): 3050 (=C–H), 2911 (C–H), 1602 (C=N); ^{1}H-NMR (300 MHz, DMSO-d_6, δ / ppm): 3.82 (3H, *s*, OCH$_3$), 3.86 (3H, *s*, OCH$_3$), 7.03–8.52 (13H, *m*, Ar-H and pyridine-H5), 9.35 (1H, *s*, pyrimidine-H2); MS (70 eV, *m/z* (relative abundance, %)): 560 (M$^+$, 28), 494 (39), 388 (100), 344 (43), 193 (10), 64 (53).

*2-(7,9-Bis(4-methoxyphenyl)pyrido[3',2':4,5]thieno[2,3-*e*][1,2,4]triazolo-[1,5-*c*]pyrimidin-2-yl)phenol (10f)*. Yield: 68 %; brown solid; m.p.: 284–286 °C; Anal. Calcd. for C$_{30}$H$_{21}$N$_5$O$_3$S (FW: 531.58): C, 67.78; H, 3.98; N, 13.17 %. Found: C, 67.69; H, 3.64; N, 13.00 %; IR (KBr, cm^{-1}): 3461 (OH), 3047 (=C–H), 2930 (C–H), 1606 (C=N); ^{1}H-NMR (300 MHz, DMSO-d_6, δ / ppm): 3.85 (3H, *s*, OCH$_3$), 3.92 (3H, *s*, OCH$_3$), 6.73–8.58 (13H, *m*, Ar-H and pyridine-H5), 9.10 (1H, *s*, pyrimidine-H2), 10.12 (1H, *s*, OH, D$_2$O exchangeable); MS (70 eV, *m/z* (relative abundance, %)): 531 (M$^+$, 17), 444 (32), 299 (56), 149 (72), 92 (79), 65 (100).

*2-(2,4-Dichlorophenyl)-7,9-bis(4-methoxyphenyl)pyrido[3',2':4,5]thieno-[2,3-*e*][1,2,4]triazolo[1,5-*c*]pyrimidine (10g)*. Yield: 64 %; brown solid; m.p.: 318–320 °C; Anal. Calcd. for C$_{30}$H$_{19}$Cl$_2$N$_5$O$_2$S (FW: 584.48): C, 61.65; H, 3.28; N, 11.98 %. Found: C, 61.62; H, 3.24; N, 11.70 %; IR (KBr, cm^{-1}): 3062 (=C–H), 2930 (C–H), 1605 (C=N); ^{1}H-NMR (300 MHz, DMSO-d_6, δ / ppm): 3.83 (3H, *s*,

OCH$_3$), 3.87 (3H, *s*, OCH$_3$), 7.01–8.58 (12H, *m*, Ar-H and pyridine-H5), 9.09 (1H, *s*, pyrimidine-H2); MS (70 eV, *m/z* (relative abundance, %)): 584 (M$^+$, 13), 414 (100), 344 (61), 193 (72), 76 (68).

*7,9-Bis(4-methoxyphenyl)-2-methylpyrido[3',2':4,5]thieno[2,3-*e*][1,2,4]tri-azolo[1,5-c] pyrimidine (10h)*. Yield: 69 %; green solid; m.p.: 182–184 °C; Anal. Calcd. for C$_{25}$H$_{19}$N$_5$O$_2$S (FW: 453.52): C, 66.21; H, 4.22; N, 15.44 %. Found: C, 66.31; H, 4.12; N, 15.28 %; IR (KBr, cm^{-1}): 3049 (=C–H), 2928 (C–H), 1606 (C=N); ^{1}H-NMR (300 MHz, DMSO-*d*$_6$, *δ* / ppm): 2.50 (3H, *s*, CH$_3$), 3.82 (3H, *s*, OCH$_3$), 3.84 (3H, *s*, OCH$_3$), 7.03–8.18 (9H, *m*, Ar-H and pyridine-H5), 9.15 (1H, *s*, pyrimidine-H2); MS (70 eV, *m/z* (relative abundance, %)): 453 (M$^+$, 100), 334 (56), 270 (59), 193 (43), 76 (60).
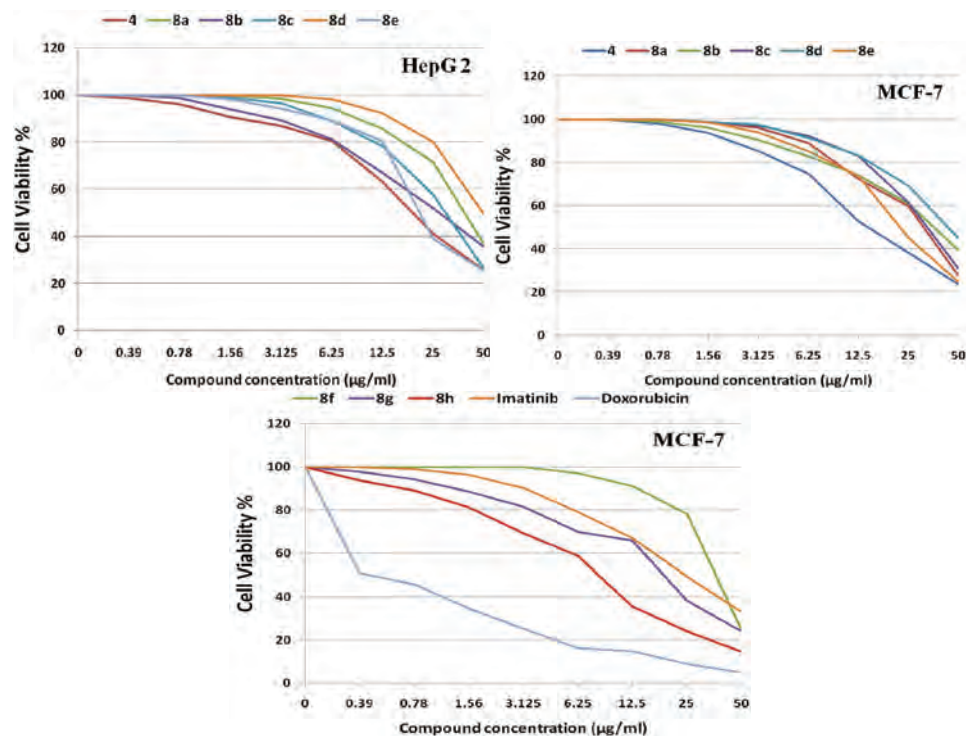
Fig. S-1. The dose response curves showing the *in vitro* inhibitory activity of compounds of the **8** series (**8a**–**h**) against hepatocellular carcinoma HepG2 and breast carcinoma MCF-7 cell lines.
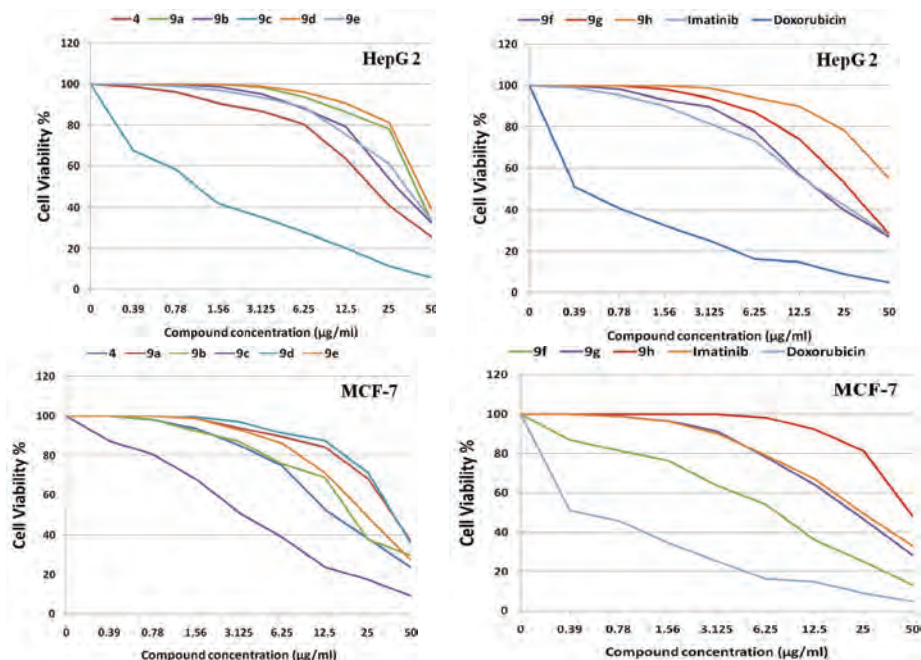
Fig. S-2. The dose response curves showing the *in vitro* inhibitory activity of compounds of the **9** series (**9a**–**9h**) against hepatocellular carcinoma HepG2 and breast carcinoma MCF-7 cell lines.
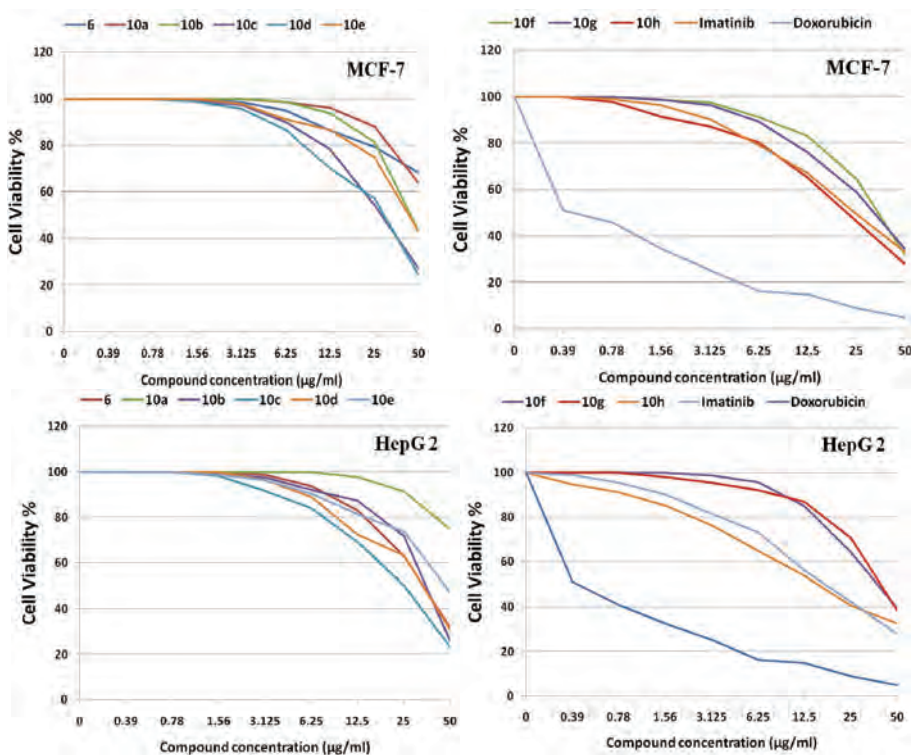
Fig. S-3. The dose response curves showing the *in vitro* inhibitory activity of compounds of the **10** series (**10a**–**10h**) against hepatocellular carcinoma (HepG2) and breast carcinoma (MCF-7) cell lines.

Green one-pot, four-component synthesis of spiro[indoline-3,4′-pyrano[2,3-*c*]pyrazole] derivatives using amino-functionalized nanoporous silica SBA-15 under solvent-free conditions

GHODSI MOHAMMADI ZIARANI[1]*, MAHSHID RAHIMIFARD[1], FATEMEH NOURI[1]
and ALIREZA BADIEI[2]

[1]*Department of Chemistry, Alzahra University, Vanak Square, P. O. Box 19938939973, Tehran, Iran and* [2]*School of Chemistry, College of Science, University of Tehran, Tehran, Iran*

Abstract: Propylamine functionalized nanoporous silica (SBA–Pr-NH$_2$) was used as an efficient heterogeneous solid basic nanoreactor in the synthesis of 6′-amino-1′*H*-spiro[indoline-3,4′-pyrano[2,3-*c*]pyrazol]-2-one derivatives **5** through a one-pot, four-component condensation of isatin derivatives **1**, activated methylene reagents **2**, hydrazine hydrate **3** and *β*-keto esters **4** under solvent-free conditions at room temperature.

Keywords: amino-functionalized nanoporous silica; solvent-free; nanoporous silica; four components; one-pot; spiro indole; pyranopyrazole.

INTRODUCTION

The indole ring is the core structure of many alkaloids, natural products and medicinal agents.[1] Compounds containing this moiety present a variety of antibacterial and antifungal activities.[2] In addition, it was reported that substitution of the indole ring with heterocycles at the 3-carbon position significantly improves biological properties.[3] The resulting spirooxindoles are found in various pharmaceutical components and natural products (Scheme 1).[4]

Heterocyclic compounds consisting of pyrano[2,3-*c*]pyrazoles with numerous biological properties, such as anticancer,[5] antibacterial,[6] antimicrobial,[7] anti-inflammatory,[8] ChK1 kinase inhibitors,[9] antifungal[10] and molluscicidal activity[11] occupy a special place in medicinal chemistry. Thus, considerable attention has been focused on the development of new modified methods for their synthesis.

Spiroindoline-pyranopyrazole derivatives can be obtained through various synthetic methods. Shestopalov *et al.* reported a four-component reaction for their synthesis by condensation of isatin, hydrazine, malononitrile and *β*-keto

---

1265

esters using triethylamine in ethanol under reflux conditions.[12] This reaction can also be affected using different catalysts, such as piperidine,[13,14] L-proline,[15] [DMBSI]HSO$_4$,[16] Mn(bpyo)$_2$/MCM-41,[17] Bmim(OH)/chitosan,[18] uncapped SnO$_2$ quantum dots,[19] 4-(dimethylamino)pyridine[20] and meglumine.[21] Another common synthetic method for the synthesis of this class of compounds is a three-component condensation of pyrazolone, malononitrile and isatin in the presence of catalysts such as triethylamine,[22] ZnS nanoparticles,[4] L-proline,[23] K$_2$CO$_3$,[24] triethanolamine[25] and NaHCO$_3$.[26] However these methods have some disadvantages, such as long reaction times, expensive and non-reusable catalysts and hard work-up or catalyst removal.

Horsfiline

Isoelacomine

Spirotryprostatin A

Scheme 1. Compounds with spirooxindole skeleton.

In recent years, mesoporous materials especially mesoporous silica, such as SBA-15 (Santa Barbara Amorphous), have attracted considerable attention. SBA-15 is a unique inorganic solid support with high surface area, large pore size and high thermal stability.[27] Grafting various organic compounds on the surface of SBA-15 could improve the catalytic activity of the silica surface. Amino functionalized SBA-15 (SBA–Pr-NH$_2$) was proved to be an efficient heterogeneous mesoporous solid base catalyst that could be used in the synthesis of various heterocyclic compounds.[28–30] In this work, an attempt was made to develop a modified methodology in the synthesis of spiro[indoline-3,4′-pyrano[2,3-*c*]pyrazole] derivatives **5** using the green solid heterogeneous base nanocatalyst SBA––Pr-NH$_2$ under solvent free conditions at room temperature *via* a one-pot four-component condensation of isatin derivatives **1**, activated methylene reagents **2**, hydrazine hydrate **3** and *β*-keto esters **4.**

RESULTS AND DISCUSSION

This report is devoted to the study of the four component condensation of isatin derivatives **1**, activated methylene reagents (malononitrile or ethyl cyanoacetate) **2**, hydrazine hydrate **3** and *β*-keto esters **4** catalyzed by nanoporous base catalyst of SBA–Pr-NH$_2$ under solvent-free conditions at room temperature (Scheme 2). In initiation of this study, various conditions employing different solvents, such as ethanol or water, and a solvent-free system with or without catalyst at room temperature were evaluated. Among the tested conditions, the best

result was obtained in the presence of SBA–Pr-NH$_2$ using the solvent-free system at room temperature (Table I).
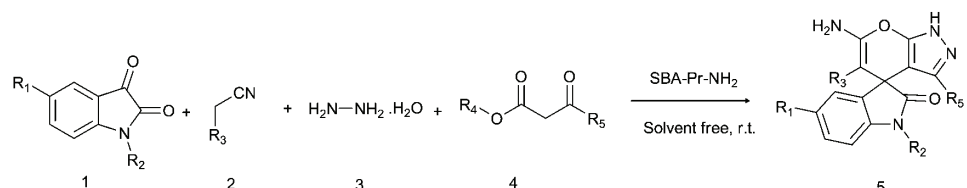
Scheme 2. Synthesis of 6′-amino-1′H-spiro[indoline-3,4′-pyrano[2,3-c]pyrazol]-2-one derivatives **5** in the presence of SBA–Pr-NH$_2$.

TABLE I. The optimization of the reaction conditions in the synthesis of **5a** at room temperature

Entry	Catalyst	Solvent	t / h	Yield, %
1	–	EtOH	8	50
2	–	H$_2$O	3	50
3	SBA–Pr-NH$_2$	EtOH	2	70
4	SBA–Pr-NH$_2$	–	0.25	80

Under the optimized conditions, various 6′-amino-1′H-spiro[indoline-3,4′-pyrano[2,3-c]pyrazol]-2-one derivatives **5a**–**f** were synthesized in the presence of SBA–Pr-NH$_2$ using several isatin derivatives **1a**–**d**, activated methylene reagents **2a** and **b**, hydrazine hydrate **3** and β-keto esters **4a**–**c**. Results are summarized in Table II. Under these conditions, the reactions were realized easily to produce spiroindoline-pyranopyrazole derivatives in good yields. It should be noted that the presence of halogens on the reacting isatins (Entries 3 and 5) decreased the reaction time in comparison to that for to isatin (Entry 1). It may be related to inductive withdrawing effects of halogens on the carbonyl group of isatin. On the other hand, replacing malononitrile with ethyl cyanoacetate increased the reaction time, which was attributed to the competing formation of the Knoevenagel adduct of isatin and the activated methylene reagents.

TABLE II. Four-component synthesis of spiro[indoline-3,4′-pyrano[2,3-c]pyrazole] derivatives **5a**–**f** in the presence of SBA–Pr-NH$_2$

Entry	R$_1$	R$_2$	R$_3$	R$_4$	R$_5$	Product	t min	Yield %	M.p. range, °C	Literature m.p., °C
1	H	H	CN	Et	Me	**5a**	15	80	278–280	279–280[26]
2	H	H	CN	Me	Me	**5a**	15	87	278–280	279–280[26]
3	Br	H	CN	Et	Me	**5b**	10	85	281–283	282–283[26]
4	H	CH$_2$Ph	CN	Et	Me	**5c**	15	78	268–270	Not reported
5	Cl	H	CN	Et	Me	**5d**	10	83	296–298	297–298[15]
6	H	H	CN	Et	Ph	**5e**	15	85	279–281	280–281[13]
7	H	H	CO$_2$Et	Et	Me	**5f**	20	80	280–282	281–282[31]
8	H	H	CO$_2$Et	Me	Me	**5f**	25	83	280–282	281–282[31]

The reusability of the catalyst was investigated under the optimized conditions for the synthesis of the model compound **5a**. As shown in Table III, the recycling process was completed four times with no significant decrease in the catalyst activity. The yields for the four runs were found to be 80, 78, 78 and 76 %, respectively.

TABLE III. Synthesis of the spiroindoline–pyranopyrazole **5a** with recycled SBA–Pr–NH$_2$

Parameter	1st run	2nd run	3rd run	4th run
Time, min	15	15	20	20
Yield, %	80	78	78	76

A possible mechanism for synthesis of 6′-amino-1′*H*-spiro[indoline-3,4′-pyrano[2,3-*c*]pyrazol]-2-one derivatives **5** is presented in Scheme 3. The initiation step begins with the two-component condensation of hydrazine hydrate **3** and β-keto esters **4** to afford the 5-alkyl-2,4-dihydro-3*H*-pyrazol-3-one **7**, which was deprotonated by SBA–Pr–NH$_2$. Then a fast Knoevenagel condensation occurred
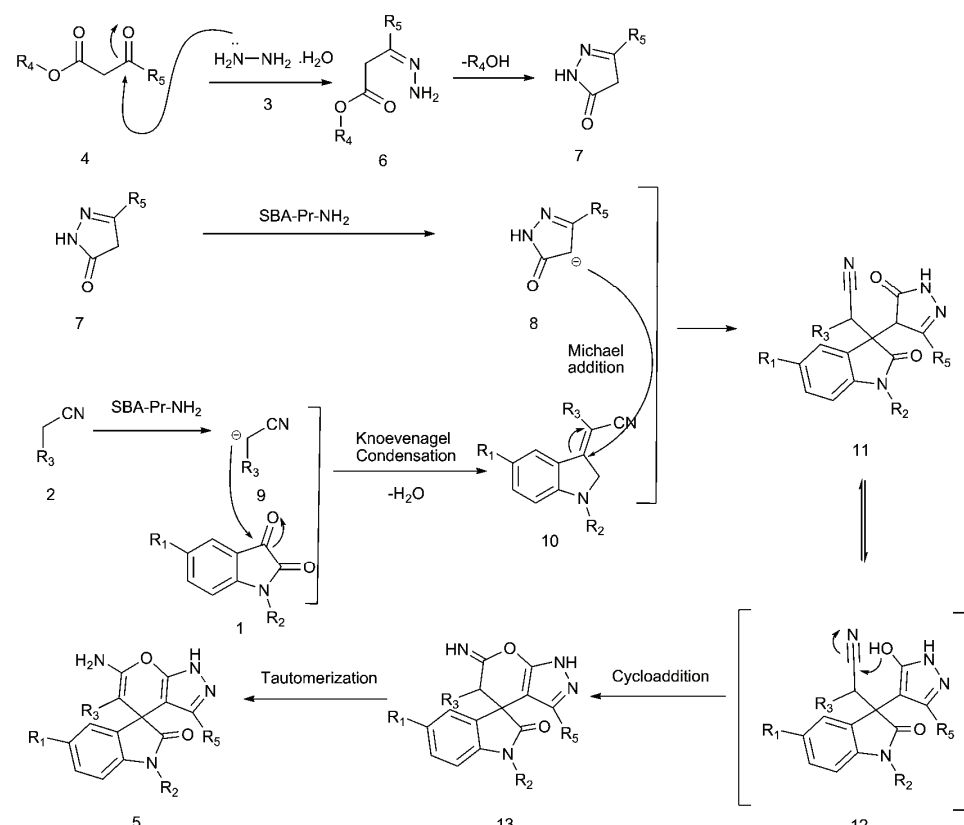
Scheme 3. Plausible mechanism.

between isatin derivatives **1** and activated methylene reagents **2**. Michael addition of **8** to **10** afforded compound **11**, which was followed by enol–keto tautomerization to yield intermediate **12**. Addition of hydroxyl to cyano group provided compound **13**. Tautomerization of compound **13** yielded the desired product **5** (Scheme 3).

Several varying conditions have been reported in the literature for the synthesis of 6′-amino-1′*H*-spiro[indoline-3,4′-pyrano[2,3-*c*]pyrazol]-2-one derivatives **5**, as given in Table IV.

TABLE IV. Comparison of several conditions

Entry	Catalyst	Solvent	Conditions	t / min	Yield, %	Year
1	N(Et)$_3$	EtOH	Reflux	5–30	76–85	2009[12]
2	Piperidine	H$_2$O	r.t.	300	80-97	2010[14]
3	Piperidine	EtOH	Ultrasound	60	73–93	2012[13]
4	[DMBSI]HSO$_4$	–	60 °C	1–2	88–96	2014[16]
5	Mn(bpyo)$_2$/MCM-41	H$_2$O	Reflux	18–24	89–92	2015[17]
6	Bmim(OH)/Chitosan		r.t.	150–210	89–93	2014[18]
7	Uncapped SnO$_2$ quantum dot	H$_2$O	r.t.	120–150	90–93	2014[19]
8	4-(Dimethylamino)pyridine	EtOH	60 °C	60	75–85	2014[20]
9	Meglumine	EtOH/H$_2$O	r.t.	27–35	90–93	2013[21]
10	L-proline	H$_2$O	80 °C	10–30	83–92	2013[15]
11	SBA–Pr-NH$_2$	–	r.t.	10–25	78–87	Present work

In the current method, the basic nanoreactor with hexagonal platelet morphology, several reusabilities, ease of handling and removal from the reaction medium could make it an economic and efficient green solid heterogeneous nanocatalyst for this synthesis. Furthermore, the short reaction time, solvent-free conditions, room temperature and simple procedure are other advantages of this method.

Structure of the catalyst

The surface of the catalyst was analyzed by different methods, such as TGA, FT-IR and others, which demonstrated that the organic groups (propylamine) were immobilized into the pores.[29]

The same ordered mesoscopic structured silica with (100), (110) and (200) reflections in the low-angle XRD patterns of SBA-15 and SBA–Pr-NH$_2$ indicated a two-dimensional hexagonal symmetrical array of nano-channels. This means that the structural integrity of SBA-15 was not affected during the functionalization reaction. Moreover, the TEM image of SBA–Pr-NH$_2$ confirmed the parallel channels were similar to the configuration of the pores in SBA-15. This indicated that during grafting of the aminopropyl-triethoxysilane (APTES) groups, the pores of SBA-15 did not collapse.[29]
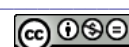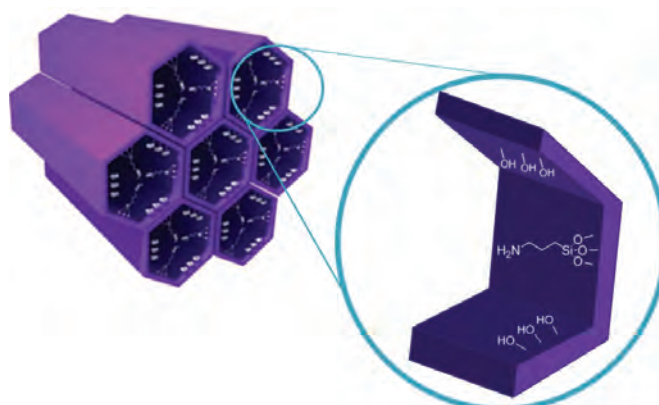
Fig. 1. Functionalized SBA-15.

EXPERIMENTAL

Materials and methods

The chemical compounds used in this work were all obtained from Merck and were employed without further purification. The IR spectra were recorded from KBr disks using a Fourier-transform (FT)-IR Bruker Tensor 27 instrument. The melting points were measured using the capillary tube method with an Electrothermal 9200 apparatus. ^{1}H- and ^{13}C-NMR were run on a Bruker DPX at 400 or 250 MHz using TMS as an internal standard. The mass spectra were obtained on an Agilent 5973 MS detector.

The physical, analytical and spectral data of compounds **5a**–**f** are given in the Supplementary material to this paper.

Synthesis and functionalization of SBA-15

The nanoporous compound SBA-15 was synthesized and functionalized according to a previous report. The triblock copolymer Pluronic P126 was used as the directing agent for the preparation of SBA-15 as nanoporous silica.[32,33] Functionalization of SBA-15 was performed through post-grafting of calcined SBA-15 with (3-aminopropyl)triethoxysilane (APTES, Fig. 1).[29]

General procedure for the synthesis of the 6'-amino-1'H-spiro[indoline-3,4'-pyrano[2,3-c]-pyrazol]-2-one derivatives

A suspension of SBA–Pr–NH$_2$ (0.02 g), isatin derivatives **1** (1 mmol), methylene reagent (malononitrile or ethyl cyanoacetate) **2** (1 mmol), hydrazine hydrate (80 %) **3** (1.4 mmol, 0.07 g) and *β*-keto ester **4** (1 mmol) was stirred at room temperature under solvent-free conditions for an appropriate time as indicated in Table II. Upon completion of the reaction as monitored by TLC (thin layer chromatography), the solid product was dissolved in hot ethyl acetate and the insoluble catalyst was removed by filtration. The filtrate was cooled to room temperature to yield pure crystals of a spiro[indoline-3,4'-pyrano[2,3-*c*]pyrazole] derivative **5**.

CONCLUSION

In conclusion, amino-functionalized SBA-15 could serve as an efficient heterogeneous solid basic nanocatalyst for the synthesis of 6'-amino-1'*H*-spiro[indoline-3,4'-pyrano[2,3-*c*]pyrazol]-2-one derivatives **5** at room

temperature and under solvent-free conditions. This procedure offers several advantages, such as short reaction times, mild reaction conditions, high yield of products, easy workup procedure, and reusability of the catalyst.

SUPPLEMENTARY MATERIAL

Physical, analytical and spectral data of compounds **5a**–**f** are available electronically from http://www.shd.org.rs/JSCS/, or from the corresponding author on request.

И З В О Д
ЗЕЛЕНА СИНТЕЗА ДЕРИВАТА СПИРО[ИНДОЛИН-3,4'-ПИРАНО[2,3-*c*]ПИРАЗОЛА], У ЈЕДНОМ РЕАКЦИОНОМ КОРАКУ, УПОТРЕБОМ АМИНО ФУНКЦИОНАЛИЗОВАНИХ НАНО-ЧЕСТИЦА СИЛИКА-ГЕЛА БЕЗ РАСТВАРАЧА

GHODSI MOHAMMADI ZIARANI[1], MAHSHID RAHIMIFARD[1], FATEMEH NOURI[1] и ALIREZA BADIEI[2]

[1]*Department of Chemistry, Alzahra University, Vanak Square, P. O. Box No. 19938939973, Tehran, Iran и* [2]*School of Chemistry, College of Science, University of Tehran, Tehran, Iran*

Нано-честице силика-гела функционализоване пропиламином употребљене су као ефикасан хетерогени нанореактор у синтези деривата 6'-амино-1'*H*-спиро[индолин-3,4'-пирано[2,3-*c*]пиразол]-2-она **5** у четворокомпонентној реакцији кондензације деривата изатина **1**, активних метиленских реагенаса **2**, хидразин-хидрата **3** и *β*-кето-естара **4** без присуства растварача, на собној температури.

REFERENCES

1. R. Sundberg, *The Chemistry of Indoles*, Vol. 18, Elsevier, New York, USA, 2012, p. 431
2. T. C. Leboho, J. P. Michael, W. A. van Otterlo, S. F. van Vuuren, C. B. de Koning, *Bioorg. Med. Chem.* **19** (2009) 4948
3. A. Abdel-Rahman, E. Keshk, M. Hanna, S. M. El-Bady, *Bioorg. Med. Chem.* **12** (2004) 2483
4. A. Dandia, V. Parewa, A. K. Jain, K. S. Rathore, *Green Chem.* **13** (2011) 2135
5. J.-L. Wang, D. Liu, Z.-J. Zhang, S. Shan, X. Han, S. M. Srinivasula, C. M. Croce, E. S. Alnemri, Z. Huang, *Proc. Natl. Acad. Sci. USA* **97** (2000) 7124
6. Z. Ren, W. Cao, W. Tong, Z. Jin, *Synth. Commun.* **35** (2005) 2509
7. E. El-Tamany, F. A. El-Shahed, B. H. Mohamed, *J. Serb. Chem. Soc.* **64** (1999) 9
8. M. E. Zaki, H. A. Soliman, O. A. Hiekal, A. E. Rashad, *Z. Naturforsch., C; J. Biosci.* **61** (2006) 1
9. N. Foloppe, L. M. Fisher, R. Howes, A. Potter, A. G. Robertson, A. E. Surgenor, *Bioorg. Med. Chem. Lett.* **14** (2006) 4792
10. M. B. Hogale, B. N. Pawar, *J. Indian Chem. Soc.* **66** (1989) 206
11. F. M. Abdelrazek, P. Metz, O. Kataeva, A. Jaeger, S. F. El-Mahrouky, *Arch. Pharm.* **340** (2007) 543
12. Y. M. Litvinov, A. A. Shestopalov, L. A. Rodinovskaya, A. M. Shestopalov, *J. Comb. Chem.* **11** (2009) 914
13. Y. Zou, Y. Hu, H. Liu, D. Shi, *ACS Comb. Sci.* **14** (2012) 38

14. S. Ahadi, Z. Yasaei, A. Bazgir, *J. Heterocycl. Chem.* **47** (2010) 1090
15. J. Yu, Y. Zhou, T. Shen, W. Mao, K. Chen, Q. Song, *J. Chem. Res.* **37** (2013) 365
16. M. Mamaghani, R. Hossein Nia, F. Shirini, K. Tabatabaeian, M. Rassa, *Med. Chem. Res.* **24** (2015) 1916
17. M. Daraie, Y. S. Beheshtiha, M. M. Heravi, *Monatsh. Chem.* **146** (2015) 191
18. P. Rai, M. Srivastava, J. Singh, J. Singh, *New J. Chem*. **38** (2014) 3181
19. S. Paul, K. Pradhan, S. Ghosh, S. De, A. R. Das, *Tetrahedron* **70** (2014) 6088
20. J. Feng, K. Ablajan, A. Sali, *Tetrahedron* **70** (2014) 484
21. R.-Y. Guo, Z.-M. An, L.-P. Mo, S.-T. Yang, H.-X. Liu, S.-X. Wang, Z.-H. Zhang, *Tetrahedron* **69** (2013) 9931
22. V. Y. Mortikov, Y. M. Litvinov, A. Shestopalov, L. Rodinovskaya, A. Shestopalov, *Russ. Chem. Bull.* **57** (2008) 2373
23. Y. Li, H. Chen, C. Shi, D. Shi, S. Ji, *J. Comb. Chem.* **12** (2010) 231
24. Y. Liu, D. Zhou, Z. Ren, W. Cao, J. Chen, H. Deng, Q. Gu, *J. Chem. Res.* **2009** (2009) 154
25. R. G. Redkin, L. A. Shemchuk, V. P. Chernykh, O. V. Shishkin, S. V. Shishkina, *Tetrahedron* **63** (2007) 11444
26. Y. Liu, Z. Ren, W. Cao, J. Chen, H. Deng, M. Shao, *Synth. Commun.* **41** (2011) 3620
27. K. Bahrami, M. M. Khodaei, P. Fattahpour, *Catal. Sci. Technol.* **1** (2011) 389
28. M. Mirza-Aghayan, N. Mohammadian, M. A. Malakshah, R. Boukherroub, A. Tarlani, *J. Iran. Chem. Soc.* **10** (2013) 559
29. G. Mohammadi Ziarani, A. Badiei, S. Mousavi, N. Lashgari, A. Shahbazi, *Chin. J. Catal.* **33** (2012) 1832
30. G. Mohammadi Ziarani, N. H. Mohtasham, N. Lashgari, A. Badiei, M. Amanlou, R. Bazl, *J. Nanostructure Chem.* **2** (2013) 489
31. E. A. A. Hafez, F. M. Abdul Galil, S. M. Sherif, M. H. Elnagdi, *J. Heterocycl. Chem.* **23** (1986) 1375
32. A. Shahbazi, H. Younesi, A. Badiei, *Chem. Eng. J.* **168** (2011) 505
33. A. Badiei, H. Goldooz, G. Mohammadi Ziarani, *Appl. Surf. Sci.* **257** (2011) 4912.

SUPPLEMENTARY MATERIAL TO

Green one-pot, four-component synthesis of spiro[indoline-3,4′--pyrano[2,3-*c*]pyrazole] derivatives using amino-functionalized nanoporous silica under solvent-free conditions

GHODSI MOHAMMADI ZIARANI[1]*, MAHSHID RAHIMIFARD[1], FATEMEH NOURI[1] and ALIREZA BADIEI[2]

[1]*Department of Chemistry, Alzahra University, Vanak Square, P. O. Box 19938939973, Tehran, Iran and* [2]*School of Chemistry, College of Science, University of Tehran, Tehran, Iran*

SPECTRAL DATA FOR THE SPIRO[INDOLINE-3,4′-PYRANO[2,3-*c*]PYRAZOLE] DERIVATIVES **5a**–**f**

6′-Amino-3′-methyl-2-oxo-1′H-spiro[indoline-3,4′-pyrano[2,3-c]pyrazole]--5′-carbonitrile (**5a**). M.p.: 278–280 °C; Anal. Calcd. for $C_{15}H_{11}N_5O_2$: C, 61.43; H, 3.78; N, 23.88 %. Found: C, 61.51; H, 3.66; N, 23.69 %; IR (KBr, cm^{-1}): 3337 (NH stretching of secondary amine), 3389 and 3131 (NH_2 stretching of primary amine), 2182 (CN stretching of nitrile), 1712 (CO stretching of amide), 1641 (C=N stretching of pyrazole ring), 1583, 1519, 1497, 1470, 1410, 1319, 1285, 1207, 1154, 1053, 930, 754, 697; ^{1}H-NMR (400 MHz, DMSO-d_6, δ / ppm): 1.52 (3H, *s*, CH$_3$), 6.90 (1H, *d*, *J* = 7.6 Hz, Ar-H), 6.97–7.04 (2H, *m*, Ar-H), 7.22–7.26 (3H, *m*, Ar-H & NH$_2$), 10.60 (1H, *s*, NH), 12.29 (1H, *s*, NH); ^{13}C--NMR (62.9 MHz, DMSO-d_6, δ / ppm): 9.4, 47.7, 55.3, 95.8, 110.1, 119.2, 123.0, 124.3, 129.3, 133.0, 135.2, 141.8, 155.7, 162.9, 178.5; EIMS (*m*/*z* (relative abundance)): 293 (4), 267 (30), 208 (12), 179 (12), 152 (14), 140 (15), 115 (17), 66 (28), 43 (63), 29 (100).

6′-Amino-5-bromo-3′-methyl-2-oxo-1′H-spiro[indoline-3,4′-pyrano[2,3-c]-pyrazole]-5′-carbonitrile (**5b**). M.p.: 281–283 °C; Anal. Calcd. for $C_{15}H_{10}BrN_5O_2$: C, 48.41; H, 2.71; N, 18.82 %. Found: C, 48.51; H, 2.69; N, 18.90 %; IR (KBr, cm^{-1}): 3346 (NH stretching of secondary amine), 3133 (NH$_2$ stretching of primary amine), 2181 (CN stretching of nitrile), 1713 (CO stretching of amide), 1643 (C=N stretching of pyrazole ring), 1608, 1580, 1499, 1473, 1412, 1297, 1206, 1156, 1053, 922, 821, 692; ^{1}H-NMR (250 MHz, DMSO-d_6, δ / ppm): 1.55 (3H, *s*, CH$_3$), 6.86 (1H, *s*, Ar-H), 7.21–7.36 (4H, *m*, Ar-H and

---

* Corresponding author. E-mails: gmziarani@hotmail.com; gmohammadi@alzahra.ac.ir

NH$_2$), 10.75 (1H, *s*, NH), 12.33 (1H, *s*, NH); ^{13}C-NMR (62.9 MHz, DMSO-d_6, *δ* / ppm): 9.4, 47.9, 54.9, 95.1, 112.2, 114.6, 119.1, 127.7, 132.2, 135.2, 135.5, 141.1, 155.6, 162.9, 178.0.

*6'-Amino-1-benzyl-3'-methyl-2-oxo-1'H-spiro[indoline-3,4'-pyrano[2,3-*c*]-pyrazole]-5'-carbonitrile (5c)*. M.p.: 268–270 °C; Anal. Calcd. for C$_{22}$H$_{17}$N$_5$O$_2$: C, 68.92; H, 4.47; N, 18.27 %. Found: C, 68.71; H, 4.39; N, 18.47 %; IR (KBr, cm^{-1}): 3390 (NH stretching of secondary amine), 3235 and 3149 (NH$_2$ stretching of primary amine), 2197 (CN stretching of Nitrile), 1708 (CO stretching of amide), 1638 (C=N stretching of pyrazole ring), 1596, 1487, 1403, 1337, 1191, 1157, 1075, 1025, 913, 752, 705; ^{1}H-NMR (400 MHz, DMSO-d_6, *δ* / ppm): 1.34 (3H, *s*, CH$_3$), 4.91 (1H, *d*, *J* = 15.6 Hz, CH$_2$), 5.00 (1H, *d*, *J* = 15.6 Hz, CH$_2$), 7.02–7.07 (2H, *m*, Ar-H), 7.12 (1H, *d*, *J*= 6.4 Hz, Ar-H), 7.25–7.34 (6H, *m*, Ar-H & NH$_2$), 7.40 (2H, *d*, *J* = 7.2 Hz, Ar-H), 12.32 (1H, *s*, NH); ^{13}C-NMR (62.9 MHz, DMSO-d_6, *δ* / ppm): 9.4, 43.6, 47.5, 55.3, 95.6, 109.7, 119.2, 123.7, 124.9, 127.9, 129.0, 129.4, 132.3, 135.3, 136.5, 142.4, 155.7, 163.1, 177.1; EIMS (*m*/*z* (relative abundance)): 383 (10), 354 (12), 292 (35), 282 (35), 267 (20), 220 (10), 125 (10), 91 (36), 73 (44), 58 (100).

*6'-Amino-5-chloro-3'-methyl-2-oxo-1'H-spiro[indoline-3,4'-pyrano[2,3-*c*]-pyrazole]-5'-carbonitrile (5d)*. M.p.: 296–298 °C; Anal. Calcd. for C$_{15}$H$_{10}$ClN$_5$O$_2$: C, 54.97; H, 3.08; N, 21.37 %. Found: C, 55.01; H, 3.10; N, 21.43 %; IR (KBr, cm^{-1}): 3346 (NH stretching of secondary amine), 3135 (NH$_2$ stretching of primary amine), 2181 (CN stretching of nitrile), 1713 (CO stretching of amide), 1644 (C=N stretching of pyrazole ring), 1611, 1580, 1498, 1476, 1413, 1299, 1207, 1157, 1051, 949, 921, 973, 823, 692; ^{1}H-NMR (250 MHz, DMSO-d_6, *δ* / ppm): 1.56 (3H, *s*, CH$_3$), 6.89–7.31 (5H, *m*, Ar-H & NH$_2$), 10.76 (1H, *s*, NH), 12.34 (1H, *s*, NH) ppm; ^{13}C-NMR (62.9 MHz, DMSO-d_6, *δ* / ppm): 9.4, 48.0, 54.9, 95.1, 11.7, 119.1, 125.0, 127.0, 129.3, 135.1, 135.2, 140.7, 155.6, 162.9, 178.2.

*6'-Amino-2-oxo-3'-phenyl-1'H-spiro[indoline-3,4'-pyrano[2,3-*c*]pyrazole]--5'-carbonitrile (5e)*. M.p.: 279–281 °C; Anal. Calcd. for C$_{20}$H$_{13}$N$_5$O$_2$: C, 67.60; H, 3.69; N, 19.71 %. Found: C, 67.71; H, 3.69; N, 19.75 %; IR (KBr, cm^{-1}): 3385 (NH stretching of secondary amine), 3307 and 3239 (NH$_2$ stretching of primary amine), 2186 (CN stretching of nitrile), 1705 (CO stretching of amide), 1651 (C=N stretching of pyrazole ring), 1599, 1582, 1497, 1472, 1408, 1320, 1209, 1058, 857, 747, 677; ^{1}H-NMR (250 MHz, DMSO-d_6, *δ* / ppm): 6.73–7.28 (11H, *m*, Ar-H & NH$_2$), 10.52 (1H, *s*, NH), 12.92 (1H, *s*, NH); ^{13}C-NMR (62.9 MHz, DMSO-d_6, *δ* / ppm): 48.0, 56.7, 95.7, 110.2, 118.9, 122.9, 124.8, 127.6, 128.6, 128.8, 129.2, 129.4, 134.4, 139.4, 142.0, 156.3, 162.2, 178.6.

*Ethyl 6'-amino-3'-methyl-2-oxo-1'H-spiro[indoline-3,4'-pyrano[2,3-*c*]pyrazole]-5'-carboxylate (5f)*. M.p.: 280–282 °C; Anal. Calcd. for C$_{17}$H$_{16}$N$_4$O$_4$: C, 59.99; H, 4.74; N, 16.46 %. Found: C, 60.08; H, 4.77; N, 16.54 %; IR (KBr, cm^{-1}):

3385 (NH stretching of secondary amine), 3281 and 3188 (NH$_2$ stretching of primary amine), 3083 & 3027 (CH stretching of aromatic ring), 2925 and 2854 (CH stretching of alkyl groups), 1715 (CO stretching of amide), 1665 (C=N stretching of pyrazole ring), 1613, 1539, 1472, 1400, 1290, 1222, 1155, 1098, 1036, 923, 767; ^{1}H-NMR (250 MHz, DMSO-d_6, δ / ppm): 0.67 (3H, t, J = 7.5 Hz, CH$_3$), 1.55 (3H, s, CH$_3$), 3.65 (2H, q, J = 7.5 Hz , OCH$_2$), 6.78–7.08 (4H, m, Ar-H), 8.02 (2H, s, NH$_2$), 10.37 (1H, s, NH), 12.16 (1H, s, NH); ^{13}C-NMR (62.9 MHz, DMSO-d_6, δ / ppm): 9.3, 13.5, 47.4, 59.1, 74.5, 97.5, 109.1, 122.0, 123.0, 127.7, 131.9, 135.1, 137.0, 142.3, 154.8, 163.2, 168.6, 180.1; EIMS (m/z (relative abundance)): 340 (2), 312 (7), 267 (100), 239 (22), 170 (8), 68 (15), 42 (25), 29 (100).

Alkylating ability of carbohydrate oxetanes: Practical synthesis of bolaform skeleton derivatives

PAVLE A. HADŽIĆ[1]*[#], MIRJANA M. POPSAVIN[2][#] and SUNČICA Z. BOROZAN[3][#]

[1]*Goša Institute, Milana Rakića 35, 11000 Belgrade, Serbia,* [2]*Faculty of Sciences, Department of Chemistry, University of Novi Sad, Trg D. Obradovića 3, 21000 Novi Sad, Serbia and* [3]*Faculty of Veterinary Medicine, University of Belgrade, Bulevar oslobođenja 18, 11000 Belgrade, Serbia*

Abstract: The alkylating ability of the oxetane ring in the carbohydrate structure was investigated and a flexible method for the construction of a bolaform amphiplile skeleton with xylose as the polar head is proposed. The method is based on oxetane ring opening in the easily accessible 3,5-anhydro-1,2-*O*-cyclohexylidenexylofuranose (**1**). One-step nitrogen alkylation in terminal diamines with **1** gave the basic cationic bolaform skeleton with xylose as potential polar head and a deliberately chosen length of the non-polar spacer. Under similar experimental conditions, but with an appropriate mole ratio of the alkylating agent, the alkylation reaction provide for selective monoalkylation of the diamines. Successful alkylation in the xanthine series (theophylline) was also achieved with **1**, giving a new 5-deoxy-5-(1,2,3,6-tetrahydro-1,3-dimethyl--2,6-dioxo-7*H*-purin-7-yl)-*α*-D-xylofuranose derivative.

Keywords: bolaform skeleton; oxetane ring; alkylation; ring opening.

INTRODUCTION

Oxiranes and oxetanes, as highly strained heterocycles, are archetypical alkylating agents. Oxetanes are widely used in organic syntheses and are considered to be less carcinogenic and lack genotoxic capacity compared to epoxides and *β*-lactones.[1] The alkylating potential of the oxetane ring is a consequence of its ring strain, which was determined to be 106 kJ mol^{-1}, a value close to that of oxirane (112 kJ mol^{-1}).[2] However, the ring-opening reactions of oxetanes usually require powerful acid catalysts, or other specific catalysts providing for particular synthetic features.[3] The oxetane ring is for steric reasons rarely encountered in carbohydrates. When present, it frequently possesses interesting pharmaceutical properties and offers numerous possibilities for chemical transformations.[4] In

---

1273

this report, the high alkylation potential of the oxetane ring in the easily accessible 3,5-anhydro-1,2-*O*-cyclohexylidene-*α*-D-xylofuranose[5] (**1**) toward the nitrogen in aliphatic diamines and in xanthine series (Scheme 1) is presented.
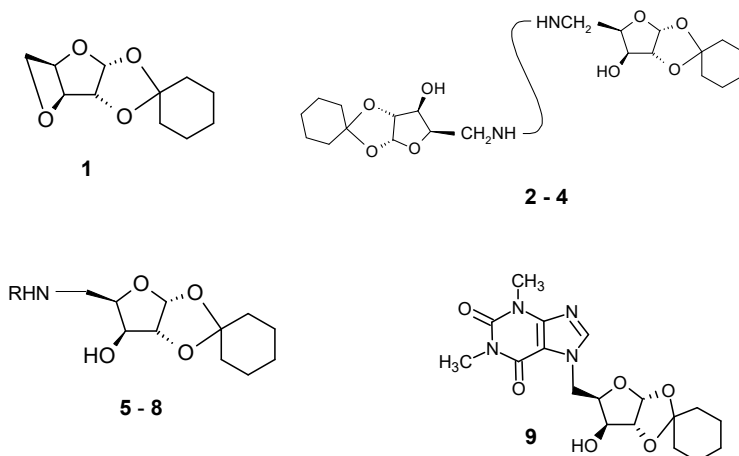
Scheme 1. Alkylation ability of 3,5-anhydro-1,2-*O*-cyclohexylidene-*α*-D-xylofuranose (**1**). Its use for basic bolaform skeleton synthesis (**2**–**4**, the graphical curve represent the hydrophobic spacer), selective monoalkylation of diamines (**5**–**8**), and alkylation in the xanthine series **9**.

From the practical standpoint, the alkylation of aliphatic diamines leads to one-step construction of basic cationic bolaform detergent skeleton, while in the xanthine series, a new type of 7-xylose substituted theophylline derivative was obtained under mild and operationally simple reaction conditions. All alkylations were performed under solvent-free reaction conditions, additionally illustrating alkylation potential of the carbohydrate oxetane ring.

EXPERIMENTAL

Thermal solid-state alkylation reactions are classical examples among solvent-free reactions, and not a new concept. In particular, the *N*-alkylation of phthalimides and heterocyclic systems, such as carbazole with alkyl halides, are known examples.[6] Unexpectedly, the high inclination of the oxetane structure in **1** toward nitrogen alkylation in this investigation enabled the realization of solvent-free reactions, giving benefits in product isolation procedures.

General reaction conditions. **1** and a diamine (1,2-diaminoethane, 1,4-diaminobutane, piperazine, *N*-methylpiperazine or theophylline from commercial suppliers and without further purification) were mixed in the appropriate mole ratio for alkylation of both nitrogen atoms, or selective alkylation of a single nitrogen in diamine compounds, with addition of water as catalyst. The reaction mixture was held in a hermetically sealed stainless steel reaction flask at temperature 110–130 °C for 12 h with occasional mixing. The products were isolated either as free bases, hydrochloride or oxalate salts (Table I).

Detailed experimental synthetic procedures and analytical data confirming the structures of the newly synthesized compounds are given in Supplementary material to this paper.

TABLE I. Products of alkylation of diamines and alkylation in xanthine series with a carbohydrate oxetane ring

Cmpd.	Alkylation position	Compound name
2	$-HNCH_2CH_2NH-$	5,5'-(1,2-Ethanediyldiimino)bis[1,2-*O*-cyclo-hexylidene-5-deoxy-*α*-D-xylofuranose]
3	$-HNCH_2(CH_2)_2CH_2NH-$	5,5'-(1,4-Butnediyldiimino)bis[1,2-*O*-cyclo-hexylidene-5-deoxy-*α*-D-xylofuranose]
4	$-N(CH_2CH_2)_2N-$	5,5'-(1,4-Piperazinediyl)bis[1,2-*O*-cyclohexylidene--5-deoxy-*α*-D-xylofuranose]
5	$H_2NCH_2CH_2NH-$	5-((2-Aminoethyl)amino)-1,2-*O*-cyclohexylidene-5--deoxy-*α*-D-xylofuranose dioxalate
6	$H_2NCH_2(CH_2)_2CH_2NH-$	5-((4-Aminobutyl)amino)-1,2-*O*-cyclohexylidene--5-deoxy-*α*-D-xylofuranose dioxalate
7	$HN(CH_2CH_2)_2N-$	1,2-*O*-Cyclohexylidene-5-deoxy-5-(1-piperazinyl)--*α*-D-xylofuranose
8	$CH_3N(CH_2CH_2)_2N-$	1,2-*O*-Cyclohexylidene-5-deoxy-5-(4-methyl-piperazin-1-yl)-*α*-D-xylofuranose
9		1,2-*O*-Cyclohexylidene-5-deoxy-5-(1,2,3,6-tetra-hydro-1,3-dimethyl-2,6-dioxo-7*H*-purin-7-yl)--*α*-D-xylofuranose

RESULTS AND DISCUSSION

Amphiphiles with two polar heads connected by a hydrophobic spacer (bola-amphiphiles) have attracted ever-increasing attention since similar structures were found in some archaebacteria cell membranes that sustain harsh environments, high salt concentrations and elevated ambient temperatures.[7] A range of bolaamphiphiles have been synthesized so far, either to imitate components of a natural cell structure, or to investigate their lipophilic–hydrophilic properties.[8] In attempts to realize specific properties, a variety of bolaform surfactants with a carbohydrate as the hydrophilic moiety have also been considered. Carbohydrate-based detergents are recognized, and convenient syntheses of compounds with variable lipophilic–hydrophilic balance based on xylose, in particular, as the polar head, or from other carbohydrate but with preserved *xylo*-configuration, are known.[9] Specifically, syntheses of bolaamphiphiles based on xylose are also described.[10] The authors affirmed earlier findings[11] on the significant impact of the length of the hydrophobic linkage (spacer) on the aggregation properties of bolaamphiphiles with sugar heads. Consequently, a simple synthetic method for the construction of the basic bolaform skeleton with xylose-based hydrophilic heads and deliberately preferred hydrophobic spacer length is intriguing. Herein, the alkylation ability of the oxetane ring in **1** toward terminal diamino compounds as a simple, practical and flexible method for the construction of the

cationic bolaform skeleton, or selective monoalkylation of aliphatic diamines and natural products are reported.

The opening of oxetane ring in 3,5-anhydro-derivatives of suitably protected[12] xylofuranose derivatives with aqueous ammonia[13] and amines[14] was investigated earlier. The reaction leads to one-step nitrogen alkylation. Under simple reaction conditions, the one-step dialkylation of α,ω-diamines of the general formula $H_2N–(CH_2)_n–NH_2$, or cyclic diamines (piperazine) with **1** lead smoothly to the basic bolaform skeleton **2**–**4**.

For further demonstration of akylating ability of carbohydrate oxetane **1**, the alkylation of diamines accomplished under essentially the same experimental conditions but with a different mole ratio of **1** toward the diamines resulted in selective monoalkylation of diamines **5**–**8**.

Frequently, prior activation of oxirane and oxetane rings is a necessary step in alkylation reactions and different catalysts are used for this purpose. Protonation of oxygen in oxetane ring significantly eases nucleophillic attack of nucleophillic species present and hence, the ring opening is facilitated by acids. As demonstrated earlier, water could also play the role of the catalyst,[15] and the present experiments afforded further experimental evidence on the subject. Particularly, water was found to be an appropriate catalyst for the alkylation tendency of **1**, owing to the expected significant strain energy release in the system of three condensed small rings in **1**.

Our previous investigations of the reactivity of the 3,5-anhydro ring in **1** towards selected nucleophiles demonstrated pronounced regioselectivity of the oxetane ring-opening process.[16] Again, it was found to be the case in the reaction of **1** with diamines. The only isolable products originated from the regioselective nucleophillic attack of nitrogen on the terminal carbon atom of xylofuranose (C-5). No detectable products of inversion at the C-3 carbon of starting **1** were found because of the hypothetic nucleophilic attack at C-3, *i.e.*, the *xylo*- configuration was preserved throughout.

To prove further the alkylating ability of the oxetane ring in the carbohydrate structure **1**, the alkylation of some natural products was considered. Many nitrogen-containing heterocycles demonstrate pronounced pharmaceutical activity. Among them, xanthine and substituted xanthine derivatives are an important class of compounds with a well-known spectrum of activity.[17] In particular, theophylline pentosides are the subject of intensive synthetic interest because of their structural resemblance to nucleosides. Theophylline-7-riboside was evaluated as a partial agonist for ubiquitous adenosine receptors[18] with the conclusion that it has characteristics between full agonists and full antagonists (xanthines). Following thee findings, further attempts were made to synthesize different 7-substituted xanthine derivatives with a modified ribose rest.[19] To the best of our knowledge, among other theophylline 7-pentofuranosides, arabinoside and xyloside are also known.[20]

In further experiments, it was found that alkylating potential of the oxetane ring in **1** could be used for the facile synthesis of a 7-xylose substituted theophylline derivative, however with a new pentose substitution pattern. Namely, all previously synthesized pentose derivatives were connected to theophylline through C1 xylose carbon.

Thus, the alkylation of theophylline with **1** smoothly gave 5-deoxy-5--(1,2,3,6-tetrahydro-1,3-dimethyl-2,6-dioxo-7*H*-purin-7-yl)-*α*-D-xylofuranose derivative **9**. However, theophylline did not react under the standard procedure (heating a mixture of diamine, oxetane **1** and water as catalyst), but further activation of the 7′-theophylline position was necessary, and hence the potassium salt of theophylline was prepared.[21]

CONCLUSIONS

The use of protected 3,5-anhydroxylofuranose as alkylating agent represent a new practical and adaptive method to reach the basic cationic bolaform skeleton with xylose-based polar heads and variable lengths of non polar spacer. The described one-step synthetic procedure give products that could be easily converted into carbohydrate polar heads with retained *xylo*-configuration, with deliberately chosen hydrophobic spacer length and in acceptable isolated yields. In the xanthine series, the alkylation provide for new 7-xylose substituted theophylline with the substitution pattern reversed to that previously described.

SUPPLEMENTARY MATERIAL

Description of specific synthesis methods and the analytical and spectral data of the synthesized compounds are available electronically from http://www.shd.org.rs/JSCS/, or from the corresponding author on request.

ИЗВОД

АЛКИЛУЈУЋИ ПОТЕНЦИЈАЛ УГЉЕНОХИДРАТНИХ ОКСЕТАНА: ПРАКТИЧНА СИНТЕЗА ДЕРИВАТА БОЛАФОРМНОГ СКЕЛЕТА

ПАВЛЕ А. ХАЏИЋ[1], МИРЈАНА М. ПОПСАВИН[2] и СУНЧИЦА З. БОРОЗАН[3]

[1]Институт Гоша, Милана Ракића 35, 11000 Београд, [2]Природно–математички факултет, Департман за хемију, Универзитет у Новом Саду, Трг Д. Обрадовића 3, 21000 Нови Сад и [3]Факултет ветеринарске медицине, Универзитет у Београду, Булевар ослобођења 18, 11000 Београд

Истражена је алкилујућа способност оксетанског прстена у структури угљених хидрата и предложена је флексибилна метода за синтезу скелета болаформних амфифила са ксилозом као поларном главом. Метода је заснована на реакцији отварања оксетанског прстена код лако доступне 3,5-анхидро-1,2-*O*-циклохексилиден ксилофуранозе (**1**). Алкиловање на атому азота код терминалних диамина са **1** даје основни болаформни скелет са заштићеном ксилозом као потенцијалном хидрофилном главом и по вољи изабраном дужином хидрофобног тела. У сличним реакционим условима, али са другачијим одговарајућим молским односом алкилујућег агенса, остварено је селективно моноалкиловање диамина. Такође, остварено је успешно алкиловање у структури ксантина, при чему је добијен раније неописани дериват ксантина 1,2-*O*-циклохекси-

лиден-5-деокси-5-(1,2,3,6-тетрахидро-1,3-диметил-2,6-диоксо-7*H*-пурин-7-ил)-*α*-D-кси-лофураноза.

REFERENCES

1. a) R. Gómez-Bombarelli, B. B. Palma, C. Martins, M. Kranendonk, A. S. Rodrigues, E. Calle, J. Rueff, J. Casado, *Chem. Res. Toxicol.* **23** (2010) 1275; b) R. G. Bombarelli, *PhD Thesis*, Universidad de Salamanca, Spain, 2011
2. a) B. Rigner, S. Sunner, H. Watanabe, *Acta Chem. Scand.* **25** (1971) 141; b) S. W. Benson, C. R. Vickshank, D. M. Golden, G. R. Haugen, H. E. O'Neal, A. S. Rodgers, R. Shaw, R. Walsh, *Chem. Rev.* **69** (1969) 279
3. a) Z. Wang, Z. Chen, J. Sun, *Org. Biomol. Chem.* **12** (2014) 6028; b) A. Harrane, N. Naar, M. Belbachir, *Mater. Lett.* **61** (2007) 3555; c) B. Guo, J. T. Njardarson, *Chem. Commun.* **49** (2013) 10802; d) R. N. Loy, E. N. Jacobsen, *J. Am. Chem. Soc.* **131** (2009) 2786
4. F. Ç. Telli, K. Ay, G. Murat, G. Kök, Y. Salman, *Med. Chem. Res.* **22** (2013) 2253
5. M. Kawana, H. Kuzuhara, S. Emoto, *Bull. Chem. Soc. Jpn.* **54** (1981) 1492
6. a) D. Bogdal, J. Pielichowsky, A. Boron, *Synlett.* (1996) 873; b) D. Bogdal, J. Pielichowsky, K. Jascot, *Synth. Commun.* **45** (1997) 715
7. a) G. H. Escamilla, G. R. Newkome, *Angew. Chem. Int. Ed. Engl.* **33** (1994) 1937; b) T. Benvegnu, M. Brard, D. Plusquellec, *Curr. Opin. Colloid Interface Sci.* **8** (2004) 469
8. a) J. H. Fuhrhop, T. Y. Wang, *Chem. Rev.* **104** (2004) 2901; b) A. Meister, A. Blume, *Curr. Opin. Colloid Interface Sci.* **12** (2007) 138
9. a) S. R. Borkar, B. N. Manjunath, B. Sivaraman, I. S. Aidhen, *Carbohydr. Res.* **358** (2012) 23; b) P. Hadzic, M. Popsavin, *Carbohydr. Res.* **345** (2010) 543
10. a) C. Damez, S. Bouquillon, D. Harakat, F. Hénin, J. Muzart, I. Pezron, L. Komunjer, *Carbohyd. Res.* **342** (2007) 154; b) M. Deleu, C. Damez, S. Gatard, K. Nott, M. Paquot, S. Bouquillon, *New J. Chem.* **35** (2011) 2258; c) M. Deleu, S. Gatard, E. Payen, L. Lins, K. Nott, C. Flore, R. Thomas, M. Paquot, S. Bouquillon, *C. R. Chim.* **15** (2012) 68
11. F. Brisset, R. Garelli-Calvet, J. Azema, C. Chebli, I. Rico-Lattes, A. Lattes, *New J. Chem.* **20** (1996) 595
12. Z. S. Kovačević, R. L. Jevrić, O. S. Podunavac-Kuzmanović, D. N. Kalajdžija, S. E. Lončar, *Acta Chim. Slov.* **60** (2013) 420
13. B. Helferich, M. Burgdorf, *Tetrahedron* **3** (1958) 274
14. P. Hadžić, N. Vukojević, *Carbohydr. Res.* **338** (2003) 1243
15. H. Reiff, D. Dieterich, R. Braden, H. Ziemann, *Liebigs Ann. Chem.* (1973) 365
16. P. Hadžić, N. Vukojević, M. Popsavin, J. Čanadi, *J. Serb. Chem. Soc.* **66** (2001) 1
17. a) R. V. Kalla, E. Elzein, T. Perry, X. Li, V. Palle, V. Varkhedkar, A. Gimbel, T. Maa, D. Zeng, J. Zablocki, *J. Med. Chem.* **49** (2006) 3682; b) R.-Y. Lin, B.-N. Wu, Y.-C. Lo, L.-M. An, Z.-K. Dai, Y.-T. Lin, C.-S. Tang, I.-J. Chen, *Pharmacol. Exp. Ther.* **316** (2006) 709; c) K. Ito, S. Lim, G. Caramori, B. Cosio, K. F. Chung, I. M. Adcock, P. J. Barnes, *Proc. Natl. Acad. Sci. USA. A* **99** (2002) 8921
18. A. P. Ijzerman, E. M. van der Venden, J. K. von Frijtag Drabbe Kűnzel, R. A. A. Mathôt, M. Danhof, P. A. Boreal, K. Varani, *Arch. Pharmacol.* **350** (1994) 638
19. a) R. V. Kalla, E. Elzein, T. Perry, X. Li, V. Palle, M. A. N. Mosselhi, *Nucleosides Nucleotides* **12** (1993) 432; b) Z. Wang, Z. Chen, J. Sun, *Org. Biomol. Chem.* **12** (2014) 6028
20. a) P. A. Levene, H. Sobotka, *J. Biol. Chem.* **65** (1925) 463; b) J. Pryde, T. R. Williams, *J. Chem. Soc.* (1933) 640
21. D. B. Ishay, *J. Chem. Soc.* (1956) 3975.

Alkylating ability of carbohydrate oxetanes: Practical synthesis of bolaform skeleton derivatives

PAVLE A. HADŽIĆ[1]*, MIRJANA M. POPSAVIN[2] and SUNČICA Z. BOROZAN[3]

[1]Goša Institute, Milana Rakića 35, 11000 Belgrade, Serbia, [2]Faculty of Sciences, Department of Chemistry, University of Novi Sad, Trg D. Obradovića 3, 21000 Novi Sad, Serbia and [3]Faculty of Veterinary Medicine, University of Belgrade, Bulevar oslobođenja 18, 11000 Belgrade, Serbia

GENERAL METHODS

The melting points were determined on a Büchi MP 50 apparatus and are not corrected. The NMR spectra were recorded on a Bruker AC250E instrument in $CDCl_3$ or D_2O, using Me_4Si as an internal standard. The mass spectra were recorded with a Thermo Finnigan Polaris Q or Finnigan MAT 8230BE spectrometer using the CI technique. TLC was performed on Silica gel DC Alufolien (Merck, Darmstadt), with 4:1 toluene–EtOAc as the mobile phase. The polarity of the mobile phase was augmented by the addition of MeOH or diethylamine when necessary. Visualization of the spots was achieved by spraying with 50 % sulfuric acid, followed by subsequent heating at 150 °C. The organic extracts were dried with anhydrous Na_2SO_4. The solutions were concentrated using a rotary evaporator under diminished pressure. Active carbon was used as decolorizing agent.

The practical way of performing the reaction of diamines with oxetane **1** consists in heating of the appropriate oxetane/amine mixture with occasional stirring in a closed vessel.

SPECIFIC SYNTHESES AND CHARACTERIZATION DATA

*5,5'-(1,2-Ethanediyldiimino)bis[1,2-*O*-cyclohexylidene-5-deoxy-α-*D*-xylofuranose] dihydrochloride (**2**)*

A mixture of oxetane **1** (3.2 g, 15 mmol), 1,2-diaminoethane monohydrate (0.35 g, 4.49 mmol) and water (5 drops) was heated in a closed vessel for 12 h at 110 °C. After cooling, the mixture was co-distilled with water to remove the

---

* Corresponding author. E-mail: pavle.hadzic@institutgosa.rs

unreacted diaminoethane; the crude product was dissolved in chloroform, washed several times with brine and evaporated to leave a red oil. The residue was dissolved in acetone and treated with a concentrated hydrochloric acid in acetone to pH 3. Light yellow precipitate was collected, air-dried and crystallized from 2-propanol–methanol to give pure **2** as the hydrochloride salt.

Yield: 0.81 g, 32.4 %; white crystals; m.p.: 240 °C (decomp.); Anal. Calcd. for $C_{24}H_{40}N_2O_8 \cdot 2HCl$: C, 51.70; H, 7.59; N, 5.02 %. Found: C, 51.56; H, 7.55; N, 5.07 %; CI MS (*m/z* (relative abundance, %)): 484 (M$^+$ for free base, 4), 405 (23), 327 (100), 242 (90), 211 (73).

*5,5′-(1,4-Butnediyldiimino)bis[1,2-*O*-cyclohexylidene-5-deoxy-α-D-xylofuranose]dihydrochloride (3)*

A mixture of oxetane **1** (4 g, 18 mmol), 1,4-diaminobutane (0.7 g, 8 mmol) and water (5 drops) was heated in a closed vessel for 12 h at 110 °C. The crude reaction mixture was dissolved in 1:1 diethyl ether–ethyl acetate, the solution washed with water, dried, decolorized and the solvent evaporated to oil. The oil was dissolved in MeOH, diluted with water to form a milky emulsion, and then left in the cold for 48 h. The separated solid was collected, air-dried and dissolved in acetone. An addition of aqueous hydrochloric acid in acetone, followed by an addition of a small amount of diethyl ether deposited the crude hydrochloride salt that was collected, air dried and recrystallized from MeOH–diethyl ether to give pure **3** as the hydrochloride salt, white crystals. The melting point determination revealed deterioration of substance without a sharp melting point at temperatures above 220 °C.

Yield: 1.42 g, 30.3 %, white crystals: Anal. Calcd. for $C_{26}H_{44}N_2O_8 \cdot 2HCl$: C, 53.33; H, 7.69; N, 4.78 %. Found: C, 53.22; H, 7.86; N, 4.80 %; CI MS (*m/z* (relative abundance, %)): 512 (M$^+$ for free base, 5), 428 (15), 412 (17), 355 (100).

*5,5′-(1,4-Piperazinediyl)bis[1,2-*O*-cyclohexylidene-5-deoxy-α-D-xylofuranose] (4)*

A mixture of oxetane **1** (2.12 g, 10 mmol), piperazine (0.5 g, 5 mmol) and water (2 drops) was heated in a closed vessel for 12 h at 130 °C. After cooling, the reaction mixture (a creamy solid) was dissolved in aqueous hydrochloric acid and washed with diethyl ether. The aqueous phase was separated, rendered alkaline (aq. Na_2CO_3) and extracted with chloroform. The extract was washed with water, dried, decolorized and evaporated to a colorless oil, which solidified spontaneously. Crystallization from dichloromethane–isooctane gave pure **4**.

Yield: 1.32 g, 52 % (based on piperazine); white crystals; m.p.: 158 °C; Anal. Calcd. for $C_{26}H_{42}N_2O_8$: C, 61.15; H, 8.29; N, 5.48 %. Found: C, 60.88; H, 8.26; N, 5.51 %; CI MS (*m/z* (relative abundance, %)): 510 (M$^+$, 5), 467 (17), 353 (100), 311 (82), 255 (137).

*5-((2-Aminoethyl)amino)-1,2-*O-*cyclohexylidene-5-deoxy-α-D-xylofuranose dioxalate (**5**)*

A mixture of oxetane **1** (2.12 g, 10 mmol), 1,2-diaminoethane monohydrate (3.9 g, 50 mmol), ethylene glycol (4 mL) and tap water (5 drops) was heated in a closed vessel for 12 h at 110 °C. The crude reaction mixture was dissolved in MeOH, diluted with water (30 mL) and concentrated to remove unreacted diaminoethane by distillation under diminished pressure. The residue was extracted with dichloromethane and the combined extracts were decolorized, dried, and evaporated. The remaining mass was dissolved in MeOH and filtered through a short pad of silica. The main fraction was evaporated, dissolved in acetone and treated with solution of oxalic acid dihydrate in acetone (2.88 g, 22.8 mmol). The white precipitate was collected and air-dried. Crystallization from methanol–water gave pure **5**.

Yield: 3.20 g, 73 %; white crystals; m.p.: 205–209 °C. Anal. Calcd. for the dioxalate, salt $C_{13}H_{24}N_2O_4 \cdot 2C_2H_2O_4$: C, 45.13; H, 6.24; N, 6.19 %. Found: C, 44.78; H, 6.45; N, 6.18 %.

*5-((4-Aminobutyl)amino)-1,2-*O-*cyclohexylidene-5-deoxy-α-D-xylofuranose dioxalate (**6**)*

A mixture of oxetane **1** (2.12 g, 10 mmol), 1,4-diaminobuthane (4.4 g, 48 mmol), ethylene glycol (4 mL) and water (5 drops) was heated in a closed vessel for 12 h at 110 °C. After cooling to room temperature, the mixture was triturated with dichloromethane, filtered and the organic solution was washed with water, dried, decolorized and evaporated to leave a light yellow oil (2.7 g). The oil was dissolved in acetone and treated with a solution of oxalic acid dihydrate (2.88 g, 22.8 mmol) in acetone to deposit a white precipitate. Recrystallization from MeOH–water gave pure **6**. The melting point determination revealed gas evolution and deterioration of the substance without melting at temperatures above 175 °C.

Yield: 3.46 g, 72 %; white crystals; Anal. Calcd. for $C_{15}H_{28}N_2O_4 \cdot 2C_2H_2O_4$: C, 47.50; H, 6.71; N, 5.83 %. Found: C, 47.71; H, 6.92; N, 5.43 %.

*1,2-*O-*Cyclohexylidene-5-deoxy-5-(1-piperazinyl)-α-D-xylofuranose (**7**)*

A mixture of oxetane **1** (2.0 g, 9.4 mmol), piperazine (3.0 g, 34.8 mmol), ethylene glycol (4 mL) and tap water (5 drops) and catalytic amount of lactic acid (one drop) was heated in a closed vessel, with occasional shaking for 12 h at 120 °C. The reaction mixture was then dissolved in chloroform and the organic layer washed several times with aqueous sodium carbonate. The chloroform solution was decolorized, dried and evaporated to leave a yellow oil that showed no presence of the starting oxetane (by TLC), but showed a minor spot for dialkylated piperazine, apart from the main spot corresponding to the monoalkylated piper-

azine. The obtained oil was dissolved in acetone; the resulting solution was decolorized again, and concentrated to a small volume. On addition of *n*-pentane while cooling, pure **7** was obtained.

Yield: 1.75 g, 62 %; white crystals; m.p.: 127–130 °C; Anal. Calcd. for $C_{15}H_{26}N_2O_4$: C, 60.38; H, 8.78; N, 9.39 %. Found: C, 60.06; H, 8.80; N, 9.17 %; CI MS (*m/z* (relative abundance, %)): 298 (M$^+$, 3), 255 (21), 183 (8), 141 (28), 99 (100).

1,2-O-Cyclohexylidene-5-deoxy-5-(4-methylpiperazin-1-yl)-α-D-xylofuranose (8)

A mixture of oxetane **1** (2 g, 9.4 mmol), *N*-methylpiperazine (1.50 g, 15 mmol) and tap water (5 drops) was heated in a closed vessel for 12 h at 110 °C. At this time, complete disappearance of the starting oxetane was found (by TLC). Unreacted *N*-methylpiperazine was removed by co-distillation with toluene under diminished pressure to leave light yellow oil that crystallized on standing. The crude crystals were dissolved in boiling hexane (80 mL), the solution concentrated to a smaller volume (25–30 mL) and left in the cold to give **8**.

Yield: 2.2 g, 73 %; white crystals; m.p.: 101–103 °C; Anal. Calcd. for $C_{16}H_{28}N_2O_4 \cdot 0.5H_2O$: C, 60.16; H, 9.10; N, 8.90 %. Found: C, 59.79; H, 9.09; N, 8.72 %; CI MS (*m/z* (relative abundance, %)): 313 (M$^+$+1, 25), 269 (32), 155 (90), 140 (23), 70 (100).

1,2-O-Cyclohexylidene-5-deoxy-5-(1,2,3,6-tetrahydro-1,3-dimethyl-2,6-dioxo--7H-purin-7-yl)-α-D-xylofuranose (9)

Theophylline, potassium salt. A solution of theophylline (9 g, 50 mmol) and potassium hydroxide pellets (2.8 g, 50 mmol) in water (50 mL) was evaporated to dryness. The remaining white mass was ground to powder and considered as the potassium salt of theophylline.

A mixture of oxetane **1** (1.4 g, 6.6 mmol), potassium salt of theophylline (2 g, 9.2 mmol), ethylene glycol (1.5 mL) and tap water (5 drops) was heated in a closed vessel for 12 h at 160 °C with occasional shaking. After this time, the TLC analysis revealed full disappearance of the starting oxetane and the formation of the product with an R_f value of 0.5 (ethyl acetate). The crude reaction mixture was dissolved in ethyl acetate, washed with brine, dried and decolorized. Evaporation of the solvent left an oil that was chromatographed on a silica gel column with ethyl acetate to give pure **9**.

Yield: 1.4 g, 54 %; colorless viscous oil; CI MS (*m/z* (relative abundance, %)): 392 (M$^+$, 19), 345 (32), 277 (36), 194 (45), 180 (100).

1
2
3
4

5   TABLE S-I. ^{1}H-NMR spectral data for **2**–**9**; cy – cyclohexylidene

Cmpd.	Chemical shifts of xylose protons, ppm						Coupling constants, Hz					Other signals, ppm
	H-1	H-2	H-3	H-4	H-5$_a$	H-5$_b$	$J_{1,2}$	$J_{3,4}$	$J_{4,5a}$	$J_{4,5b}$	$J_{5a,5b}$	
2[a]	6.18 (d)	4.80 (d)	4.46 (d)	4.60 (m)	3.49–3.75 (m)		3.5	1.6				1.41–1.91 (*m*, cy); 3.49–3.75 (*m*, N–**CH₂CH₂**–N)
3[a]	6.06 (d)	4.69 (d)	4.31 (d)	4.44 (m)	3.32 (dd)	3.42 (dd)	3.7	2.7	7.3	3.4	13.6	1.31–1.90 (*m*, cy and N–CH₂**CH₂CH₂**CH₂–N); 3.14 (*m*, N–**CH₂**CH₂CH₂**CH₂**–N)
4[b]	5.93 (d)	4.46 (d)	4.27 (d)	4.09 (m)	2.82 (dd)	3.05 (dd)	3.7	2.2	2.4	2.6	14.5	1.12–1.75 (*m*, cy); 2.05–4.0 (*bs*, piperazine); 7.60 (*bs*, OH)
5[a]	6.06 (d)	4.68 (d)	4.32 (d)	4.44 (m)	3.33–3.55 (m)		3.6	2.8				1.28–1.73 (*m*, cy); 3.33–3.55 (*m*, N–**CH₂CH₂**–N)
6[a]	6.17 (d)	4.80 (d)	4.42 (d)	4.55 (m)	3.44 (dd)	3.54 (dd)	3.5	2.6	7.5	3.5	13.7	1.36–1.94 (*m*, cy and N–CH₂**CH₂CH₂**CH₂–N); 3.08–3.30 (*m*, N–**CH₂**CH₂CH₂**CH₂**–N)
7[b]	5.93 (d)	4.45 (d)	4.27 (d)	4.10 (m)	2.32–2.97 (m)	3.06 (dd)	3.6	2.2		2.7	14.7	1.28–1.75 (*m*, cy); 2.32–2.97 (*m*, piperazine protons, NH)
8[b]	5.89 (d)	4.41 (d)	4.23 (d)	4.07 (m)	2.81 (dd)	3.03 (dd)	3.7	2.5	2.8	2.8	14.5	1.25–1.66 (*m*, cy); 2.19 (*s*, CH₃); 2.24–2.65 (*bs*, piperazine); 7.60 (*bs*, OH)
9[c]	5.93 (d)	4.54 (d)	4.19 (d)	4.33 (td)	4.38 (dd)	4.76 (dd)	3.6	2.6	4.8	6.3	13.2	1.23–1.69 (*m*, cy); 3.37 (*s*, N–CH₃); 3.56 (*s*, N–CH₃); 7.74 (s, H8 from xanthine)

6   [a]D₂O; [b]CDCl₃; [c]CDCl₃+D₂O

7

8   TABLE S-II. ^{13}C-NMR spectral data for **2**–**9**; cy – cyclohexylidene

Cmpd.	Chemical shifts of xylose carbons, ppm						Other signals, ppm
	C-1	C-2	C-3	C-4	C-5	C-1cy	
2[a]	107.10	87.02	77.47	78.54	49.69	116.61	25.90, 26.31, 26.87, 37.45, 38.23 (cy), 46.36 (–**CH$_2$**–**CH$_2$**–)
3[a]	107.08	87.03	77.43	78.65	49.02	116.55	25.36 (–CH$_2$**CH$_2$CH$_2$**CH$_2$–); 25.90, 26.31, 26.86, 37.43, 38.21 (cy), 50.05 (–NHCH$_2$–)
4[b]	104.22	85.01	77.82	76.75	56.85	111.90	23.47, 23.80, 24.83, 35.49, 36.26 (cy), 54.62 (piperazine carbons)
5[a]	107.10	87.01	77.45	78.56	49.65	116.62	25.87, 26.29, 26.84, 37.42, 38.17 (cy), 38.17 & 47.50 (–**CH$_2$**–**CH$_2$**–), 169.17 (carbonyl from oxalate)
6[b]	107.07	87.01	77.41	78.63	49.00	116.54	25.90, 26.30, 26.68, 37.41, 38.19, 25.21, 26.84 (cy & –HN–CH$_2$**CH$_2$CH$_2$**CH$_2$–NH–), 41.60 & 50.10 (–HN–**CH$_2$**CH$_2$CH$_2$**CH$_2$**–NH–), 169.05 (carbonyl from oxalate)
7[b]	104.31	85.13	77.87	76.93	57.78	111.94	23.55, 23.88, 24.90, 35.58, 36.36 (cy), 46.03, ((CH$_2$)$_2$NH), 55.94 ((**CH$_2$)$_2$**N–**CH$_2$**–)
8[b]	104.20	85.02	77.70	76.85	56.92	111.81	23.44, 23.76, 24.80, 35.49, 36.30 (cy), 45.77 (CH$_3$), 54.51 and 54.99 (piperazine carbons)
9[c]	104.15	84.78	73.96	79.96	44.90	112.44	23.35, 23.67, 24.64, 35.32, 36.09 (cy), 28.06 and 29.78 (2×CH$_3$), 106.61, 142.63, 148.95, 151.19 & 155.74 (C-5, C-8, C-4, C-2 and C-6 from xanthine part

9   [a]D$_2$O; [b]CDCl$_3$; [c]CDCl$_3$+D$_2$O

Enhancement of amylase production by *Aspergillus* sp. using carbohydrates mixtures from triticale

BILJANA DOJNOV[1]*, MARICA GRUJIĆ[2], BOJANA PERČEVIĆ[2] and ZORAN VUJČIĆ[2]

[1]*Department of Chemistry, Institute of Chemistry, Technology and Metallurgy, University of Belgrade, Njegoševa 12, Belgrade, Serbia and* [2]*Department of Biochemistry, Faculty of Chemistry, University of Belgrade, Studentski trg 12–16, Belgrade, Serbia*

Abstract: With the purpose of finding a suitable available inducer in combination with starvation, carbohydrate mixtures from triticale were used and compared with well-known amylase inducers in fungi. Carbohydrate mixtures from triticale induced the production of an amylase cocktail (*α*-amylase and glucoamylase) in *Aspergillus niger*, unlike induction with well-known inducers that induce only glucoamylase, shown by zymography and TLC analysis of the carbohydrate mixtures before and after fermentation. Glucoamylase production by *A. niger* was the highest in the presence of the extract obtained after autohydrolysis of starch from triticale (95.88 U mL^{-1}). Carbohydrate mixtures from triticale induced the production of *α*-amylase in *A. oryzae*. More *α*-amylase isoforms were detected when using a complex carbohydrate mixture, compared to induction with maltose or starch. A 48-h induction was the most efficient using a triticale extract (101.35 U mL^{-1}). Carbohydrates from triticale extracts could be used as very good cheap amylase inducers. Triticale, still not fully utilized, could be taken into consideration as an inducer in amylase production by *Aspergillus* sp, and in such a way, it could be used as the sole substrate in fermentation.

Keywords: *α*-amylase; glucoamylase; maltose; starch; enzyme production; fungi.

INTRODUCTION

The fungi *Aspergillus* sp. are well-known producers of amylases, which are industrially important enzymes. Filamentous fungi produce hydrolytic enzymes in the form of enzymes mixtures – cocktails. Glucoamylase and *α*-amylase are produced concomitantly in fungal fermentations.[1–4]

Maximal production of the enzymes may be achieved by using appropriate inducer molecules. Induction is the main controlling mechanism in the pro-

1279

duction of amylases in fungi. The effects of small molecules on amylase production were examined even when using complicated bioreactors.[5] It is known that α-amylase and glucoamylase are inducible enzymes in *Aspergillus* sp.[6] The induction mechanism of amylase production in *Aspergillus* sp. has been successfully studied.[7,8] Induction study of α-amylase production in *A. oryzae* began in 1961.[9] Starch and its hydrolysis products, mostly studied is maltose, are known inducer of α-amylase in *A. oryzae*.[10–12] Maltose is also a good glucoamylase inducer in *A. niger*.[13] Starvation launches a special mechanism leading to increased amylase production in *Aspergillus* sp.[14]

Considering all the above known, the induction mechanisms and the fact that *Aspergillus* sp. produce concomitantly α-amylase and glucoamylase, a cost-effective fermentation could be optimized by using inducers for the production of special amylase cocktail. This brought about the idea to examine the possibility of using a carbohydrate mixture from triticale (x *Triticosecale*, Wittmak). Triticale is an important industrial crop insufficiently utilized yet. Triticale cultivation has many benefits compared to other crops and its production and use have been intensively studied.[5,15] Triticale contains high amounts of starch (about 60 %) and protein (from 12 to 15 %).[16] It also contains higher amounts of major mineral elements (K, P and Mg) and nutritionally important minor elements (Na, Mn, Fe, Cu and Zn) than wheat.[17]

The opportunity of using cost effective and available carbohydrate mixtures from triticale as inducers of amylase in the two most important fungal producers of amylase, *A. niger* and *A. oryzae*, were examined in this study. Two kinds of triticale extracts, starchy extract and the extract obtained after starch hydrolysis by endogenous amylases were used as the sole fermentation substrates in submerged fermentation (SmF) and were compared with synthetic media containing the known inducers maltose and starch. The induction mechanisms were combined with mycelial starvation to cover all known methods of induction.

EXPERIMENTAL

Reagents

All used reagents and solvents were of the highest purity and purchased from Merck and Sigma–Aldrich. Triticale (x *Triticosecale* sp.) "Rtanj" line was obtained from the "Center for Small Grains Kragujevac", Kragujevac, Serbia.

Microorganisms and fermentation conditions

Aspergilus niger ATCC 10864 and *A. oryzae* ATCC 56747 strains were cultivated while obtaining matured spores. Spore suspensions were prepared in a 0.1 % Tween 80 solution at a concentration of 5.9×10^5 spores mL^{-1}.

Fermentations

Two parallel fermentations were performed with *A. niger* and *A. oryzae*. Submerged fermentations (SmF) were performed for 73 h at 30 °C and 210 rpm. The spore suspensions (10 vol. %) were inoculated in Czapec solution with 0.5 % yeast extract. Fungal mycelia

obtained in 18 h (5 %) were transferred into induction or non-induction media, as shown in experiments scheme in Fig. 1. Fungal mycelia were washed twice with water and dried with filter paper between the experimental phases shown in schematic diagram. Fermentations were stopped after scheduled time (Fig. 1) by centrifugation of the biomass for 15 min at 5000×g.
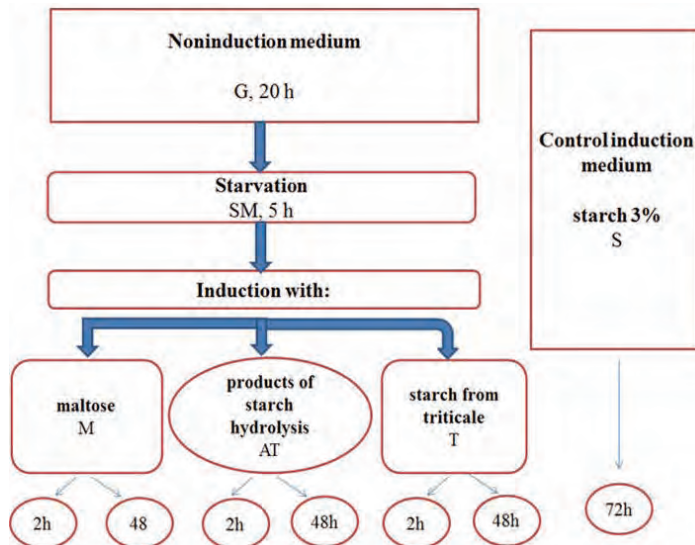
Fig. 1. Schematic presentation of amylase induction in *A. niger* and *A. oryzae*. MG – medium with glycerol, SM – starvation medium, MM – medium with maltose, AT – autohydrolysate of triticale extract, T – Triticale extract, MS – Medium with starch. Compositions of specified substrates are given in Table I.

TABLE I. The compositions of the media used in the fermentations by *A. niger* and *A. oryzae* following the scheme shown in Fig. 1

Medium		Composition
MG	Medium with glycerol	Peptone 20 g L^{-1}; glycerol 30 g L^{-1}; KH$_2$PO$_4$ 5 g L^{-1}; MgSO$_4$ 2.5 g L^{-1}
SM	Starvation medium	KH$_2$PO$_4$ 5g L^{-1}; MgSO$_4$ 2.5 g L^{-1}
MM	Medium with maltose	Peptone 20 g L^{-1}; maltose 30 g L^{-1}; KH$_2$PO$_4$ 5g L^{-1}; MgSO$_4$ 2.5 g L^{-1}
AT	Autohydrolysate of triticale extract	Decanted extract obtained after incubation of milled triticale (x *Triticosecale* sp.) and water in 1:3 ratio, autohydrolysis at 60 °C for 3 h[a]
T	Triticale extract	Decanted extract obtained from mixing milled triticale (x *Triticosecale* sp.) and water in 1:3 ratio without auto hydrolysis of starch
MS	Medium with starch	Peptone 20 g L^{-1}; raw starch 30 g L^{-1}; KH$_2$PO$_4$ 5 g L^{-1}; MgSO$_4$ 2.5 g L^{-1}

[a]Preparation of autohydrolysate of the triticale extract is described in the Experimental, *Media preparation*

Media preparation

The compositions of the media used in the examination of the induction of amylase production by *Aspergillus* sp. are given in Table I.

Triticale was finely ground to flour using a "Bragal" mill. The triticale flour was suspended in water (1:3 *w/V* ratio), mixed and strained through a strainer to obtain the triticale extract (T). The autohydrolysate of triticale (AT) was prepared by incubation of suspension of triticale flour and water (1:3 *w/V* ratio) for 3 h at 60 °C.[18] The obtained suspension was strained through a strainer to separate the liquid from solid part. The liquid phase was used as the AT. The other media were prepared by mixing the individual components. All media were autoclaved under standard conditions prior to use.

Amylase activity assay

The amylase activity was assayed at pH 5.0 according to the dinitrosalicylic acid (DNS) procedure[19] using of 1.0 % (*w/V*) soluble starch as substrate, for 30 min at 35 °C. Maltose was used as the standard. Each data point represents the mean of three independent assays (standard error, SE, values were less than 5 % of the means). One unit of α-amylase activity was defined as the amount of enzyme required to produce 1 µmol of maltose in 1 min at 35 °C.

Glucoamylase activity assay

Glucoamylase activity was assayed at pH 5.0 using 1.0 % (*w/V*) soluble starch as the substrate in 30 min at 35 °C. Glucose (final product of the reaction) was detected in the reaction mixture by coupled reaction with glucose oxidase and horseradish peroxidase (HRPO, Trinder reagent). Each data point represents the mean of three independent assays (*SE* values were less than 5 % of the means). One unit of glucoamylase activity was defined as the amount of enzyme required to produce 1 µmol of glucose in 1 min at 35 °C.

Zymographic detection of α-*amylase and glucoamylase*

α-Amylase and glucoamylase were detected simultaneously using zymography.[4] α-Amylase was detected in a PAA (polyacrylamide) gel with copolymerized β-limit dextrins, stained by iodine solution. The α-amylase activity appeared as clear bands on a purple background. Both amylases were detected as clear bands on a blue background, using soluble starch as substrate and iodine solution for staining, in the native EF (electrophoresis) PAA gel after printing. Glucoamylases were detected on an NC (nitrocellulose) membrane using a substrate solution (1.0 % (*w/V*) starch in buffer) and a reaction mixture for glucose detection (glucose oxidase, HRPO and 4-Cl-α-naphthol as substrate). Specific reaction product, purple and insoluble, appeared on the NC in bands corresponding to glucoamylase.

Starch, reducing sugar and glucose concentrations

The concentrations of starch in triticale extract and triticale autohydrolysate were determined by the iodine dextrine color (IDC) method by measuring the absorbance at 590 nm.[20] Reducing sugars were determined by the 3,5-dinitrosalicylic acid (DNS) method[19] using maltose as the standard, while glucose concentration was measured by Trinder reagent.

TLC analysis of carbohydrates in triticale extract and triticale autohydrolysate

Carbohydrates were detected by thin layer chromatography (TLC) on silica plates, 4.5 cm×6 cm (Silica gel 60 F-254, Merck, Darmstadt, Germany), using a Camag development chamber in the tank configuration. The plates were developed by the double-ascending method in a solvent system consisting of butan-1-ol, ethanol, water and glacial acetic acid (5:3:2:0.5 volume ratio). Standard solution of the oligosaccharides mixtures (1.0 mg mL^{-1}
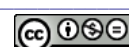
each) was prepared in water and they consisted of: glucose (C1), maltose (C2), maltotriose (C3), maltotetraose (C4), maltopentaose (C5), maltohexaose (C6) and maltoheptaose (C7) (Across and Sigma Aldrich, USA). All separations were performed at ambient temperature (22±2 °C). The carbohydrates were detected by spraying the plates with an ethanolic solution containing 0.5 % (w/V) α-naphthol and 5 vol. % H_2SO_4, followed by heating for 10 min at 120 °C.

RESULTS AND DISCUSSION

Induction of amylase cocktails in *A. niger* and *A. oryzae* were examined by submerged fermentations (SmF) according to scheme showed in Fig. 1. The impact of two kinds of triticale extracts were compared with the impacts of known amylase inducers using various media, the compositions of which are given in Table I.

Carbohydrate composition of triticale extract and triticale autohydrolysate

Triticale extract (T) and triticale autohydrolysate (AT) differed in their carbohydrate contents, especially in their starch contents, Table II. Triticale grains contain more than 60 % starch, classifying it as a starchy cereal.[16,21] The concentration of starch in the triticale extract used in this research was 10 mg mL^{-1}, which represents the quantity of starch available to the fungi during fermentation. Only a trace of starch was detected in triticale autohydrolysate because of starch hydrolysis during the autohydrolysis process by the α-amylase contained in the triticale. The amount of reducing sugars was increased 12.5 times after autohydrolysis, which corresponds to the decreased starch content.

TABLE II. Starch, reducing sugar and glucose contents in triticale extract and triticale autohydrolysate

Sample	Starch, mg mL^{-1}	Reducing sugars, mM	Glucose, mM
Triticale extract (T)	10.24	16.60	11.04
Triticale autohydrolysate (AT)	0.75	201.09	146.18

The TLC analysis revealed that the triticale extract contained a wide range of carbohydrates, Fig. 2C, lane T. Maltose was the most abundant carbohydrate, apart from glucose and maltotriose, in triticale extract after autohydrolysis, Fig. 2C, lane AT. These differences suggest potential different induction of α-amylase and glucoamylase in *Aspergillus* sp.

Induction of amylase production in Aspergillus *sp.*

Non-growing mycelia of *Aspergillus* sp. are a good model system of amylase induction.[11] For this reason, 20-h cultures of both *Aspergillus* species were used. Starvation before addition of carbohydrates is well known as good method for enzyme induction.[11,14,22] Starvation of *Aspergillus* mycelia for 5 h was applied before adding the inducers to the medium, Fig. 1. This enables fungi to meta-

bolize all ingredients present in growth medium and to maximalize the uptake of new molecules added after starvation. All inductions were monitored after 2 h (rapid induction) to compare the impact of maltose and starch[11] with the impact of the triticale extract and of the triticale autohydrolysate. The inductions were further monitored and production levels were determinate in 48 h, which is actually 72 h after the start, because it is commonly used fermentation time for fungi SmF.
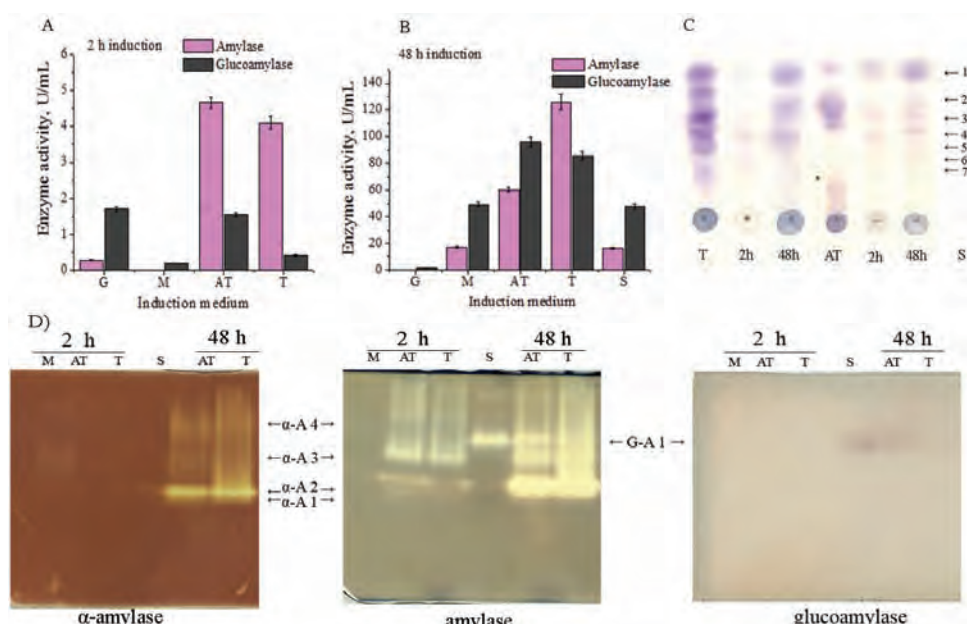
Fig. 2. Glucoamylase and *α*-amylase production by *A. niger* depending on the type of inducers (carbohydrate source) after 2 and 48 h. A) Enzymatic activities, U mL^{-1}, after 2 h of induction; B) enzymatic activities, U mL^{-1}, after 48 h of induction; C) TLC analysis of the carbohydrates in the SmF samples; S – standard carbohydrates: 1 – glucose, 2 – maltose, 3 – maltotriose, 4 – maltotetraose, 5 – maltopentaose, 6 – maltohexaose and 7 – malto-heptaose; D) zymographic detection of *α*-amylase and glucoamylase in the SmF samples. The arrows indicate the positions of the *α*-amylase isoforms (*α*-A1 to *α*-A4) and the glu-coamylase isoform (G-A1). G – glycerol, MM – medium with maltose, AT– autohydrolysate of the triticale extract, T – triticale extract and MS – medium with starch.

Induction of glucoamylase and ɑ*-amylase production in* A. niger

The impact of all inducers on *A. niger* amylases production were monitored by enzymatic assays, TLC analysis of the obtained carbohydrates, and zymogram detection of *α*-amylase and glucoamylase in the fermentation extracts and the results are presented in Fig. 2.

Rapid induction (after 2 h) with triticale extract and triticale autohydrolysate led only to a noticeable increase in the α-amylase production, as evidenced by the enzymatic assay and zymogram, Fig. 2A and D. Low levels of both amylases were detected in all the examined extracts, indicating that 2 h was too short for production.

The glucoamylase level was lower in the medium with maltose than in medium with glycerol, which is contrary to literature results.[11] However, as this was not the case after the 48 h of fermentation with induction (Fig. 2B), it could be because the mycelia had not started to express the induced enzymes within 2 h. Levels of enzymes detected after 2 h in medium with glycerol originated from the standard enzyme pool. The results obtained for *A. oryzae* confirmed this assumption, Fig. 3A and B. The observation indicated that it is necessary to monitor the fermentation for 48 h.
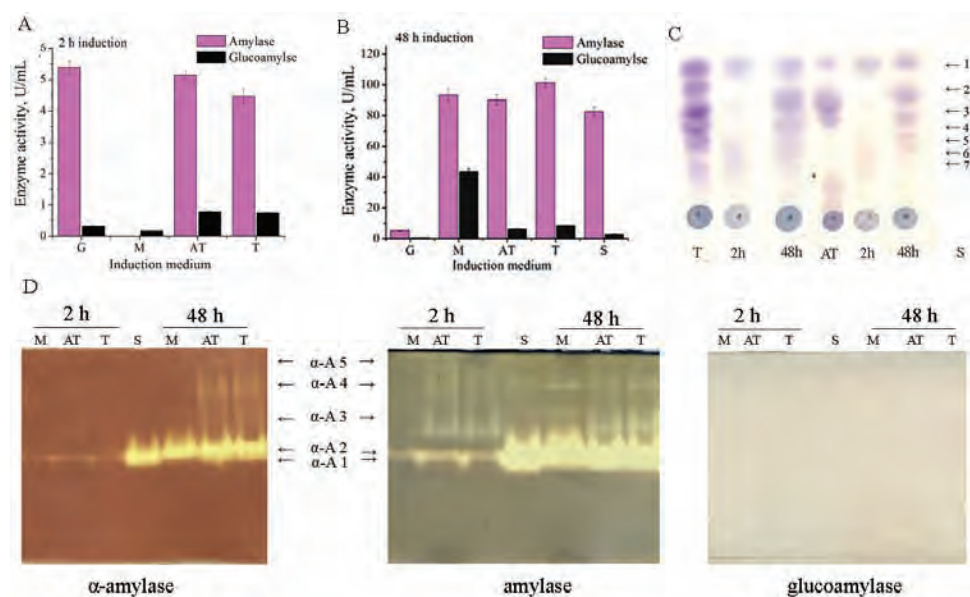
Fig. 3. Production of α-amylase by *A. oryzae* in dependence on the type of inducer (carbohydrate source) after 2- and 48-h fermentation. A) and B) Enzymatic activities, U mL^{-1}, after 2 and 48 h of induction, respectively; C) TLC analysis of carbohydrates in the SmF samples; S – standard carbohydrates: 1 – glucose, 2 – maltose, 3 – maltotriose, 4 – malto-tetraose, 5 – maltopentaose, 6 – maltohexaose and 7 – maltoheptaose; D) zymographic detection of α-amylase and glucoamylase in the SmF samples. The arrows indicate the positions of the α-amylase isoforms (α-A1 to α-A5). G – glycerol, MM – medium with maltose, AT– autohydrolysate of the triticale extract, T – triticale extract and MS – medium with starch.

The fact that glucoamylase and α-amylase were produced concomitantly is often ignored and *A. niger* was shown as a producer of glucoamylase solely.[23–25]

The results prove that *A. niger* produce glucoamylase and *α*-amylase in different ratio, depending on the applied inducers. Maltose was a strong inducer of glucoamylase after 48 h, Fig. 2B and D, which was shown by using maltose and AT as inducers. Maltose was the most abundant carbohydrate in AT according to TLC analysis, Fig. 2C. The high level of glucoamylase in the fermentation with AT was confirmed by enzymatic assay, specific zymogram detection and TLC, as well the detection of a high quantity of glucose. Maltose is a well-known glucoamylase inducer.[13,26] The obtained results confirmed this, and showed that maltose was a better glucoamylase inducer when used in a mixture with the other carbohydrates (maltotriose and glucose) in AT. *A. niger* produced glucoamylase when cultivated on starch as a carbon source – control medium, and with T. This proves that starch is a good amylase inducer and the starch hydrolysis products formed during fermentation are especially good amylase inducers. The use of T as an inducer favors the production of *α*-amylase in *A. niger*, Figs. 2B and D. The choice of the carbohydrate mixture as inducer affects various amylase complexes leading to enrichment with glucoamylase if AT was used or *α*-amylase if T was used.

Induction of α-*amylase production by* A. oryzae

The impacts of all the examined carbohydrates as inducers on the production of amylases by *A. oryzae* were monitored in the same way as for *A. niger* and the results are shown in Fig. 3.

A. oryzae produced only *α*-amylase isoforms in all the examined fermentations, Fig. 3D. The period of 2 h was too short for production according to the obtained low level of amylase, Fig. 3A. T and AT proved to be better *α*-amylase inducers than maltose and starch after 48 h induction. The triticale extract, containing a mixture of carbohydrates C1 to C7 (Fig. 3C lane T), induced the highest amount of *α*-amylase production after 48 h (Fig. 3B). Carbohydrate profile of starch hydrolysis products corresponded to typical fungal *α*-amylase profiles after 48 h fermentation with T and AT inducers (Fig. 3C).[14]

Starch and its hydrolysis products are well known inducers of *α*-amylase.[10,11] This was also shown in the presented results obtained using starch as the carbon source (control medium) and, particularly, the triticale extract in the fermentation. The best-known and most studied inducers of *α*-amylase in *Aspergillus* sp. are maltose and isomaltose, arising from maltose during fermentations.[7,9,11] Moreover, the obtained results confirmed that maltose is a good inducer for *α*-amylase in *A. oryzae*, using maltose and AT, which contained a high amount of maltose (Fig. 3C line AT).

lead to increase in *α*-amylase production after 48 h, of which the triticale extract was the most effective, Fig. 3B. The TLC analysis (Fig. 3C) showed that the T extract contained a spectrum of carbohydrates from C1 to C5, responsible

for the highest level of α-amylase production. Both types of triticale extracts induced as many as five α-amylase isoforms, Fig. 3D. Major α-amylase isoform (α-A2) was presented in all tested samples. However, only α-A1 and α-A2 were present when *A. oryzae* was cultivated on starch. This further favors the usage of the triticale extracts as the α-amylase inducer in *A. oryzae* because the presence of more enzyme isoforms in an enzyme preparation provides easier adaptation to the required industrial conditions of starch hydrolysis.

CONCLUSIONS

The presented results satisfied the aims set out in the Introduction section, *i.e.*, improving amylase production levels and allowing the use of a single fungal strain and a cheap and accessible inducer for the production of specific amylase complexes that might give different product profiles of starch hydrolysis depending on the industrial requirements. This could open a new chapter in triticale utilization. It could be considered as a universal means, as was proven for the two most widely used fungal amylase producer strains. The benefits derived from the consequences of the presented results might be a greater use of triticale, otherwise insufficiently used, as well as higher fungal amylase production.

И З В О Д
ПОВЕЋАЊЕ ПРОДУКЦИЈЕ АМИЛАЗА СМЕШОМ УГЉЕНИХ ХИДРАТА ИЗ ТРИТИКАЛА КОРИШЋЕЊЕМ *Aspergillus* sp.

БИЉАНА ДОЈНОВ[1], МАРИЦА ГРУЈИЋ[2], БОЈАНА ПЕРЧЕВИЋ[2] и ЗОРАН ВУЈЧИЋ[2]

[1]Центар за хемију, Институт за хемију, технологију и металургију Универзитета у Београду, Његошева 12, Београд и [2]Катедра за биохемију, Хемијски факултет, Универзитет у Београду, Студентски трг 12–16, Београд

У циљу проналажења одговарајућег лако доступног индуктора гљивичних амилаза у комбинацији са гладовањем, смеша угљених хидрата из тритикала је испитана и упоређена са већ описаним и познатим индукторима. Смеша угљених хидрата из тритикала је код *Aspergillus niger* индуковала продукцију амилазног коктела (α-амилазе и глукоамилазе), за разлику од индукције са добро познатим индукторима који индукују само глукоамилазу, што је показано зимограмом и TLC анализама угљених хидрата смеша пре и после ферментације. Продукција глукоамилазе *A. niger* је била највећа у присуству екстракта добијеног после аутохидролизе скроба из тритикала (95,88 U/mL). Смеша угљених хидрата из тритикала је код *A. oryzae* индуковала продукцију α-амилазе. Значајно више α-амилазних изоформи је детектовано коришћењем комплексних смеша угљених хидрата као индуктора, у поређењу са малтозом или скробом. Индукција у трајању од 48 h је најефикаснија када се користи екстракт тритикала (101,35 U mL^{-1}). Угљени хидрати из екстраката тритикала могу да се користе као веома добри и јефтини индуктори амилазе. Тритикале, житарица која још увек није у потпуности искоришћена, може се узети за разматрање као индуктор у производњи амилаза коришћењем *Aspergillus* sp., и то тако да
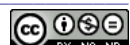
се користи као једини супстрат у подлози за ферментације без додатка других нутритивних елемената.

(Примљено 17. марта, ревидирано 7. маја, прихваћено 12. маја 2015)

REFERENCES

1. H. Gasdorf, P. Atthasampunna, V. Dan, D. Hensley, K. Smiley, *Carbohydr. Res.* **42** (1975) 147
2. A. Yuhki, T. Watanabe, K. Matsuda, *Starch* **29** (1977) 265
3. A. K. Dubey, C. Suresh, R. Kavitha, N. G. Karanth, S. Umesh-Kumar, *FEBS Lett.* **471** (2000) 251
4. B. Dojnov, Z. Vujčić, *Anal. Biochem.* **421** (2012) 802
5. A. Rakha, P. Åman, P. Andersson, *J. Cereal Sci.* **54** (2011) 7
6. N. Bansal, R. Tewari, R. Soni, S. K. Soni, *Waste Manage.* **32** (2012) 1341
7. N. Kato, Y. Murakoshi, M. Kato, T. Kobayashi, N. Tsukagoshi, *Curr. Genet.* **42** (2002) 43
8. Y. Murakoshi, T. Makita, M. Kato, T. Kobayashi, *Appl. Microbiol. Biotechnol.* **94** (2012) 1629
9. K. Tomomura, H. Suzuki, N. Nakamura, K. Kuraya, O. Tanabe, *Agric. Biol. Chem.* **25** (1961) 6
10. J. A. Erratt, P. E. Douglas, F. Moranelli, V. L. Seligy, *Can. J. Biochem. Cell Biol.* **62** (1984) 678
11. M. Yabuki, N. Ono, K. Hoshino, S. Fukui, *Appl. Environ. Microb.* **34** (1977) 6
12. S. N. Jordan, G. J. Mullen, *Waste Manage.* **27** (2007) 1820
13. L. Barton, K. Georgy, D. Lineback, *J. Bacteriol.* **111** (1972) 6
14. M. F. Chaplin, *The use of enzymes in starch hydrolysis*, http://www1.lsbu.ac.uk/water/enztech/starch.html (05.09.2014)
15. D. F. Salmon, M. Mergoum, H. Gómez Macpherson, in *Triticale improvement and production*, M. Mergoum, H. Gomez-Macpherson, Eds., FAO, Rome, 2004, p. 27
16. R. J. Pena, in *Triticale improvement and production*, M. Mergoum, H. Gomez-Macpherson, Eds., FAO, Rome, 2004, p. 37
17. K. Lorenz, F. W. Reuter, C. Sizer, *Cereal Chem.* **51** (1974) 376
18. D. Pejin, L. J. Mojović, V. Vučurović, J. Pejin, S. Denčić, M. Rakin, *Fuel* **88** (2009) 1625
19. P. Bernfeld, in *Methods in enzymology*, Vol. I, P. S. P. Colowick, N. O. Kaplan, Eds., Deutcher Academic Press, San Diego, CA, 1955, p. 149
20. D. E. Briggs, *J. Ind. Brew.* **67** (1961) 4
21. P. Stacey, P. Kiely, O. R. Hacket, F. P. Mara, *Irish J. Agr. Food Res.* **45** (2006) 12
22. T. S. Yu, *J. Biol. Chem.* **271** (1996) 26998
23. H. Pedersen, M. Beyer, J. Nielsen, *Appl. Microbiol. Biotechnol.* **53** (2000) 272
24. P. Selvakumar, L. Ashakumary, A. Pandey, *Bioresour. Technol.* **65** (1998) 83
25. Q. H. Wang, X. Q. Wang, X. M. Wang, H. Z. Ma, *Process Biochem. (Oxford, U.K.)* **43** (2008) 280
26. M. I. Rajoka, A. Yasmeen, *World J. Microbiol. Biotechnol.* **21** (2005) 179.

A new zinc(II) supramolecular square: synthesis, crystal structure, thermal behavior and luminescence

XIU-YAN WANG*, ZHONG-YU ZHAO, QIAN HAN, MIAO YU and DE-YU KONG

Key Laboratory of the Preparation and Application of Environmental Friendly Materials, Ministry of Education, College of Chemistry, Jilin Normal University, Siping 136000, China

Abstract: A new square-shaped Zn(II) complex, $[Zn_4(L)_4(phen)_4]\cdot6H_2O$ (**1**, L = = 2-hydroxynicotinate and phen = 1,10-phenanthroline), was synthesized under hydrothermal condition. The crystal of **1** belongs to triclinic, space group P–1 with a = 10.773(2) Å, b = 12.641(3) Å, c = 13.573(3) Å, α = 107.44(3)°, β = = 102.66(3)°, γ = 93.89(3)°, $C_{72}H_{56}N_{12}O_{18}Zn_4$, FW = 1638.77, V = 1702.8(6) Å³, Z = 1, D_c = 1.598 g/cm³, S = 1.045, μ(MoK$_\alpha$) = 1.475 mm^{-1}, F(000) = 836, R = 0.0472 and wR = 0.0919. Four L ligands bridge four Zn(II) atoms to form a square-shaped structure, where four phen ligands are respectively located on the four corners of the square. The π–π stacking interactions extend adjacent squares into a 1D supramolecular chain. The thermal behavior of **1** was characterized. Moreover, the solid-state luminescence property of the complex was studied at room temperature.

Keywords: crystal structure; supramolecular square; luminescence; 2-hydroxynicotinate.

INTRODUCTION

Over the past few decades, precise control over the shape and size of supramolecular architectures *via* self-assembly has been a major driving force for chemists.[1–6] Well-designed supramolecular architectures can show various physical properties and functionalities in molecular recognition, sensing and magnetism.[7–10] To date, a number of complexes with regular arrays, such as grids, wires and rings, were synthesized using various synthetic methods.[11,12] In a variety of typical cases, successful assemblies of molecular architectures with precise shapes and sizes mainly relied on the angles of the organic ligands and the coordination geometry of the metal ions.[13–18] Therefore, through rational ligand design and metal ion selection, a controllable arrangement of metal ions in multinuclear complexes could be achieved.[19,20] In this regard, tetranuclear

---

complexes with square-shaped arrangements of metal ions are of intense interest to chemists owing to their potential application as molecular devices.[21] By rationally combining the planar *N*-donor chelating ligand and the angular bridging carboxylate-containing ligand square grid-like complexes could be afforded.[22]

Based on the above consideration, in this work a planar *N*-donor chelating 1,10-phenanthroline (phen) ligand and an angular bridging carboxylate-containing 2-hydroxynicotinate (L) were selected, and their complexation behavior was investigated. This paper describes the syntheses, crystal structure, and luminescent property of a new Zn(II) square-shaped complex, $[Zn_4(L)_4(phen)_4]\cdot6H_2O$ (**1**). The compound was characterized by elemental analysis, IR spectrum, TG and X-ray crystallography. In addition, its luminescent property was also investigated.

EXPERIMENTAL

All the materials were of analytical reagent grade and used as received without further purification. The C, H and N elemental analyses were conducted on a Perkin–Elmer 240C elemental analyzer. The emission spectra were measured on a Renishaw inVia Raman Microscope at room temperature. The IR spectrum was recorded in the range of 4000–400 cm^{-1} on an Alpha Centauri FT-IR spectrophotometer using the KBr pellet technique. Thermal stability experiment was performed on a TG SDT2960 thermal analyzer (TA Instruments) under a nitrogen atmosphere.

Synthesis of [Zn$_4$(L)$_4$(phen)$_4$]·6H$_2$O (1)

A mixture of Zn(OAc)$_2$·2H$_2$O (0.2 mmol, 0.044 g), H$_2$L (0.15 mmol, 0.021 g), phen (0.1 mmol, 0.018 g) and KOH (0.1 mmol, 0.006 g) was dissolved in distilled water (10 mL). Then the mixture was transferred and sealed in a 25 mL Teflon-lined stainless steel container. The container was heated at 417 K for 4 days. After the mixture had been cooled to room temperature at a rate of 10 °C·h^{-1}, pale yellow crystals of **1** were obtained. Yield: 21 %. Anal. Calcd. for C$_{72}$H$_{56}$N$_{12}$O$_{18}$Zn$_4$: C, 52.76; H, 3.44; N, 10.75 %. Found: C, 52.31; H, 3.22; N, 10.26 %; IR (KBr, cm^{-1}): 3435(*w*), 1615(*w*), 1564(*m*), 1474(*w*), 1408(*m*), 1254(*w*), 1139(*s*), 1070(*w*), 994(*w*), 952(*w*), 850(*w*), 832(*w*), 786(*w*), 726(*w*), 618(*m*), 539(*w*), 515(*w*).

X-Ray crystallography

Single-crystal X-ray diffraction data for **1** was obtained on a Rigaku R-Axis-Rapid diffractometer with graphite-monochromatized MoK$_\alpha$ (λ = 0.71073 Å) radiation using an ω–ϕ scan method at 293(2) K. The structure was solved by direct methods with SHELXS-97 program and refined with SHELXL-97 by the full-matrix least-squares techniques on F^2.[23,24] Non-hydrogen atoms of the compound were refined with anisotropic temperature parameters. All H atoms on carbon atoms were positioned geometrically (C–H = 0.93 Å) and refined as riding, with U_{iso}(H) = 1.2U_{eq}(carrier). The H atoms of O1W and O2W were included in the model. A summary of the crystallographic data and structure analysis are given in Table S-I of the Supplemrntary material to this paper, and selected bond lengths and bond angles are listed in Table S-II of the Supplementary material.

RESULTS AND DISCUSSION

Crystal structure of *1*

The asymmetric unit of **1** is composed of two Zn(II) atoms, two L ligands, two phen ligands, and three lattice water molecules. Noticeably, the two Zn(II) atoms are both in a penta-coordinated environment, completed by two oxygen atoms from one hydroxyl and one carboxylate of the same L anion, and three nitrogen atoms of one phen ligand and one L anion (Fig. 1). However, the two Zn(II) atoms exhibit different coordination spheres: Zn1 is in a slightly distorted square-pyramidal geometry with a τ value of 0.27, and Zn2 shows a nearly ideal trigonal–bipyramid sphere with a τ value of 0.90.[25]
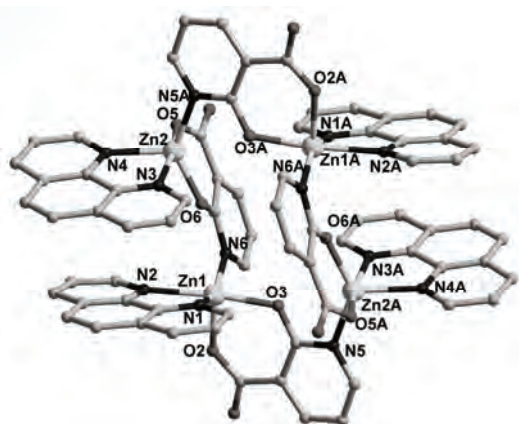
Fig. 1. View of square-shaped structure of **1** and the coordination environments of Zn(II) atoms in **1**.

As given in Table S-II, the Zn–O distances range from 1.971(3) to 2.057(3) Å, and the Zn–N distances vary from 2.023(4) to 2.196(4) Å, which are very similar to the ones found in other related compound [Zn(bpea)(phen)] (bpea = = 1,4,4'-(1*E*)-1,2-ethenediyl-bisbenzoate).[26] Each L ligand adopts a tridentate coordination mode by using its one pyridine nitrogen, one hydroxyl oxygen and one carboxylate oxygen. In this way, four L ligands bridge four Zn(II) atoms to yield a rare square-shaped molecular arrangements with the Zn(II)···Zn(II) distance of 4.66 Å. Four phen ligands are respectively located on the four corners of the square. It is clear that the bis-chelating phen ligands play a key role in the formation of the square.

Significantly, π–π stacking interactions exist among neighboring L ligands in adjacent squares (the face-to-face distance is *ca*. 3.51 Å). Furthermore, these π–π stacking interactions extend adjacent squares into a 1D supramolecular chain (Fig. 2). Moreover, in complex **1**, there are O–H···O hydrogen-bonding inter-actions among water oxygen atoms and the carboxylate oxygen atoms of the L ligands (Table I). These hydrogen-bonding interactions further stabilize the 1D supramolecular architecture of **1**.
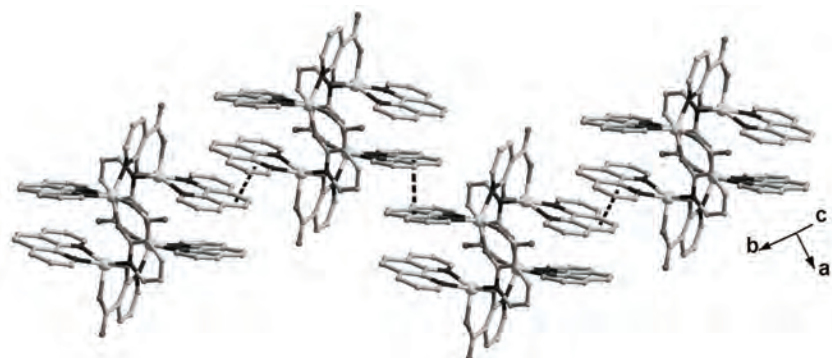
Fig. 2. View of the 1D supramolecular ladder structure of **1** constructed by π–π interactions.

TABLE I. Hydrogen-bonding parameters for **1**; symmetry transformations were used to generate equivalent atoms: B: x+1, y–1, z; C: –x+2, –y, –z+2; D: –x+1, –y, –z+2

D–H···A	d(D–H) / Å	d(H···A) / Å	d(D···A) / Å	$\angle$DHA / °
O(2W)–HW21···O(3W)[B]	0.854(10)	2.027(14)	2.864(6)	167(5)
O(2W)–HW22···O(1W)[C]	0.854(10)	1.999(13)	2.845(6)	170(5)
O(1W)–HW11···O(2)[D]	0.848(10)	2.019(14)	2.862(5)	172(6)
O(1W)–HW12···O(1)	0.851(10)	1.926(16)	2.765(6)	168(6)

Notably in **1**, the L is a doubly deprotonated species coordinated to Zn(II) centers *via* two O atoms and one N atom. It is evident that the pH value of the reaction mixture plays an important role in the double deprotonation of the H_2L ligand and the formation of the final complex. In the present experiment, potassium hydroxide was used to adjust the pH value. Nevertheless, only at pH around 6.5 can be the reaction mixture produce single crystals of **1** with the completely deprotonated L dianion. Moreover, the hydrothermal reaction is necessary for the formation of **1**. At room temperature or under milder conditions, no crystals of **1** were obtained. It could be inferred that the hydrothermal reaction improved the solubility of the reaction mixture, and favored the crystallization of **1** during the cooling-down process. Moreover, the hydrothermal reaction accelerated the complete deprotonation of the H_2L ligand.

Thermal behavior

To know the stability of compound **1**, its thermogravimetric curve was recorded at a heating rate of 10 °C min^{-1}. As shown in Fig. 3, there were two main steps of weight loss. The first step of 6.5 % from 25 to 159 °C can be ascribed to the release of the free water molecules (calcd. 6.6 %), and the second step of 73.3 % in the temperature range of 178–598 °C corresponds to the removal of the organic ligands (L and phen; Calcd. 77.5 %). The residual weight 20.2 % (Calcd. 19.9 %) could probably be attributed to the formation of ZnO. These thermal behaviors agree with the formula of the title compound.
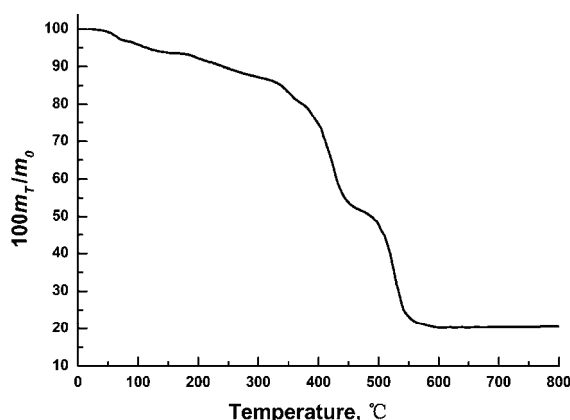
Fig. 3. TG curve of **1** recorded at a heating rate of 10 °C min⁻¹.

Luminescent property

The d^{10} metal-based luminescent compounds are of great interest because of their potential applications as chemical sensors and in photochemistry.[27,28] In this work, the emission spectra of the free organic ligand H$_2$L and compound **1** were recorded in the solid state at room temperature (Fig. 4). The spectrum of H$_2$L shows a maximum emission peak at 393 nm (λ_{ex} = 325 nm) which could be attributed to a π–π* transition, together with a broad shoulder at about 480 nm tentatively attributable to an n–π* transition.[29] The spectrum of **1** exhibited a main peak at 523 nm (λ_{ex} = 325 nm) that was red-shifted by 25 nm with respect to the band shown by the phen ligand (λ_{em} = 498 nm).[26] The red shift may be attributed to a ligand to metal charge transfer (LMCT) transition.[30]
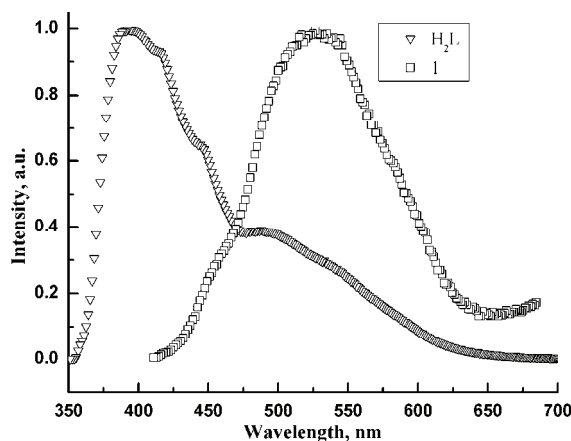
Fig. 4. Emission spectra of H$_2$L and **1** in the solid state at room temperature.

CONCLUSIONS

A new square-shaped molecule was prepared from a planar *N*-donor chelating ligand, 1,10-phenanthroline, and the angular bridging carboxylate-con-

taining 2-hydroxynicotinate under hydrothermal conditions. In **1**, the four L ligands bridge the four Zn(II) atoms to form a square-shaped structure, in which four phen ligands are respectively located on the four corners. The π–π stacking interactions extend adjacent squares into a 1D supramolecular chain. Moreover, compound **1** exhibits intense luminescence in the solid state at room temperature.

SUPPLEMENTARY MATERIAL

The supplementary crystallographic data for this paper are deposited at The Cambridge Crystallographic Data Centre under CCDC-1046844 (1). These data can be obtained free of charge from www.ccdc.cam.ac.uk/data_request/cif.

Crystal data and structure refinement, and selected bond lengths and angles for **1** are available electronically from http://www.shd.org.rs/JSCS/, or from the corresponding author on request.

ИЗВОД

НОВИ СУПРАМОЛЕКУЛСКИ КВАДРАТНО-ПЛАНАРНИ ЦИНК(II) КОМПЛЕКС: СИНТЕЗА, КРИСТАЛНА СТРУКТУРА, ТЕРМИЧКО ПОНАШАЊЕ И ЛУМИНИСЦЕНЦИЈА

XIU-YAN WANG, ZHONG-YU ZHAO, QIAN HAN, MIAO YU и DE-YU KONG

Key Laboratory of Preparation and Application of Environmental Friendly Materials, Ministry of Education, College of Chemistry, Jilin Normal University, Siping 136000, China

Применом хидротермалних услова синтетизован је нови квадратно-планарни цинк(II) комплекс, опште формуле $[Zn_4(L)_4(phen)_4]\cdot6H_2O$ (**1**, L = 2-хидроксиникотинат и phen = 1,10-фенантролин). Нађено је да комплекс **1** припада триклиничном кристалном систему са P–1 просторном групом и a = 10,773(2) Å, b = 12,641(3) Å, c = 13,573(3) Å, α = 107,44(3)°, β = 102,66(3)°, γ = 93.89(3)°, $C_{72}H_{56}N_{12}O_{18}Zn_4$, FW = 1638.77, V = = 1702,8(6) Å^3, Z = 1, D_c = 1,598 g/cm^3, S = 1,045, μ(MoKα) = 1,475 mm^{-1}, F(000) = 836, R = 0,0472 и wR = 0,0919. У комплексу **1** четири лиганда L повезују четири Zn(II) јона мостом и граде структуру квадратно-планарне геометрије у којој се четири phen лиганда налазе на угловима квадрата. Преко π–π интеракција квадратно-планарне јединице су повезане у 1D супрамолекуларни ланац. Описано је термичко понашање комплекса **1**. Такође, испитивано је луминесцентно понашање овог комплекса на собној температури.

(Примљено 4. фебруара, ревидирано 8. маја, прихваћено 6. јуна 2015)

REFERENCES

1. F. A. Cotton, C. Lin, C. A. Murillo, *Inorg. Chem.* **40** (2001) 478
2. S. Leininger, B. Olenyuk, P. J. Stang, *Chem. Rev.* **100** (2000) 853
3. M. Fujita, *Chem. Soc.* Rev. **27** (1998) 417
4. Y.-F. Han, G.-X. Jin, *Acc. Chem. Res.* **47** (2014) 3571
5. S.-L. Huang, Y.-J. Lin, Z.-H. Li, G.-X. Jin, *Angew. Chem. Int. Ed. Engl.* **53** (2014) 11218
6. Z.-Q. Yu, M. Pan, J.-J. Jiang, Z.-M. Liu, C.-Y. Su, *Cryst. Growth Des.* **12** (2012) 2389
7. J. Malberg, M. Bodensteiner, D. Paul, T. Wiegand, H. Eckert, R. Wolf, *Angew. Chem. Int. Ed. Engl.* **53** (2014) 2771

8. D. Whang, K. Kim, *J. Am. Chem. Soc.* **119** (1997) 451
9. A. Noor, E. S. Tamne, B. Oelkers, T. Bauer, S. Demeshko, F. Meyer, F. W. Heinemann, R. Kempe, *Inorg. Chem.* **53** (2014) 12283
10. V. Vrdoljak, B. Prugovečki, D. Matković-Čalogović, T. Hrenar, R. Dreos, P. Siega, *Cryst. Growth Des.* **13** (2013) 3773
11. B. Manimaran, A. Vanitha, M. Karthikeyan, B. Ramakrishna, S. M. Mobin, *Organometallics* **33** (2014) 465
12. F. A. Cotton, C. Y. Liu, C. A. Murillo, X. Wang, *Inorg. Chem.* **45** (2006) 2619
13. A. M. Najar, I. S. Tidmarsh, H. Adams, M. D. Ward, *Inorg. Chem.* **48** (2009) 11871
14. V. Yin, G.-C. Huang, C.-K. Kuo, M.-D. Fu, H.-C. Lu, J.-H. Ke, K.-N. Shih, Y.-L. Huang, G.-H. Lee, C.-Y. Yeh, C.-H. Chen, S.-M. Peng, *J. Am. Chem. Soc.* **130** (2008) 10090
15. Y. Hou, M. A. Rodriguez, M. Nyman, *Cryst. Growth Des.* **12** (2012) 1422
16. J. Park, Y.-P. Chen, Z. Perry, J.-R. Li, H.-C. Zhou, *J. Am. Chem. Soc.* **136** (2014) 16895
17. S. Khullar, S. K. Mandal, *Cryst. Growth Des.* **14** (2014) 6433
18. T. Matsumoto, T. Shiga, M. Noguchi, T. Onuki, G. N. Newton, N. Hoshino, M. Nakano, H. Oshio, *Inorg. Chem.* **49** (2010) 368
19. L. K. Thompson, O. Waldmann, Z. Xu, *Coord. Chem. Rev.* **249** (2005) 2677
20. Y. Wang, X. Ma, S. Hu, Y. Wang, C. Tan, Y. Wen, X. Zhang, T. Sheng, X. Wu, *Polyhedron* **83** (2014) 137
21. M. Ruben, J. Rojo, F. J. Romero-Salguero, L. H. Uppadine, J.-M. Lehn, *Angew. Chem. Int. Ed. Engl.* **43** (2004) 3644
22. T. Shiga, T. Matsumoto, M. Noguchi, T. Onuki, N. Hoshino, G. N. Newton, M. Nakano, H. Oshio, *Chem. Asian J.* **4** (2009) 1660
23. *SHELXS 97,* G. M. Sheldrick, *Program for the Solution of Crystal Structure*, University of Göttingen, Göttingen, 1997
24. G. M. Sheldrick, *SHELXL 97, Program for the Refinement of Crystal Structure*, University of Göttingen, Göttingen, 1997
25. A. W. Addison, T. N. Rao, J. Reedijk, J. van Rijn, G. C. Verschoor, *J. Chem. Soc., Dalton Trans.* (1984) 1349
26. X.-L. Wang, C. Qin, E.-B. Wang, L. Xu, *Cryst. Growth Des*. **6** (2006) 2061
27. Z.-M. Chen, Y.-L. Feng, Y.-Q. Yang, W. Li, Z.-J. Yi, M.-S. Chen, *Chin. J. Struct. Chem.* **31** (2012) 1803
28. Z. G. Kong, X. Y. Wang, L. Carlucci, *Inorg. Chem. Commun.* **12** (2009) 691
29. Q.-M. Wang, B. Yan, *J. Organomet. Chem.* **691** (2006) 3567
30. Z.-G. Kong, S.-N. Guo, Y.-X. Zhao, D. Song, *J. Serb. Chem. Soc.* **79** (2014) 669.

SUPPLEMENTARY MATERIAL TO

A new zinc(II) supramolecular square: synthesis, crystal structure, thermal behavior and luminescence

XIU-YAN WANG*, ZHONG-YU ZHAO, QIAN HAN, MIAO YU and DE-YU KONG

Key Laboratory of the Preparation and Application of Environmental Friendly Materials, Ministry of Education, College of Chemistry, Jilin Normal University, Siping 136000, China

TABLE S-I. Crystal data and structure refinement for **1**

Parameter	Value
Chemical formula	$C_{72}H_{56}N_{12}O_{18}Zn_4$
Formula weight	1638.77
Wavelength, Å	0.71073
Temperature, K	293(2)
Crystal system	Triclinic
Space group	P-1
a / Å	10.773(2)
b / Å	12.641(3)
c / Å	13.573(3)
α / °	107.44(3)
β / °	102.66(3)
γ / °	93.89(3)
V / Å^3	1702.8(6)
Z	1
D_{calc} / g cm^{-3}	1.598
μ / mm^{-1}	1.475
F(000)	836
$(\theta_{min} - \theta_{max})$ / °	3.15–25.03
Diffraction measured fraction, θ_{max} / °	25.03
Refined difference density, max/min	0.450/–0.363
Reflection collected/unique (R_{int})	13258 / 5920 (0.0597)
Data/restraints/parameters	5920/6/494
Goodness-of-fit on F^2	1.045
R indices (all data)	$R_1 = 0.0472$, $wR_2 = 0.0919$
Final R indices ($I > 2\sigma(I)$)	$R_1 = 0.0863$, $wR_2 = 0.1076$

* Corresponding author. E-mail: wangxiuyan2004@sohu.com

TABLE S-II. Selected bond lengths (Å) and angles (°) for **1**; symmetry transformations used to generate equivalent atoms: A: $-x+2$, $-y+1$, $-z+2$

Bond	Value	Bond	Value
Bond length, Å			
Zn(1)–N(1)	2.125(3)	Zn(1)–N(2)	2.196(4)
Zn(2)–N(3)	2.192(3)	Zn(2) –N(4)	2.124(4)
Zn(2)–N(5)^A	2.023(4)	Zn(1)–N(6)	2.034(3)
Zn(1)–O(2)	2.009(3)	Zn(1)–O(3)	2.038(3)
Zn(2)–O(5)	2.057(3)	Zn(2)–O(6)	1.971(3)
Bond angle, °			
O(2)–Zn(1)–N(6)	99.99(13)	O(2)–Zn(1)–O(3)	89.18(12)
N(6)–Zn(1)–O(3)	95.62(13)	O(2)–Zn(1)–N(1)	110.16(13)
N(6)–Zn(1)–N(1)	149.54(15)	O(3)–Zn(1)–N(1)	89.16(12)
O(2)–Zn(1)–N(2)	92.84(14)	N(6)–Zn(1)–N(2)	98.16(14)
O(3)–Zn(1)–N(2)	165.50(11)	N(1)–Zn(1)–N(2)	76.66(13)
O(6)–Zn(2)–N(5)^A	136.09(14)	O(6)–Zn(2)–O(5)	88.94(12)
N(5)^A–Zn(2)–O(5)	92.79(14)	O(6)–Zn(2)–N(4)	113.64(15)
N(5)^A–Zn(2)–N(4)	110.12(15)	O(5)–Zn(2)–N(4)	92.33(14)
O(6)–Zn(2)–N(3)	89.50(12)	N(5)^A–Zn(2)–N(3)	96.66(13)
O(5)–Zn(2)–N(3)	167.89(14)	N(4)–Zn(2)–N(3)	77.31(13)

Effect of transition metal cations on the commensurate freezing of *n*-hexane confined in micropores of ZSM-5

RADMILA HERCIGONJA[1]*, VLADISLAV RAC[2], VESNA RAKIĆ[2]
and ALINE AUROUX[3]

[1]*Faculty of Physical Chemistry, University of Belgrade, 11000 Belgrade, Studentski trg 12, Serbia,* [2]*Faculty of Agriculture, Nemanjina 6, 11080 Belgrade-Zemun, Nemanjina 6, Serbia and* [3]*Université Lyon 1, CNRS, UMR 5256, IRCELYON, Institut de recherches sur la catalyse et l'environnement de Lyon, 2 avenue Albert Einstein, F-69626 Villeurbanne, France*

Abstract: Besides its importance concerning fundamental studies on gas adsorption in narrow pores, investigation of the commensurate freezing of a fluid within a zeolite is of practical importance in the application of zeolites in the processes of adsorption, separation and catalysis. In this work, the adsorption of *n*-hexane on HZSM-5 and its transition metal ion-exchanged modified forms was studied at 303 K by means of microcalorimetry. The thermal molar entropies changes of adsorption were calculated and thereby, the freezing-like behaviour of *n*-hexane inside the structure of the zeolite as a confinement media was noticed. This effect is governed by the attractive interactions between *n*-hexane molecules and the pore walls, and is influenced by the length of the pores and the nature of the charge-balancing cations. Among the investigated zeolites, a solid-like phase of *n*-hexane in the pores of zeolites with Fe(II) ions was the most similar to solid bulk *n*-hexane, while Cu(II) ions contributed to the lowest ordering of the obtained solid-like *n*-hexane phase.

Keywords: confinement media; adsorption; entropy; microcalorimetry; ZSM-5.

INTRODUCTION

The confinement of fluids in limited spaces, such as narrow pores, is a very interesting phenomenon. The behaviour of fluid confined in a pore is influenced by many factors, such as pore size and geometry, and the atomic structure of the pore surface. Consequently, its properties are distinctly different from those of bulk phase. For example, a confined fluid can have a higher density or can be in a different aggregation state from its analogue under normal conditions. There are many experimental and theoretical studies reporting that the phase behaviour of

---

1297

different fluids under extreme confinement is qualitatively different from that of the bulk.[1–13] In the confinement medium, the presence of fluid–pore wall and fluid–fluid forces can lead to interesting surface-driven phase changes. These include new types of phase transitions not found in the bulk phase and shifts in transitions. In a bulk system, freezing is considered a first-order phase transition accompanied by an infinitely sharp change in a suitable order parameter, usually density or composition. In a confinement medium, the freezing phase transition is possible but with evident effects of confinement. The freezing temperature of a fluid confined in pores is determined by the bulk freezing temperature, pore wall–solid and pore wall–fluid surface tensions, the molar volume of the liquid, the latent heat of melting in the bulk and pore width.[14] A decrease or increase in the freezing temperature due to confinement is strongly affected by the strength of the attractive forces between the fluid molecules and the pore walls.[14,15] For repulsive or weakly attractive pore walls, the shift in the freezing temperature is negative.[16,17] For highly attractive adsorbents where the adsorbate–pore wall interactions are strong compared to the adsorbate–adsorbate interactions, an increase in freezing temperature over the bulk value is observed.[15,18,19–22]

Zeolites are regular crystalline solid microporous materials with peculiar structural characteristics (a three-dimensional lattice with well defined pores, high internal surface area and curvature, high ion-exchange capacity and remarkable thermal stability). Zeolites are extensively used in the chemical industry as catalysts and for the separation of gases, particularly hydrocarbons.[23–25] Therefore, the adsorption of hydrocarbons, especially *n*-alkanes, has been widely studied.[4,6,26–29] According to the molecular dimensions of their pores, zeolites may be considered as confinement media and the effect of confinement on fluids adsorbed in zeolites may be expected. For example, investigations of hexane and heptane adsorption at room and at slightly higher temperatures on silicalite-1 and ZSM zeolite revealed anomalous behaviour of these two hydrocarbons compared to other alkanes.[2–6] An explanation was given for the first time by Smit and Maesen.[30] Their interpretation is that the adsorption of straight chain hydrocarbons on silicalite leads to a phase transition of the hydrocarbons inside the pores of the silicalite. Bearing in mind that silicalite-1 and ZSM have two types of channels, straight and zigzag (sinusoidal) connected *via* intersections, they showed that phase transition occurred when the lengths of the adsorbed molecules were similar to the length of the channels. Indeed, the length of *n*-hexane and heptane molecules are 1.03 and 1.16 nm, respectively, while the length between the centres of channel intersections of the silicalite structure is 1.2 nm, *i.e.*, they are comparable. Under the above conditions, fluid can freeze in a configuration that is commensurate with the pore structure.[30–33] Phase transitions of hexane and heptane between the gas, liquid and solid phases in the pores of silicalite-1 and ZSM are generally accepted and were the subject of many studies.[34–41]

Commensurate adsorption of hydrocarbons (*e.g.*, *p*-xylene, *n*-hexane, *n*-heptane, benzene, *etc*.) was found in several different types of zeolites, for instance, MFI, ITW, ERI, CHA, LTA, AFX and silicalites.[42–46]

Evidence for freezing of *n*-hexane molecules inside the channels of ZSM can be seen from the adsorption isotherms, which can show a step or kink when half of the maximum loading (about 4 molecules per unit) is achieved; such isotherms were obtained for adsorption measurements at temperatures above 338 K.[4,6,30,47–49] Lohse *et al.*[50] did not provide evidence for a kink at half of the loading because the temperature of adsorption (298 K) was too low. Additionally, Meansen[30] showed in a simulation that the kink becomes more pronounced with increasing temperature. The adsorption isotherms measured by Zhu *et al.*[51] showed a kink in the temperature region 338–373 K, but not at 303 K. The volumetric adsorption isotherms of *n*-hexane on HZSM-5 zeolite and its transition metal modified forms were reported,[52] but they did not show a kink since a low temperature of adsorption (303 K) was applied.

In addition to isotherms, temperature programmed desorption (TPD) profiles also gave evidence of commensurate freezing of *n*-hexane in the zigzag channels of zeolite. The TPD studies showed that among the linear alkanes, hexane and heptane behave distinctly differently.[28,32,44,45,48,53–57] While other linear alkanes showed a single desorption step, *n*-hexane and especially *n*-heptane exhibited two-step desorption profiles. The first desorption peak of *n*-hexane and *n*-heptane occurred at lower temperatures than expected based on the chain length of these two *n*-alkanes. This low temperature peak corresponds to desorption from the zigzag channels and should be caused by a relatively high gain in entropy upon desorption compared to the other *n*-alkanes. The relatively high gain in entropy upon desorption can only be the result of a low entropy value in the constrained position of the adsorbed *n*-hexane and *n*-heptane molecules at high loadings. Partial desorption then allows a rearrangement of the adsorbed *n*-hexane or *n*-heptane molecules, resulting in an ordering similar to the ordering of the other *n*-alkanes with normal entropy values. The high temperature peak corresponds to desorption from the straight channels and it occurs at temperatures that are in accordance with the chain length of the *n*-alkane. It was reported[58] that the TPD profiles of *n*-hexane sorbed on ZSM-5 were composed of two well-defined peaks in the temperature region from 300 to 550 K, consistent with the results of other researchers.[28,32,44,54,56] Accordingly, this indicated that the phase transition of freezing occurred when *n*-hexane was adsorbed on the samples of ZSM used in the present study.

In the last decade, among the transition metal ion-containing zeolites, the Fe-, Cu- and Mn-MFI zeolites have received much attention because they are catalytically active in some important reactions, such as N_2O and NO decomposition, reduction of NO_x to N_2 in the reaction with various hydrocarbons[59–61] and catal-

ytic cracking of hydrocarbons.[62–64] Many experimental results indicate that the physical adsorption of *n*-alkane reactants contributes to the kinetics of catalytic reactions.[65–67]

In this work, the phase transition of commensurate freezing of *n*-hexane confined in microporous of HZSM-5 and in its forms modified by different charge balancing cations: Cu(II), Mn(II) and Fe(II), was investigated. It is known that attractive adsorbate–pore wall interactions in zeolite partly originate from the charge balance cation–adsorbate interactions, and hence, an influence of transition metal cations on the adsorption of *n*-hexane and on its commensurate freezing could be expected. Recently, molecular dynamics (MD) simulation studies[31] clearly showed that the behaviour of *n*-hexane at a loading of 4 mol per unit cell (u.c.) in silicalite-1 should not be ascribed to an enthalpy effect but to an entropy change of the system approaching 4 mol (u.c.)$^{-1}$, which was in agreement with the results of Smit *et al.*[1] Therefore, in order to investigate the influence of the nature of the charge balancing cation on the commensurate freezing of *n*-hexane inside the zeolite structure, one physical property, thermal molar entropy, was studied, which was chosen for two reasons: first, the appearance of a low temperature peak in TPD profile, as confirmation that commensurate freezing is associated with the entropy change, and secondly, the property in relation to the molar entropy of liquid and solid *n*-hexane may cast insight into the freedom of the *n*-hexane molecules within the zeolite and thus, could provide evidence for the occurrence of commensurate freezing.

EXPERIMENTAL

The parent self-produced NaZSM-5 (Si/Al = 20) was synthesized hydrothermally. HZSM-5 and under-exchanged forms of HZSM-5 containing Cu(II), Fe(II) or Mn(II) cations (mono- or bi-metallic) were obtained by appropriate common wet ion-exchange procedures, fully described previously.[22] The crystallinity of the parent NaZSM-5, HZSM-5 and ion--exchanged forms was proved by X-ray diffraction. The measurements were performed on a Bruker (Siemens) D5005 diffractometer at room temperature using CuK$_\alpha$ radiation (0.154 nm), 2θ from 3 to 80°, in 0.02° steps with 1 s per step, and the results showed that the structure of the ZSM-5 zeolite remained unchanged during the ion-exchange process. XRD analysis proved that the structure was also not changed by adsorption of *n*-hexane. The differential heats and the isotherms of *n*-hexane adsorption were collected using a coupled microcalorimetric–volumetric line, using the procedure fully described elsewhere.[23] Briefly, the heats of adsorption were measured in a heat-flow microcalorimeter (C80, Setaram) linked to a glass volumetric line that permitted the admission of successive known doses of adsorbed gas, until a final equilibrium pressure of 66 Pa. Subsequently, the sample was pumped, the desorption peak was recorded and re-adsorption was performed at the same temperature. Before the adsorption, the samples were pre-treated in vacuum (10^{-3} Pa) overnight at 673 K, while the adsorption temperature was maintained at 303 K. In order to clarify the states of cation species in the investigated samples, UV–Vis diffuse reflectance spectra were recorded, in 190–1000 nm spectral region, using a Perkin Elmer Lambda 35 UV–Vis spectrometer equipped with a diffuse reflectance accessory. The powder samples were placed in the sample cup and BaSO$_4$ was used as a reference.

The thermal entropy of sorbed *n*-hexane was calculated from the values of the entropy change of adsorption, ΔS^0, obtained from calorimetric measurements.[52] The obtained values of entropy change of adsorption are in good agreement with the values from the litera-ture.[44,56,68,69] The following expression was used to calculate ΔS^0 from the microcalorimetry data:

$$\Delta S^0 = R \ln \frac{p^0}{p} + \frac{\Delta H^0}{T} \tag{1}$$

where T is the adsorption temperature, p^0 is the standard pressure, p is the equilibrium pres-sure at temperature T and ΔH^0 is the standard enthalpy change in the adsorption process. These values were obtained from microcalorimetry as differential heats of adsorption. The entropy change accompanying the adsorption process can be expressed as:

$$\Delta S^0 = S_g^0 - S_s^* \tag{2}$$

where S_g^0 is the molar entropy of *n*-hexane vapour at standard pressure p^0 and temperature T, while S_s^* is the differential molar entropy of adsorbed *n*-hexane. The differential molar entropy, is a finite, positive quantity that may be separated into thermal and configurational entropy components.[70] In this case, S_s^* can be represented by:

$$S_s^* = S_c + S_{th} \tag{3}$$

where S_c and S_{th} are the differential molar configurational and differential molar thermal entropies, respectively. When the density of the molecules adsorbed in the channels of the zeolite is high, it is generally assumed that these molecules attempt to pack closely together and take up the walls of the anion framework. With such a localized sorption process, S_c, may be calculated with the equation:

$$S_c = R \ln \frac{x}{1-x} \tag{4}$$

where $x = W / W_0$ (W is the amount adsorbed at equilibrium pressure p, and W_0 is the total adsorption capacity at 303 K).[71] Subtraction of Eq. (4) from S_s^* gives S_{th}:

$$S_{th} = S_s^* - R \ln \frac{x}{1-x} \tag{5}$$

RESULTS AND DISCUSSION

The values of differential molar entropy, differential molar configurational and differential molar thermal entropies were calculated for the adsorption of *n*-hexane with different loadings (expressed as N, number of molecules adsorbed per unit cell), on both parent HZSM-5 and its cation modified forms using Eqs. (2)–(5). The profiles of differential molar thermal entropies plotted *vs.* the amount adsorbed are shown in Fig. 1.

The profiles of the S_{th} values *vs.* loading gave evidence that the differential molar thermal entropies of the *n*-hexane adsorbed on zeolite was dependent on the nature of the environment of the adsorbate molecules, *i.e.*, the porous zeolite lattice with its charge balance cations. It can be seen from Fig. 1 that the S_{th} of parent HZSM-5 was altered by the incorporation of transition metal cations in its

lattice. Furthermore, the presence of transition metal cations increased the adsorption capability of HZSM-5 zeolite from 4 (obtained in the case of HZSM-5) to 6 molecules of *n*-hexane per unit cell (found for zeolites with transition metal cations). Different numbers (from 2 to 8) of sorbed *n*-hexane molecules per unit cell were reported in the literature,[4,32,72] while the theoretical loading limit for ZSM-5 was 8 hexane molecules per unit cell.[73] It could be inferred that the charge balance cations influence the values of S_{th} since they result from *n*-hexane attractive interactions with the zeolite pore wall, originating from the macro-anion framework and extra-framework charge-balancing cations.
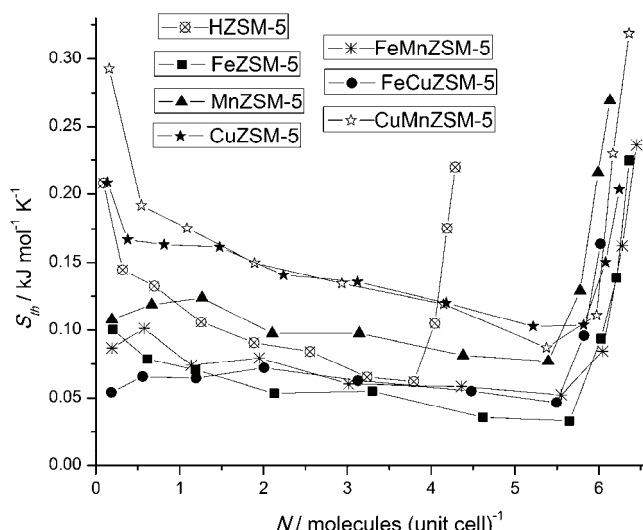
Fig. 1. Differential molar thermal entropies (S_{th}) as a function of loading N (molecules per unit cell) of *n*-hexane.

In a study of *n*-hexane adsorption on ZSM, several facts must be taken into account. First, the length of the *n*-hexane molecule is almost the same as the distance between channel intersections and hence, these molecules cannot be wholly located in the channel segments and the possibility of adsorbate–adsorbate interaction at the channel intersections always exists at high surface loadings. In fact, adsorbate–adsorbate interaction are enhanced for a loading of 4 *n*-hexane molecules per unit cell; while for even higher values (4–8 molecules per unit cell), the adsorbed molecules arrange in such way that additional side-on interactions can occur; while with further increase in the N values, closer packing of *n*-hexane molecules occurs and thus, repulsion interactions become significant.[4,47,74,75]

For all the investigated zeolites, the S_{th} *vs.* loading profiles can be divided into three regions of loading. It could be seen from Fig. 1 that these regions are:

$N < 2$, $2 < N < 6$ and $N > 6$. The S_{th} values found for n-hexane adsorption on HZSM-5, CuZSM-5 and CuMnZSM-5 decreased sharply in the initial, micro--pore-filling region ($N < 2$). This is probably due to the fact that the first molecules entering the micropores occupy the most favourable sites, which results in their fast ordering and fast loss in S_{th}. In the case of adsorption on FeZSM-5, the S_{th} values decreased very slowly up to $N < 2$. However, it is important to notice that in this low-surface coverage region, the S_{th} values measured for n-hexane adsorption on MnZSM-5, FeMnZSM-5 and FeCuZSM-5 showed increased values with a more or less marked maxima. Barrer *et al.*[70,76] reported that strong energetic heterogeneity is reflected in a maximum in the entropy curves against coverage for low adsorbate uptakes. Indeed, it seems that on these samples, the ordering of adsorbed molecules occurred as a result of interaction with surface active sites. After the maximum values of S_{th} were reached on MnZSM-5 and on the samples containing Fe(II) cations (FeZSM-5, FeMnZSM-5 and FeCuZSM-5), the S_{th} values remained almost constant in the medium surface coverage region ($2 < N < 6$), thus indicating highly localized adsorption. In contrast, the S_{th} values of HZSM-5 and the zeolites containing Cu(II) cations (CuZSM-5 and CuMnZSM-5) slightly decreased from the constant values, thus indicating that there were some deviations of the localized sorption. For high surface coverages ($N > 4$ for HMnZSM-5 and $N > 6$ for all other samples), the S_{th} values increased sharply as a result of repulsion interactions among the closely packed n-hexane molecules.

At low surface coverage, the adsorbate molecules can move freely in the zigzag channels and thus fill one part of the intersections for some time. As a consequence, further adsorption would become restricted, since the intersections are blocked while the straight channels are too short to accommodate n-hexane molecules. To fill the zeolite completely, the molecules adsorbed in a zigzag channel have to be confined in their position, which leads to a loss in entropy.[8] It is accepted that when a coverage of half a loading per unit cell is achieved, the intersections are blocked. Then, the adsorbed molecules in the zigzag zeolite channels undergo phase transition, which is known as commensurate freezing. The S_{th} values of n-hexane adsorbed that are achieved at half-loading (≈ 3 molecules per unit cell) may be compared with the entropy of liquid n-hexane at 303 K (300 J mol^{-1} K^{-1}) and the sum of the vaporization entropy change (94 J mol^{-1} K^{-1}) and the fusion entropy change of n-hexane (72 J mol^{-1} K^{-1}) at 178 K.[77] According to Eq. (3), the values of the differential molar entropy at half-loading enable the derivation the S_{th} part of the respective differential molar entropy since $S_c = 0$. These values of S_{th} are listed in Table I.

The S_{th} part of the respective S_s^* obtained for the configurational entropy $S_c = 0$ of n-hexane adsorbed within the channels of FeZSM-5, FeMnZSM-5 and FeCuZSM-5 were between 55 and 62 J mol^{-1} K^{-1}; values sufficiently lower than the sum of the vaporization entropy change and the fusion entropy change of n-hex-

TABLE I. The S_{th} part of respective S_s^* (for $S_c = 0$)

Zeolite	S_s^* $(= S_{th})$ / J mol^{-1} K^{-1} ($S_c = 0$)
CuMnZSM-5	134
CuZSM-5	136
MnZSM-5	98
FeMnZSM-5	60
FeZSM-5	55
FeCuZSM-5	62

ane at 178 K to suggest that degree of ordering of the molecules adsorbed in the pores of these zeolites was similar to that in solid *n*-hexane. Similar results were found for *n*-hexane adsorbed on MnZSM-5. In this case, the S_{th} part of the respective S_s^*, for $S_c = 0$ equalled 98 J mol^{-1} K^{-1}, which is more than the S_{th} found in the case of the zeolites containing Fe(II) cations, but still less than the sum of the vaporization entropy change and the fusion entropy change of *n*-hexane at 178 K. The S_{th} parts of the respective S_s^* obtained for $S_c = 0$ within the channels of CuMnZSM-5 and CuZSM-5 were practically equal (134 and 136 J mol^{-1} K^{-1}) and also less than the sum of the vaporization entropy change and the fusion entropy change of *n*-hexane at 178 K. Obviously, the presence of Mn(II), Cu(II) and especially Fe(II) cations changes the attractive interactions between *n*-hexane molecules and the pore walls in such a way to enable the adsorbed *n*-hexane molecules to be arranged as in a solid-like state of *n*-hexane. It is noteworthy that the S_{th} values obtained for the samples containing Fe(II) cations were about 100 J mol^{-1} K^{-1} lower than the sum of the vaporization entropy change and the fusion entropy change of *n*-hexane at 178 K, while the S_{th} values for the samples containing Cu(II) ions were only about 20 J mol^{-1} K^{-1} lower than the above mentioned sum, indicating a higher ordering of the hexane molecules in the zeolites containing Fe(II) cations than inside those containing Cu(II) cations. The general conclusion, based on the values of S_{th}, is that a phase transition from gaseous *n*-hexane to a solid-like structure of *n*-hexane, *i.e.*, commensurate freezing of *n*-hexane, occurred in the pores of ZSM-5 containing transition metal ions. The commensurate freezing occurred at 303 K, well above the temperature of the bulk freezing of *n*-hexane (178 K). Increasing of the freezing temperature is a characteristic of fluids confined in a confinement medium with highly attracting pore-walls, as is the case with the investigated zeolites.

In order to better illustrate the influence of the extra framework cations on decreasing S_{th}, the difference between S_{th} and S_g^0 was calculated and plotted as $(S_{th} - S_g^0)$ *vs.* loading (Fig. 2).

At the very beginning of the sorption, the entropy loss followed the order: FeCuZSM-5 > FeMnZSM-5 > FeZSM-5 > MnZSM-5 > HZSM-5 > CuZSM-5 > CuMnZSM-5. At half of the maximum loading, the entropy loss followed the order: FeZSM-5 > FeCuZSM-5 = FeMnZSM-5 > HZSM-5 > MnZSM-5 >

CuZSM-5 = CuMnZSM-5, while at the maximum loading ($N = 6$), the entropy loss followed the order: FeZSM-5 > FeCuZSM-5 > FeMnZSM-5 > MnZSM-5 > CuMnZSM-5 > CuZSM-5.
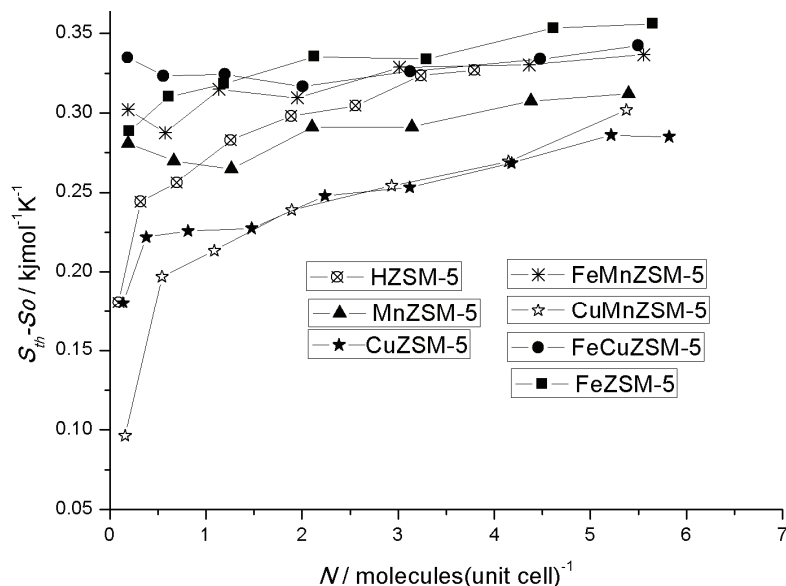
Fig. 2. Dependence of the entropy loss $(S_{th} - S_g^0)$ of adsorbed n-hexane on loading N.

The maximum entropy loss was achieved for n-hexane adsorption in the zeolites with Fe(II) cations and the minimum entropy loss was found for n-hexane adsorption in zeolites with Cu(II) cations. The rigid zeolite structure is the same in all these samples, which means that the presence of the charge-balancing cations influences the distribution and ordering of n-hexane molecules inside the zeolite channels, and thus the S_{th} values. It is important to note that[27] Al MAS NMR experiments showed that the HZSM-5 investigated in this work does not contain extra framework Al, which means that some steric hindrance for n-hexane adsorption was not to be expected.[78] The different values of the S_{th} part of respective S_s^* (for $S_c = 0$) of the samples with different charge balancing cations indicate that the created solid-like phase was not always the same and depended on the type of the extra framework cations. Cu(II), Mn(II) and Fe(II) have the same charge, but different ion radii (Cu: 0.73 nm, Mn: 0.82 nm and Fe: 0.78 nm) and hence, they create different electrostatic interactions with n-hexane molecules. In addition, Cu(II), Mn(II) and Fe(II) have different electron configurations, $i.e.$, (Mn(II) possesses five and Fe(II) four incomplete d-orbitals, while Cu(II) has only one unpaired electron in the $4s^1$ orbital). The electrons of uncompleted orbitals can form bonds with oxygen atoms from the lattice, as well with

adsorbed *n*-hexane molecules. If these electrons "react" with the oxygen of the lattice, the reaction of *n*-hexane with oxygen atoms is reduced, while the cations partly lose the possibility of interaction with *n*-hexane. Both effects cause an increase in S_{th}. However, the interaction of spin unpaired electrons with *n*-hexane molecules produce the opposite effect, *i.e.*, a decrease in S_{th}. The low S_{th} obtained for samples with Mn(II) and Fe(II) cations shows that Mn(II) and Fe(II) present in zeolite lattice coordinated the electrons of adsorbed *n*-hexane easier than the electrons of the oxygen atoms from the lattice. Therefore, the S_{th} of the samples containing Mn(II) and Fe(II) ions are influenced both by ion-induced dipole interactions, while the additional interactions originate from the possibility of Mn(II) and Fe(II) to behave as electron acceptors. On the contrary, considering that Cu(II) ions have only one unpaired electron in the $4s^1$ orbital, the S_{th} value of samples possessing Cu(II) ions is mostly determined by ion-induced dipole interactions through electrostatic and dispersive forces. If all the interactions achieved between *n*-hexane molecules and the samples possessing Fe(II) and Mn(II) ions are compared, it could be concluded that Fe(II) ions can achieve stronger electrostatic (its ionic radius is smaller), but weaker additional interactions (Fe(II) possesses four uncompleted d-orbitals, Mn(II) five). Based on the values of S_{th}, it seems that both these interactions are stronger in the samples containing Fe(II) cations, which led to better ordering of the adsorbate and finally to the formation of a solid-like phase in the course of a phase transition known as commensurate freezing.

CONCLUSIONS

The results obtained in this work show that the phase transition of commensurate freezing of *n*-hexane occurred during the adsorption of *n*-hexane into the parent HZSM-5 and its transition metal modified forms: CuZSM-5, MnZSM-5, FeZSM-5, CuMnZSM-5, FeMnZSM-5 and FeCuZSM-5. Freezing of *n*-hexane, the molecules of which "fit" the zigzag channels of ZSM-5, occurred at 303 K, which is well above the freezing temperature of bulk *n*-hexane (178 K). The positive shift in the freezing temperature was affected by the strong attractive forces between the *n*-hexane molecules and pore walls of the zeolite, originating from the presence of charge balancing cations. The results showed that above the circumstances of reduced dimensionality, such is in the case of zeolite lattice, the type (size and charge) and nature (electron configuration) of the charge balancing cation determine the ordering of the solid like phase of *n*-hexane obtained in the phase transition of commensurate freezing. Among the investigated zeolites, the solid-like phases obtained in zeolites possessing Fe(II) cations (FeZSM-5, FeMnZSM-5 and FeCuZSM-5) were the most similar to the solid *n*-hexane phase. Obviously, the presence of Fe(II) as the charge balancing cation facilitated the ordering of the adsorbed *n*-hexane molecules inside the zeolite. The smallest

ordering of the solid like phase of *n*-hexane obtained in the process of commensurate freezing was in the zeolites with Cu(II) as the charge balancing cations (CuMnZSM-5 and CuZSM-5).

ИЗВОД

УТИЦАЈ КАТЈОНА ПРЕЛАЗНИХ МЕТАЛА НА "МРЖЊЕЊЕ" ХЕКСАНА У ОГРАНИЧЕНОМ ПРОСТОРУ МИКРОПОРА ZSM-5 ЗЕОЛИТА

РАДМИЛА ХЕРЦИГОЊА[1], ВЛАДИСЛАВ РАЦ[2], ВЕСНА РАКИЋ[2] и ALINE AUROUX[3]

[1]Факулȳеȳ за физичку хемију, Универзиȳеȳ у Беоīраду, Сȳуденȳски ȳрī 12, 11 000 Беоīрад, [2]Пољоȳривредни факулȳеȳ, Универзиȳеȳ у Беоīраду, Немањина 6, 11080 Беоīрад-Земун и [3]Université Lyon 1, CNRS, UMR 5256, IRCELYON, Institut de recherches sur la catalyse et l'environnement de Lyon, 2 avenue Albert Einstein, F-69626 Villeurbanne, France

Commensurate freezing је назив за појаву фазног прелаза првог реда (мржњења) гасова на температурама које су знатно изнад температуре сублимације слободног гаса, у условима када се гас адсорбује у уским порама чије димензије одговарају димензијама молекула гаса. Поред значаја у основним испитивањима адсорпције гасова, испитивање "мржњења" флуида унутар зеолита као микропорозног материјала је од практичног значаја у примени зеолита у процесима адсорпције, раздвајања компонената и катализи. У овом раду је проучавана адсорпција *n*-хексана из гасне фазе на ZSM-5 зеолиту, као и његовим облицима модификованим јонима прелазних метала, применом микрокалориметрије на температури од 303 K. ZSM-5 зеолит има два типа канала, праве и синусоидалне (цик-цак) који се међусобно секу. Дужина молекула *n*-хексана (1,03 nm) одговара растојању између центара пресека правих и цик-цак канала зеолита (1,2 nm), тако да под овим условима *n*-хексан може да се адсорбује на такав начин да је његово кретање толико ограничено да може да се схвати као замрзавање у каналима зеолита. Ова појава је у литаратури названа *commensurate freezing* и повезана је са променом ентропије система, па је у раду на основу израчунатих вредности промене термалне моларне ентропије адсорпције потврђено да је дошло до формирања структуре *n*-хексана која личи на чврсти *n*-хексан. Такође је показано да наведена фазна промена *n*-хексана зависи од природе катјона прелазних метала (електронске конфигурације, димензија и наелектрисања) који компензују негативно наелектрисање решетке. Међу испитиваним зеолитима, у оном са Fe(II) јонима је постигнут највећи степен уређености молекула *n*-хексана тако да је у том случају он у стању које је најсличније чврстом док је у зеолиту са Cu(II) јонима постигнута његова најмања уређеност.

(Примљено 3. фебруара, прихваћено 21. апила 2015)

REFERENCES

1. B. Smit, T. Maesen, *Chem. Rev.* **108** (2008) 4125
2. G. Rakhmatkariev, K. Zhalalov, K. Akhmedov, *Uzb. Khim. Zh.* **3** (1998) 68
3. M. Dubinin, G. Rakhmatkariev, A. Isirikyan, *Izv. Akad. Nauk. SSSR Ser. Khim.* **10** (1989) 2333
4. F. Eder, J. Lercher, *Zeolites* **8** (1997) 75
5. F. Eder, J. Lercher, *J. Phys. Chem., B* **101** (1997) 1273
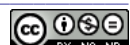
6. H. Zhang, S. Peng, L. Mao, X. Zhou, J. Liang, C. Wan, J. Zheng, X. Ju, *Phys. Rev., E* **89** (2014) 89
7. C. Malheiro, B. Mendiboure, J. Miguez, M. Pineiro, C. Miqueu, *J. Phys. Chem., C* **118** (2014) 24905
8. C. Bilgic, A. Askin, *J. Chromatogr., A* **1006** (2003) 281
9. A. Chica, A. Corma, P. Miguel, *Catal. Today* **65** (2001) 101
10. J. Delgado, T. Nijhuis, F. Kapteijn, J. Moulijn, *Chem. Eng. Sci.* **59** (2004) 2477
11. J. Denayer, G. Baron, J. Martens, P. Jacobs, *J. Phys. Chem., B* **102** (1998)3077
12. L. Domokos, L. Lefferts, K. Seshan, J. Lercher, *J. Catal.* **203** (2001) 351
13. J. Ndjaka, G. Zwanenburg, B. Smit, M. Schenk, *Micropor. Mesopor. Mat.* **68** (2004)37
14. M. Pera-Titus, *J. Phys. Chem., C* **115** (2011) 3346
15. M. Miyahara, K. Gubbins, *J. Chem. Phys.* **106** (1997) 2865
16. K. Morishige, K. Kawano, *J. Chem. Phys.* **110** (1999) 4867
17. M. Sliwinska-Bartkowiak, J. Gras, R. Sikorski, R. Radhakrishnan, L. Gelb, K. Gubbins, *Langmuir* **15** (1999) 6060
18. J. Klein, E. Kumacheva, *Science* **269** (1995) 816
19. J. Klein, E. Kumacheva, *J. Chem. Phys.* **108** (1998) 6996
20. M. Miyahara, M. Sakamoto, H. Kanda, K. Higashitani, *Stud. Surf. Sci. Catal.* **14** (2002) 411
21. U. Raviv, P. Laurat, P. Klein, *Nature* **413** (2001) 51
22. R. Radhakrishnan, K. Gubbins, A. Watanabe, K. Kaneko, *J. Chem. Phys.* **111** (1999) 9058
23. K. Sirkar, *Chem. Eng. Commun.* **157** (1997) 145
24. S. Bates, R. Van Santen, *Adv. Catal.* **42** (1998) 1
25. B. Newalkar, N. Choudary, U. Turaga, R. Vijayalakshmi, P. Kumar, S. Komarneni, T. Bhat, *Chem. Mater.* **15** (2003) 1474
26. R. Kolvenbach, L. Gonzalez-Pena, F. Luis, A. Jentys, J. Lercher, *Catal. Lett.* **143** (2013) 1116
27. T. Vlugt, M. Schenk, *J. Phys. Chem., B* **106** (2002) 12757
28. S. Bates, M. Gillan, G. Kresse, *J. Phys. Chem., B* **102** (1998) 2017
29. P. Jacobs, H. Beyer, J. Valyon, *Zeolites* **1** (1981) 161
30. B. Smit, T. Maesen, *Nature* **337** (1995) 42
31. N. Floquet, J. Simon, J. Coulomb, J. Bellat, G. Weber, G. Andre, *Micropor. Mesopor. Mater.* **122** (2009) 61
32. D. Olson, P. Reischman, *Zeolites* **17** (1996) 434
33. W. Well, J. Wolthuizen, B. Smit, J. Hooff, R. Santen, *Stud. Surf. Sci. Catal.* **105** (1997) 2347
34. M. Henri, H. Loven, *Phys. Rev. Lett.* **85** (2000) 366 8
35. D. Majda, W. Makowski, *J. Therm. Anal. Calorim.* **101** (2010) 519
36. H. Morell, K. Angermund, A. Lewis, D. Brouwer, C. Fyfe, H. Gies, *Chem. Mater.* **14** (2002) 2192
37. J. Coulomb, P. Llewellyn, Y. Grillet, J. Rouquerol, *Stud. Surf. Sci. Catal.* **87** (1994) 535
38. U. Müller, H. Reichert, E. Robens, K. Unger, Y. Grillet, *Anal. Chem.* **3** (1989) 433
39. P. Llewellyn, J. Coulomb, Y. Grillet, J. Patarin, H. Lauter, H. Reichert, J. Rouquerol, *Langmuir* **9** (1993) 1846
40. D. Dubbeldam, S. Calero, T. Maesen, B. Smit, *Phys. Rev. Lett.* **90** (2003) 245901
41. G. Manos, L. Dunne, M. Chaplin, Z. Du, *Chem. Phys. Lett.* **335** (2001) 77
42. R. Krishna, S. Calero, B. Smit, *Chem. Eng.* **88** (2002) 81

43. W. Makowski, D. Majda, *Thermochim. Acta* **412** (2004) 31
44. W. Makowski, D. Majda, *Appl. Surf. Sci.* **252** (2005) 707
45. W. Haohan, Q. Gong, D. Olson, J. Li, *Chem. Rev.* **112** (2012) 836
46. D. Olson, A. Lan, J. Seidel, K. Li, J. Li, *Adsorption* **16** (2010) 559
47. R. Richards, L. Rees, *Langmuir* **3** (1987) 35
48. R. Marguta, S. Khatib, J. Guil, E. Lomba, E. Noya, J. Perdigon-Melon, S. Valencia, *Micropor. Mesopor. Mater.* **142** (2011) 258
49. T. Vlugt, R. Krishna, B. Smit, *J. Phys. Chem., B* **103** (1999) 1102
50. U. Lohse, H. Thamm, M. Noack, B. Fahlke, *J. Incl. Phenom.* 5 (1987) 307
51. W. Zhu, F. Kapteijn, B. Linden, A. Moulijn, *Phys. Chem. Chem. Phys.* **3** (2001) 1755
52. R. Hercigonja, V. Rac, V. Rakic, A. Auroux, *J. Chem. Thermodyn.* **48** (2012) 112
53. S. Ashtekar, A. McLeod, M. Mantle, P. Barrie, L. Gladden, J. Hastings, *J. Phys. Chem., B* **104** (2000) 5281
54. Y. Yang, C. Rees, *Micropor. Matter.* **12** (1997) 117
55. B. Millot, A. Methivier, H. Jobic, *J .Phys. Chem., B* **102** (1998) 3210
56. D. Majda, W. Makowski, *J. Therm. Anal. Calorim.* **101** (2010) 519
57. W. Makowski, L. Ogorzale, *Thermochim. Acta* **465** (2007) 30
58. V. Rac, V. Rakic, S. Gajinov, V. Dondur, A. Auroux, *J. Therm. Anal. Calorim.* **84** (2006) 239
59. J. Pieterse, S. Booneveld, R. van den Brink, *Appl. Catal., B-Environ.* **51** (2004) 215
60. R. Burch, P. Millington, *Appl. Catal., B-Environ.* **2** (1993) 101
61. S. Yashnik, Z. Ismagilov, V. Anufrienko, *Catal. Today* **110** (2005) 310
62. X. Li, B. Shen, C. Xu, *Appl. Catal., A-Gen.* **375** (2010) 222
63. O. Bortnovsky, P. Sazama, B. Wichterlova, *Appl. Catal., A-Gen.* **287** (2005) 203
64. K. Kohei, I. Hajime, N. Seitaro, I. Akira, *Catal. Commun.* **29** (2012) 162
65. W. Haag, R. Dessau, R. Lago, *Stud. Surf. Sci. Catal.* **60** (1991) 255
66. T. Narbeshuber, H. Vinek, J. Lercher, *J. Catal.* **157** (1995) 388
67. W. Haag, *Stud. Surf. Sci. Catal.* **84** (1994) 1375
68. W. Makowski, B. Gil, D. Majda, *Catal. Lett.* **120** (2008) 154
69. J. Janchen, H. Stach, L. Uytterhoven , W. Mortier, *J. Phys. Chem.* **100** (1996) 12489
70. R. Barrer, J. Suterland, *Proc. R. Soc. A-Math. Phys.* **237** (1956) 439
71. W.J. Mortier, *Compilation of Extra-Framework Sites in Zeolites*, Butterworth Scientific Limited, Guildford, 1982
72. P. Jacobs, H. Beyer, J. Valyon, *Zeolites* **1** (1981) 161
73. K. De Meyer, S. Chempath, J. Denayer, J. Martens, R. Snurr, G. Baron, J. *Phys. Chem., B* **107** (2003) 10760
74. P. Titus, *J. Phys. Chem., C* **115** (2011) 3346
75. K. M. A. De Meyer, M. Kurt, S. Chempath, J. Denayer, J. Martens, A. Johan, R. Snurr, G. Baron, *J. Phys. Chem., B* **107** (2003) 10760
76. R. Barrer, R. Gibbons, *Trans. Faraday Soc.* **59** (1963) 2875
77. NIST Chemistry WebBook, http://www.webbook.nist.gov/chemistry/
78. H. Zou, M. Li, J. Shen, A. Auroux, *J. Therm. Anal. Calorim.* **72** (2003) 209.

Hollow-fiber micro-extraction combined with HPLC for the determination of sitagliptin in urine samples

RAHEME REZAEE, MAHNAZ QOMI* and FOROOZAN PIROOZI

Medicinal Chemistry Department, Pharmaceutical Sciences Research Center, Pharmaceutical Sciences Branch, Islamic Azad University, Tehran, Iran

Abstract: In this study, a three-phase, hollow-fiber, liquid-phase micro-extraction (HF–LPME) method coupled with high performance liquid chromatography was successfully developed for the determination of trace levels of the anti-diabetic drug sitagliptin (STG) in urine samples. Sitagliptin was extracted from 15 mL of the basic sample solution with a pH of 8.5 into an organic extracting solvent (*n*-octanol) impregnated in the pores of a hollow fiber and then back extracted into an acidified aqueous solution in the lumen of the hollow fiber with a pH of 3. After extraction, 20 µL of the acceptor phase was injected into HPLC system. In order to obtain high extraction efficiency, the parameters affecting the HF–LPME, including pH of the source and receiving phases, type of organic phase, ionic strength, stirring rate, extraction time, the volume ratio of donor phase to acceptor phase and temperature, were studied and optimized. Under the optimized conditions, enrichment factors up to 88 were achieved and the relative standard deviation of the method was in the range from 3 to 6 %. The results indicated that the HF–LPME method has an excellent clean-up capacity and a high pre-concentration factor and could serve as a simple and sensitive method for monitoring the drug in urine samples.

Keywords: anti-diabetic drug; drug analysis; chromatography; biological sample; pre-concentration.

INTRODUCTION

Type 2 diabetes mellitus is a common chronic condition that causes significant morbidity and mortality worldwide and is a growing global public health concern.

Sitagliptin (STG), (*R*)-4-oxo-4-[3-(trifluoromethyl)-5,6-dihydro[1,2,4]triazolo[4,3-a]pyrazin-7(8*H*)-yl]-1-(2,4,5-trifluorophenyl)butan-2-amine, is an orally active, potent and selective inhibitor of dipeptidylpeptidase-4 (DPP-4 inhibitor), for the treatment of type 2 diabetes.[1,2] STG was the first DPP-4 inhibitor to gain

---

1311

the approval of the Food and Drug Administration (FDA) in October 2006 for both monotherapy and in combination with other anti-diabetic agents for the treatment of type 2 diabetes mellitus.[3] Following oral administration of a 100-mg tablet, the absolute bioavailability is approximately 87 % and therapeutic concentration (c_{max}) is 950 nmol L^{-1} in healthy individuals. Eighty seven percent of STG is eliminated *via* renal excretion (79 % unchanged) with a renal clearance in the region of 350 mL min^{-1}.[1,2,4]

Several liquid chromatographic methods with ultraviolet and mass spectrometric detection have been reported in the literature for the quantitative determination of STG in biological fluids. Techniques utilizing HPLC alone do not have an adequate lower limit of quantification (*LLOQ*) suitable for monitoring sitagliptin in low concentrations.[5] Recent LC/MS/MS methods showed improvement in sensitivity, however, a mass spectrometer is very expensive.[6,7] Therefore, due to the low concentration of sitagliptin in biological samples, a pretreatment and pre-concentration step is generally required prior to determination of trace amounts of the drug. Various sample preparation procedures have been applied for STG in biological fluids, such as liquid–liquid extraction (LLE) and solid phase extraction (SPE).[5,8] The liquid micro extraction method is a relatively new method for sample preparation. This method has some advantages over conventional extraction methods such as LLE and SPE.[9–11] In 1999, Pedersen-Bjergaard and Rasmussen suggested using porous hollow polypropylene fibers as a retainer to maintain the extraction phase, a method known as hollow fiber liquid phase micro extraction (HF–LPME).[12,13]

HF–LPME can be performed in two or three micro-extraction phase modes. The three phases involved in the extraction are the analyte solution (donor), an organic phase and second aqueous phase into which the extraction is conducted (acceptor phase). During the extraction, the desired analyte under proper conditions is first transferred into the organic phase and then into the acceptor phase. The rate of conducting the extraction depends on the rate of mass transfer between the two interfaces of the donor/organic phase and the organic/acceptor phase. The main reported limitation of this method is that it is only applicable for species which are capable of ionization.[14,15] In the present study, a simple, inexpensive and sensitive three-phase hollow fiber micro-extraction technique combined with high performance liquid chromatography-ultraviolet detection (HPLC––UV) is described for the extraction and determination of STG in urine samples.

EXPERIMENTAL

Chemicals and materials

Sitagliptin reference standard was kindly donated by the Food and Drug Organization (Tehran, Iran). A stock solution containing 200 μg mL^{-1} of sitagliptin was prepared in HPLC grade methanol and stored at 4 °C. Working solutions (from 2 to 300 μg L^{-1}) were freshly prepared in HPLC grade water by dilution of the stock solution and filtered using a Millipore

filter (0.45 μm) each day prior to use. All chemicals were of analytical reagent grade unless otherwise stated. The urine samples were obtained from the Taleghani Clinic (Tehran, Iran). The samples were diluted using deionized water and were used for method development and calibration. The working standards for real sample analysis were prepared by spiking STG to 15 mL of urine samples, which were diluted 1:1 with ultra-pure water.

Apparatus and chromatographic conditions

The chromatographic separations were realized on a Youngling HPLC instrument equipped with a YL 9110 quaternary HPLC pump, a 20 μL sample loop and YL 9120 UV-Vis detector. The chromatographic data were collected and analyzed using a Younglin Autochro-3000. The separations were performed on a C_{18} column (150 mm×4.6 mm, with 5 μm particle size) from Teknokroma (Barcelona, Spain). A mixture of methanol and 0.1 % perchloric acid (40:60) at a flow rate of 1.0 mL min^{-1} was used as the mobile phase. The injection volume was 20 μL for all the standards and samples, and the detection was performed at a wavelength of 268 nm. The pH measurements were performed using a GPHR 1400A pH meter (Berlin, Germany). A magnetic stirrer model MR Hei-Standard (Heidolph Company, Germany) and a 25 μL syringe model 702 NR from Hamilton (Bonaduz, Switzerland) were also used. The ultrapure water was from a MilliQ Ultrapure water purification system (Millipore, Bedford, MA, USA). All extractions were realized using a Q3/2 Accrual polypropylene hollow fiber membrane from Membrana (Wuppertal, Germany) with a 0.2 μm pore size, 600 μm internal diameter and 200 μm wall thickness.

Extraction procedure

Initially, the polypropylene fibers were cut to the size of 8.5 cm (the volume of these fibers was approximately 22 μL). The fibers were completely washed with acetone in an ultrasonic bath for 10 min and then dried at room temperature before use for extraction. In order to avoid any possible memory effects, a new fiber was used for each extraction. In the extraction procedure, 15 mL of the sample solution with a known concentration and alkaline pH was transferred to a 20-mL sample vial containing a magnetic stirring bar. The sample vial was placed on a Heidolph MR 3001 K magnetic stirrer. Thirty μL of an acceptor phase with an acidic *pH* was withdrawn by a 25 μL Hamilton micro-syringe and the syringe needle was inserted into the hollow fiber segment. The fiber was immersed in an organic solvent for 10 s (*n*-octanol) to impregnate the fiber pores with the organic solvent. The fiber was then placed in distilled water for 30 s in order to wash the extra solvent from its surface. The acceptor phase inside the syringe was injected into the lumen of the fiber. The end of the fiber was blocked by a piece of aluminum foil. The U-shaped fiber was placed in the sample vial. The sample solution was agitated at 1000 rpm. At the end of the extraction (after 50 min), the fiber was removed from the sample solution and the acceptor phase was then retracted back into the syringe. Finally, the extraction phase (20 μL) was injected directly into the HPLC system in order to analyze the drug. In 2006, Pawliszyn and co-workers successfully automated the HF–LPME technique with a CTC CombiPal autosampler, and a new device was designed for the automation of HF–LPME in this study.[16]

RESULTS AND DISCUSSION

In this study, a three-phase hollow-fiber micro-extraction technique combined with HPLC–UV was used for the extraction and determination of STG in biological samples. Furthermore, the effect of different experimental parameters on the efficiency of extraction, such as the type of organic solvent, the pH of the

donor and acceptor phases, the stirring time, the ionic strength of the donor phase, temperature, the stirring rate and the volume ratio of donor phase to acceptor phase were all investigated and optimized to obtain the best analytical performance.

Type of organic solvent

It is important to select a suitable solvent in order to achieve maximum extraction, good sensitivity, selectivity and high accuracy. The chosen solvent should enter easily into the fiber pores, be non-toxic, and ultimately have a high boiling point (be non-volatile) and a proper viscosity to be stable during the extraction process.[10,17,18]

In order to select a proper solvent, several solvents (*n*-octanol, *n*-octane, 1-decanol, 4-methyl-2-pentanone and benzyl alcohol) were examined. The highest extraction efficiency was obtained using *n*-octanol (Fig. 1).
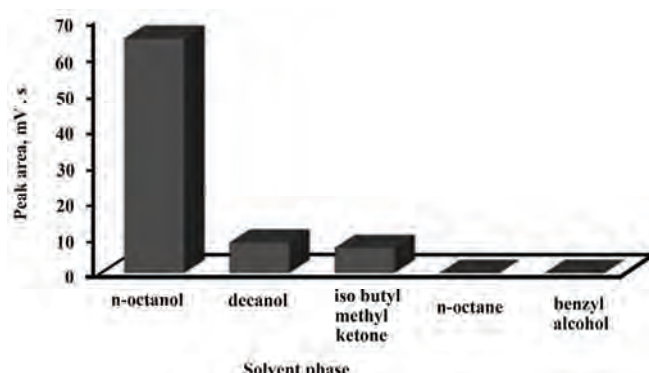
Fig. 1. The effect of organic solvent on HF–LPME efficiency in the determination of sitagliptin.

pH of acceptor phase and donor phase

The pH values of the donor and acceptor solutions are important factors in a three-phase LPME. For ionizable analytes, acid–base dissociation is the most common reaction utilized to facilitate the extraction of the analyte from the donor to the acceptor phase.[18–20] The pH difference between the donor and acceptor phases can promote the transfer of analytes. For practical applications, the pH should differ from the pK_a value of the analyte (the pK_a of STG is 7.7) by at least 3 units.[21]

To promote extraction, the pH of the donor solution was adjusted in order to deionize the analyte. Therefore, the effect of the donor phase pH on the extraction efficiency was studied by changing the sample pH from 8.0 to 12.5. The maximum efficiency of the analyte extraction was achieved at pH 10.5.

The effect of the pH of the acceptor phase from 2.0 to 4.0 was studied. At pH of 3, the extraction rate increased because STG had an ionic structure at this pH and transferred easily into the aqueous phase.

Accordingly, pH values of 10.5 and 3 were selected as optimum values for the donor and acceptor phases respectively.

Stirring rate of analyte solution

Stirring the sample during extraction reduces the thermodynamic equilibrium time and increases the extraction efficiency as stirring provides a fresh donor solution for the organic phase to extract and enhances analyte transport from the donor phase to the organic solvent. To evaluate the effect of sample stirring, the aqueous donor sample was stirred for 50 min at different rates (from 250 to 1200 rpm). The efficiency of extraction increased with increasing stirring speed. However, at 1200 rpm there was a decrease in the extraction efficiency, probably due to the high speed creating air bubbles on the surface of the hollow fiber that ultimately leads to poorer precision and possible failure of the experiment.[10,22,23] Finally, a stirring speed of 1000 rpm was adopted for the subsequent experiments.

Ionic strength of the donor phase

In this stage, the effect of adding salt to the donor phase on the extraction rate was investigated. Generally, two phenomena occur simultaneously when salt is added to water. The first phenomenon is known as salting-out (this can increase the efficiency of the extraction) and the second phenomenon is electrostatic interactions between the analyte molecules and the salt,[18,19] which reduces the mobility of the analyte molecules and increases the thickness of the emission layer between the sample solution and fibrated organic layer, that reduces the extraction efficiency. Furthermore, the addition of salt could increase the viscosity of the sample solution and change the physical properties of the fiber wall, which could reduce the movement of analyte from the donor to solvent phase. Overall, it is fair to comment that the addition of salt depends on the nature of the analyte and could increase, decrease or, in some cases, not change the efficiency of extractions.[24,25]

In this study, the effect of salt addition (NaCl) from 0 to 350 g L^{-1} was investigated on the extraction rate. NaCl addition significantly increased the drug extraction. The concentration of 350 g L^{-1} was selected as the optimum value for further studies.

Thus, according to the nature, structure and the pK_a value (7.7) of STG, the salting out phenomenon was dominant in this process and, therefore, increasing the salt concentration, increased the extraction rate of the drug.
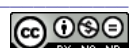
Extraction time

The extraction and recovery of an analyte is affected by the stirring time of the sample solution, which facilitates the transfer of an analyte from the donor phase to the organic phase and finally to the acceptor phase. In this study, the effect of extraction time between 20 and 60 min was examined.

Normally, if the extraction time is too long, the loss of solvent and the formation of air bubbles may occur, both of which affect the extraction efficiency.[17,10,26,27]

The obtained results showed that with increasing time, the extraction rate increased. Based on thee results, an extraction time of 50 min was selected as a suitable extraction time.

Temperature

In this study, the effect of temperature on extraction rate was investigated in the range from 22 to 45 °C. The results demonstrated that the extraction efficiency was reduced on increasing the temperature. This could be due to solvent evaporation and bubble formation on the fiber wall.[19] Therefore, 25 °C was chosen as the optimum temperature for the extractions.

Volume ratio of donor phase to acceptor phase

In the three phase HF–LPME, an analyte transfers from an aqueous donor phase to an organic solvent and finally to an acceptor phase existing in the fiber during an emission process. Pre-concentration factor (*PF*) in this process is calculated based on the equation:

$$PF = \frac{100V_d R}{V_a}$$

where V_d and V_a are the volumes of the donor phase and acceptor phase, respectively, and R is the extraction efficiency.[20,25]

In this study, the volume of the acceptor phase was kept constant (20 µL), and the volume of donor phase was altered and the effects of these changes on the extraction rate were investigated. Based on the obtained results, 15 mL was selected as the optimum volume of the donor phase.

Validation method

The calibration curve for STG in aqueous solutions was plotted in the concentration range from 0.05 to 10 mg L^{-1}. For each level, three replicate extractions were performed under the optimum pre-concentration conditions (Table I).

TABLE I. Optimum conditions for the pre-concentration of sitagliptin

V_d / mL	T / °C	[NaCl] / g dL^{-1}	t / min	Stirring rate, rpm	pH of AP	pH of DP	Solvent
15	25	35	50	1000	3	10.5	*n*-Octanol

The corresponding regression equation, coefficient of determination (R^2), dynamic linear range (*DLR*), limit of detection (*LOD*) and pre-concentration factor (*PF*) of STG were calculated and are summarized in Table II. The *LOD* was calculated at a signal-to-noise ratio of 3 and was obtained by adding the standard STG solution to drug-free urine samples. The results indicated that the proposed method displayed good reproducibility to determine sitagliptin with intra-day *RSD* value of 3.4 % and inter-day *RSD* value of 5.25 % (for 3 consecutive days, the extraction was performed at an STG concentration of 1 mg L^{-1}). Under the optimized conditions, enrichment factors of up to 88 were achieved.

TABLE II. The values of the corresponding regression equation and the analytical characteristics of the proposed HF–LPME method; *PF*, pre-concentration factor; *LOD*, limit of detection; *LOQ*, limit of quantification; R^2, coefficient of determination; *DLR*, dynamic linear range and *RSD* %: relative standard deviation; Analyzed concentrations, mg L^{-1}: 0.05, 0.2, 0.5, 3, 5, 7, 9 and 10

Inter-day *RSD* / %	Intra-day *RSD* / %	*DLR* range ng mL^{-1}	R^2	Intercept	Slope mV s L mg^{-1}	*LOQ* ng mL^{-1}	*LOD* ng mL^{-1}	*PF*
5.25	3.4	2.5–200	0.999	25.881	328.09	3.0	1.0	88

Extraction of sitagliptin from urine samples

Under the optimized conditions, the developed HF–LPME–HPLC technique was applied to the pre-concentration and determination of sitagliptin in urine samples. The pH of the real samples was adjusted to 10.5 by the addition of 0.1 mol L^{-1} NaOH solution. Prior to the spiking and extraction of the target drug, the urine samples were diluted 1:1 with water. Typical chromatograms for spiked and non-spiked urine samples obtained by the HF–LPME–HPLC method are shown in Figs. 2 and 3, respectively.
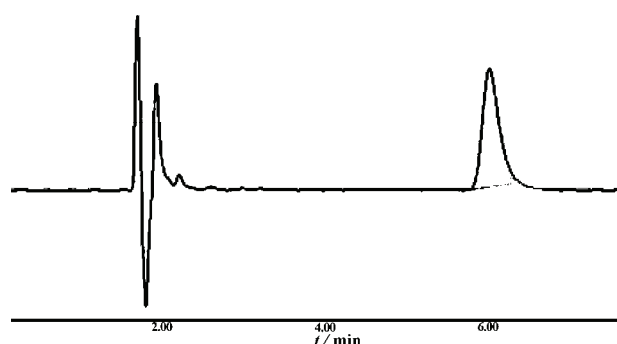
Fig. 2. Representative HF–LPME–HPLC chromatograms of urine sample spiked with 10 ng/mL of sitagliptin under the optimum conditions (*n*-octanol as organic solvent; the donor phase *pH* of 10.5; the acceptor phase *pH* of 3; stirring speed of 1000 rpm; concentration of NaCl 35 g dL^{-1}; extraction time of 50 min; temperature of 25 °C; volume of donor phase of 15 mL).
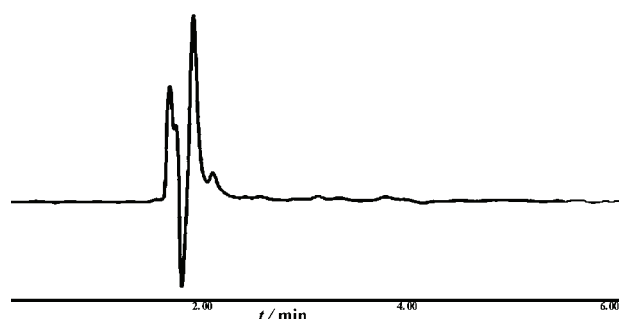
Fig. 3. Representative HF–LPME–HPLC chromatograms of control urine sample.

Comparison of the present method with other reported methods

The present method was compared with other studies in terms of the method of extraction, validation, and precision. The method compares well with those mentioned in Table III. As can be seen, the *LOD* value of this method is comparable with those obtained in previous studies, and even lower than those reported in the literature. In addition, due to the simplicity and low cost of the extraction device, the hollow fiber, it can be discarded after each extraction to avoid carry-over and cross-contamination.

TABLE III. Comparison of the proposed method with other developed methods for determination of sitagliptin in biological samples

Determination method	Extraction method	*LOD* μg mL^{-1}	*DLR* μg mL^{-1}	*LOQ* μg mL^{-1}	*RSD* %	Real sample	Ref.
HPLC–UV	HF–LPME	0.001	0.0025–0.2	0.003	3.4	Urine	Present work
HPLC	LLE	–	0.75–100	0.75	10>	Plasma	28
LC/MS/MS	LLE	–	0.001–1	0.001	2–6.1	Plasma	6
HTLC/MS/MS	TFO[a]	–	0.1–50	0.1	2.3–6.5	Urine	29
RP-LC	–	0.02	0.25–200	0.075	0.93–1.62	Plasma	30
LC/MS/MS	LLE	–	0.001–0.25	0.001	<6	Plasma	7
LC	MISPE[b]	0.03 (μg L^{-1})	0.1–100 (μg L^{-1})	0.1 (μg L^{-1})	0.4	Urine	8

[a]TFO: turbulent flow online, [b]MISPE: molecularly imprinted solid-phase extraction

CONCLUSIONS

This work introduced a three-phase HF–LPME method combined with HPLC–UV for the extraction, pre-concentration and determination of STG in urine samples. The LPME technique proved to have several advantages over the other extraction methods such as liquid–liquid extraction (LLE) and solid phase extraction (SPE). A simple, fast and inexpensive HF–LPME–HPLC–UV with

high accuracy and good sensitivity for the extraction and determination of STG in human urine samples was developed and validated.

И З В О Д

ЕКСТРАКЦИЈА ШУПЉИМ ВЛАКНИМА КОМБИНОВАНА СА HPLC ЗА ОДРЕЂИВАЊЕ СИТАГЛИПТИНА У УЗОРЦИМА УРИНА

RAHEME REZAEE, MAHNAZ QOMI и FOROOZAN PIROOZI

Medicinal Chemistry Department, Pharmaceutical Sciences Research Center, Pharmaceutical Sciences Branch, Islamic Azad University, Tehran, Iran

У овом раду је успешно развијена трофазна микроекстракција шупљим влакнима у течној фази (HF–LPME) спрегнута са високоефиксном течном хроматографијом (HPLC) за одређивање трагова лека, антидијабетика ситаглиптина (STG), у узорцима урина. Ситаглиптин је екстрахован из 15 mL основног раствора, на pH 8,5 у органски растварач (*n*-октанол) у порама шупљег влакна и ре-екстархован у закишељен раствор у лумену шупљег влакна на pH 3. После екстракције, 20 µL акцепторске фазе је ињектирано у HPLC систем. У циљу боље ефикасности екстракције, испитивани су и оптимизовани параметри који утичу на HF–LPME, као што су pH донорске и акцепторске фазе, тип органске фазе, јонска јачина, брзина мешања, време екстракције, запремински однос донорске и акцепторске фазе и температура. Под оптималним условима је постигнут фактор преконцентрисања од 88 и добијена релативна стандардна девијација у опсегу 3–6 %. Резултати указују да HF–LPME метода има одличан капацитет за пречишћавање и висок фактор преконцентрисања, па може бити примењена као једноставна и осетљива метода за праћење лекова у узорцима урина.

(Примљено 27. децембра 2014, ревидирано 14. маја, прихваћено 24. маја 2015)

REFERENCES

1. R. Pathak, M. B. Bridgeman, *P&T* **35** (2010) 509
2. D. K. Badyal, J. Kaur, *JK Science* **10** (2008) 97
3. E. Fleury-Milfort, *J. Am. Acad. Nurse Pract.* **20** (2008) 295
4. A. J. Scheen, *Diabetes Obes. Metab.* **12** (2010) 648
5. S. Terabe, *Anal. Chem.* **76** (2004) 241A
6. W. Zeng, Y. Xu, M. Constanzer, E. J. Woolf, *J. Chromatogr., B* **878** (2010) 1817
7. R. Nirogi, V. Kandikere, K. Mudigonda, P. Komarneni, R. Aleti, R. Boggavarapu, *Biomed. Chromatogr.* **22** (2008) 214
8. R. Rao, P. Maurya, S. Khalid, *Talanta* **85** (2011) 950
9. A. Rodríguez, S. Pedersen-Bjergaard, K. E. Rasmussen, C. Nerín, *J. Chromatogr., A* **38** (2008) 1198
10. K. M. Al Azzama, A. Makahleaha, B. Saada, S. Mansorb, *J. Chromatogr., A* **1217** (2010) 3654
11. Y. Tao, J. F. Liu, X. L. Hu, H. C. Li, T. Wang, G. B. Jiang, *J. Chromatogr., A* **1216** (2009) 6259
12. S. Pedersen-Bjergaard, K. E. Rasmussen, *Anal. Chem.* **71** (1999) 2650

13. K. E. Rasmussen, S. Pedersen-Bjergaard, M. Krogh, H. G. Ugland, T. Grønhaug, *J. Chromatogr., A* **873** (2000) 3
14. K. E. Rasmussen, S. Pedersen-Bjergaard, *Anal. Chem.* **23** (2004) 1
15. L. Hou, H. K. Lee, *Anal. Chem.* **75** (2003) 2784
16. G. Ouyang, J. Pawliszyn, *Anal. Chem.* **78** (2006) 5783
17. S. Shariati, Y. Yamini, A. Esrafili, *J. Chromatogr., B* **877** (2009) 393
18. E. Tahmasebi, Y. Yamini, A. Saleh, *J. Chromatogr., B* **877** (2009) 1923
19. M. Saraji, M. T. Jafari, H. Sherafatmand, *J. Chromatogr., A* **1217** (2010) 5173
20. H. Ebrahimzadeh, Y. Yamini, H. A. Firozjaei, F. Kamarei, N. Tavassoli, M. R. Rouini, *Anal. Chim. Acta* **665** (2010) 221
21. S. Pedersen-Bjergaard, K. E. Rasmussen, *J. Chromatogr., A* **1184** (2008) 32
22. J. Xiong, J. Chen, M. He, B. Hu, *Talanta* **82** (2010) 969
23. M. Saraji, B. Farajmand, A. A. Ensafi, A. R. Allafchian, Z. M. Zare, *Talanta* **82** (2010) 1588
24. Y.-J. Dong, *J. Chin. Chem. Soc.* **56** (2009) 549
25. M. Liu, B. Qiu, X. Jin, L. Zhang, X. Chen, G. Chen, *J. Sep. Sci.* **31** (2008) 622
26. F. Barahonaa, A. Gjelstad, S. Pedersen-Bjergaard, K. E. Rasmussen, *J. Chromatogr., A* **1217** (2010) 1989
27. Y. Yang, J. Chen, Y. P. Shi, *J. Chromatogr., B* **878** (2010) 2811
28. X. F. Jiu, D. W. Shang, Y. Chen, X. G. Li, X. M. Wan, T. Y. Zhou, W. Lu, *J. Chin. Pharm. Sci.* **20** (2010) 63
29. W. Zeng, D. Musson, A. Fisher, L. Chen, M.S. Schwartz, E. J. Woolf, *J. Pharm. Biomed. Anal.* **46** (2008) 534
30. R. El-Bagary, E. F. Elkady, B. M. Ayoub, *Talanta* **85** (2011) 673.

Secondary-school chemistry textbooks in the 19th century

VESNA D. MILANOVIC[1#], DRAGICA D. TRIVIC[2*#] and BILJANA I. TOMASEVIC[2#]

[1]*Innovation Centre of the Faculty of Chemistry, Studentski trg 12–16, Belgrade, Serbia and* [2]*University of Belgrade, Faculty of Chemistry, Studentski trg 12–16, Belgrade, Serbia*

Abstract: The teaching of chemistry in Serbia as a separate subject dates from 1874. The first secondary-school chemistry textbooks appeared in the second half of the 19th century. The aim of this study was to gain insight, by analysing two secondary-school chemistry textbooks, written by Sima Lozanić (1895) and Mita Petrović (1892), into the amount of scientific knowledge from the sphere of chemistry was presented to secondary school students in Serbia in the second half of the 19th century, and the principles textbooks written at the time were based on. Within the framework of the conducted research, we defined the criteria for assessing the quality of secondary-school chemistry textbooks were defined in the context of the time they were written. The most important difference found between the two textbooks under analysis pertained to the way in which their contents were organised. Sima Lozanić's textbook is characterised by a greater degree of systematicness when it comes to the manner of presenting its contents and consistency of approach throughout the book. In both textbooks, the authors' attempts to link chemistry-related subjects to everyday life, and to indicate the practical significance of various substances and their toxicity can be perceived.

Keywords: chemistry teaching; chemistry textbook; structural components of textbooks; textbook quality.

INTRODUCTION

Textbooks are representative samples of the time in which they were written, for they reflect the trends and principles that existed in a particular area of education.[1] In a way, the books are built into the generations of students after which they were taught, for it is through them that a certain way of thinking, a strategy of learning, general intellectual skills and habits, ones attitude towards that which is being learnt, towards science and knowledge in general are cultivated.[2] A review and analysis of various chemistry textbooks from their beginnings to the

present day affords insight into the development of ideas about chemistry and the intellectual achievements of many generations of students in the realm of this science.[3] A textbook reflects the characteristics of the context that it was created in, as well as the academic knowledge and beliefs of its author(s), reflecting their views of what science is or what it should be.[4] It may be viewed as a conversation between chemistry as a scientific discipline, the context for teaching/learning, the author's personal characteristics and the burden that each society imposes upon one.[5] Textbook writers are confined to the margins of scientific communities, they share various cultures and they are under strong social, economic, and political pressures.[6] Moreover, textbooks are read and used by a great variety of audiences with different aims, expectations and reading practices. Scientific textbooks are, therefore, at the crossroad between disciplines such as the of science, the history of education and the history of books and reading.[7] By analysing textbooks that were used in the past, one can form a picture of the quality of teaching at that time can be formed. Insight can be gained into the relationship between science and education, into how fast scientific knowledge was built, into the process of education and the extent to which they represented a response to the needs of society at the time. It could be said that textbooks are sorts of archaeological traces of former regimes of knowledge.[6] Textbooks can be viewed as focal points for many of the historical contingencies that shape not only scientific practice, but also the roles of science and scientists in society. Although most easily treated as part of the history of the book, they also carry historical significances that transcend that genre.[8]

Textbooks turned into an independent and characteristic genre of scientific publication in the 19th century when science education became compulsory in a number of European universities as well as in primary and secondary education. A reason for the rise of the textbook was its instrumentality in the development of the national structures of education, in particular, the nineteenth-century implementation of secondary education.[9]

The teaching of chemistry as an independent subject in secondary schools in Serbia dates back to 1874.[10] Prior to that, chemistry was studied within the framework of physics and mineralogy. It was taught in the fourth grade, four classes per week. In the guidelines sent to teachers in 1874, it is stated that inorganic and organic chemistry with experiments should be taught. Of the four classes per week, one had to be dedicated to conducting experiments, which is indicative of the significance attached to experimental work in the course of teaching chemistry.

By analysing two secondary-school chemistry textbooks written by Sima Lozanić (1895) and Mita Petrović (1892), the aim of this study was to gain insight into the amount of scientific knowledge from the sphere of chemistry

presented to young people in Serbia in the second half of the 19th century, and into principles on which textbooks written at the time were based.

Sima Lozanić (1847–1935) was a chemist, scientist, Professor, Chairman of the Academy of Sciences, the first Rector of Belgrade University, Ambassador to London, Minister of the Economy and Minister of Foreign Affairs, a diplomat. In the mid-1880's, at the time of a reform and modernisation of grammar schools, Lozanić worked on compiling a modern chemistry curriculum and introducing teaching through experiments in secondary schools.[11] Apart from chemistry, Sima Lozanić also studied pedagogy (1868–1870) at the well-known school of pedagogy in Küsnacht near Zurich. At Zurich University, Lozanić studied chemistry under Johannes Wislicenus (1835–1902), and subsequently spent one year at the August Wilhelm von Hofmann's (1818–1892) laboratory for organic chemistry.[12]

For many years, Mita Petrović (1848–1891) worked at the Serbian Teacher-training School in Sombor, where he taught mathematics and natural sciences. He had organized and equipped a chemical laboratory in Sombor where he did research in the sphere of natural sciences, especially physics and chemistry. He also wrote a large number of textbooks on all subjects he taught. These were mainly based on contemporary German language textbooks which Petrović translated and adjusted to the level and needs of his students. He was a correspondent member of the Serbian Academy of Science, and member of numerous other learned societies. Mita Petrović received many accolades for his work.[13]

The rules on writing secondary-school textbooks in Serbia were passed in 1895. A commission was formed the task of which was to establish whether suitable textbooks existed for all the subjects taught at school. In March 1895, the commission informed the Board of Education that there was no suitable chemistry textbook for the fourth grade of grammar school. Within one year, Lozanić wrote a textbook and submitted it for publication in March 1896 (although on the cover 1895 remained as the year of publication). In March 1896, Lozanić sent the textbook to the Minster of Education and to the Board of Education for review. The reviewer Marko Leko submitted a negative review, containing 36 objections, of the textbook to the Board.[14]

The Board of Education, which was composed of secondary school teachers who opposed Lozanić's terminology, decided not to accept Lozanić's book as an official textbook. It was in vain that Lozanić tried to respond to the criticisms addressed to him.[15–19] Through the Board of Education, the polemic between him and Leko continued throughout 1897, until *The Educational Gazette* announced that the editorial board would accept no further correspondence pertaining to the said polemic. Lozanić's textbook was only recommended for use in secondary schools at the beginning of the 20th century. Until then, Mita Petrović's textbook was used.[11]

THE METHODOLOGY OF THE RESEARCH

The textbook sample analysed within the framework of this research was the first edition of Sima Lozanić's textbook *Chemistry for Secondary Schools*, dating from 1895, and the third edition of Mita Petrović's textbook *Chemistry for Secondary Schools, based on Prokop Prohaszka and Others*, dating from 1892. Sima Lozanić's textbook had a total of five editions (1895, 1897, 1903, 1910, and 1925). For the purpose of this analysis, the first edition was chosen in view of the above-mentioned criticism, which reflects the context in which the textbook was created.

Mita Petrović's textbook, despite the fact that it was not in accordance with the curriculum dating from 1881, was used in schools with the permission of the Ministry of Education until the beginning of the 20th century, even after the publication of Sima Lozanić's textbook.[12] The first edition of this textbook came out in 1883, but herein, the third edition, dating from 1892, was analysed as the preceding two editions were not available.

In order to achieve the set goal, first a methodology for analysing and evaluating the quality of these textbooks within the context of the period when they were created required development.

Some characteristics of a textbook can be quantified, whereas others require a qualitative analysis. The main purpose of the qualitative approach is to understand and interpret various meanings that the textbook being analysed carries, following which the elements of the meanings are established.[20] The present analysis of the selected secondary-school chemistry textbooks dating from the 19th century was supposed to provide answers to the following questions:

1. What contents were presented in the chemistry textbooks from the second half of the 19th century?

2. To what extent were the contents presented in the examined textbooks in keeping with the then current level of knowledge in chemistry?

3. What experiments are presented and described in the textbooks?

4. To what extent did the textbooks analysed establish a connection between the textbook contents and everyday life?

5. To what extent does the textbook caution the students to take care when dealing with certain substances?

6. To what extent were the contents of the textbooks in keeping with the chemistry curriculum then in effect?

7. To what extent did the textbooks deal with events from the history of chemistry?

8. How were the analysed textbooks supported in terms of graphic design and illustrations?

9. What were the structural and organisational components of the analysed textbooks?

10. How were the contents of the textbooks shaped in terms of didactics?

The chemistry-related contents of the analysed textbooks were followed through the following: the themes, the index, the symbols and names of the elements mentioned in the textbook, the formulas of chemical compounds and their names, the equations depicting particular chemical reactions. With the exception of the themes reviewed, all the other parameters monitored within the framework of this part of the research were quantified. The degree to which the contents of the analysed textbooks were in keeping with the current level of knowledge in chemistry was assessed based the presence of current discoveries in the sphere of chemistry in the text (for example, the discovery of the periodical system of the elements, the Arrhenius theory of acids and bases, *etc*.).

The extent to which the students' understanding of chemistry was supported through experiments was also monitored. The experiments described in chemistry textbooks brings the question whether laboratory techniques can be appropriated by students when reading textbooks and provide information about the teaching practices in the context of the local resources.[6] The possibilities for developing meanings on the basis of the textbook (the meaningfulness of the textbook material) and insight into the practical importance of the knowledge of chemistry were monitored on the basis of the existing links between the chemistry-related contents and their application in everyday life, and also on the basis of indicating the toxicity of certain substances, their influence on human health and precautions to be taken when dealing with such substances.

The contents of the analysed textbooks were compared with the chemistry curriculum from 1881, the latter being closest in time to their publication dates.

On the basis of the presence of contents related to the history of chemistry, we reviewed the extent to which the textbooks supported the development of an appropriate idea of this science in the students' minds.[21,22] Furthermore, we monitored the ways in which the analysed textbooks were supported in terms of illustrations and graphic design and what kind of information was supplied through the illustrations, *i.e.*, what was their purpose, were monitored. One of the ways of checking the extent to which textbooks achieve their aims is to evaluate the questions that they contain.[23] In the textbooks analysed, the thought processes that they initiated, *i.e.*, the form of learning they initiated, were evaluated.

The structural and organisational components that were monitored within the framework of this analysis are given in Table S-I of the Supplementary material to this paper.

The content of a textbook should be didactically shaped in such a way that it ensures the students' minds are activated, that the basic structure of knowledge is accepted by those for whom the textbook is intended.[20] The indicators of didactic organisation that were followed in the analysed textbooks were as follows: I) the existence of scientific terms, II) the functional use of pictorial means of expression, III) the diversity of the examples provided, IV) the meaningfulness of the organisation of the textbook contents and V) whether the textbook material has any connection with everyday life out of school.

Whether the language of the textbook in question was compatible with the current language of the science of chemistry at the time when the textbooks analysed were written was also monitored during the analysis of the textbooks.

RESULTS AND DISCUSSION

From the introductory statements of both textbooks, their intentions and views on how the study of chemistry should be organised could be seen.

In the preface to the first edition of his textbook, Sima Lozanić pointed out that students found it easier to understand the formulation of the laws of chemistry based on experiments conducted in class. He was of the opinion that it was easier for beginners to learn about general terms in the sphere of chemistry in a separate section of the book and that by doing so enabled the presentation of this part in a systematic manner, thus forming a basis for understanding inorganic and organic chemistry. The method of "placing the general part within the framework of a special part", which was included in the curriculum, could lead to learning without real understanding. In his introductory statement, Sima Lozanić explained that his approach to organising the contents of organic chemistry was

through homologous series. He stressed that he paid greater attention to applied chemistry and to interpreting chemical phenomena in nature, for he was of the opinion that in this way "young men were not only enriched through knowledge but also developed a greater interest in science".

At the beginning of the third edition of Mita Petrović's textbook *Chemistry for Secondary Schools, based on Prokop Prohaszka and Others,* dating from 1892, the preface to the first edition of this textbook, dating from 1883, is included. In this preface, Mita Petrović states that the presentation of the contents of chemistry, the body of knowledge of which has greatly increased, in a manner suitable for beginners to this area, while at the same time including its development as a science, is a problem. He indicated that the organisation of the textbook material was such that the theoretical explanations provided by chemistry were not given in succession, but alternated with experimental parts, and were placed so that the students should be able to understand them when they reached them. In his opening statement, the author pointed out that, when deciding on the scope of the textbook material, he was guided by the curriculum prescribed for grammar schools in the Kingdom of Serbia.

The quantitative data on the analysed textbooks are presented in Table S-II of the Supplementary material. The scope of the textbook material in the analysed textbooks differs: Sima Lozanić's textbook has 163 pages, whereas Mita Petrović's textbook has 110 and is smaller in format. In Sima Lozanić's textbook, the table of chemical elements, containing their symbols, names and atomic mass, comprises 68 elements, of the 70 that were known at the time. The table presented in Mita Petrović's textbook contains such data for 36 elements. In Sima Lozanić's textbook, there are a greater number of chemical formulas. Those are, for the most part, molecular formulas, whereas the number of structural formulas is small in both textbooks.

Both textbooks comprise contents related to general, inorganic and organic chemistry. In Sima Lozanić's textbook, the contents are organised into three sections: general chemistry, inorganic chemistry and organic chemistry. Following a brief opening part, explaining several fundamental terms in the sphere of chemistry, the contents of Mita Petrović's textbook are organised into two sections: inorganic chemistry and organic chemistry.

These two textbooks differ in how their contents are organised. Sima Lozanić's textbook first explains the basic concepts, principles and laws in the sphere of chemistry, and only then proceeds to consider inorganic chemistry through the families of elements, and organic chemistry through the classes of compounds and homologous series. In Mita Petrović's textbook, the material related to inorganic chemistry, within the framework of which chemical elements are considered individually, is interspersed with segments of material in which general chemical

principles and laws are reviewed (which is referred to as "placing the general part within the framework of a special part").

In the general section of Sima Lozanić's textbook, the fundamental concepts and laws in the sphere of chemistry, the division of elements into metalloids and metals, and the nomenclature of chemical compounds are explained. The following fundamental chemical laws are discussed: the law of constant mass ratio, the law of multiple proportions, the law of conservation of mass, and Avogadro's law. The material is conceived in such a way that the corresponding experiments, or the results of experiments that preceded the discovery of the law in question are first presented, followed by the formulation of the law. At the end of the general section, the author explains how the remainder of the textbook is organised, announcing that the most important elements and compounds are discussed, that carbon compounds are especially emphasised because they are so numerous, and thus, that the entire sphere of chemistry is divided into two parts: inorganic chemistry, within the framework of which elements and their compounds are presented, and organic chemistry, within the framework of which carbon compounds are studied.

As opposed to the general section of Sima Lozanić's textbook, which contains 28 subtitles, in the opening section of Mita Petrović's textbook, there are four subtitles. In the section entitled *Things change*, various kinds of physical and chemical changes known from everyday life are presented (changes in the aggregation state of water, sliding a bow across a string, charging a resin bar with electricity, sliding a magnet across steel, the dissolution of sugar in water, the burning of wood and the fermentation of grapes). In the section entitled *Transient and essential changes*, differences between the types of changes are presented, which is followed by their classification into two groups and finally their definition as physical and chemical changes. In the section entitled *The directions of chemical changes*, some experiments are presented, following which the meanings of the terms analysis and synthesis are defined. The last section in the introductory part of the textbook is entitled *The difference between a mixture and a compound*, in which the difference between the two is defined.

In the section of Sima Lozanić's textbook that deals with inorganic chemistry, the chemical elements are presented based on the family of elements to which they belong, They are considered in the following order: the hydrogen family (H), the halogen family (F, Cl, Br and I), the oxygen family (O, S, Se and Te), the nitrogen family (N, P, As, Sb, Bi, B, V, Nb and Ta), the carbon family (C, Si, Ge, Sn, Ti, Zr and Th), the alkali family (Li, Na, K, Rb and Cs), the earth alkali family (Ca, Sr and Ba), the magnesium family (Be, Mg, Zn and Cd), the mercury family (Hg, Cu, Ag and Au), the lead family (Pb), the aluminium family (Al, Ga, In, Tl, Ce, La, Di, Sm, Y, Er, Yb and Sc), the iron family (Fe, Co, Ni, Cr and Mn), the platinum family (Pt, Pd, Ir, Rh, Ru and Os) and the molybdenum

family (Mo, W and Ur). A consistent manner of presentation was used for each of the above families of chemical elements. First the name of the family is given, followed by an enumeration of all elements belonging to it, together with their valences, and then the elements are studied individually. The organisation of the presentation of material when considering each individual element is as follows: after the section title, which contains the name of the element in Serbian and, in most cases, in Latin, its atomic mass, as well as molecular mass if the element occurs in nature in molecular form, the author proceeds to speak of the forms in which it occurs in nature, both in its elementary state and as part of compounds, then of the ways in which it can be obtained, its physical and chemical properties, and finally of its use, that is, its practical application. The physical properties include the state of aggregation, colour, taste, solubility in water and less polar solvents, for example, alcohol and CS_2. The chemical properties include the reactivity of the given element with some other element or compound. Concerning the use of elements, first their use in everyday life is presented, be it in their elementary state or in compounds. This order of presentation of the material is retained when considering the important compounds of the elements previously presented. In the case of compounds where characteristics analogous to those of previously presented compounds featuring elements of the same family can be observed, the similarity in their physical and chemical characteristics are emphasised. At the beginning of the presentation of the majority of the elements, the year when a particular element was discovered and who discovered it are briefly mentioned. In the section dealing with nitrogen, a three-atom molecule of nitrogen, N_3, referred to as argon, as an allotropic modification of nitrogen, analogous with oxygen and ozone, was mentioned (which was deleted from the next edition of the textbook, published in 1897). The mention of N_3 as an allotropic modification of nitrogen was criticised by Marko Leko, and constitutes one of his objections contributing to his negative review of the textbook.

A lot of attention is paid to ores and minerals that contain certain elements and to where they can be found, and the most important mines are enumerated, both in Serbia and outside its boundaries at the time. This points to the significance of mineralogy and to the importance that was attached to it in the sphere of education in the 19th century.

As was already stated, the contents of the inorganic chemistry section of the textbook *Chemistry for Secondary Schools, based on Prokop Prohaszka and Others* are organised based on the principle of "placing the general part within the framework of a special part", which was applied in the chemistry curriculum dating from 1881. This textbook contains separate sections for studying metals and non-metals. The section dealing with non-metals includes a lot of subjects from the sphere of general chemistry, alternating with segments wherein the characteristics of individual elements and their compounds are considered. The

textbook section entitled *Metals* deals with individual metals and their characteristics. The presentation of the contents related to inorganic chemistry begins with the section entitled *On air*. At the very beginning of this section, the following experiment is described – the heating of tin inside a closed vessel, along with measuring the mass of the solid substances before and after the reaction, identical to the one on which Lavoisier (Antoine Laurent Lavoisier, 1743–1794) established the Law of conservation of mass. However, Lavoisier's work is not mentioned here, nor is the law that he discovered; the latter is subsequently explicitly stated within the framework of the section entitled *The quantitative ratios of compounds*. There follows a description of experiments for obtaining nitrogen and oxygen. After this, the characteristics of oxygen and nitrogen are discussed individually, primarily the physical ones, and when considering the characteristics of oxygen, the process of oxidation and the creation of oxides are explained. The next section is entitled *On water*, and it considers hydrogen. The author expounds on the dilemma of whether hydrogen should be classified among non-metals or metals. There follows a general part again in which the following are defined: chemical affinity, atoms and molecules. After neutralisation, there is a detailed presentation of chlorine and sulphur (the way they appear in nature, how they are obtained, their properties, use, *etc*.). Within the framework of the section entitled *The quantitative ratios of compounds*, for the first time an equation of a chemical reaction is presented, namely, the one depicting the creation of water, wherein the reactants are presented in their atomic form. Within the next section, entitled *The important compounds of the elements considered so far*, the following compounds are presented: HCl, H_2S, HNO_3 ($HO \cdot NO_2$), NO_2, NO, H_2SO_4 and $(HO)_2SO_4$. Described is how they occur in nature, how they are obtained, their properties and their use. The next element to be considered is carbon, its allotropic modifications, and the types of coal. Particular attention is paid to the sites of coal deposits and the sources of mineral water in Serbia. Together with carbon, its compounds are considered, which was not the case for the preceding elements. *Valence*, as a topic belonging to the general section, is introduced after carbon. There follows a section entitled *On flame and burning*, wherein the last considered non-metal, phosphorus is introduced.

At the beginning of the section dealing with the study of metals, it is stated that metals are divided into light and heavy ones. The light metals are: K, Na, Ca, Mg, Ba, Sr and Al. The others are heavy metals. What is presented next is the division of metals based on valence follows: one-valence metals (K, Na and Ag), two-valence metals (Ba, Sr, Ca, Mg, Zn, Cd, Pb, Cu and Hg), three-valence metals (Bi and Au), four-valence metals (Al, Mn, Fe, Co, Ni and Cr). It is pointed out that some metals, as well as some non-metals, have more than one valence, that they form two lines of compounds, but that it is still not known

what valence depends on and how it changes, except that it often occurs at high temperatures. Subsequently, the important metals and metal compounds are studied individually, and it should be noted that the "*affinity*" of certain metals is stressed. The section of Mita Petrović's textbook dealing with inorganic chemistry ends with an explanation of the spectral analysis method and a description of the main parts of the spectroscope. As opposed to Mita Petrović's textbook, spectral analysis is not dealt with in Sima Lozanić's textbook, even though in the general section of the textbook, the author did mention the importance of this method and said that he would discuss it later.

At the beginning of the section dealing with organic chemistry, Sima Lozanić states that organic chemistry studies carbon compounds, whether those in the "*kingdom of life*" or those artificially produced in laboratories. Then he presents a classification of organic compounds based on their composition: hydrocarbons, halogen derivatives of hydrocarbons, alcohols, aldehydes, acids, carbohydrates, nitro compounds, amines, amides, nitriles, unstudied compounds (terpenes, camphors, resins and caoutchouc, natural colours and the like, alkaloids, proteins). When speaking of a class of compounds, it is stated whether a particular compound exists in nature, whether it is extracted from certain plants or animals, and how this is realised, whether such compounds exist in the human body and what sort of function they perform. Along with homologous series of carbohydrates, the text presents the boiling and melting temperatures of various elements of the series, on the basis of which conclusions may be draw about their state of aggregation under the same conditions. The importance that was attached to fuel is evident from the amount of space dedicated to oil, the way it is obtained, its refining and various fractions. When considering proteins, the molecular formulas of albumin, haematin and haemoglobin are presented ($C_{72}H_{112}N_{18}SO_{22}$, $C_{68}H_{70}N_8Fe_2O_{10}$ and $C_{600}H_{960}N_{154}FeS_3O_{17}$), but it is stressed that these are their presumed formulas, and that the exact composition of these compounds is still unknown, except that they are characterised by a high molecular mass. The ensuing section contains detailed descriptions of various types of fermentation that contribute too many important processes unfolding in nature, and to processes for producing various compounds. Within the framework of the section entitled *The processes inside an animal organism*, there is a description of the composition of blood and urine, of the process of breathing and digestion. This chapter also contains advice for healthy eating and presents information on the daily needs of the human organism for various kinds of food in order to function properly.

In Mita Petrović's textbook, the first section dealing with organic chemistry, entitled *The ingredients of organic compounds*, contains an explanation of the elements that are part of the composition of organic compounds, while organic chemistry is determined in the following way: "If we heat wood, a feather, paper,

cotton, egg-white, etc. in a glass tube which is heated at one end, after a while they will all turn black and turn into coal. All organic matter contains carbon without exception. An object that does not contain carbon is not organic. We can therefore say that organic chemistry is the chemistry of carbon compounds." Paraffins are considered first, of which methane is presented in some detail, as are its halogen derivatives, along with four equations depicting chemical reactions for its gradual chlorination. After that, cyan compounds, alcohols, ethers, aldehydes and acids are described. Not much attention is dedicated to aldehydes, while acids are considered individually and in more detail within the framework of two sections. Regarding carbohydrates, the following are described individually: plant fibre (cellulose), starch, dextrin, grape sugar, cane sugar (sucrose) and milk sugar. Their occurrence in nature and the method of their extraction from natural products are described, and an experimental method of distinguishing between reducing and non-reducing sugars (Fehling's test) is presented. Within the section entitled Alcohol fermentation, the processes of producing wine, beer and various kinds of brandy are described in detail. A significant amount of attention is dedicated to tannin, in order to indicate its use for tanning leather, making ink, *etc*. Subsequently, aromatic compounds are considered, i.e., how to obtain benzene and its nitro and amino derivatives, and their characteristics. Several alkaloids are enumerated, and their physiological effect on man is indicated. The penultimate section is dedicated to natural colours, and the final one to proteins.

Sima Lozanić's textbook contains the descriptions of 13 experiments, while that of Mita Petrović contains 29 descriptions. A list of experiments featured in the textbooks is given in Table S-III of the Supplementary material. Some of the experiments are featured in both textbooks. The experiments are not individually marked and separated from the main text. From the manner of the presentation of the material, it could be concluded that the authors intended them for demonstration in class, and having presented them, both authors subsequently referred to the experiments already presented when considering new material.

All the experiments featured in Sima Lozanić's textbook pertain to the contents related to general and inorganic chemistry, whereas in Mita Petrović's textbook, two of the experiments belong to the sphere of organic chemistry.

In both textbooks, one can observe the connection between the textbook material and everyday life outside school, be it when it comes to the practical application of certain elements and compounds, or the occurrence and function of organic molecules in the human organism, plants or animals. There are 158 such examples in Sima Lozanić's textbook and 174 examples in Mita Petrović's textbook.

In both textbooks, apart from pointing out the practical use of various substances, the authors stress that certain substances have a toxic effect on human

health. These include not only substances that can be found in a chemical laboratory, but also substances that are encountered in everyday life, or those that easily occur as a result of processes unfolding in the surroundings (such as carbon monoxide gas). In Sima Lozanić's textbook, there are 14 examples testifying to the toxicity of certain substances and their harmful effects on humans, although, there is no direct reference to precautions that should be taken or first-aid measures to be applied if any accident should happen, which is a shortcoming of this textbook. In Mita Petrović's textbook, there are 34 such examples, and in some cases the author points to precautions that should be taken when handling such substances, as well as first-aid measures to be applied.

Sima Lozanić's textbook contains 43 illustrations, whereas that of Mita Petrović contains 10. All the illustrations featured in both the analysed textbooks follow the main text and contribute to a better understanding of chemical concepts and processes. The illustrations in both textbooks are numerically marked, but contain no captions explaining their contents. The main text contains references pointing to a particular illustration through its number. In Sima Lozanić's textbook, the illustrations are used to present apparatuses (ten illustrations), experiments (two illustrations), industrial plants or their segments (nine illustrations), various types of furnaces (eight illustrations), crystallographic structures (two illustrations), structures seen under a microscope (two illustrations), certain processes or parts of them (seven illustrations), chemical vessels and equipment (three illustrations). The first four illustrations are featured in the general section of the textbook, 36 illustrations are to be found within the framework of the inorganic chemistry section, whereas only three illustrations are included in the section of the textbook dealing with organic chemistry. In Mita Petrović's textbook, the illustrations are used to present apparatuses (two illustrations), experiments (four illustrations), processes (two illustrations), laboratory vessels (one illustration) and instruments (one illustration). All the illustrations are included in the textbook section dedicated to inorganic chemistry, specifically, in the part dedicated to studying non-metals.

Contents pertaining to the history of chemistry, mention of essential discoveries in the sphere of chemistry and names of great chemists are to be found in Sima Lozanić's textbook, 27 cases in all, whereas in Mita Petrović's textbook, there are only two references to the historical development of chemistry. In his textbook, Sima Lozanić points to turning points in the development of the science of chemistry (disproving the phlogiston theory, disproving the vitalist theory by means of the Wöhler synthesis of urea), and also to the development of certain production processes that have a broad scope of practical usefulness (the production of ceramic dishes, the production of glass), from time immemorial to the period when the textbook was written, based on which conclusions could be

draw about the development of science through history and its beneficial effect on mankind.

Concerning the monitored structural components in the analysed textbooks, both of them contain: the main text, illustrations and questions. Apart from the three components, Mita Petrović's textbook also contains instructions and references to other parts of the text. Concerning the organisational components, the following were observed in both textbooks: a table of contents, an introductory explanation of the textbook structure as part of the preface, an index of terms arranged in alphabetical order, tables of chemical elements. In Mita Petrović's textbook, there is a brief note on the author, consisting of a few sentences included on the title page. Neither textbook contained a separate list of the literature used in compiling the books, but in their prefaces both authors refer to the authors on whose books they had relied when writing their textbooks. Sima Lozanić states that when writing the present textbook, he had relied on his own textbooks of inorganic and organic chemistry that he had previously written for the High Schools, while Mita Petrović explains in the introductory section that his role model for writing the present textbook was the book written by Prokop Prohaszka, professor of the Czech High School in Prague, entitled *Chemie učebna kniha pro čtvrtu tridu škol realnih, založena na pokuseh*, and that he also relied on Sima Lozanić's inorganic and organic chemistry textbooks for the High Schools.

Indicators of the didactic organisation of a textbook, such as explanations of scientific terms, a functional use of illustrative means of expression and variety of the examples used are for the most part similar in these two textbooks. In both of them, when a term is mentioned for the first time, it is printed in bold letters, and immediately next to it there is an explanation. In both textbooks, definitions of a certain concept, process or phenomenon are supported by diverse specific examples, before or after the formulation of the definition.

In the general section of Sima Lozanić's textbook, there are five questions, followed by answers, whereas in Mita Petrović's textbook, in the course of studying inorganic chemistry, 12 questions are posed, but no specific answers to them are provided. The questions and instructions found in both textbooks analysed are presented in Table S-IV of the Supplementary material.

In Sima Lozanić's textbook, a uniform manner of presenting the material contained in the textbook is consistently applied almost throughout the book (the only exception being the section entitled *Unstudied compounds*, which encompasses terpenes, camphors, resins and caoutchouc, natural colours, alkaloids and proteins), which is not the case with Mita Petrović's textbook.

The contents of both textbooks to a large degree cover the chemistry curriculum of 1881. Both authors observed the recommendation from the curriculum on what should be taught about an element, *i.e.*, how it is obtained, its physical

and chemical properties, how it occurs in nature, its use. Even though Sima Loza-nić's textbook covers the contents relating to inorganic chemistry prescribed by the curriculum, there is a difference between the textbook and the curriculum concerning the organisation of the contents. Mita Petrović's textbook follows the organisation of the contents prescribed by the curriculum more closely ("placing the general part within the framework of a special part"). The essential difference between the 1881 curriculum and the organisation of the contents in both text-books lies in the way organic compounds are systematised. The curriculum, which was actually based on Sima Lozanić's textbook for the High School, sys-tematised organic compounds according to the number of carbon atoms they con-tain, whereas in the textbooks, the compounds are systematised in accordance with homologous series. In Sima Lozanić's textbook, much emphasis is placed on this particular way of systematising compounds, whereas in Mita Petrović's textbook, the compounds are systematised in this way without defining the notion of homologous series.

One characteristic of textbooks is the translations from the language in a sci-entific discipline into the local or national language[7]. A difference was observed concerning the terminology used between the curriculum and Sima Lozanić's textbook, whereas the terminology used in Mita Petrović's textbook is in keeping with the curriculum. In Mita Petrović's textbook, the scientific terms used are adjusted to the Serbian language, that is to say, they are "Serbianised". In Sima Lozanić's textbook, the scientific terminology corresponds to the terminology that we still use today, with minor changes. The names of compounds in Sima Lozanić's textbook are mainly in the nominative case (for example, potassium chloride), while in Mita Petrović's textbook the names of compounds are given in the genitive case (for example, chloride of potassium).[24] At the time, a discus-sion between scientists (not exclusively chemists) was ongoing – should science terminology be "Serbienisied" or not.

Sima Lozanić's textbook also contains topics that go beyond the curriculum contents, mainly related to organic chemistry, whereas Mita Petrović's textbook does not cover several topics from the sphere of inorganic chemistry, nor does it cover the topics contained in the curriculum supplement relating to: the chemical difference between plants and animals, breathing and life-giving heat, and the feeding of plants. Furthermore, it contains no topic beyond those prescribed by the curriculum.

In the major part of both textbooks, the knowledge available at the time is accurately presented, with the exception of the valences of some elements, the symbol of fluorine, the formulas of certain compounds and the equations of che-mical reactions in Mita Petrović's textbook, and the controversial allotropic modification of nitrogen in Sima Lozanić's textbook. Neither textbook mentions Arrhenius's theory of electrolytic dissociation or Mendeleev's periodical system

of the elements. Arrhenius's theory of electrolytic dissociation was posited in 1884, and the textbooks analysed were published in 1892 and 1895, respectively. The omittance of this theory may be explained by the fact that, for a number of years, Arrhenius's theory was under dispute among the scientific public. Neither of the analysed textbooks mentions the periodical system of the elements that Mendeleev published in 1869. This was not the case with the second edition of Sima Lozanić's textbook, dating from 1897. It is surprising that Sima Lozanić did not include the periodical system of the elements in his secondary-school textbook, considering it was included in his previously published inorganic chemistry textbook for High Schools.

CONCLUSIONS

Towards the end of the 19th century, general, inorganic and organic chemistry in secondary schools in Serbia were studied based on the textbooks *Chemistry for Secondary Schools* by Sima Lozanić and *Chemistry for Secondary Schools, based on Prokop Prohaszka and Others* by Mita Petrović. In these two textbooks, a difference in the organisation of the contents of the textbooks is apparent. The discussion was ongoing for years: should general chemistry be presented under inorganic chemistry or as a special section of textbooks. In the former, general chemistry, with the basic chemical concepts, principles, theories and laws, is presented in the opening section, thus forming a basis for inorganic and organic chemistry in the remainder of the textbook. In the latter textbook, the two largest sections are taken up by inorganic and organic chemistry and contents related to general chemistry are presented within the inorganic chemistry section, in those places that the author considered to be the most convenient for the students' understanding of the said contents. Based on the authors' introductory statements, the impression is given that both approaches are the result of their thinking and assessment of the type of organisation of the textbook contents would contribute to the students' better understanding chemistry. The latter author's approach followed more closely the organisation of the then chemistry curriculum, but the former author's approach has been retained in today's chemistry curricula. It may be assumed that the said approach was developed during the course of Sima Lozanić's studies under Wislicenus and Hofmann. However, the approach applied by Sima Lozanić was criticised by Marko Leko, the reviewer of the *Chemistry for Secondary Schools* textbook. The only justification for criticising Sima Lozanić's textbook, based on the present analysis, lies in the fact that he mentioned a controversial allotropic modification of nitrogen. It may be assumed that this arose out of a wish to make the textbook's contents as up-to-date as possible, but in this case, the said scientific information was insufficiently verified. In the second edition of the textbook, Sima Lozanić had already left out the controversial allotropic modification of nitrogen.

The analysed textbooks differ in terms of the scope of their contents, Sima Lozanić's textbook being the more voluminous of the two. As regards the accuracy of the textbooks' contents, several segments of Mita Petrović's textbook were assessed to be inaccurate.

Both textbooks link theoretical contents with corresponding experiments, with the experiments presented in Sima Lozanić's textbook being better suited to the lesson at hand, thus providing a better grounding for understanding the theoretical contents. Both textbooks contain examples that stress the practical significance of chemistry and its connection with everyday life. Also, in both textbooks the authors point out the toxicity of certain substances. Sima Lozanić's textbook, compared to that of Mita Petrović, to a greater extent includes contents related to the history of chemistry which, at the time, could acquaint young people with the nature of science and scientific/research work, the essential turning points in science and the contribution of science to the development of society.

Concerning the structural components, both textbooks contain: the main text, with in-built descriptions of experiments and their results, illustrations and questions. Apart from these components, Mita Petrović's textbook also contains instructions and references to other parts of the text. With regards to the organisational components, both textbooks contain: a table of contents, an introductory explanation of the structure of the textbook within the framework of the preface, an alphabetically arranged index of terms and tables of the elements.

In the final analysis, it could be concluded that Sima Lozanić's textbook is of a better quality compared to that of Mita Petrović, not so much in terms of the choice of contents but in the way the contents are presented and the presentation order.

SUPPLEMENTARY MATERIAL

Structural and organisational components and quantitative data of the textbooks analysed, as well as experiments described and questions and instructions found in them, are available electronically from http://www.shd.org.rs/JSCS/, or from the corresponding author on request.

И З В О Д

УЏБЕНИЦИ ХЕМИЈЕ ЗА СРЕДЊУ ШКОЛУ У 19. ВЕКУ

ВЕСНА Д. МИЛАНОВИЋ[1], ДРАГИЦА Д. ТРИВИЋ[2] и БИЉАНА И. ТОМАШЕВИЋ[2]

[1]*Иновациони центар Хемијског факултета у Београду, Студентски трг 12–16, Београд и*
[2]*Универзитет у Београду, Хемијски факултет, Студентски трг 12–16, Београд*

Настава хемије, као самостални предмет у Србији, датира од 1874. године. Први уџбеници хемије за средњу школу појавили су се у другој половини 19. века. Циљ овог рада јесте да се кроз анализу два средњошколска уџбеника из хемије, аутора Симе Лозанића (1895) и Мите Петровића (1892), сагледа шта се од научних знања из хемије презентовало ученицима у средњим школама у другој половини 19. века и према којим принципима су тада писани уџбеници. У оквиру истраживања дефинисани су критеријуми за праћење квалитета средњошколских уџбеника хемије у контексту времена у коме су настали. Најбитнија нађена разлика између два анализирана уџбеника односи се на организацију садржаја. Уџбеник Симе Лозанића карактерише већа систематичност у излагању садржаја и доследност у приступу кроз цео уџбеник. У оба уџбеника видљива су настојања да се садржаји хемије повежу са свакодневним животим, као и да се поред практичног значаја супстанци укаже на њихову токсичност.

(Примљено 26. септембра 2014, ревидирано 30 маја, прихваћено 8. јуна 2015)

REFERENCES

1. J. C. Bailar, *J. Chem. Educ.* **70** (1993) 695
2. J. Pešić, *One view on critical thinking and its application in the design of textbooks*, University of Belgrade, Faculty of Philosophy, Belgrade, 2006 (in Serbian)
3. S. D. Tarbell, A. T. Tarbell, *J. Chem. Educ.* **54** (1977) 266
4. R. Seligardi, *Sci. Educ.* **15** (2006) 713
5. K. Souza, P. Porto, *Sci. Educ.* **21**(2012) 705
6. B. Bensaude-Vincent, *Sci. Educ.* **15** (2006) 667
7. J. R. Bertomeu-Sanchez, A. Garcia-Belmar, A. Lundgren, M. Patiniotis, *Sci. Educ.* **15** (2006) 657
8. K. M. Olesko, *Sci. Educ.* **15** (2006) 863
9. J. Simon, *Hist. Sci.* **50** (2012) 339
10. *The Curriculum*, 28.8.1874, Školstvo i prosveta u 19. veku, The Ministry of Education, Belgrade, p. 101 (in Serbian)
11. S. Bojović, *Honourable Serbs: Sima Lozanić*, Princip, Belgrade, 1996 (in Serbian)
12. S. Bojović, *Chemistry in secondary schools in Serbia in the nineteenth and twentieth centuries,* University of Belgrade, Faculty of Chemistry, Belgrade, 2009 (in Serbian)
13. I. Gutman, D. Prodanović, Mita (Dimitrije) Petrović (1848–1891), in *Lives and work of the Serbian scientist,* M. R. Sarić, Ed., Serbian Academy of Sciences and Arts, Belgrade, 2002, p. 29
14. M. Leko, *Educ. Gazette* **17** (1896) (in Serbian)
15. M. Leko, *Educ. Gazette* **18** (1897) 177 (in Serbian)
16. M. Leko, *Educ. Gazette* **18** (1897) 369 (in Serbian)
17. S. M. Lozanić, *Educ. Gazette* **18** (1897) 55 (in Serbian)
18. S. M. Lozanić, *Educ. Gazette* **18** (1897) 298 (in Serbian).
19. S. M. Lozanić, *Educ. Gazette* **18** (1897) 439 (in Serbian)
20. J. Herron, *J. Chem. Educ.* **54** (1977) 15

21. I. Ivić, A. Pešikan, S. Antić, *Guide for a good textbook - overall standards for textbooks quality*, Platoneum, Novi Sad, 2009 (in Serbian)
22. L. Leite, *Sci. Educ.* **11** (2002) 333
23. E. T. Pappa, G. Tsaparlis, *Chem. Educ. Res. Pract.* **12** (2011) 262.
24. S. Bojović, *Chem. Rev*. **30** (1989) 88.

Secondary-school chemistry textbooks in the 19th century

VESNA D. MILANOVIC[1#], DRAGICA D. TRIVIC[2*] and BILJANA I. TOMASEVIC[2#]

¹Innovation Centre of the Faculty of Chemistry, Studentski trg 12–16, Belgrade, Serbia and
²University of Belgrade, Faculty of Chemistry, Studentski trg 12–16, Belgrade, Serbia

TABLE S-I. The structural and organisational components monitored in the textbooks analysed

Structural components	Organisational components
The basic text	Overview of the contents
Terms, concepts, principles, theories and laws	An introductory explanation of the textbook
Chemical symbols, formulas and chemical equations	structure
	Index of the terms used
Contents related to everyday life and health-related contents	Various kinds of supplementary tables
	Literature used
Contents related to the history of chemistry	Note on the author
Precautions to be taken when dealing with certain substances	
Pointing out new terms	
Photographs, pictures, illustrations	
Experiment descriptions	
Questions, instructions, tasks	
Referring to other parts of the book	

TABLE S-II. The quantitative data on the textbooks analysed

Quantitative data	Sima Lozanić *Chemistry for Secondary Schools*	Mita Petrović *Chemistry for Secondary Schools, Based on Prokop Prohaszka and Others*
Number of pages	163	110
Number of titles and subtitles	259	118
Number of highlighted terms	420	482
Number of terms in the index	490	439
Number of elements whose symbols, names and atomic mass are given	68	36
Number of formulas of compounds	383	202

* Corresponding author. E-mail: dtrivic@chem.bg.ac.rs

TABLE S-II. Continued

Quantitative data	Sima Lozanić *Chemistry for Secondary Schools*	Mita Petrović *Chemistry for Secondary Schools, Based on Prokop Prohaszka and Others*
Number of equations of chemical reactions	119	25
Number of experiments presented	13	29
Number of examples connecting knowledge from the sphere of chemistry with its practical application in everyday life	158	174
Number of warnings concerning the toxicity of certain substances and precautions to be taken when handling them	14	34
Number of illustrations	43	10
Number of episodes from the history of chemistry	27	2
Number of questions and instructions	5	12

TABLE S-III. The experiments described in the analysed textbooks

The experiments featured in Sima Lozanić's textbook	The experiments featured in Mita Petrović's textbook
Making a mixture of iron and sulphur	Dehydrating copper sulphate and then hydrating it anew
Heating a mixture of iron and sulphur	Making a mixture of iron and sulphur and separating its constituent from each other
Electrolysis of water, gases collected together	Heating a mixture of iron and sulphur
Dissolving salt in water and subsequent evaporation of the water	Heating tin (lead, zinc, mercury) and measuring the mass of the substance before and after the reaction
A reaction between sodium and water	Heating tin and paraffin, and measuring the mass of the substances before and after heating
Analysis of "red dust" (HgO)	Burning phosphorus inside a bell jar, investigating the characteristics of the gas left in the bell jar
Electrolysis of water, gases collected separately	Obtaining oxygen from red HgO, investigating the characteristics of oxygen
Synthesis of water	Making a mixture of nitrogen and oxygen
Obtaining hydrogen from zinc and sulphuric acid	Burning sulphur in oxygen
Obtaining chlorine from HCl and MnO_2	Burning pieces of coal on a spiral wire in oxygen
Obtaining oxygen from $KClO_3$	Electrolysis of water and investigating the characteristics of the gases obtained
	Obtaining hydrogen from zinc and sulphuric acid (prescribing the exact masses of the reactants)
	Burning hydrogen, covering the flame and obtaining water (chemical harmonica)
	Creating explosive gas in soap suds

TABLE S-III. Continued

The experiments featured in Sima Lozanić's textbook	The experiments featured in Mita Petrović's textbook
Retention of nitrogen after burning phosphorus in the air inside a bell jar Obtaining NH_3 from NH_4Cl and $Ca(OH)_2$	Obtaining NH_3 from NH_4Cl and $Ca(OH)_2$ (prescribing the exact masses of the reactants) Obtaining hydrogen from KOH (prescribing the exact masses of the reactants) and nitrogen from KNO_3 and iron (prescribing the masses of the reactants) and their reaction The neutralisation reaction of ammonia and sulphuric acid Obtaining chlorine from HCl and MnO_2, and investigating its characteristics Obtaining HCl from table salt, water and sulphuric acid Obtaining HFl from $CaFl_2$ and H_2SO_4 Obtaining H_2S from FeS and HCl in a Woulff bottle Sedimentation of Ag_2S, PbS, As_2S_3 Obtaining HNO_3 from KNO_3 and H_2SO_4 Obtaining NO from copper and nitric acid Obtaining CO_2 from $CaCO_3$ and HCl, and investigating its characteristics Decomposition of $CaCO_3$ and the reaction of its product with water Obtaining KOH by boiling K_2CO_3 with $Ca(OH)_2$ Reactions of various sugars with NaOH in $CuSO_4$ Making colour from indigo, $FeSO_4$ and NaOH (prescribing the exact masses)

TABLE S-IV. Questions and instructions found in Sima Lozanić's and Mita Petrović's textbooks

Sima Lozanić's textbook	Mita Petrović's textbook
1) Does the matter of water change when it freezes and when it evaporates? 2) Is it possible to decompose mercury, hydrogen and oxygen into even simpler components? 3) Do these elements of ours make up other cosmic bodies as well? 4) Is the composition of compounds permanent, which is to say, do they always contain the same elements, joined in the same ratio?	1) In what order shall we arrange the halogen elements based on the strength of their affinity? 2) What are the molecular weights of H_2O and NH_3? 3) What are the molecular weights of oxygen and hydrogen? 4) Thus the volume weight of steam equals 9, as we have seen before. Why? 5) What are the volume weights of HCl and NH_3? 6) Thus all chlorides, iodides, bromides, fluorides and sulphides are salts. What acids are they created from? How shall we explain this process? Which of these salts are already familiar to us? Write their chemical formulas, along with the formulas of their acids.

TABLE S-IV. Continued

Sima Lozanić's textbook	Mita Petrović's textbook
5) What keeps molecules and atoms bound together?	7) Sulphuric carbon burns with a bluish flame. What are the products of its burning? 8) According to this, in how many ways could we put out a fire? 9) Sodium occurs in compounds only, and is obtained artificially in the same way as potassium is obtained from its carbonate. What is the chemical equation of this process? 10) $BaCl_2$ and $Ba(NO_3)_2$ are important as reagents to H_2SO_4 and sulphates, with which they produce a heavy white sediment. What is the composition of the sediment? 11) When aluminium sulphate is mixed with sodium sulphate or ammonia sulphate, what is created sodium or ammonia alum. Write their formulas. 12) Galenite is melted with iron particles, which extract sulphur from it through the greater intensity of its affinity. What is the Equation of this reaction?